Genetic and developmental analysis of the *Drosophila* Central Complex: Generation and organisation of distinct neuronal subsets

Joanna Young

Thesis presented for degree of Ph.D.

Institute for Adaptive and Neural Computation

2008

Abstract

The distinct structure of the Central Complex (CC) spanning the midline is one of the most prominent features of the *Drosophila* brain. The CC is highly conserved across insect species and is thought to be required for several behaviours. Although analyses have been performed on the organisation of this structure in the adult brain, few investigations have addressed its ontogeny. Unlike the Mushroom bodies, the CC is an exclusively imaginal structure differentiating in the early half of metamorphosis. Characterisation of the development and neuroarchitecture of this structure is critical for elucidation of function. By employing a combination of immunohistochemical techniques, enhancer trap technology and mutant analysis, this thesis has analysed the cellular structure and development of the CC.

In this study the expression patterns from a subset of genes encoding cell adhesion molecules generated three developmental series datasets from which a developmental timeline for the CC was determined. The *echinoid* gene displayed elevated expression in the Horizontal fibre system allowing a detailed developmental characterisation of this set of isomorphic neurons. Analysis using enhancer trap lines revealed genetic subdivision of neurons and isolation of several isomorphic CC neuron sets in the adult brain. These lines were subsequently used to assess the development of CC neurons. These experiments determined CC development to be in the first 48 hours after puparium formation. The CC neuron structure is established in a series of increments, with sets of isomorphic neurons projecting to their targets within defined time intervals commencing with the Horizontal and Vertical Fibre Systems.

This study includes details of CC structure indicated by projection patterns of neurons and by mutant analysis. In addition, the investigation of one of the genes involved in development, *echinoid*, is further analysed for a potential pathfinding function in the Optic lobe. Finally, this thesis presents the advantages conferred by the use of enhancer trap lines for developmental study of the CC and has isolated a novel set of these lines that will be beneficial for future studies into structure, development and behaviour of the CC.

Table of Contents

List of Tables

List of Figures

List of Abbreviations

APF	After Puparium Formation
AL	Antennal Lobe
CAM	Cell Adhesion Molecule
CBT	Cell Body fibre Tract
CC	Central Complex
CNS	Central Nervous System
DPC	dorsal posterior commissural system
DPL	lateral dorso posterior lineages
DPM	medial dorso posterior lineages
EB	Ellipsoid body
FB	Fan-shaped body
GFP	Green Fluorescent Protein
HFS	Horizontal Fibre System
IgSF	Immunoglobulin Superfamily
LTR	Lateral Triangles
L3	3rd instar larva
MARCM	Mosaic Analysis with a Repressible Cell Marker
MB	Mushroom bodies
Nb	Neuroblast
NO	Noduli
PB	Protocerebral bridge
PNS	Peripheral Nervous System
SAT	Secondary lineage Axon Tract
trCM	transverse system
UAS	upstream activation sequence
VBO	Ventral bodies
VFS	Vertical Fibre System

VNC	Ventral Nerve Cord
a ch	anterior chiasma
gc	great commissure
p ch	posterior chiasma
p fbd c	posterior commissure of the dorsal Fan shaped body
s ar	superior arch

Gene and Protein abbreviations

ccb	*central complex broad*
cbd	*central body defect*
ceb	*central brain deranged*
ed	*echinoid*
ibx	*icebox*
nrg	*neuroglian*
robo	*roundabout*
shg	*shotgun*
Dscam	Down syndrome cell adhesion molecule
De-cadherin	*Drosophila* epithelial cadherin
Dn-cadherin	*Drosophila* neural cadherin

Neuron Nomenclature

Central Complex Neurons

Small Field Neurons

HFS	Horizontal Fibre System (*w*, *x*, *y* and *z* fibre bundles)
	Connecting the PB, FB and VBO
VFS	Vertical Fibre System
	Connecting the PB, FB and NO
Pontine neurons	Type P*c d* : Pontine contralateral dorsal (P*i*)
	Type P*c v* : Pontine contralateral ventral (P*ii*)
	Type P*a* : Pontine adjacent segments
	Type P*l* : Pontine layer (P*iii*)
	(These neurons were renamed as P*i-iii* in publications from this thesis)
fb-eb	Connecting the FB and EB
fb-ltr	Connecting the FB and LTR
fb-no	Connecting the FB and NO
fb-eb-no	Connecting the FB, EB and NO
pb-no	Connecting the PB and NO
pb-fb	Connecting the PB and FB
pb-eb	Connecting the PB and EB
pb-eb-ltr	Connecting the PB, EB and LTR
pb-fb-fb	Connecting the PB, FB and FB
pb-eb-no	Connecting the PB, EB and NO
pb-fb-eb	Connecting the PB, FB and EB
pb-eb-vbo	Connecting the PB, EB and VBO

eb-no	Connecting the EB and NO
eb-pb-vbo	Connecting the EB, PB and VBO
vbo-ltr	Connecting the VBO and LTR

Large Field Neurons

R neurons	Type A : R1-R4 (Characteristic ring neurons connecting LTR and EB)
	Type B : ExR1 (Connecting FB, EB and VBO)
	Type C : ExR2 (Connecting VBO, LTR and EB)
F*l* neurons	Fan shaped lateral neurons
F*m* neurons	Fan shaped medial neurons
	F*m*1
	F*m*2
	F*m*3

Optic Lobe Neurons

R cells	R1- R6 target the Lamina
(photoreceptors)	R7 target the M6 layer of the Medulla
	R8 target the M3 layer of the Medulla
L1-5	Laminar neurons

Synonyms

Synonym	Species	Drosophila equivalent	Comments
Bulb	New name	Lateral triangle (LTR)	(newly established term for *Drosophila* as of 11/5/08)
Central body	*Schistocerca gregaria* *Musca domestica*	FB and EB	
Central body lower division (CBL)	*Schistocerca gregaria*	FB	
Central body lower division (CBU)	*Schistocerca gregaria*	EB	
Column	*Schistocerca gregaria*	segment	EB segments are radial not columnar
Columnar neuron of the PB and CBU (CPU1)	*Schistocerca gregaria*	HFS	
Columnar neuron of the PB and CBU (CPU4)	*Schistocerca gregaria*	VFS	
Lateral accessory lobes (LAL)	*Schistocerca gregaria*	Ventral bodies (VBO)	(newly established term for *Drosophila* as of 11/5/08)
Pontine neuron of the CBU (PoU)	*Schistocerca gregaria*	P*i* neuron	(P*i* neuron = proposed term for *Drosophila* in this thesis)
Tangential neuron	*Schistocerca gregaria* *Tenebrio molitor*	Large field neuron	
Tether	New name	Secondary axon tracts (SATs)	(Tether: established for *Drosophila* as of 11/5/08)
		Cell body fibre tracts (CBT)	
w, *x*, *y*, *z* fibres	*Schistocerca gregaria* *Tenebrio molitor*	Only refer to HFS projections in *Drosophila*	
		Projections from all cells originating from that cluster/ lineage	(proposed to be adopted for *Drosophila* in this thesis)

Acknowledgements

This study was funded by a scholarship award from the Medical Research Council and performed under the supervision of Dr. Douglas Armstrong at the University of Edinburgh.

I would like to thank the following people for their suggestions, support and advice during this project: My supervisor Douglas Armstrong and my second supervisor Andrew Jarman. Also, David Willshaw, Mark Longair, Petra zur Lage, Lynn Powell, Raphie Kitson-Pantano, Bilal Malik and Jane Ewins.

For financial assistance to attend various academic conferences to present my work I would like to thank the Institute for Adaptive and Neural Computation, the Informatics Graduate School and the EMBL in Heidelberg.

Finally, special thanks go to my Parents and family for their unwavering support and encouragement throughout this project and my University career. I would also like to thank numerous friends and colleagues for their support. Finally, for general mischief collaboration thanks must go to my lab and office mates.

Declaration

This study has not been presented for any other qualification or degree. All work was undertaken by the author with the following exception.

The mapping of enhancer trap lines to chromosomes was carried out jointly between the author and Mark Longair.

1

Introduction

1.1 The *Drosophila* Central Nervous System

1.1.1 The Composition of the Nervous system

Investigations into the structure and function of the insect brain have been occurring since the pioneering studies by Kenyon in the nineteenth century (Kenyon, 1896). Their nervous system is small but insects display a variety of complex behaviours and several studies have implicated key brain regions in the elucidation of these behaviours (Strausfeld, 1976; Strauss & Heisenberg, 1993; Strauss, 2002; Keene & Waddell, 2007). Understanding the intricate neural circuitry underlying behaviour is a key objective in Neuroscience. With its manipulable genetic system and short life cycle, *Drosophila* provides an ideal model to study brain development, structure and function.

The insect Central Nervous System (CNS) exists as a series of ganglia with the brain as the main association centre located in the head capsule. The brain is divided in to the Supraesophageal ganglion, comprised of the protocerebrum, deuterocerebrum, tritocerebrum and the subesophageal ganglion. The insect brain is divided into neuropil masses (Power, 1943; Strausfeld, 1976), several of which are clearly identifiable. The tritocerebrum and neurons from the subesophageal ganglion

innervate the mouth parts and the deuterocerebrum is innervated by the antennal nerve and the major olfactory centre (Strausfeld, 1976; Nassif et al., 1998). The protocerebrum is the largest of the divisions where prominent structures such as the Mushroom bodies, the Central Complex and the Optic lobes are found. The *Drosophila* brain is a complex organisation of fibres consisting of ~100,000 neurons (Truman et al., 1993). The CNS of the fly contains only motoneurons and interneurons, with sensory neurons limited to the Peripheral Nervous System (Truman, 1990).

Despite functional and evolutionary similarities (Ghysen, 2003) the structure of the insect neuron differs from that of vertebrate neurons. Due to the small size of the organism, neurons are much smaller than their vertebrate counterparts. In addition, insect neurons are mainly unipolar, with only one primary neurite emanating from a perikaryon (Strausfeld, 1976), unlike the heteromultipolar vertebrate neurons. In contrast to the vertebrate body plan, Perikarya in the Fly brain lie in the cortex and axons project inwards to the neuropil forming a dense fibrous network of connections. Insect neurons do not have postsynaptic dendrites on the Perikaryon, instead processes branch off at various points along the axon and these are referred to as dendrites (Landgraf et al., 2003; Sanchez-Soriano et al., 2005). The axon hillock is found ectosomatically, beyond the dendrites (Strausfeld, 1976).

1.1.2 Development of the Nervous System

Neural generation occurs in two major phases in the holometabolous *Drosophila* life cycle; during embryogenesis and metamorphosis. During embryogenesis neurons required for larval life develop, designed to control feeding and foraging behaviours in addition to locomotion (Nassif et al., 1998). In the larval brain several neuroblasts can be detected dividing to produce clusters of immature neurons that do not appear to be functionally active at this stage, suggesting these are required for adult life (Truman, 1990; Dumstrei et al., 2003a; Dumstrei et al., 2003b; Nassif et al., 2003). Throughout metamorphosis extensive remodelling of the larval

brain occurs involving neuronal birth, pruning and apoptosis. The brain increases in size and changes shape, forming separate optic lobes flanking the central brain. The first 12-14 hours of metamorphosis are consigned to disposing or pruning of larval neurons representing a degenerative phase that occurs primarily in the Ventral nerve cord and to a more limited extent in the brain (Truman, 1990). Equally, this time is also when several adult specific neurons commence axonogenesis, such as the Photoreceptors of the Optic lobe (Meinertzhagen et al., 1993). Early metamorphosis is therefore a key phase in CNS development, as both degenerative processes and axonal targeting are taking place concurrently. This extensive remodelling process is mainly a result of the action of ecdysteroids, hormones that regulate the action of transcription factors in the nuclear receptor family (Riddiford et al., 2003). With the exception of the Optic lobes (Meinertzhagen et al., 1993) and the Mushroom bodies (Lee et al.,1999; Armstrong et al., 1998) limited research has been conducted into the development of adult brain structures during metamorphosis in *Drosophila,* though extensive studies have been performed on metamorphosis of the Ventral nerve cord (Truman et al., 1993; Truman et al., 2004; Williams & Truman, 2005).

1.2 The Central Complex

1.2.1 The Central Complex in the Insect brain

The insect Central Complex (CC) is an intricate, symmetrical structure that is located on the midline of the protocerebrum. The CC has been implicated in coordination of motor behaviour (Strauss & Heisenberg, 1993; Strauss, 2002), flight control (Ilius et al., 1994), multimodal information processing (Muller et al., 1997), courtship behavior (Popov et al., 2003; Popov et al., 2004), visual pattern learning (Liu et al., 2006) and spatial orientation (Heinze & Homberg, 2007). The CC neuropil is highly conserved between arthropods (Loesel et al., 2002) and the adult neuroarchitecture of this structure has been previously documented (*Musca*: Strausfeld 1976; *Drosophila*: Hanesch et al., 1989; Renn et al., 1999; *Schistocerca*:

Homberg, 1991; Muller et al., 1997; *Tenebrio*: Wegerhoff & Breidbach, 1992). These studies do not adhere to a common nomenclature system regarding either sub-structures or neuronal types despite shared projection and innervation patterns in several cases. For example, the term 'Central body' in *Musca* refers to the FB, EB and NO collectively. The *Drosophila* CC is comprised of four sub-structures, the Protocerebral bridge (PB), the Fan shaped body (FB), the Ellipsoid body (EB) and the paired Noduli (NO) as shown in Figure 1.1. Two accessory regions are associated with the CC; these are the Lateral triangles (LTRs) and the Ventral bodies (VBO), satellite to the CC. In this thesis the nomenclature system conforms to that documented in the *Drosophila* brain by Hanesch et al. (1989).

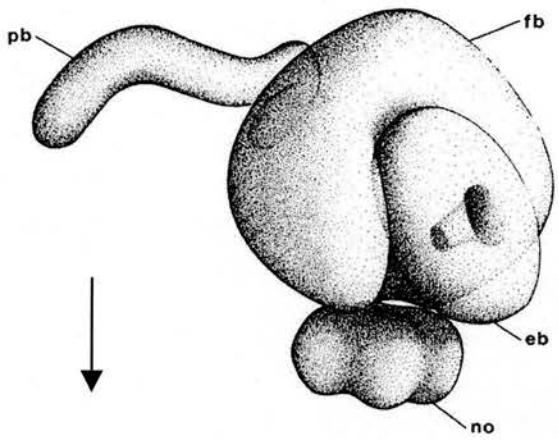

Figure 1.1: The Central Complex of *Drosophila melanogaster* (Hanesch et al., 1989). Arrow points in a ventral direction. fb, FB; eb, EB; no, NO; pb, PB.

1.2.2 Compartmentalisation and Neuronal Structure of the Central Complex

The columnar elements and stratifications of the CC neurons make it possible to compartmentalise the CC sub-structures forming a sophisticated matrix. The PB is divided into sixteen glomeruli (eight per hemisphere) on the transverse axis. The FB can be divided into six horizontal layers and eight vertical segments when viewed frontally as well as four shells on the antero-posterior axis (Hanesch et al.,1989). The NO consist of two pairs of glomeruli adjacent to the midline located ventral to the FB. The doughnut shaped EB is partially embedded in the concave FB and the dorsal side lies more posterior to the ventral edge (Hanesch et al.,1989). This is represented schematically in Figure 1.2. The number of EB segments has not been determined in the *Drosophila* brain. In *Musca* the radial segments of the EB display homolateral connections to the FB segments (Strausfeld, 1976). This may also be the case in *Drosophila.*

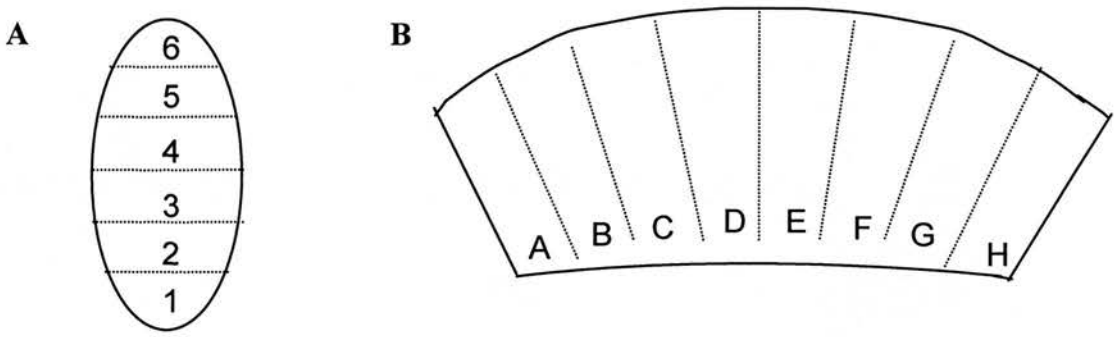

Figure 1.2: Compartmentalisation of the FB. A, The FB is divided into six (1-6) horizontal layers, viewed here as a lateral cross section. **B**, The FB is divided into eight segments (A-H) along the transverse axis (Hanesch et al., 1989).

The total number of cells that comprise the intricate CC neuroarchitecture is unknown but over fifty neuron types have been identified (Hanesch et al., 1989; Renn et al., 1999). The neurons of the CC can be categorised into two major groups; the Large field neurons that display arborisations prior to innervating the CC (such as F neurons and R neurons) and Small field neurons that connect regions within the CC (including the HFS, VFS and Pontine neurons). These are represented schematically in Figure 1.3. The most prominent fibre systems of the CC are the Horizontal and Vertical fibre systems (HFS and VFS) with Perikarya in the dorsal cortex innervating the PB and FB before targeting satellite neuropil regions. The HFS is comprised of 3-4 neurons per PB glomerulus and all but the most lateral neurons innervate segments of the FB contralaterally before targeting the VBO. The VFS consists of 2 neurons per glomerulus innervating FB segments ipsilaterally then target the contralateral NO. Additional small field elements innervate specific segments of the FB forming a columnar matrix. Connections have been observed between all substructures (Hanesch et al.,1989). Large field F neurons arborise outside the CC before targeting from a lateral direction and crossing the FB contralaterally to form transverse strata that has been tentatively labelled as six FB layers.

Although studies have addressed the development of prominent neuropil such as the Mushroom bodies (Ito & Hotta, 1992; Tettamanti et al., 1997; Armstrong et al., 1998; Lee et al., 1999) and the Optic lobes (Meinertzhagen et al., 1993), few studies have detailed the differentiation of the CC beyond the larval stage (Renn et al., 1999). In other arthropods, the elaboration of the CC has been investigated. In *Schistocerca*, the CC commences differentiation during mid embryogenesis (Boyan & Williams, 1997; Williams et al., 2005), in *Tenebrio* the CC develops throughout the larval instars (Wegerhoff & Breidbach., 1992) *Drosophila* differs from these species in that the CC does not appear to be required for larval life. Detailed maps of the embryonic (Nassif et al., 1998) and the late larval brain (Dumstrei et al., 2003b; Pereanu & Hartenstein, 2006; Younoussi-Hartenstein et al., 2006) exist that can now facilitate the study of brain development during metamorphosis. Unlike the Mushroom bodies that are identifiable in late embryogenesis (Ito & Hotta, 1992), the

CC is an exclusively imaginal structure, differentiating in the early half of metamorphosis (Hanesch et al., 1989). In the 3rd instar larva the CC is present as a series of interhemispheric commissures (Hanesch et al.,1989; Strauss et al., 1992) and a structure resembling that of the PB has been observed at this stage (Schneider et al., 1993). In the Ventral nerve cord, adult specific neurons are born in larval life but their development into mature functional neurons is delayed until metamorphosis (Truman, 1990). This may be the case for the neurons that comprise the interhemispheric commissure tracts, though it has been suggested that there are too few of these (1970 fibres) to comprise the complete cellular composition of the CC (Strauss, 2002) suggesting additional neurons are born in metamorphosis. A recent report has determined lineages and projections in the late 3rd instar that has identified a series of different fibre systems originating from several lineages thought to eventually constitute the CC (Pereanu & Hartenstein., 2006). By establishing the developmental characteristics of the CC during metamorphosis, it will be possible to trace the generation of this structure from neuroblasts to fibre systems.

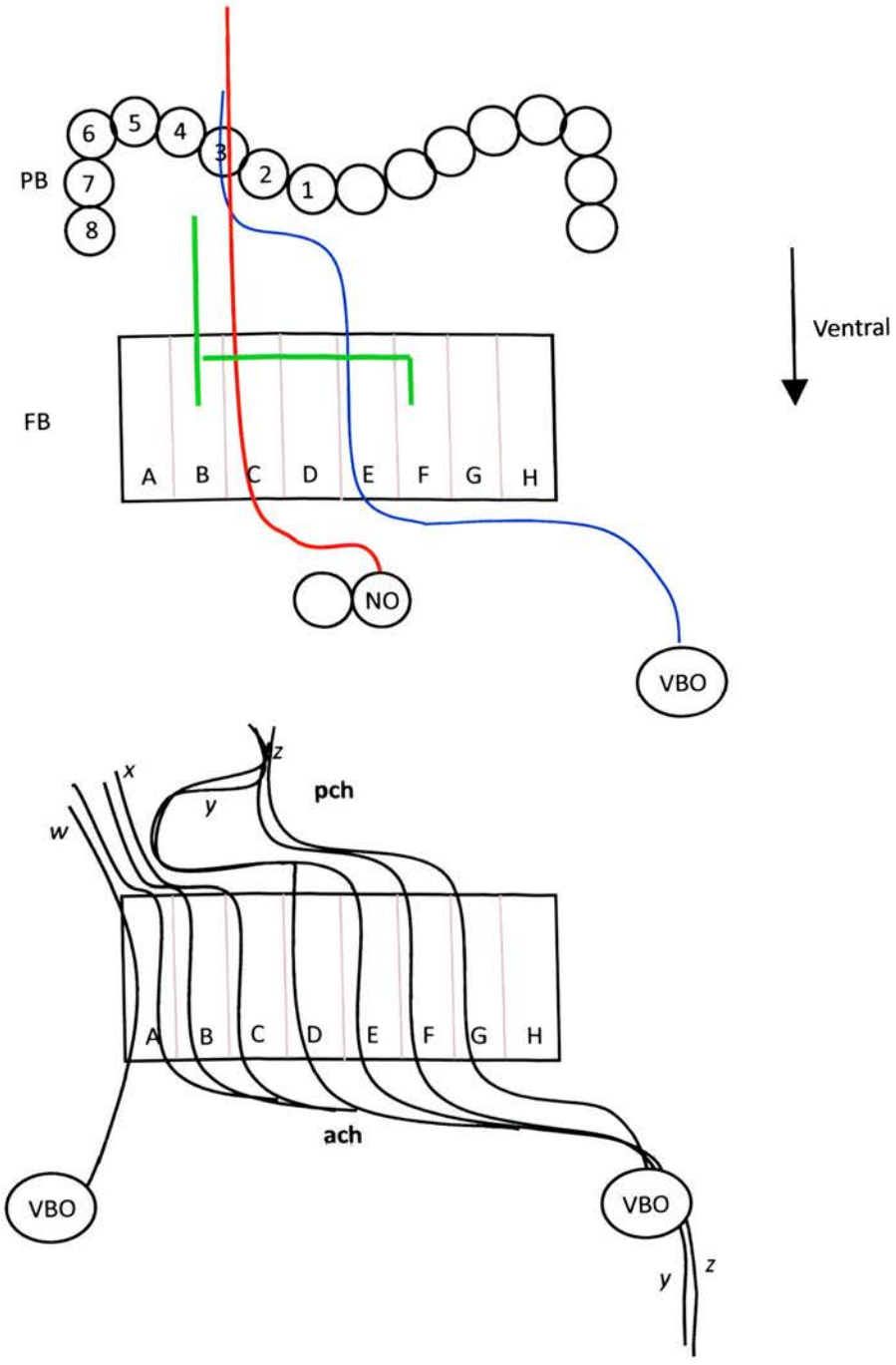

Figure 1.3: Compartmentalisation of the FB by small field neurons. **A**,Three types of small field neurons from three known isomrphic sets are shown. The fibre bundles of the VFS (red) target the FB ipsilaterally then cross to the contralateral NO. One of the neurons from the *y* fibre bundle of the HFS (blue) innervates glomerulus 3 of the PB then crosses contralaterally to innervate segment E of the FB prior to innervating the VBO. The Pontine neurons (green) branch to innervate 2 contralateral segments of the FB that are 4 segments removed. **B**, Projections of the HFS from one hemisphere to the FB. Sixteen HFS fibre bundles innervate the FB.

1.3 Information flow through the Central Complex

1.3.1 Input and Output neurons of the Central Complex

Information flow through the CC has been inferred from the appearance of neurons revealed by Golgi stains, with 'blebbed' axon endings considered presynaptic and 'spiny' endings as postsynaptic (Strausfeld, 1976; Hanesch et al., 1989). Input to the CC is through Large field neurons such as the stratified Fan shaped (F) neurons and the R neurons of the EB (Hanesch et al., 1989). These neurons first arborise with spiny terminals in regions outwith the CC or the satellite regions of the Ventral bodies (VBO) or the Lateral Triangles (LTR) and have blebbed endings in the CC. The VBOs also receive information from the CC through the small field neurons such as the HFS neurons, which are thought to be the main output neurons of the CC (Hanesch et al., 1989).

The symmetrical structure and contralateral connective neuroarchitecture of the CC suggests a role in information exchange between brain hemispheres. Previous reports have shown the EB (type A) R neurons to be GABA-ergic (inhibitory) and the FB, NO and posterior EB to be excitatory (Buchner et al., 1986) leading to the formation of the hypothesis that Small field neurons elicit the actual behavioural output whereas Large field neurons such as the type A R neurons exert modificational control (Hanesch et al., 1989). The F neurons have also been implicated in visual pattern recognition (Liu et al., 2006). Although no direct connections between the Mushroom bodies and the CC have been reported, F neurons have been shown to arborise in the region of the MB leading to the hypothesis that F neurons with presynaptic terminals in the CC receive input from the MB output neurons (Ito et al., 1998). These presynaptic F neurons have been implicated in a locomotor circuit with columnar, small field *pb-eb-no* neurons (Martin et al.,1999) which have been previously inferred as a potential looped pathway within the CC structure (Hanesch et al., 1989). Additionally, connections are now known to exist between the CC and sensory regions; connections to the EB

from the Ventral nerve cord (thoracic ganglion) via the lateral accessory lobes (VBO in *Drosophila*) have been reported in *Schistocerca* (Homberg, 1994), further supporting the theory that the CC is an integrative decision centre for locomotion. These studies contribute to the understanding of CC neural circuitry though elucidation of information flow through the CC still requires further investigation.

1.3.2 Central Complex Structural Mutants

Previous structural and functional analyses of the CC have utilised mutant strains with structural defects in the CC (Strauss & Heisenberg, 1993; Bouhouche et al., 1993; Ilius et al., 1994; Martin et al., 1999; Renn et al., 1999). Such defects include distortion and incomplete formation of the FB (*central body defect, cbd*), a dorsal to ventral cleft down the FB (*central brain deranged, ceb,* an allele of *neuroglian*) and an unfused EB (*icebox, ceb, cbd*). Although the gross CC structure has been recorded for these mutants, no analysis has been performed at the cellular level. The mutants can provide valuable data on CC structure due to these distortions as it can allow visualisation of regions of the CC that are otherwise difficult to isolate. The development nature of how these CC phenotypes occur has not been investigated, though gene mutations have now been mapped to several loci (Strauss & Heisenberg, 1993; Carhan et al., 2005). This now permits further study into gene function in the CC.

The extensive behavioural and structural studies on the insect brain over the last century have also been noted by fields such as informatics, prompting studies to model insect behaviour in robots. Such studies have proposed a general insect brain control architecture for obtaining adaptive behaviour in robots that involves the CC, Mushroom bodies and thoracic ganglia (Wessnitzer & Webb, 2006). A combined approach of robotic and biological research should provide a novel insight into CC function in the future.

1.4 Techniques for neuroanatomical studies

Several fundamental neuroanatomical studies on the insect brain were performed before the advent of modern techniques and tracing neuronal remodelling during metamorphosis often proved difficult with conventional methods. Modern genetic and immunohistochemical applications can now facilitate the study of neuroanatomical development (Lee et al., 1999; Renn et al., 1999; Landgraf et al., 2003; Dumstrei et al., 2003b) allowing us to build on neuroarchitecture recorded in previous studies. Traditionally, silver staining or dye injections were used to visualise individual or groups of neurons (Strausfeld, 1976; Strausfeld & Miller, 1980; Hanesch et al., 1989). The advantage of this methodology was that it rendered individual cells clearly visible when viewed under the microscope, allowing visualisation of branches and terminals in addition to trajectory patterns, but there are limitations to using this technique. Firstly, neurons adopt the stain stochastically therefore it is difficult to reproduce exact staining patterns for further examination, a requirement that is mandatory for developmental analysis. Secondly, categorising neurons into isomorphic sets is difficult with only individual cellular projection patterns since comparing trajectories from different preparations is not reliable.

Recent neuroanatomical studies on the *Drosophila* brain have used modern methods of analysis such as immunohistochemistry (Nassif et al., 1998; Dumstrei et al., 2003b; Nicolas & Preat, 2005), clonal analysis (Lee et al.,1999) and enhancer trap lines (Yang et al., 1995; Armstrong et al., 1998; Renn et al., 1999; Landgraf et al., 2003). Immunohistochemistry using known neural markers is effective because it is reproducible and efficient. To use this technique for developmental analysis it is necessary to initially satisfy three criteria; firstly, the target molecule must be on neurons of interest, secondly, expression must remain constant on these neurons to trace their projection patterns and thirdly, the target molecule must be membrane tethered to reveal neuronal structure. Due to the range of antibodies available this is an effective method to use if a specific marker is known for the neurons of interest. A disadvantage to using immunohistochemistry is that markers tend to stain a large number of fibre tracts meaning subsequent visualisation of individual tracts or fibre

systems is problematic.

Clonal analysis is a technique that is used in several studies of the *Drosophila* nervous system. With the advent of techniques such as the Mosaic Analysis with a Repressible Cell Marker (MARCM) (Lee & Luo, 2001) it has become possible to trace neurons originating from the same neuroblast by induction of mitotic recombination producing clones that contain common driver and reporter lines. This is particularly useful when conducting lineage analysis. The disadvantage to this technique is that obtaining flies with the desired genotype is time consuming. For developmental studies it is necessary to have several reproducible preparations over a series of timepoints and the MARCM technique may not reliably produce the same number or set of clones. Finally, in order to visualise the clones it is necessary to use a P{Gal4} driver that is specific to a cell type and is expressing at the desired timepoints. Regarding a developmental analysis of the CC, for which few specific driver lines are known in either the adult or developing structure, this would not be an ideal technique with which to start.

In contrast, using the Gal4-UAS system (Brand & Perrimon, 1993) alone is highly efficient for developmental analysis (Armstrong et al, 1998; Renn et al., 1999; Landgraf et al., 2003). As with clonal analysis, P{Gal4} driver lines are used to drive expression of a fluorescent reporter construct under the control of a UAS sequence in specific neurons. A variety of membrane tethered reporters are available for visualisation. For whole neurons, UAS-mCD8::GFP (a membrane tethered mouse surface molecule; Brand, 1995) or UAS-lacZ (Tettamanti et al., 1997) can be used. To visualise dendritic arborisations a flourescently tagged membrane segment encoded by exon 17.1 of *Drosophila Down syndrome cell adhesion molecule* (*Dscam*) can be expressed ectopically in neurons and will specifically target to dendrites (Wang et al., 2004). Equally, to observe presynaptic sites a flourescently tagged construct of neuronal Synaptobrevin can be expressed. The advantage of this system is that, like immunohistochemistry, it is reproducible both temporally and spatially in a defined set of neurons. Equally, expression patterns may reveal genetic and morphological relationships between sets of neurons. The main limitation to this

technique is determination of temporal and spatial expression patterns. Enhancer trap lines have previously been shown to alter their expression patterns throughout development (Armstrong et al., 1998; Ward et al., 2002). Prior to neuroanatomical analysis, it is necessary to first isolate enhancer trap lines for the neurons of interest then assess their expression patterns in development for consistency.

For a study of the developing CC, we have to first consider that there are remarkably few markers known for this structure since previous anatomical studies relied on cellular injections, as mentioned above. As our knowledge of CC lineage and markers is limited, it would not be prudent to commence an investigation of the developing CC using a clonal analysis. Instead, a combined methodology using both immunohistochemistry and enhancer trap analysis was considered the optimal approach by which to conduct this study. In order to investigate the functions of the Central Complex it is critical to understand the intricate circuitry of this structure. Analysis of the CC during development will not only provide fundamental knowledge of the differentiation of this structure but will allow visualisation of neurons during axonogenesis and as connections are formed. Tracking neurons through the less dense neuropilar framework of metamorphosis facilitates the study of neuronal organisation in the brain. This approach has several advantages; firstly, we can visualise sets neurons more easily, secondly, formation of connections between neurons may indicate information flow through the CC and thirdly, we may discover connections previously unreported.

This thesis focuses on the structure and development of the CC during metamorphosis, in addition to the determination of genetic and neuronal relationships within this structure. In this study, analysis of CC development is performed using a combined approach of immunohistochemical markers and enhancer trap lines. The main aims are to identify novel markers for the CC in the adult brain and during development, to determine the developmental characteristics of the intricate structure of the CC and infer further structural insights into CC neuroarchitecture and finally to assess the genetic relationships between neurons and

the potential role of novel genes present in the differentiating CC.

2

Materials & Methods

2.1 *Drosophila* strains & husbandry

2.1.1 Fly husbandry

Flies were reared on standard cornmeal food at 25°C on a 12 hour:12 hour light:dark cycle in either vials or bottles in LMS cooled incubators. Food was 'Dundee food' (a standard yeast/ cornmeal/ agar medium) prepared in the Swann media kitchen, Kings buildings at 18°C or room temperature. Temperature sensitive strains were reared at 18°C as appropriate.

Precise numbers of flies were not maintained in vials but stocks were kept healthy by frequent changes into fresh food when required judging on the size of individuals and mobility of larvae. Stocks were tipped frequently to avoid mite pests and yeast paste (made from dried Allisons yeast mixed with water) was added to vials with sick stocks when required. Small volumes (~1-3ml) of water were occasionally added to vials or bottles when required to prevent food from drying out. When culturing sick stocks 'humidifiers' made from paper towels soaked in water were added to bottles.

Alternatively, flies were transferred to cages containing grape juice plates to lay eggs, then the contents of the plate were added to a food bottle.

2.1.2 Fly strains

For a detailed list of strains used in this study refer to Table 2.1. The wildtype *Drosophila* strain used as a control for chapters 3, 4 and 6 was Oregon R and for chapter 5 wildtype strain Canton S was used.

Central Complex mutants (*ccb* ^{KS127}, *cbd*^{KS96} and *cbd* ^{KS171}) were obtained from Martin Heisenberg. Mutants were originally isolated in mass histology following ethylmethane sulfonate mutagenesis (*Heisenberg and Bohl, 1979*). All mutations are X-linked. All strains were outcrossed to Canton S, a wildtype strain obtained from Scott Waddell (University of Massachussetts) and still displayed CC phenotypes

Crosses for experiments with both enhancer trap lines and CC structural mutants are as described in the previous section. The cross performed for analysis of the Central Complex in *echinoid* mutants was a null mutant, *ed*^{K01102}*/ Cyo* to a deficiency, *Df(2L)ed-dp/ SM1* that produced delayed hatching escapers (1/70).

2.1.3 Enhancer trap lines

The enhancer trap lines used here originated from a mutagenesis that generated a total collection of 1800 P{Gal4} inserts (Yang et al 1995) by standard techniques (Brand and Perrimon 1993). From this original screen, 300 P{Gal4} lines were isolated and have been maintained in the Armstrong lab for several years. The enhancer trap lines used in this study were selected from this subset on the basis of FB expression (see *www.flytrap.org*).

Reporters used included UAS-mCD8::GFP on chromosomes II and III, used in conjunction with a rabbit anti-GFP primary antibody (Molecular Probes, product A11122 dilution 1:5000) and Goat anti-rabbit Alexa Flour 488 (dilution 1:400). No reporter gene expression was detected in the brain in the absence of a P{Gal4} driver. For both adult and developmental expression analysis, females from a UAS-mCD8::GFP reporter strain were crossed to males from an enhancer trap line and the resulting heterozygous male progeny were dissected in all cases except for X linked enhancer trap lines, when females were dissected. Crosses were performed in bottles with approximately 5-10 females and 3-8 males in each.

In order to map P{Gal4} insertions to chromosomes, males from enhancer trap lines were crossed to *w- /w- ; Kr/Cyo ; D^1 / Tm6B* females and the F1 was scored for eye colour and wing phenotype. Then males from non X-linked strains were crossed back to *csw-* females and again scored for eye colour and wing phenotype to ascertain insertion position.

For enhancer trap and CC structural mutant crosses, enhancer trap lines were first crossed to UAS-mCD8::GFP lines (ensuring P{Gal4} insertions and UAS-mCD8::GFP constructs were on separate chromosomes), then male heterozygotes were crossed with CC mutant females. Hemizygous males were selected from the resulting F2 progeny. To ascertain which flies carried the desired markers they were rendered unconscious by placing the vials at -20°C for 1 hour, this method proved to be more effective in keeping the flies unconscious for longer than using CO_2. Flies were then analysed for GFP reporter expression under a Leica MZFLIII Fluorescence microscope. Males positive for expression were dissected for analysis. In all cases, flies between 3-10 days old were dissected.

2.2 Developmental timeseries

2.2.1 Pupal timeseries

All fly strains used in each developmental time series were raised in bottles at 25°C. Stationary white pre-pupae (both male and female) that had climbed up the bottle and had extended spiracles were collected (Time, t = 0). Collections were accurate to ±30 mins (Ashburner, Golic & Hawley, 2005) using this method. Pupae were transferred to vials and raised at 25°C. Timepoints were every four hours thereafter recorded as APF (hours After Puparium Formation) as performed in Renn et al (1999). Dissection times were accurate to 10 minutes. Pupae were collected when available therefore not in relation to the diurnal cycle. Between 2-5 individuals (n) were dissected per timepoint for the developmental series screens. Length of time to eclosion was timed as approximately 106 ± 4 hours at 25°C in wildtype and enhancer trap/GFP strains. The initial expression analysis in chapter three was performed to 96 hours APF, the enhancer trap study up to 52 hours APF.

2.2.2 Mutant pupal timeseries

Staging of $ed^{4.12}/ed^{4.12}$ mutants followed the same protocol as above but several more individuals were dissected, n = 15-20 per timepoint. In order to ascertain genotypes for non viable *echinoid* mutant pupae accurately the Black cell (bc) larval marker was used. $ed^{6.1}/Cyo$ and ed^{K01102} / *CyO* flies were first crossed with w^{118}; *ln(2LR)Gla,wg*^{elp} *Bc / CyO*. The resulting mutant/ *bc* F1 progeny were then crossed. F2 larvae were collected from the bottle and analysed under the dissecting microscope for the absence of the *bc* marker. These flies were then replaced in a vial and collected as above. Collection times were accurate to approximately 30 mins - 2 hours. Delayed adult eclosion times indicated slower development (data not shown) which may have affected

R cell outgrowth. These mutants were semi-lethal in what appeared to be between 24-48 APF (data not shown), therefore there were few individuals obtained at later stages of metamorphosis.

2.3 Tissue preparation and Immunohistochemistry

2.3.1 Dissection and fixation

Adult dissection : Adult males (except in cases of X-linkage) between 3-10 days old were dissected using two pairs of Inox forceps. Flies were anesthetized with CO_2 and pinned through the thorax in a dorsal to ventral direction on a Sylgard/gel mix plate flooded with PBS (Tablets - Sigma). Brains were dissected immediately (dissection time per brain ~1 minute) using a Nikon dissecting microscope and fixed in 100µl 4% paraformaldehyde in a microtitre plate for 30 minutes. Brains were then washed for 5 minutes in PBS followed by incubation for 1 hour in PBT (PBS + 0.1 % Triton X-100) before immunohistochemistry. Incubation with antibodies as below. Brains were washed in PBT for 2 hours at 4°C after removal of secondary antibody.

Adult dissection (mAb nc82 protocol): Dissection as above. Brains were fixed in 4% paraformaldehyde on ice for 30 minutes then washed for 5 minutes in PBS. Two further 20 minute washes were then performed in PBT. After incubation with the secondary antibody, brains were washed in PBT for 2-5 days before confocal analysis.

Pupal dissection: Pupal dissections were performed at 4 hour intervals throughout metamorphosis for a range of strains. Dissections were performed using Inox forceps in a 5cm x 5cm watch glass filled with PBS. Brains were dissected out (dissection time ranged from 3-10 minutes) and fixed and washed as above.

Larval dissection: Wandering 3rd instar larvae were picked from the wall of the food bottle and immersed individually in a 5cm x 5cm watch glass filled with PBS. Brains were dissected (Dissection time 30-60 seconds) by gripping the larvae at the mouthparts and one third of the way down the body then pulling the tissue apart to reveal the brain and VNC. Fixation occurred as above.

Embryo preparation: In the initial *echinoid* expression screen embryos were assayed for expression in the CNS. Embryos were collected on grape juice plates in cages overnight, rinsed with water and caught in a sieve. Embryos were then dechorionated in 50% bleach for 4 minutes then rinsed with dH_2O before fixation with a mix of 3.25ml dH_2O, 0.5ml 10xPBS and 1.25ml formaldehyde and 5ml Heptane for 20 minutes. The lower phase of the solution was then removed. Devitellinisation was performed by adding 10ml of Methanol, embryos were then washed twice with Methanol. Rehydrate embryos with PBT. Embryos were then blocked in 2% Bovine Serum Albumin in PBT for two hours at room temperature prior to staining.

2.3.3 Immunohistochemistry

For details on antibodies used in this study refer to Tables 2.2 and 2.3.

Primary antibodies were diluted as required in PBT kept at 4°C. Embryos and whole brains of all stages were incubated in 100µl of diluted antibody overnight at 4°C in microtitre plates. Initial experiments with brains included between 20 – 50µl of 2% BSA in PBT and 25µl NGS but results showed no difference without these therefore use was discontinued. Embryos were incubated with 25µl NGS and 125µl 2% BSA in PBT in addition to diluted antibody. When obtained, antibodies were divided into 200µl aliquots and stored at 4°C or -20°C as required.

Secondary antibodies were diluted 1:400 in PBT kept at 4°C. Embryos and

whole brains of all stages were incubated in 100µl of diluted antibody overnight at 4°C in microtitre plates. Plates were kept in the dark.

To control for anomalous expression all secondary antibodies (1:400) were tested on brains that had not been previously incubated in Primary antibodies. There was no detectable staining pattern. Brains untreated by immunohistochemistry were detectable under the confocal microscope but showed no comparable expression patterns.

2.3.4 Preparing tissue mounts

Whole tissue mounts were prepared after immunohistochemistry. For adult brains, a twin frost slide (Agar Scientific) was first placed on a Kaiser heating plate and two 24mm x 24mm coverglasses (Agar Scientific, thickness 1) were stuck on flat at the slide edges. Coverglasses were stuck on using Glycerol Gelatin (Sigma) that had been heated for 10 seconds at medium strength in a microwave oven. The slide was then left to cool on the bench for 5 minutes. Tissue preparations were transferred on to the centre of the slide between coverglasses using a Gilson pipette and excess PBT was removed using tissue paper. A small volume of Vectashield mounting medium (Vector laboratories, inc) was added covering the brains. A 60mm x 20mm coverglass (Agar Scientific, thickness 0) was then placed over the tissue and stuck to the two coverglasses using Glycerol Gelatin. The slide was then sealed using Glycerol Gelatin. Between 2-4 brains were included on one slide. Slides were prepared with a single genotype at a time to avoid confusion.

For embryos, larval and pupal brain preparations mounts used one 24mm x 24mm coverglass over vectashield that was sealed with Glycerol Gelatin. Between 2-4 brains were included on one slide. In contrast, approximately 50 embryos were included on one slide. Only brains of the same genotype and timepoint shared a slide to avoid confusion. Slides were stored in the dark at room temperature until required for

microscope analysis.

2.4 Microscopy and Imaging

2.4.1 Dissection and Flourescence microscopy

Drosophila were scored, phenotyped and dissected using Nikon dissection microscopes. Flies were analysed for GFP expression using a Leica MZFLIII flourescence microscope.

2.4.2 Confocal microscopy and image capture

Images were scanned using a Zeiss LSM 5 Pascal confocal microscope using excitation (495 nm) and detection (519 nm) filters for flourescein and excitation (560 nm) and detection (572 nm) filters for Cy3-based secondary antibodies. Images were captured using Zeiss Plan-neofluar lenses (x20, x40, x63) as Z stacks unless otherwise stated. Images focused on the whole brain or specific section (Central Complex, Central Brain, Optic lobe). Double stained preparations were scanned sequentially to avoid crosstalk between channels. Single channel scans are presented in monochrome, double channel scans were presented in green (488) and magenta (546), with co-expression visualised as white.

The Pascal Software was used for image capture. Images were analysed and annotated using three different programs; open source software ImageJ (1.37 v and 1.4g, Wayne Rasband, NIH), Osirix version 2.0 (Osirix foundation, Geneva) and licensed Amira version 3.1 (Visage Imaging). A rotatable stage was installed for the confocal

microscope in the later stage of this project therefore some final images were captured when able to use this feature. Projections were generated using the Pascal and ImageJ programs.

Stock	Gene/ description	Synonym(s)	Source	Reference
cadN^{M12} pr^{1} c^{1} px^{1} sp^{1}/CyO	dn-cadherin	-	Bloomington 229	
Canton S	Wildtype		Scott Waddell, UMASS	
cbd^{KS171}	central body defect	*cbd^{2}*	M.Heisenberg, Universitat Wurzburg	Strauss & Heisenberg, 1993
cbd^{KS96}	central body defect	*cbd^{1}*	M.Heisenberg, Universitat Wurzburg	Strauss & Heisenberg, 1993
ccb^{KS127}	central complex broad	*ccb^{1}*	M.Heisenberg, Universitat Wurzburg	Strauss & Heisenberg, 1993
ceb^{849}	neuroglian	*ceb^{1}, nrg^{849}, nrg^{S213L}*	Troy Zars, University of Missouri	Strauss & Heisenberg, 1993 Dorsch, 1985
ceb^{892}/FM7	neuroglian	*ceb^{2}, nrg^{892}*	Patrick Callaerts, University of Leuven	Strauss & Heisenberg, 1993
cnbw ed^{ts}	echinoid (temperature sensitive)	-	H.Vaessin, Columbus OH	Ahmed et al. 2003
ed$^{4.12}$/ ed$^{4.12}$	echinoid	-	A. Jarman, University of Edinburgh	Rawlins et al. 2003
ed$^{6.1}$/CyO	echinoid	-	A. Jarman, University of Edinburgh	Rawlins et al. 2003
ed^{K01102}/ CyO	echinoid	-	A. Jarman, University of Edinburgh	Rawlins et al. 2003
Df(2L)ed-dp/CyO	Deficiency arm 2L, echinoid - dumpy	-	A. Jarman, University of Edinburgh	Rawlins et al. 2003
FM7	Balancer	-	Armstrong lab	-
FM7/CyO	Balancer	-	Bloomington 4558	-
Gal80^{ts} /Gal80^{ts} ; TM2/TM6	Temp sensitive Gal 80	-	Bloomington 7019	-
GMR-Gal4 #12	glass multimer receptor-Gal4	-	A. Jarman, University of Edinburgh	-
GMR-Gal4 #15	glass multimer receptor-Gal4	-	A. Jarman, University of Edinburgh	-
icebox 7N/FM7	neuroglian	-	Armstrong lab	Carhan et al, 2005

kr/Cyo ; D^1/TM6B	Balancer	-	A. Jarman, University of Edinburgh	-
nrg^3	Neuroglian (temp. sensitive)	n^{ts}	S.Godenschwege	Godenschwege et al 2006
Oregon R	Wildtype		Armstrong lab	
PM181-Gal4	R7 Gal4 driver	-	Chi Hon Lee, NIH, Bethesda	Lee et al. 2001
P{rh1-GAL4}1; ry506	R1-R6 Gal4 driver	-	Bloomington 8688	-
w[*];P{w[+ mC]=Pan-R7-GAL4}2/CyO ; TM2/MKRS	R7 Gal4 driver	-	Bloomington 8603	-
UAS-mCD8::GFP on II	-	-	Armstrong lab	-
UAS-mCD8::GFP on III	-	-	Bloomington 5130	-
UAS-nSyb::GFP on II	-	-	Bloomington 6921	-
UAS-Gal4	-	-	A.Jarman, University of Edinburgh	Hassan ?
UAS-ed^{ICD}-HA/ TM6B	echinoid dominant negative	-	A.Jarman, University of Edinburgh	Rawlins et al. 2003a
UAS-ato-1	atonal	-	A.Jarman, University of Edinburgh	Rawlins et al. 2003b
w^{118}; ln(2LR)Gla,w g^{elp} Bc / CyO	-	-	Bloomington 5439	-
w ; shg[R6]/ SM6B	shotgun (encodes De-cadherin)	-		
w; 181-Gal4/ CyO	R7 cell marker	-	Chi Hon Lee, NIH, Bethesda	Lee et al. 2001
w; ; 181-Gal4 / Tm6b	R7 cell marker	-	Chi Hon Lee, NIH, Bethesda	Lee et al. 2001
w;;182-Gal4UAS-mcd8::GFP/	R7 cell marker	-	Chi Hon Lee, NIH, Bethesda	Lee et al. 2001

Tm6b				
w;181-Gal4UAS mCD8::GFP/ CyO6; Tm2/Tm6G	R7 cell marker	-	Chi Hon Lee, NIH, Bethesda	Lee et al. 2001
y1w;P{Rh5-GAL4}2;TM2 /TM6B, Tb1*	R7 & R8 cell marker	-	Bloomington 7458	
106-68-Gal4	R8 Gal4 driver	-	A.Jarman	Rawlins et al. 2003

Table 2.1 : Fly Stocks

Antigen	ID tag	Host	Source	Dilution	Description
Bruchpilot	nc82	Mouse	UIOWA	1:10	Neuropil marker
CNS	BP102	Mouse	UIOWA	1:10	CNS axon marker
Chaoptin	24B10	Mouse	UIOWA	1:50	R cell marker
DE-cadherin	DCAD2	Rat	UIOWA	1:20	
$Delta^{ECD}$		Mouse	Jarman lab	1:50	Extracellular domain
DN-cadherin	DN-Ex #8	Rat	UIOWA	1:20	
Echinoid	ed	Rabbit	Jarman lab	1:2000	
Elav	-	Mouse	Jarman lab	1:100	Neuronal marker
FasII	1D4	Mouse	UIOWA	1:20	MB, EB
GFP	-	Rabbit	Molecular Probes, A11122	1:5000	
HA		Mouse	Jarman lab	1:1000	Hemagglutinin
Neuroglian	BP104	Mouse	UIOWA	1:50	
Neurotactin	BP106	Mouse	UIOWA	1:50	
$Notch^{ICD}$	N^{ICD}	Mouse	Jarman lab	1:50	Intracellular domain
$Notch^{ECD}$	N^{ECD}	Mouse	Jarman lab	1:40	Extracellular domain
Prospero	Pro	Mouse	Jarman lab	1:100	R7 marker
Senseless	Sens	Guinea pig	H.Bellen	1:1000	R8 marker

Table 2.2: Primary Antibodies. UIOWA; University of Iowa hybridoma bank

Target	Host	Flurophore	Source	Dilution
anti-Rabbit	Goat	Alexa Fluor 488	Molecular probes	1:400
anti-Rabbit	Goat	Alexa Fluor 546	Molecular probes	1:400
anti-Mouse	Goat	Alexa Fluor 546	Molecular probes	1:400
anti-Mouse	Donkey	Alexa Fluor 488	Molecular probes	1:400
anti-Rat	Goat	Alexa Fluor 488	Molecular probes	1:400
anti-Guinea pig	Goat	Alexa Fluor 488	Molecular probes	1:400

Table 2.3: Secondary Antibodies

3

Analysis of Central Complex development using Selected Markers

3.1 Introduction

3.1.1 Selection of markers

Due to the limited information available on immunohistochemical markers for the developing CC, appropriate structural markers had to be found that labelled the developing tracts of this neuropil. Therefore a subset of candidate genes (shown in Table 3.1) were selected that were of interest both as markers and for potential developmental functions. Genes were selected based on the criterion that they encoded membrane tethered molecules with extracellular domains to facilitate whole cell visualisation. In addition, previously reported genetic and proteomic relationships inferred between candidates were taken into account.

Alleles of *neuroglian* have been shown to display CC structural phenotypes (Strauss & Heisenberg, 1993; Carhan et al., 2005) thereby indicating a potential function

in the developing CC. The Cadherins had previously been shown to be expressed on several axon tracts in the larval central brain development (Dumstrei et al., 2003a) in addition to pathfinding and targeting roles in the photoreceptors (Lee et al, 2001; Iwai et al., 2002; Prakash et al., 2005; Ting et al., 2005). *echinoid* encodes a homophilic Cell adhesion molecule similar to that of the L1-type molecules (Rawlins et al., 2003a). Echinoid was selected for analysis as it has been shown to demonstrate relationships with both De-cadherin and Neuroglian (Islam et al., 2003; Wei et al., 2005) and for its homophilic binding properties, leading to the hypothesis that it is also involved in CC structural development.

Gene	Family	Primary Reference	Alleles/ constructs used	Homologs
echinoid	IgSF	Rawlins et al (2003)	$ed^{4.1}$ (Rawlins et al., 2003a) ed^{K01102} (Rawlins et al., 2003a) *UAS-*ed^{ICD}*-HA* (Rawlins et al., 2003a) ed^{ts} (Ahmed et al 2003)	-
neuroglian	IgSF	Bieber et al (1989)	*ibx* (Carhan et al 2005) ceb^{849} (Strauss & Heisenberg 1993) ceb^{892} (Strauss & Heisenberg 1993)	Mouse L1-CAM
de-cadherin	Cadherin	Dumstrei et al (2003)	-	Vertebrate Classic cadherins
dn-cadherin	Cadherin	Iwai et al (2002)	-	Vertebrate Classic cadherins

Table 3.1: Genes used in this study for expression analysis including protein famillies and known homologs in vertebrates. The primary reference refers to the most relevant publication to this study. Alleles used for each gene are listed including the study from which they originated.

Currently, most analysis of specific genes and their roles in neuronal development in the CNS has been performed using either the Optic lobe or the Mushroom Bodies as models. This is due to the well characterised topography and development of these neuropil. The CC has an intricate neuronal topography and provides a fundamental, symmetrical structure in the central brain that is unique in being unpaired and spanning the midline. Existing publications that have studied the behavioural applications of the CC have analysed several mutants of this structure (Bouhouche et al., 1993; Strauss and Heisenberg, 1993). The CC offers a unique model with which to study features of midline development in the fly brain.

In addition to identifying genes involved in CC development and function, we can isolate genes that are expressed in specific populations of neurons. This may indicate different genetic controls between neuronal types. The advantages of using immunohistochemistry over more traditional neuron staining techniques is that it is easily reproducible and provides additional data on potential molecules involved in developmental processes. By aiming to address both the genetic and structural development of the CC, this study could facilitate future projects aiming to fully understand the developmental, genetic and structural features of the CC. The data for this section was generated prior to publications detailing a digital atlas of the late larval brain (Pereanu and Hartenstein, 2006) and the role of the Robo proteins in the developing CC (Nichols and Preat, 2005) that would have provided information on alternative structural markers.

3.1.2 Chapter overview

This chapter reveals novel gene expression patterns in addition to a structural and temporal development timeline for the CC. The findings from this chapter laid the framework for the remainder of this thesis.

3.2 Aims

1. To identify structural markers for neurons of the developing Central Complex
2. To investigate the developing structure of the Central Complex

3.3 Gene expression in the developing and adult Central Complex

Unlike the Mushroom bodies that initially develop during embryogenesis (Ito & Hotta, 1992), the CC of *Drosophila* is exclusively an imaginal structure therefore the majority of investigation into CC development described here is limited to metamorphosis. All genes were first analysed for expression in the adult CC and central brain of the 3rd instar larva. Next, the developing CC was examined by performing a complete developmental analysis throughout metamorphosis to eclosion. Table 3.2 illustrates the temporal and spatial expression patterns for each gene.

3.3.1 Adult expression analysis

Initial experiments were performed to determine the expression patterns of four selected genes in the wildtype adult Central Nervous System. Several other genes were also included in the initial screen; *notch* and *delta* (known signalling molecules in neurogenesis; Rawlins et al., 2003a), *bruchpilot* (synaptic neuropil marker, Vosshall et al., 2000), *fas II* (adult MB and EB marker), *elav* (pan neuronal marker), BP102 (CNS axonal marker) and BP106 (neurotactin) but were rejected either because they were not expressed in the CC or because the staining pattern was too general making it difficult to isolate CC neurons (data not shown). Only *dn-cadherin* and *neuroglian* expression could be detected in the adult CC (data not shown). *dn-cadherin* expression appears to be widespread throughout the neuropil but is not present on any fibre tracts in the CC.

In contrast to *dn-cadherin, neuroglian* expression seemed to be mainly axonal, and was not visible on perikarya. The distinct appearance of lobes of the Mushroom Bodies are discernible and the *neuroglian* expression pattern clearly highlights several fibres of the CC. Due to the number of tracts stained it was difficult to isolate specific CC cell types, though the pattern appears reminiscent of the VFS and HFS. It is also

possible that *pb-fb-no* neurons are included. Neuroglian is not detected on any arborisations of this fibre system which occur in the glomeruli of the Protocerebral bridge or the layers of FB. Expression of *neuroglian* is not exclusive to any individual fibre system of the Central Complex but it does seem to be mainly present on axons.

The other two selected genes, *de-cadherin* and *echinoid*, were not detected in the adult brain of 4-9 day old adults. In order to assess if these were not present at any stage during adulthood, an adult expression analysis was performed by dissecting every six hours after eclosion. This revealed *echinoid* expression in the NO and Optic lobes detectable up to 24 hours after eclosion, indicating *echinoid* may be expressed in these structures during metamorphosis. This is the first time *echinoid* expression has been reported in the CNS. *de-cadherin* expression was not detected in the adult brain.

3.3.2 Larval expression analysis

Further to the adult expression analysis the brain of the 3rd instar larva was examined. This revealed an overlap of expression between genes in several cells. De-cadherin, Echinoid and Neuroglian were all detected on the Secondary lineage Axon Tracts (SATs), also known as Cell Body fibre Tracts (CBTs) (CBT, Strausfeld 1976; SAT, Dumstrei et al. 2003b) highlighting the clear radial trajectory of these tracts from clusters of dividing neuroblasts as shown in Figure 3.1 (A-D). Both *echinoid* and *neuroglian* could be found on commissures crossing the midline [Figure 3.1(B,C)]. Previous reports have stated that the Protocerebral bridge can be detected in the late 3rd instar larval stage (Schneider et al. 1993) and this was confirmed here by *neuroglian* and *dn-cadherin* expression in PB glomeruli [Figure 3.1(C,D)]. The PB is recognisable by its characteristic handlebar shape but it is not fused at the midline at L3, instead it exists as two separate structures, one in each hemisphere, appearing as a paired structure. It was not possilbe to determine the specific neuronal structure of the PB at this stage with

these markers. This is the only instance of *neuroglian* expression on dendritic fibres in the CC. The commissure that is visible with α-Echinoid staining in the late 3rd instar [Figure 3.1(B)] could potentially be early CC neurons, though the exact projection patterns were not discernable at this stage. Reports previous to this have referred to a CC in the larval brain as interhemispheric commissures (Hanesch et al, 1989; Truman et al., 1993) and several of these can be seen crossing the midline with in α-*neuroglian* staining.

All genes were expressed in either the 3rd instar larval central brain or the adult CC. These expression patterns suggested that they could be involved in the formation of the CC during metamorphosis. Indeed *de-cadherin* has previously been reported to play a role in SATs formation during the third instar (Dumstrei et al., 2003b). Expression was also detected in other larval brain regions. Both *neuroglian* and *dn-cadherin* were expressed in the larval Mushroom Bodies [Figure 3.2(A)] and all four were detected in the optic lobes. All four genes were subsequently included in the resulting developmental series throughout metamorphosis. Interestingly *bruchpilot* (nc82) is strongly expressed in the 3rd instar larva, then hardly at all during early metamorphosis. It is not detectable again until late metamorphosis. This is likely due to the entensive neuronal remodelling, pruning and cell death that occurs in the first 12 hours of metamorphosis, greatly reducing the synaptic neuropil.

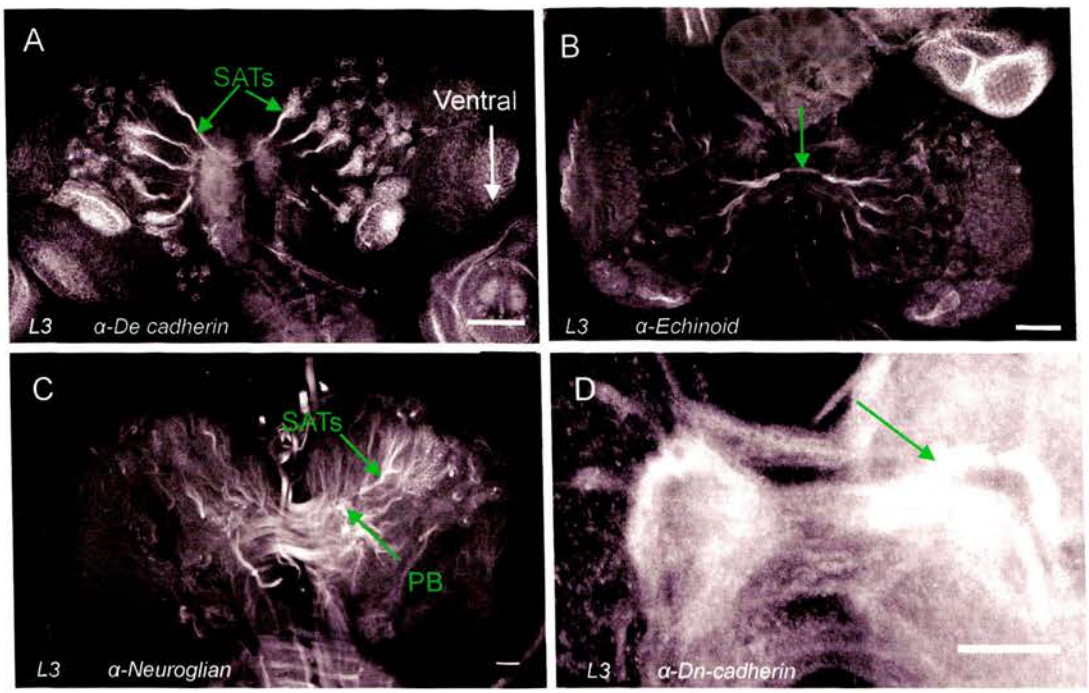

Figure 3.1: Late Larval expression patterns revealing possible CC tracts and the Protocerebral bridge (PB). **A,** Neuroblasts, secondary neurons and Secondary lineage Axon tracts (SATs) projecting with radial trajectories as visualised with ∝-De-cadherin. **B**, Secondary lineage Axon tracts and interhemispheric commissures (magenta arrow) visualised with ∝-Echinoid. Neuroblasts are faintly visible. **C**, SATs and several interhemispheric commissures are visible with ∝–Neuroglian staining. It is also possible to see the early Protocerebral bridge (PB). **D**, ∝-Dn-cadherin reveals the early PB (arrow). Scale bars 25μm. L3; 3rd instar.

3.3.3 Metamorphosis expression analysis

Previous reports have stated CC development is completed in the first half of metamorphosis (Hanesch et al., 1989; Renn et al. 1999). This expression analysis was designed to ensure a detailed analysis of the first 72 hours of metamorphosis. This generated three data sets of images for analysis. *de-cadherin* could not be detected after 4 APF therefore analysis of this marker was discontinued. *echinoid, neuroglian* and *dn-cadherin* were expressed extensively throughout the CC during metamorphosis. Table 3.2 illustrates the temporal and spatial expression patterns for the main fibre systems and neuron types in the Central Complex for each gene. In the case of *dn-cadherin* expression only the substructures are included due to the lack of expression on fibre tracts. *echinoid* was revealed as a novel marker for the developing HFS. These data revealed novel expression patterns for genes which have not been characterised in postembryonic brain development. Further to this it provided a clear timeline for CC development using three different markers.

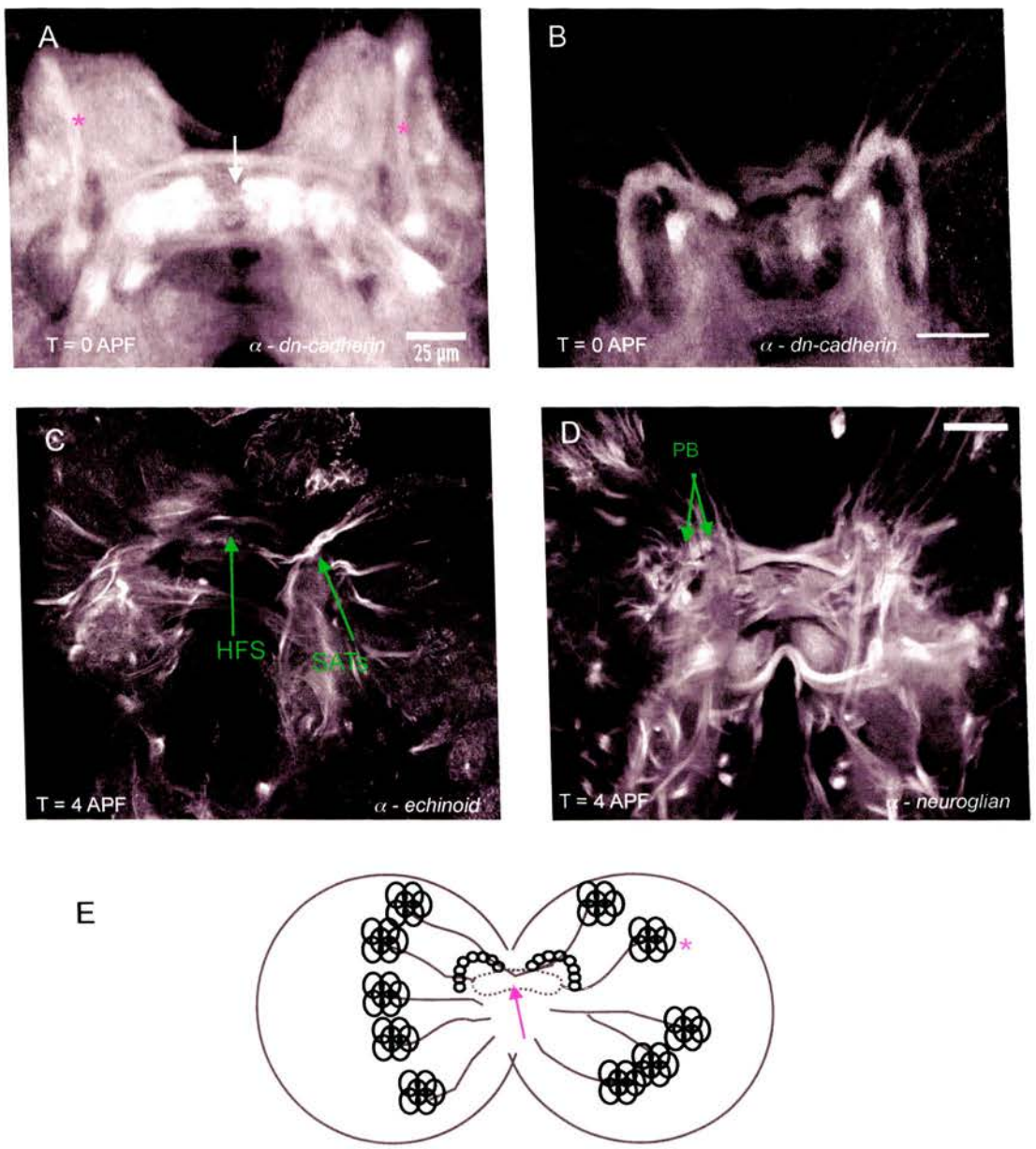

Figure 3.2: The existing Central Complex at 0-4 APF. **A**; brain from a white prepupa stained with *α-dn-cadherin* showing the early FB (arrow) and MBs (asterix) at 0 APF. **B**, same preparation as A showing the PB at 0 APF. **C;** pupal brain at 4 APF showing *echinoid* expression revealing SATs and the projecting fibre bundles of the HFS. **D**; Pupal brain at 4 APF showing *neuroglian* expression revealing several interhemispheric commissures and glomeruli of the early PB. **E**; Schematic of the CC at 0 the white prepupa. SATs can be seen projecting from clusters of cell bodies (asterix) arranged in a radial pattern to the CC where the PB and FB (arrow) are already evident. SATs, Secondary lineage axon tracts; HFS, Horizontal Fibre System; PB, Protocerebral bridge. Scale bars 25µm.

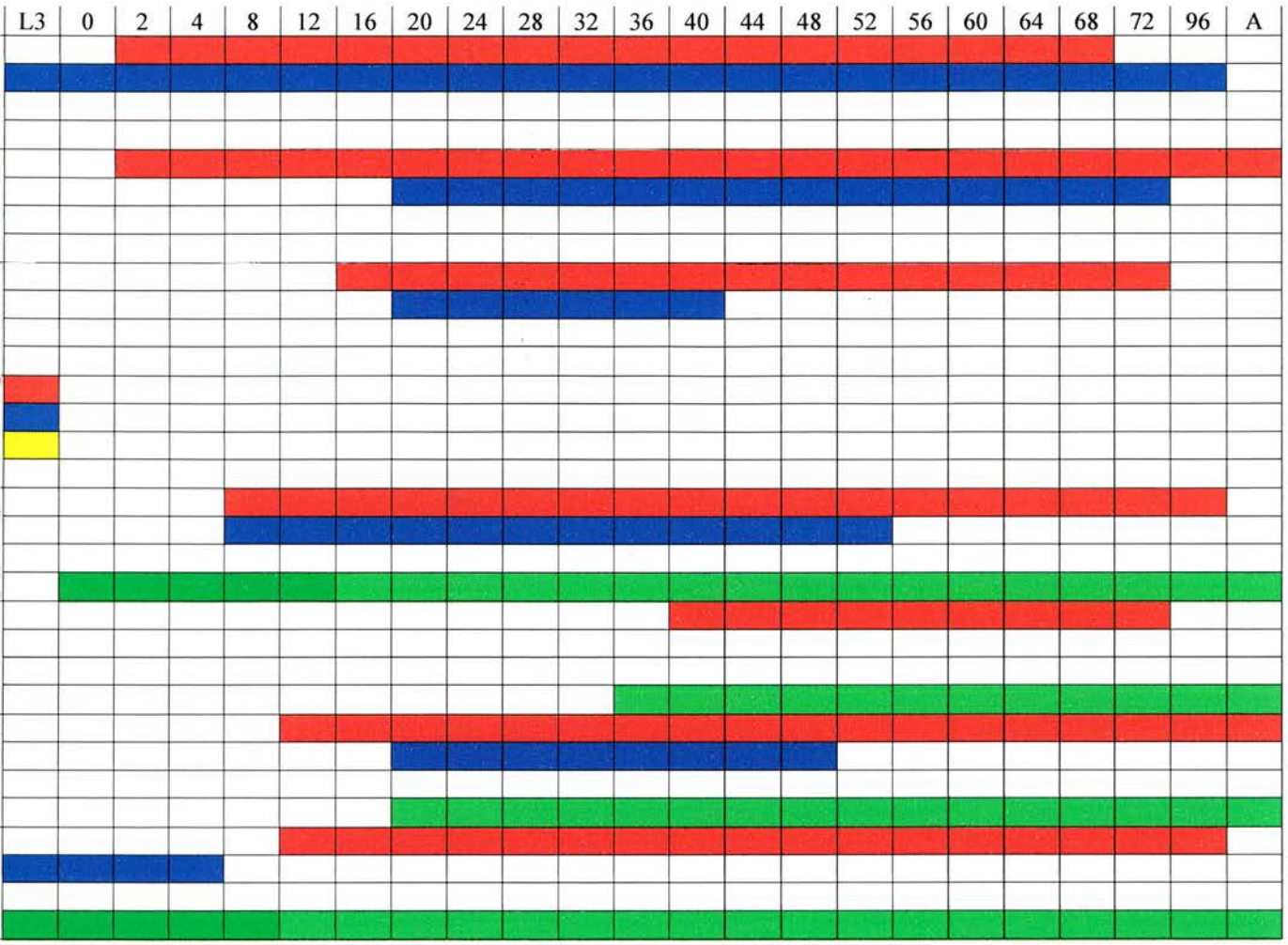

Table 3.2 : Anatomical & Spatial Expression Patterns. Coloured boxes denote detected expression of a specific CAM marker (Echinoid – Red; Neuroglian – blue; De-cadherin – yellow; Dn-cadherin – green) and numbers indicate the number of hours after puparium formation (APF). Only Echinoid and Neuroglian were clearly visible on axon tracts. De-cadherin was faintly detectable on SATs during the first hours of metamorphosis. L3 (3rd instar larva), A (Adult), VFS (Vertical Fibre System), HFS (Horizontal Fibre System), F*m* (Large field Fan Shaped body neurons - medial), F*l* (Large Field Fan Shaped Body neurons - lateral), SAT (Secondary lineage Axon Tracts), fb-no (Fan shaped Body to Noduli neurons), FB (Fan Shaped body), EB (Ellipsoid body), NO (Noduli) and PB (Protocerebral bridge).

3.4 Developmental Timeline for the Central Complex

From these developmental series' it was possible to infer a timeline of development for the CC. Staining in and around the CC becomes more dense as metamorphosis continues, subsequently it becomes more difficult to see specific neurons and their connections. From these observations we can conclude that the gross central complex structure appears to be complete by 48 APF (when metamorphosis is approximately 50% complete) as shown in Figure 3.10 (A,B). At this point the characteristic architecture of the CC closely resembles that observed in the adult brain. Figure 3.11 gives a detailed account of the development of each substructure and neuronal types revealed by the expression data.

3.4.1 Early CC development (0-20 APF)

The CC starts to differentiate in the larval stages, with an immature FB and PB structure already evident by 0 APF [Figure 3.2(A,B,D)]. At 2 APF it was still difficult to identify CC fibres, though tracing backwards from later stages revealed that the first fibres of the HFS were visible at this stage visible with α-Echinoid staining. These appeared to be only the most medial tracts (*z* tracts) running ventrally then making a medial turn and crossing the midline to create the early Posterior chiasma as shown in Figure 3.2 (C).

3.4.1.1 The Horizontal fibre system (HFS)

Each of the *y* and *z* fibre bundles in each hemisphere can be traced back via an individual SAT to one cluster of perikarya in the dorsal cortex. All cell clusters are dorsal but that of the *z* fibres is in the medio-anterior cortex and those of the *y* fibres are in the posterior cortex. The cell clusters are visible at 4 APF. This suggests a common lineage for each set (*w, x, y* or *z*) of fibre bundles. The fibre bundles of the more lateral fibres (*w* and *x*) were not traceable using this staining. The SATs do not branch until

reaching the area that will be occupied by the FB. By 8 APF the individual bundles (*w, x, y* and *z*) of the HFS are visible making a ventral turn then targeting the developing dorsal section of the FB [Figure 3.3(A-C)]. Between 8 - 16 APF the *z* and *y* fibre bundles are clearly visible but the more lateral HFS bundles (*w* and *x*) are not. By 12 APF the *z* and *y* fibre bundles are clearly apparent targeting to their specific segments as the FB has extended both laterally and dorso-ventrally [Figure 3.4(A)]. Zones of arborisation are visible in the segments thought to originate from the HFS. By 16 APF the projections of the *z* and *y* fibre bundles have exited the ventral FB and targeted the VBO [Figure 3.4(B,C)]. It is not until 20 APF that the *w* and *x* fibre bundles are clearly visible reaching the VBO [Figure 3.5(A,B)]. It may be the case that these fibre bundles reach their targets later. Tracing the SATs of these fibres was problematic due to the density of staining. It may be that they originate from a lineage lateral to the one of *x* and *y* fibre bundles. By 20 APF the anterior chiasma is visible as shown in Figure 3.5(A,B). The fibre bundles of the HFS can be seen projecting to the VBO. Interestingly, the y and z fibre bundles can be seen projecting in a ventral direction beyond the VBO, a feature that has not been previously reported. It may be that these are projecting to the thoracic ganglion. There is no evidence of arborisation in the protocerebral bridge at the early stages, a characteristic of the HFS. Echinoid staining revealed this arborisation later, at 12 APF when arborisations were also visible in the segments. This indicates that arborisation may occur from the HFS axons in both the FB segments and PB at the same time. Figure 3.6 summarises HFS development schematically.

3.4.1.2 The Vertical fibre system (VFS)

Due to the density of α-Neuroglian staining at the midline it was difficult to isolate axons from specific cell types. It was possible to ascertain that the VFS, like the HFS, is also complete by 20 APF. By 28 APF, when the brain and sub-structures have enlarged both the completed HFS and the VFS can be seen clearly with α-Neuroglian [Figure 3.7(A,B)]. These two major sets of isomorphic neurons are complete early in metamorphosis, by 20 APF.

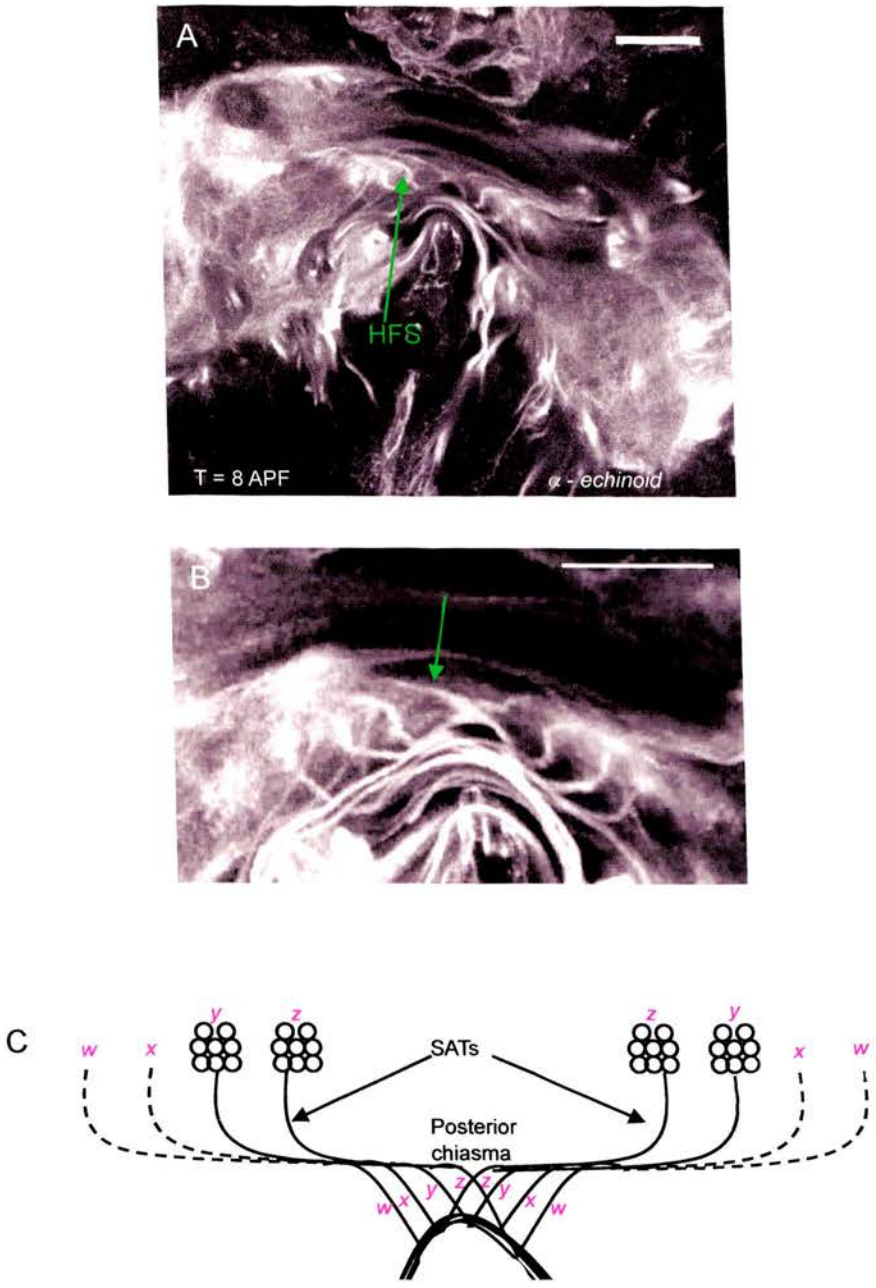

Figure 3.3: The Central Complex at 8 APF. Both images are from the same preparation. **A**,**B**; *echinoid* expression reveals the fibres of the HFS making a ventral turn into the early FB. **C**, Schematic representation of the HFS at 8 APF. Fibre bundles are visible as single fasciculated projections targeting the midline. Only the *z* fibre bundles can be seen clearly crossing contralaterally at this stage, though it is likely that the other fibre bundles are also crossing. The *y* and *z* fibre bundles can be traced to separate clusters of perikarya in the dorsal cortex (see text). The *x* and *w* fibre bundles were not traceable therefore the dashed lines represent theoretical positions for their origins. SATs, Secondary lineage Axon Tracts; HFS, Horizontal Fibre System. Scale bar 25μm.

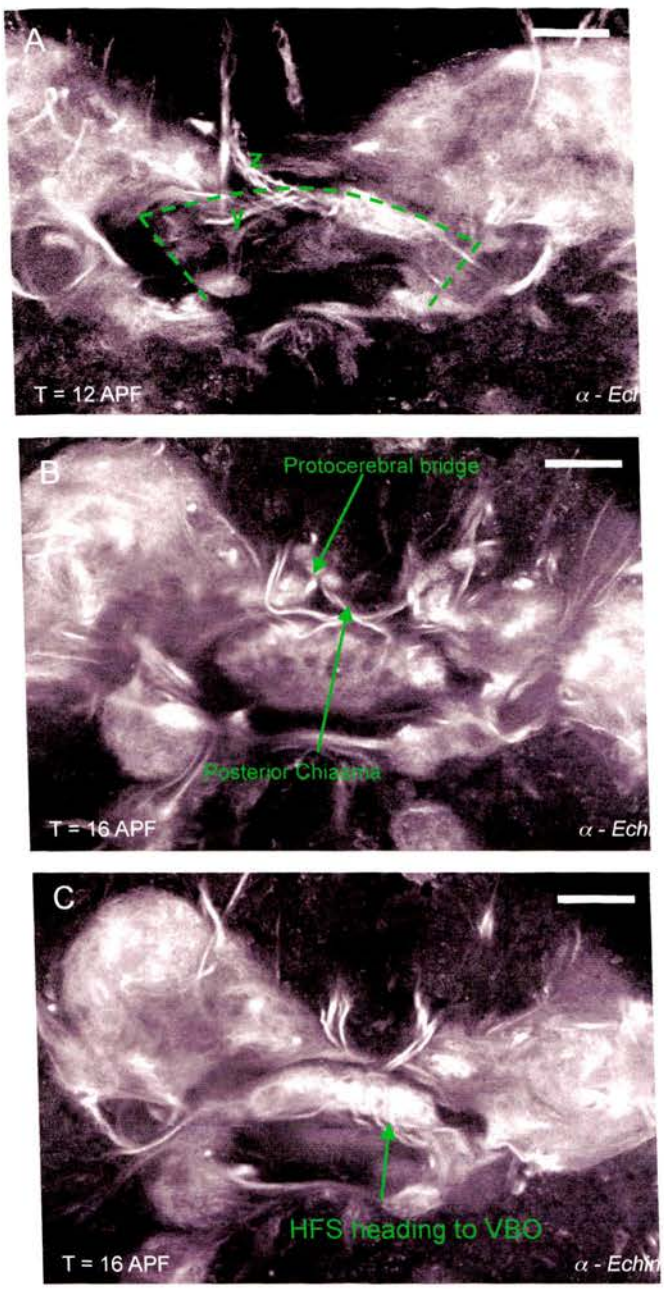

Figure 3.4: The Central Complex at 12 - 16 APF. A, at 12 APF the *z* and *y* fibre bundles can be seen extending further into the FB (outlined by dotted line) and targeting predetermined segments. **B,** fibre bundles can be seen innervating the PB and crossing contralaterally. **C**; By 16 APF these fibre bundles can clearly be seen innervating FB segments then performing a lateral turn to target the VBOs. VBO, Ventral bodies; HFS, Horizontal fibre system. Scale bars 25μm.

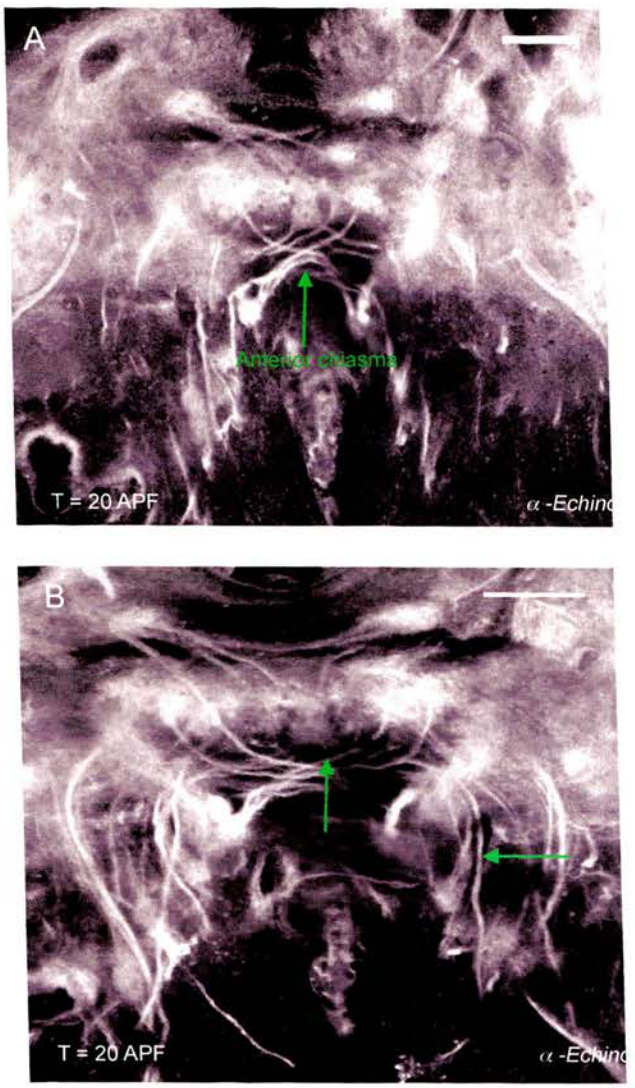

Figure 3.5: The Central Complex from 20 APF. A, By 20 APF the *w* and *x* fibre bundles of the HFS can be seen innervating individual segments than projecting to the VBOs. The anterior chiasma is clearly visible. **B**, Interestingly, the *z* and *y* fibres can be seen targeting beyond the VBO (green arrow) then turning to project in a ventral direction. Scale bars 25µm.

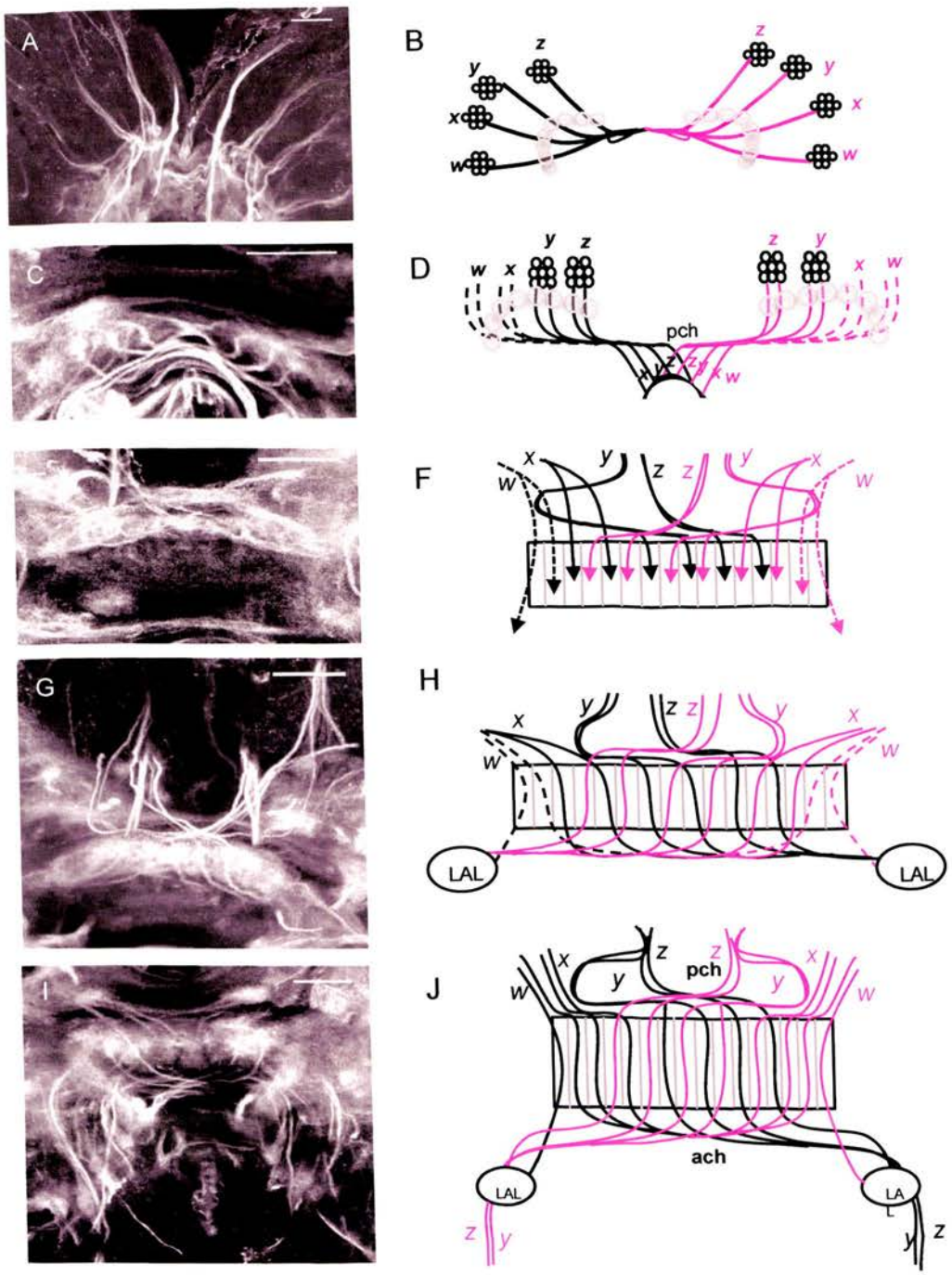

Figure 3.6: Schematics of the HFS during early Central Complex development. Neurons originating from the right brain hemisphere (pink) are superimposed on the neurons from the left hemisphere (black). **A**,**B**, at 2 APF the SATs containing the w,y,x,and z fibres can be seen targeting the central brain. **C,D**, by 8 APF these fibres have created the posterior chiasma. **E,F;** by 12 APF the HFS fibres have arborised in their target segments. **G,H;** by 16 APF the HFS fibres have targeted the VBOs. **I,J;** by 20 APF the HFS appears complete with the posterior and anterior chiasma clearly visible. The y and z tracts can be seen projecting to the ventral ganglia. ach, anterior chiasma; pch, posterior chiasma; VBO, Ventral bodies.

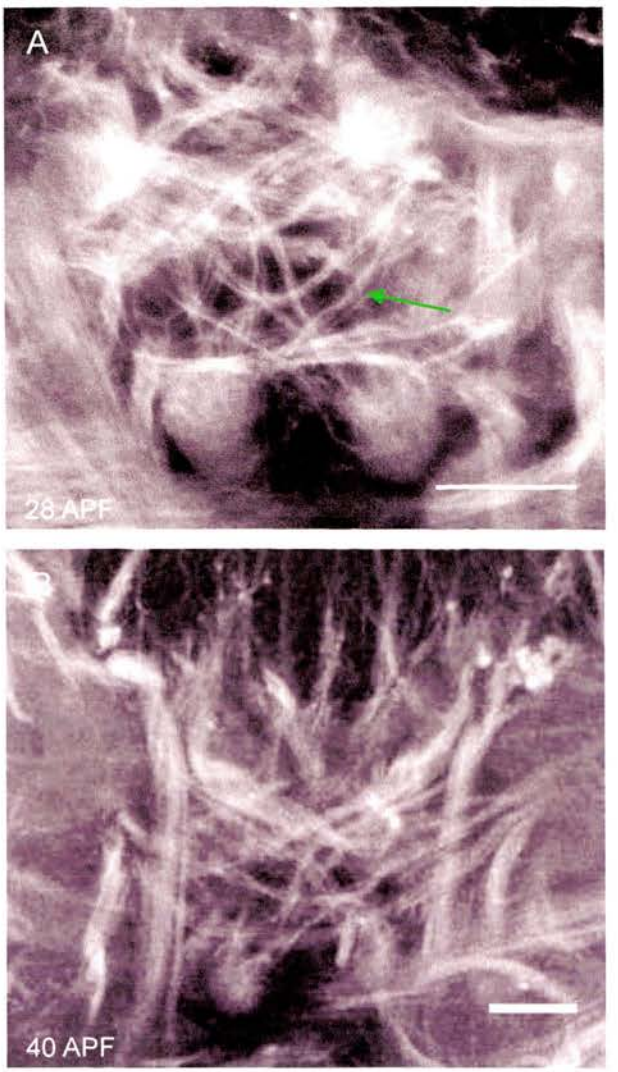

Figure 3.7 : The VFS shown by Neuroglian staining**. A**, the axons of the VFS can be seen clearly at 28 APF. **B**, Similar to A, at 40 APF. Scale bars 25µm.

3.4.1.3 Other neurons and whole sub-structures

The HFS are the most prominent fibre tracts visualised with α-Echinoid staining. Few other tracts can be detected in early CC development. Tracts that can be tentatively classified as the VFS neurons can be faintly detected at 16 APF, though their targeting phase is not detectable. The Superior arch commissure is faintly visible at 4 and 8 APF with α-Echinoid staining but is not discernable after these timepoints. Neuroglian staining reveals the Superior arch commissure from the 3rd instar larva in addition to an early FB structure. At 8 APF connections can be seen faintly from the Superior arch to the LTRs and on to the early VBO (data not shown).

CC sub-structures as a whole can be documented more easily than individual neurons as all four sub structures could be visualised with one of the candidate genes. As mentioned above, the PB is detectable from the late 3rd instar larva [Figure 3.1(C,D). The NO are first visible at 12 APF but are not located adjacent to the midline but at the lateral edges of the developing FB, they remain in this position throughout early CC development [Figure 3.11(E)]. The visibility of the NO at these stages is likely to be due to the VFS. The EB is not visible until 24 APF as previously reported (Renn et al., 1999). The development of CC sub-structures is shown schematically in Figure 3.11.

3.4.2 Mid CC development (20- 32 APF)

During mid CC development the fibres of the HFS are still detectable with α-Echinoid staining. The FB segments can be distinguished; at 24 APF two F*l* neurons were detected traversing layer five at the anterior edge of the FB, one from each hemisphere. Branches from the F*l* neurons could be seen faintly making a ventral turn in each segment. It is possible that these are the same F*l* neurons mentioned above, as

observed in early CC development. It was not possible to visualise these neurons after 24 APF due to the density of staining in the FB, though it is likely that they are branching and arborising in FB segments. In addition, several axons (thought to be F*l* neurons) are faintly visible traversing the now distinguishable FB layers throughout mid CC development. Clear horizontal neuronal strata are visible in the FB from 24 APF onwards [Figure 3.9 (B)], though it is difficult to isolate these later in development. At this stage the FB is visible as an curved barbell shape [Figure 3.11 (G)].

By 24 APF the PB has altered in appearance in terms of glomeruli orientation and the NO have moved further towards the midline [Figure 3.9(A,B)]. These movements are likely to be due to the overall structural change of the brain. By 28 APF the early unfused EB structure can be seen very faintly. By 32 APF the enlarged brain results in the PB and FB appearing further apart, more like that of the adult. The NO are still not adjacent to the midline and the PB is not fused at the midline.

3.4.3 Late CC development (32-48APF)

By 36-40 APF the PB and the NO appear in a more medial position [Figure 3.9(B)]. The NO do not reach their adult formation until 48 APF. Both the PB and the NO show this gradual migration to the midline between 12-48 APF. This may be due to the overall changing shape of the brain at this time. The smooth appearance of the PB (i.e. not as set of isolated glomeruli) is not obvious until 76 APF. The ring of the EB was visible at 36 APF using these markers. The R neurons are not clearly visible, however the doughnut shape of the EB is apparent and appears almost fully developed at this point, therefore it is likely that these candidate genes are expressed too late to observe development of this structure in this study. The FB is the largest and most complex of the sub-structures in the CC. It is also the last to develop fully. It has a smaller, more rounded appearance in the early stages which gradually differentiates into the adult form. The final FB displays the shape reminiscent of the adult form by 48-52 APF.

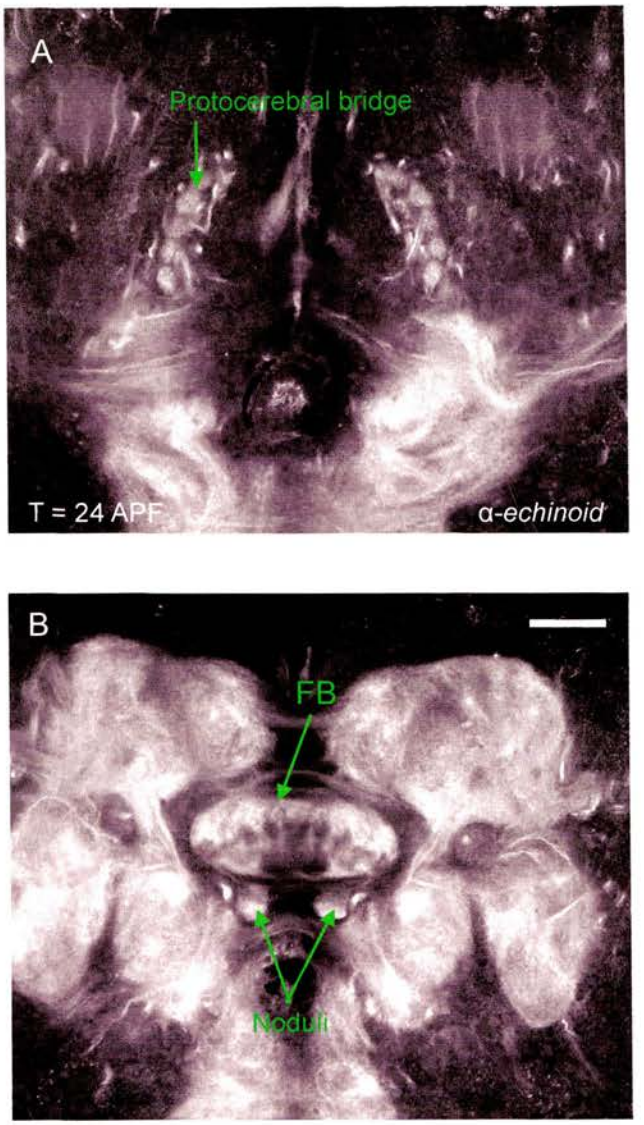

Figure 3.8: Mid-development of the Central Complex. Both images are from the same preparation. **A**, Glomeruli of the PB (only six glomeruli visible on each side as this image is a brain section – the other glomeruli are in a more anterior position) **B,** The Noduli are not yet adjacent to the midline and the FB has a more rounded shape. FB, Fan shaped body. Scale bar 25µm.

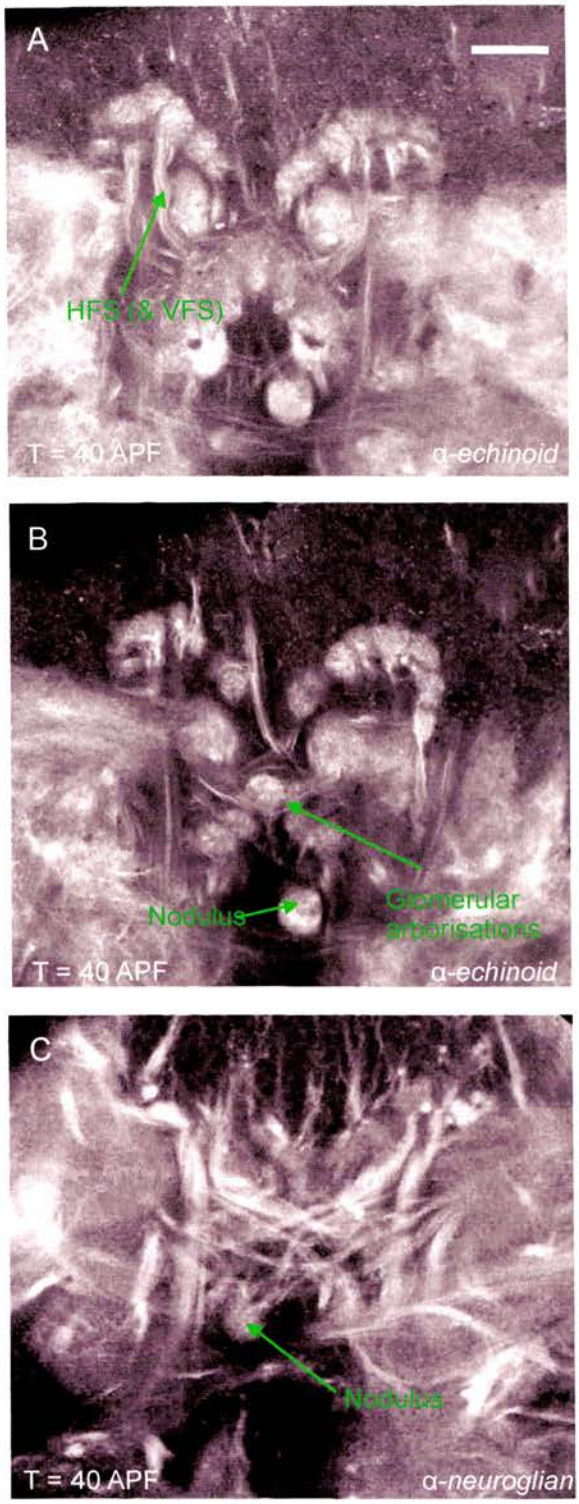

Figure 3.9: Selected late Central Complex developmental stages. **A,** The fibres of the VFS and HFS can be seen targeting the FB as thick bundles. **B**, Glomerular arborisations visible in segments of the FB at 40 APF, these are likely to be arborisations from the HFS. **C,** Axons of the VFS and HFS. VFS, Vertical fibre system; HFS, Horizontal fibre system. Scale bar 25μm.

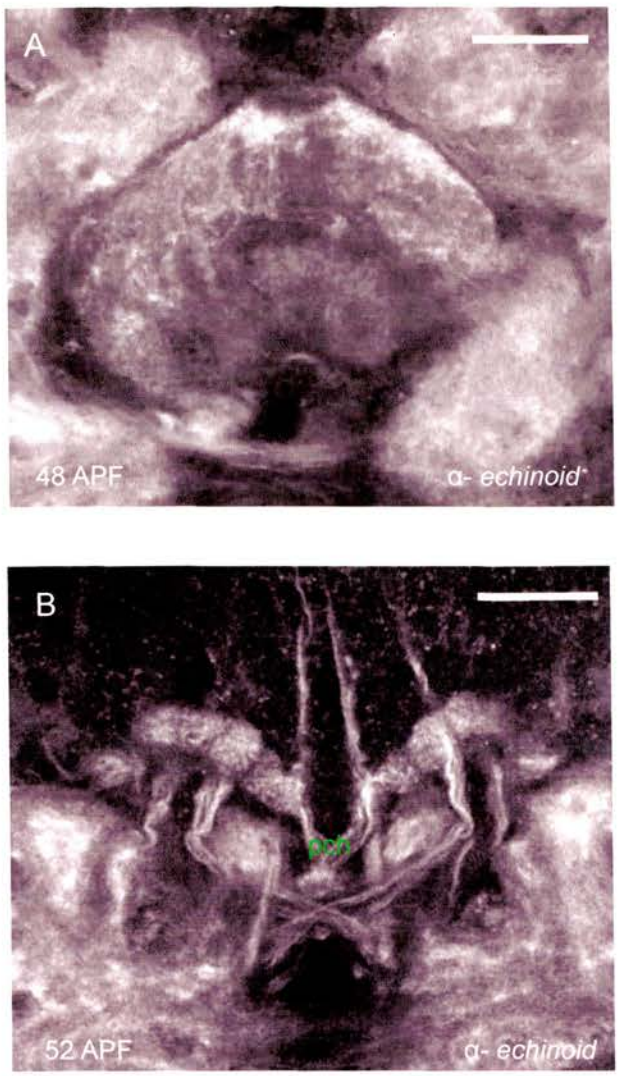

Figure 3.10: The fully formed Central Complex. **A**, The FB at 48 APF. **B**, 52 APF the posterior an danterior chiasma are visible and the fibres from the HFS can clearly be seen exiting the PB. pch, Posterior chiasma. FB, Fan shaped body; PB, Protocerebral bridge. Scale bars 25µm.

A

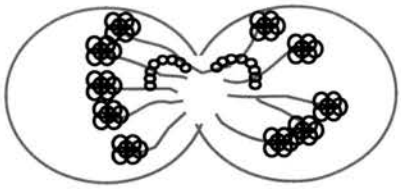

L3: Secondary axon tracts (SATs) projecting into the neuropil. The PB is visible but unfused at the midline.

B

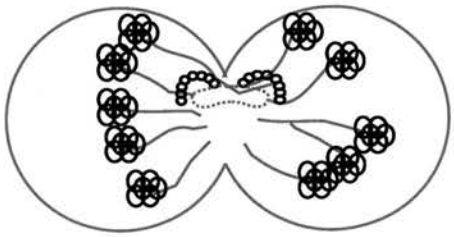

0 APF: Secondary axon tracts (SATs) projecting into the neuropil. The PB and early FB (dotted line) are visible.

C

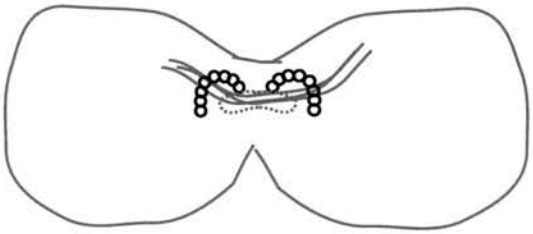

4 APF – The first fibres of the HFS (Horizontal fibre system) and the PB (Protocerebral bridge) are visible.

D

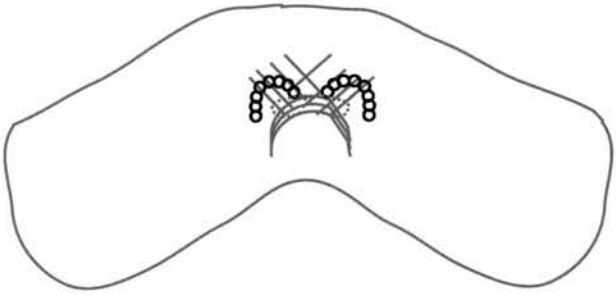

8 APF – The fibres of the HFS (Horizontal fibre system) have formed the posterior chiasma.

E

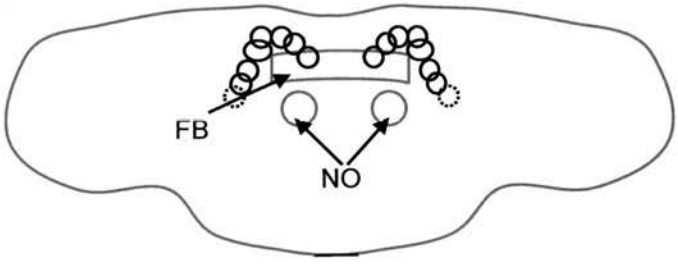

12 APF – The Fan shaped body (FB) is starting to adopt its characteristic shape. The Noduli (NO) are ventral to the FB. The PB has adopted a handlebar shape.

F

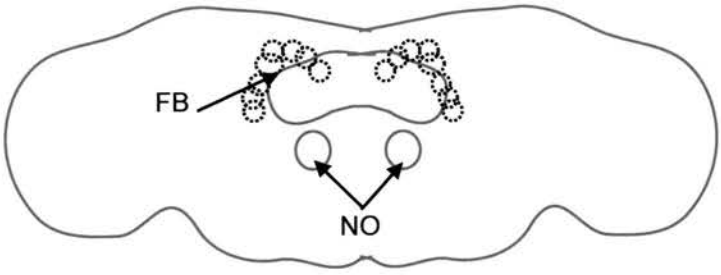

16 APF – The Fan shaped body (FB) elongates.

G

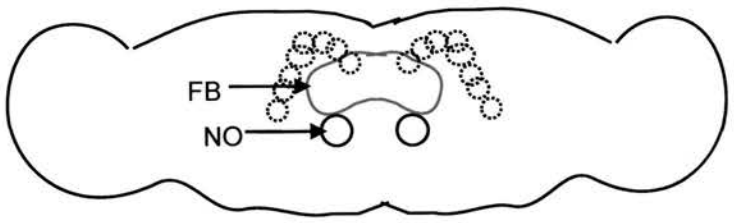

20 APF – Further elongation and change of shape of the FB.

H

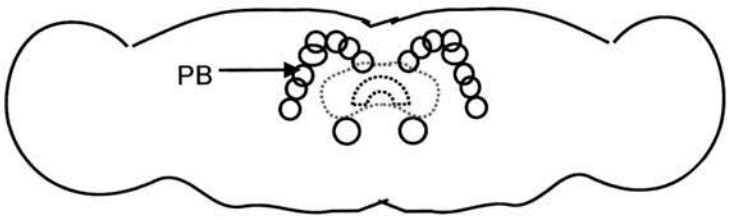

24 APF – Further elongation of the FB. The EB visible as an unfused semi circle.

I

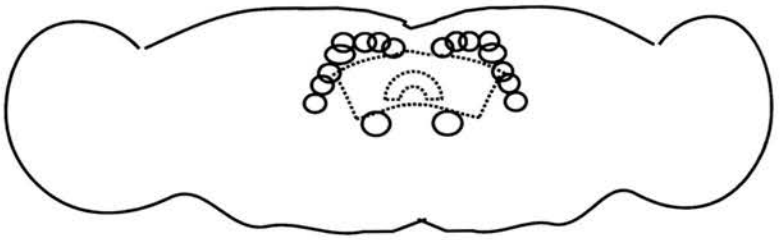

28 APF – Further elongation of the FB and the brain. The EB visible as an unfused semi circle.

J

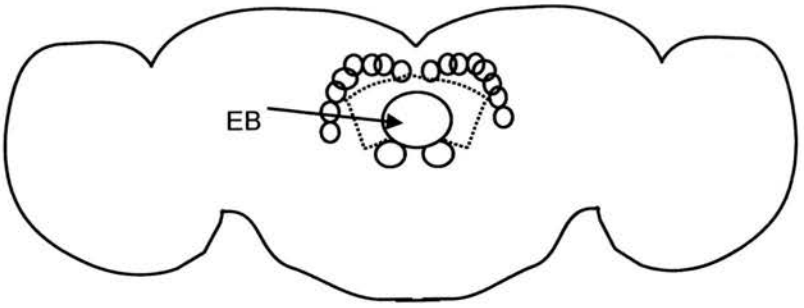

32-36 APF –The brain is starting to adopt its adult form. The EB is visible as its adult form.

K

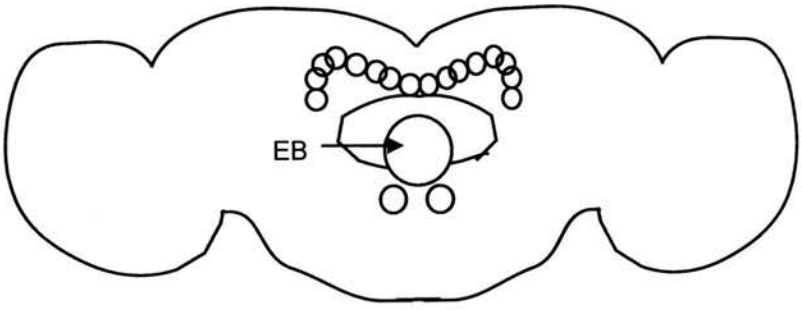

40 APF –The CC is reminiscent of the adult CC. The Noduli are still not adjacent to the midline.

L

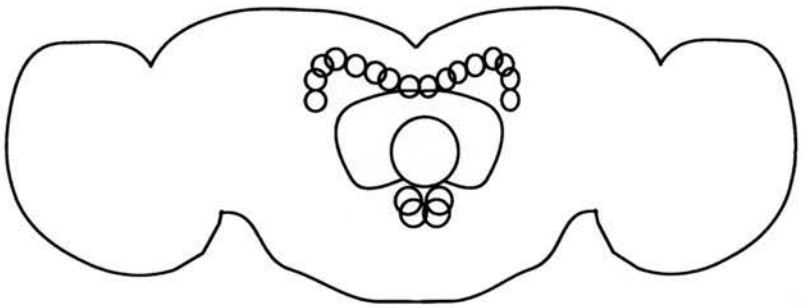

44 APF – The paired Noduli can be seen in their adult form.

M

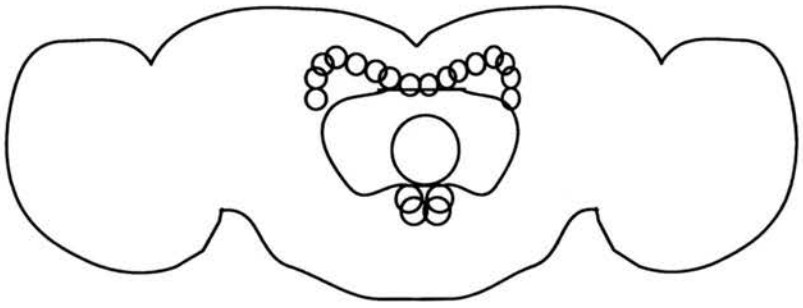

48-52 APF – Further elongation of the FB.

Figure 3.11: The development of the CC sub-structures. This details the development of substructures. The changing shape of the brain is also included. Schematics are not drawn to scale. **A-G**; early CC development. **H-J**; mid CC development; **K-M**, late CC development.

3.4.4 Summary

The expression patterns of the candidate genes revealed the development of a major isomorphic set of Small Field Neurons (the HFS), a type of Large Field Neurons (F*l* neurons) in addition to individual sub-structures. The fibre bundles of the HFS have all reached the VBO by 16-20 APF, and the *x* and *y* fibre bundles appear to continue ventrally. The targets of these fibre bundles beyond the VBO were not resolvable in this study. The *w* and *x* fibres may also continue past the VBO but this was not visualised in these data. The first of the substructures to be recognised is the PB, though this sub structure does not reflect its adult conformation until much later in development. Taking into account data for a previous study (Renn et al., 1999) then it is likely that the EB is the first to achieve its adult form at 24-32 APF, followed by the NO, the FB and finally the PB, producing a recognisable CC by 48-52 APF, though a final adult version is more likely to be at 76 APF considering the earlier glomerular appearance of the PB. It is important to note that this data is based on the expression of selected genes, therefore developmental interpretations are dependant on expression patterns of these genes.

3.6 Discussion

3.6.1 Tracing the lineage of CC neurons

Three previous studies mention, but do not elaborate on the presence of a primordium to the CC in the larval brain referring to it as either the interhemispheric commissure (Hanesch et al.,1989; Truman, 1990) or the trCM (transverse system) & DPC1 (dorsal posterior commissural system) (Pereanu & Hartenstein, 2006). From the data generated here, α-Neuroglian staining reveals several interhemispheric commissures present in the 3rd instar larva [Figure 3.1(C)] but it is difficult to isolate specific tracts. This study can confirm the presence of the protocerebral bridge in the 3rd instar larva as previously reported (Schneider et al.,1993) and an immature FB by the white prepupal stage. SATs are clearly visible in the central brain of the 3rd instar larva forming axon bundle trajectories in a radial pattern projecting towards the midline. Although these were not as clear during metamorphosis it was possible to trace the *x* and *y* fibre bundles from the HFS back through their SAT origins to the initial source of fibre tracts. From this information it is possible to assign previously determined lineages to these fibres (Pereanu & Hartenstein, 2006) forming a direct link between adult fibres and cell lineage. Projections of the *z* and *y* fibre bundles indicates that each of the fibre bundles of the HFS originates from a separate SAT and therefore separate lineage (or sub-lineage). Positions of these clusters of Perikarya suggest that the HFS are from the DPM (medial dorso posterior lineages; *z* and *y*) and possibly DPL (lateral dorsoposterior lineages; *x* and *w*) which are then further subdivided into 5-6 sub categories (Pereanu and Hartenstein, 2006; Yonoussi-Hartenstein et al., 2006).

These data support a hypothesis that each fibre bundle originates from a separate lineage sub category like that of *Schistocerca* (Williams et al., 2005), and subsequently two lineages in total. In order to confirm this it would be necessary to clearly visualise the entire length of the individual fibre bundles of the HFS and counter stain with a

neuroblast and secondary lineage marker (such as α-De-cadherin) to reveal lineage positions. Unfortunately this was not possible here for a number of reasons; firstly, distinguishing the whole length of the individual fibre bundles of the HFS was problematic due to density of staining external to the CC; secondly, differentiating between HFS fibre bundles prior to 12 APF is difficult; thirdly, it was not possible to counter stain α-Echinoid with α-De-cadherin at a late enough stage to visualise the SATs due to temporal expression of these markers (De-cadherin is not detectable after 8 APF). Co-expression of *shotgun* (De-cadherin) and *echinoid* in the 3rd instar displayed co-expression on several SATs but this was not traceable to specific lineages for individual HFS fibre bundles as they were not yet visible.

3.6.2 Developmental features of the CC using these markers

These results revealed that the first evidence of the CC is the unfused PB structure, identifiable from the 3rd instar larval brain. By the white prepupal stage an immature barbell shaped FB was also visible. The first identifiable neurons were the early HFS (visible by 2 APF). This early projection to the VBO (20 APF) of the HFS and VFS suggests that these neurons provide a structural framework for the CC. The continued projections of the *x* and *y* fibre bundles in a ventral direction past the VBO have not been previously reported. Due to the density of staining at this point in development it was not possible to resolve the final targets of these neurons. This raises interesting question about their ultimate targets. Are they targeting a region in the subesophageal ganglion or further to the thoracic ganglion? This reinforces the need for a specific HFS marker to trace these projections as it may reveal previously unknown connections with motor control centres in the Ventral nerve cord.

The late development of the EB from 24 APF indicates that the R neurons project later. There is faintly detectable segmentation of the FB at the prepupal stage

however it is not clear what causes this as it is visible prior to innervation from the HFS. This may be from undetected neurons or glial cells. A characteristic of brain metamorphosis is the differentiation of secondary neurons producing dendritic branches (Pereanu and Hartenstein, 2006). Consistent with this view, Echinoid staining of the HFS revealed that dendritic processes are not detectable in the CC until 12 APF, in the PB. This raises the question of what neurons are forming the early PB structure?

The latter half of CC development appears to be mainly influenced by the changing shape of the brain and further branching and arborisation of Large field neurons. The changing brain shape results in the fusion of the handlebar of the PB and also the gradual shift in position of the NO to adjacent sides of the midline. The FB also does not adopt its characteristic Fan shaped structure until 32 APF. Prior to this it has either a barbell like appearance (0-12 APF) or a more rounded shape (16-28 APF) that gradually elongates along the transverse and dorso-ventral axes. This shape alteration causes a subsequent shift in neuronal perikarya position in the case of the F*l* neurons often making them difficult to trace in timepoints of subsequent preparations.

The data analysed in this chapter indicates that a structure reminiscent of the adult CC is recognisable by 48 APF. The expression patterns from these genes allowed visualisation of a major fibre system and a set of F*l* neurons. In addition it was possible to document the development of individual sub-structures. It is important to note that the developmental data is limited to analysing only neurons that express these candidate genes. Subsequently it was not possible to visualise the development of other neurons of the CC. These limitations combined with the knowledge that several CC neurons have been unaccounted for dictate that this study cannot be considered comprehensive. In addition, although these candidate genes showed unique and identifiable patterns, the expression in brain regions external to the CC often made neuronal tracing and identification difficult. To address these issues it is necessary to adopt a methodology that allows visualisation of small numbers of neurons alone. Ideally, this should reveal both individual projection patterns and sets of isomorphic neurons in tandem to facilitate

cell type identification.

This study has given an insight into expression of selected genes in specific neuron types. Equally it has highlighted features of these gene products. *neuroglian* appears to be almost completely restricted to axonal expression. *echinoid* expression also appears to be restricted to neurites and certain neuron types, showing elevated expression in the HFS. This indicates a genetic separation between neuronal populations in the CC. Equally, *dn-cadherin* was not detected on fibre tracts but shows a pattern reminiscent of that of *bruchpilot* suggesting a synaptic function.

Although the gross structure of the CC is recognisable at 48 APF during metamorphosis it is unlikely that the CC is 'complete' at this time. Continued detection of *echinoid*, *neuroglian* and *dn-cadherin* suggests that development is ongoing. Subsequent synaptic formation and branching may occur. This study aimed to analyse overall neuronal structure. No evidence of pruning in the Horizontal or Vertical fibre systems or F neurons was observed using these genes/ CAMs as markers. This is not unexpected; most neuronal remodelling during metamorphosis is likely to be of neurons that were required for larval life. These observations have shown that an immature form of the PB is present in the late 3rd instar larva in *Drosophila* suggesting that the CC may have a functional role at this stage. This could be for locomotor behaviour, indeed CC mutants have been shown to be defective in larval locomotion assays (Varnam et al.,1996). To establish a role for the larval CC in locomotion conditional knockouts of neuronal subpopulations in this structure and further analysis of the extrinsic connections to motor centres are required.

4

Analysis of Central Complex structure and development using Enhancer Trap lines

4.1 Introduction

4.1.1 P{Gal4} enhancer trap system

Results from the candidate gene immunohistochemistry study in the previous chapter produced an initial timeline of development for all sub-structures in addition to characterising the development of the HFS and VFS. The data also invited hypotheses on the lineage of the CC and uncovered novel gene expression patterns. Structural analysis was limited by the specific expression patterns of these genes and staining in the region of the CC was often too dense to analyse populations of neurons accurately. In order to analyse the developing CC in detail it was necessary to use markers capable of isolating distinct neuronal populations throughout metamorphosis.

The P{Gal4} enhancer trap system is an ideal method with which to perform an anatomical analysis at the cellular level. The cell autonomous Gal4 transcription factor

activates any sequence downstream of a UAS construct (Brand and Perrimon, 1993). In order to visualise neurons P{Gal4} enhancer trap lines can be used to drive a membrane tethered GFP construct in the cell that can then be captured as a high resolution image. The technology provides a replicable method by which to study specific populations of neurons and allows us to infer potential genetic relationships between cells. This system has been used successfully for similar studies of brain structures such as the Mushroom bodies (Yang et al., 1995; Armstrong et al., 1998) and the EB (Renn et al., 1999). These studies built upon the initial anatomical study of the *Drosophila* CC that utilised Golgi staining (Hanesch et al.,1989). The enhancer trap system avoids the random cellular marking technique in every preparation characteristic of the Golgi staining method and is better suited to a developmental study tracing populations of neurons as opposed to individual neurons.

In order to further assess the polarity of the CC, this study used a novel approach to assessing polarity using P{Gal4} lines and UAS-Dscam(exon 17.1)::GFP reporter line. The *Dscam* gene generates over 12,000 isoforms of an immunoglobulin superfamily cell-surface protein and regulates dendritic patterning in Olfactory Projection Neurons (Zhu et al., 2006). We have driven a GFP tagged UAS-Dscam construct that can be used as a dendritic marker in the Flybrain. Using the P{Gal4} lines we aim to identify dendritic regions in the CC, with the aim of providing some insight into information flow of this structure.

4.1.2 Overview

There are now several collections of enhancer trap lines in use in the *Drosophila* community. The enhancer trap lines used in this study were first isolated in a study by Yang et al (1995). For the analysis of the developing CC in this study, 300 P{Gal4} lines were initially screened for expression focusing on the adult FB. The resulting lines

were then subjected to a developmental expression screen. This chapter gives a detailed description of the morphology, development and potential genetic relationships of several identifiable neuronal populations in the CC.

4.2 Aims

1. To isolate a set of P{Gal4} lines marking neuronal subsets in the adult FB

2. To determine a set of P{Gal4} lines that are expressed during Central Complex development

3. To perform an anatomical analysis of these neuronal sets throughout CC development.

4.3 Characterisation of individual P{Gal4} lines isolated in a developmental screen

Three hundred enhancer trap lines were screened for expression in the adult FB. This resulted in fourteen lines being isolated from the collection. These adult neuronal expression patterns are shown in Table 4.1. Whole brain images for selected lines are shown in Figure 4.1. All fourteen lines were crossed to a UAS-mCD8::GFP reporter line and initially assessed for expression at three stages; the white prepupal stage, 24 APF and 48 APF. No expression was detected for four lines (121y, 227y, c5, and c259) at any of these stages. For two lines (23y, 52y) expression in the Central Complex was detected later at either 24APF (23y) or 48APF (52y). Further analysis revealed that 23y was faintly detectable from 20 APF. Line 52y was faintly detectable from between 28-48 APF. The screen identified seven P{Gal4} lines that showed expression from the start of CC development through to 52 APF and beyond.

Nine of the enhancer trap lines are further detailed in this section. The aim of this part of the study was to use the FB enhancer trap lines to trace the structure and development of specific neurons in the Central Complex. As reported in the previous chapter, the typical structure of the Central Complex is complete by 48 APF therefore it was initially necessary to determine which enhancer trap lines were expressed before this point. Developmental expression patterns are shown in Table 4.2. All images are frontal sections unless otherwise specified.

Enhancer trap Line	Chromosome (location)	Neuron type	Synonym in *Schistocerca*	Figure reference in this thesis	Perikarya position ap	dv	ml	Projections	Cross ref to Fig Hanesch (1989)
23y	2	*Fm2*	Tangential	4.1 (B) 4.2 (A)	a	m	m		-
		Fld	Tangential	4.1 (B) 4.2 (A)	p	d	l		-
52y	3L (69e)	R1		4.1(A) 4.3 (A) 4.4(A,B)	a	m	m		Fig 20 (a, d)
		R2		4.1(A) 4.3 (A) 4.4(A,B)	a	m	m		Fig 20 (b, d)
		R3		4.1(A) 4.3 (A) 4.4(A,B)	a	m	m		Fig 20 (c, d)
		R4		4.1(A) 4.3 (A) 4.4(A,B)	a	m	m		Fig 20 (a, d)
		P *cv*		4.2 (B)	p	m	m		-
62y	2	*Fm*	Tangential	4.2(C)					-
		Fld	Tangential	4.2(C)	p	d	l		-
71y	3	*Fm2*	Tangential	4.2(D)	a	m	m		-
		Fld	Tangential	4.1(C) 4.2(D)	p	d	l		-
		ExR1			p	d	m		Fig 21(a)
104y	2L (26D)	*Fld*	Tangential	4.1(D) 4.2(E) 4.5(A,B)	p	d	l		-
		Fm2	Tangential	4.1(D) 4.2(E) 4.5(A)	p	d	l		-
121y	Unknown	*Fld*	Tangential	4.2(F)	p	d	l		-
210y	3L	*Fm1*	Tangential	4.2(G)	p	d	l		Fig 22(c)
		Fld	Tangential	4.2(G)	p	d	l		-
227y	X (1A)	*Fld*	Tangential	4.2(H)	p	d	l		-
		Fm1	Tangential	4.2(H)	p	d	l		Fig 22(c)
c5	3	*Fld*	Tangential	4.2(I)	p	d	l		-
c61	X	*Fld*	Tangential	4.1(E) 4.2(J)	p	d	l		-
		Fm1	Tangential	4.1(E) 4.2(J)	p	d	l		Fig 22 (c)
c159b	2	*P cd*	PoU	4.1(F) 4.2(K)	p	d	m		Fig 8
		fb-eb		4.1(F) 4.2(K)	p	d	m		Fig 13 (a)
c255	3L	ExR1		4.1(G) 4.2(L) 4.3(B) 4.6(A,B)	p	d	m		Fig 21 (a)
		Fm2	Tangential	4.1(G) 4.2(L) 4.3(B) 4.6(A,B)	a	m	m		-
c259	Unknown	*Fm1*	Tangential	4.2(M)	p	d	l		Fig 22(c)
		Fld	Tangential	4.2(M)	p	d	l		-
c465	2	VFS I	CPU4a	4.1(H) 4.2(N)	p	d	m		Fig 5 (a, b)
		VFS II	CPU4b	4.1(H) 4.2(N)	p	d	m		Fig 5 (a, b)
		VFS III	CPU4c	4.1(H) 4.2(N)	p	d	m		Fig 5 (a, b)
		HFS	CPU1a	4.1(H) 4.2(N)	p	d	m		Fig 6 (a, b)
		R2		4.3(C)	a	m	m		Fig 20 (b, d)
		R3		4.3(C)	a	m	m		Fig 20 (c, d)
		fb-eb		4.3(C)	p	d	m		Fig 13 (a)

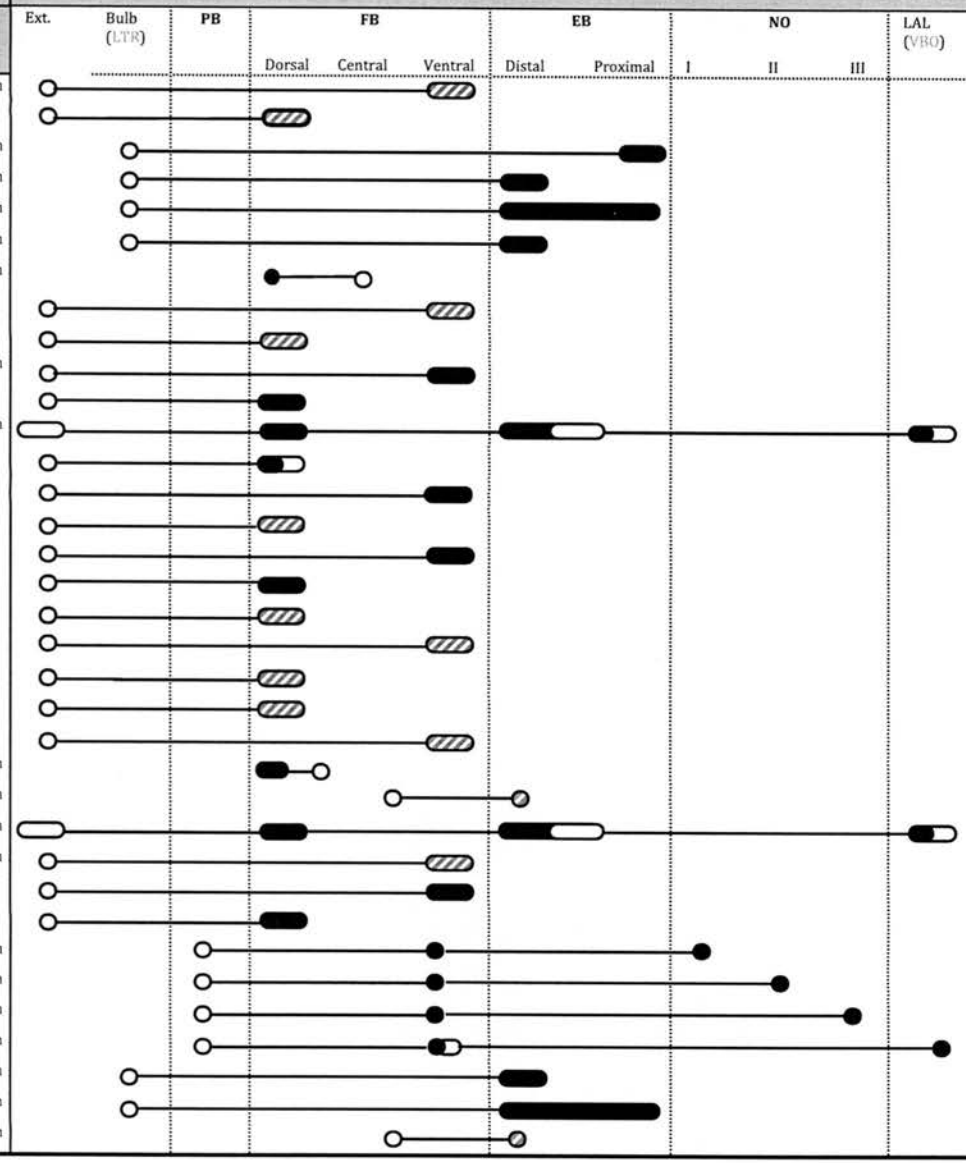

Table 4.1: Types of CC neurons revealed by enhancer trap expression, their connectivity and polarity. Both large and small field neurons are represented. Filled (black) circles indicate presynaptic expression and open (white) circles indicate dendritic expression. If a circle contains both this indicates mixed terminals. Hatching represents unknown terminals. Synonyms from other insect species are included in column 4. Figure references to this publication are in column 5. The perikarya position of each neuron (column 6) is described according to its position on the anteroposterior(ap), dorsoventral(dv) and mediolateral(ml) axes. References to Hanesch et al. (1989) are in the rightmost column. Ext., extrinsic arborisations (outwith the CC); PB, protocerebral bridge ; FB, fan shaped body; EB, ellipsoid body; NO, noduli with layers I, II and III; LAL, lateral accesory lobes.

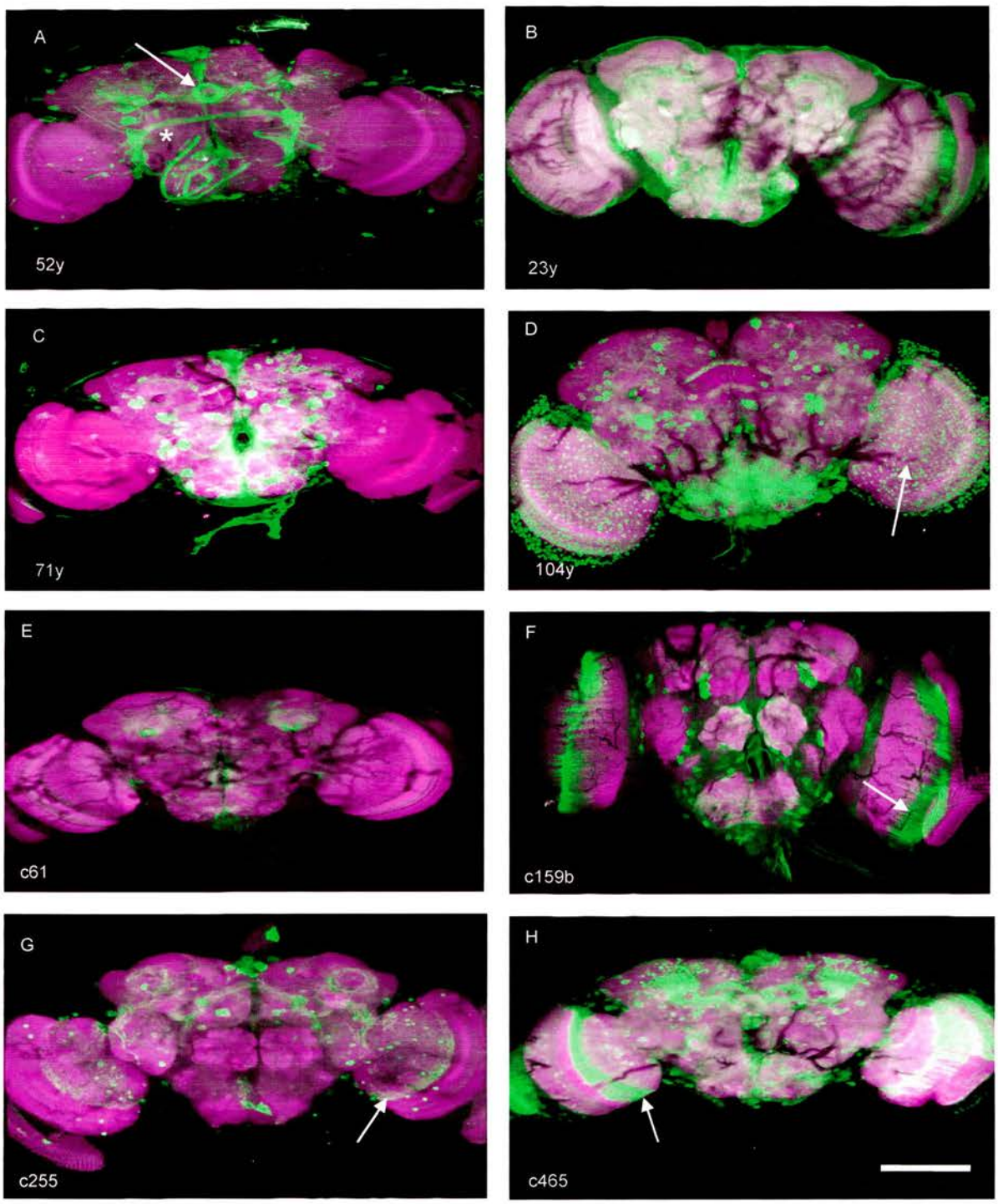

Figure 4.1: Whole brain adult expression patterns of selected enhancer trap lines. The enhancer trap line is in the lower left corner of each image. **A**, line 52y shows the EB (arrow) and the great commissure (asterix). **B,C**, lines 23y and 71y show general staining in the central brain. **D,F,G,H**, In several lines clear expression can also be observed in the visual system (arrows). Images are from 3D projections. Green: α-GFP, Magenta: nc82. Scale bar 100µm.

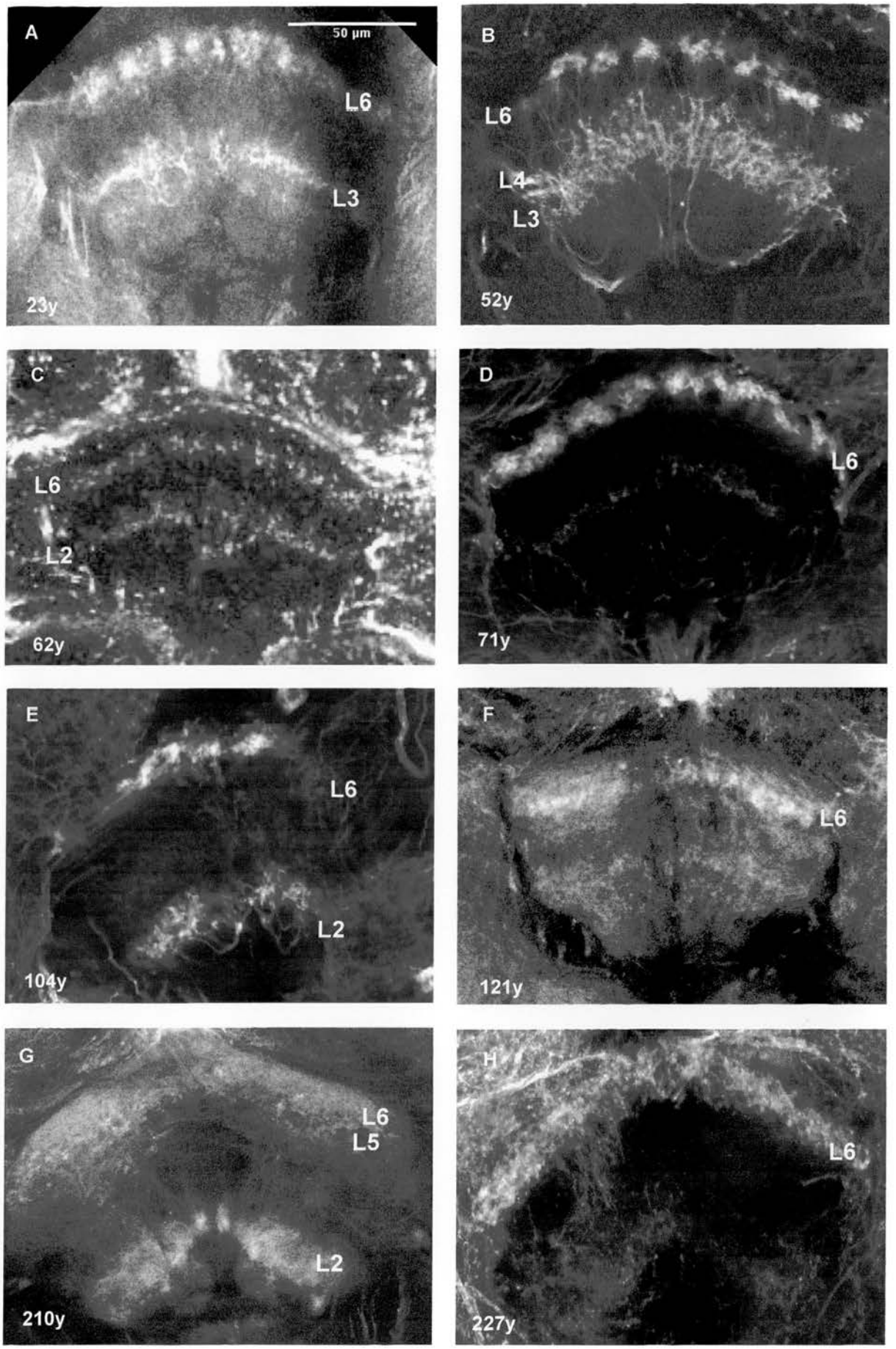
A
50 µm
L6
L3
23y
B
L6
L4
L3
52y
C
L6
L2
62y
D
L6
71y
E
L6
L2
104y
F
L6
121y
G
L6
L5
L2
210y
H
L6
227y

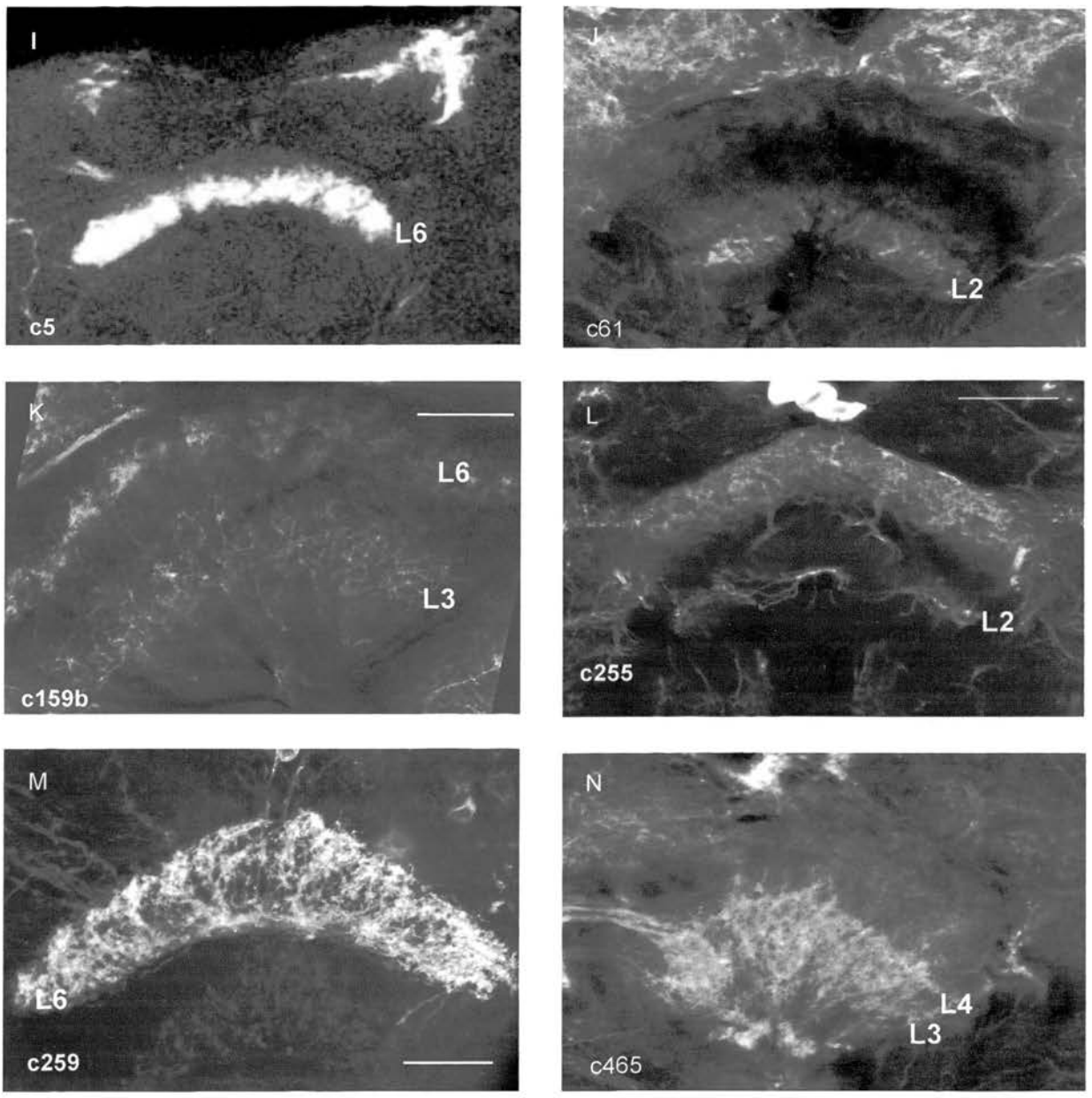

Figure 4.2: Adult FB expression patterns of enhancer trap lines used in the developmental screen (this page and previous page). In all cases neurons were observed as sets. L1-6 refers to layers in the FB. **A**, line 23y shows expression in F*l* neurons in layer 6 and Fm neurons in layer 2. **B**, line 52y expression reveals Pontine neurons. **C,** 62y shows both F*l* and F*m* neurons. **D,** line 71y expression in F*l* neurons. **E**, line 104y expression also reveals Fl neurons in layers 1 and 6. **F,** line 121y shows F*l* neurons. . **G**, line 210y expression does not show axons clearly but reveals arborisations. **H,** line 227y shows both F*l* and F*m* neurons. **I**, line c5 shows elevated expression in the dorsal FB. **J**, line c61 is expressed in the dorsal and ventral FB layers. **K,** line c159b shows widespread expression in the FB from both Pontine neurons and F*l* neurons. **L**, line c255 is expressed in F*m* neurons and shows elevated expression in the Superior arch. **M,** c259 shows F*l* neurons **N**, line c465 reveals the fibre bundles of the HFS and VFS in addition to other Small field neurons (see text). All lines except 210y and c465 show segmented arborisations in upper layers (not visible with c255 in this view). Scale bars 50µm.

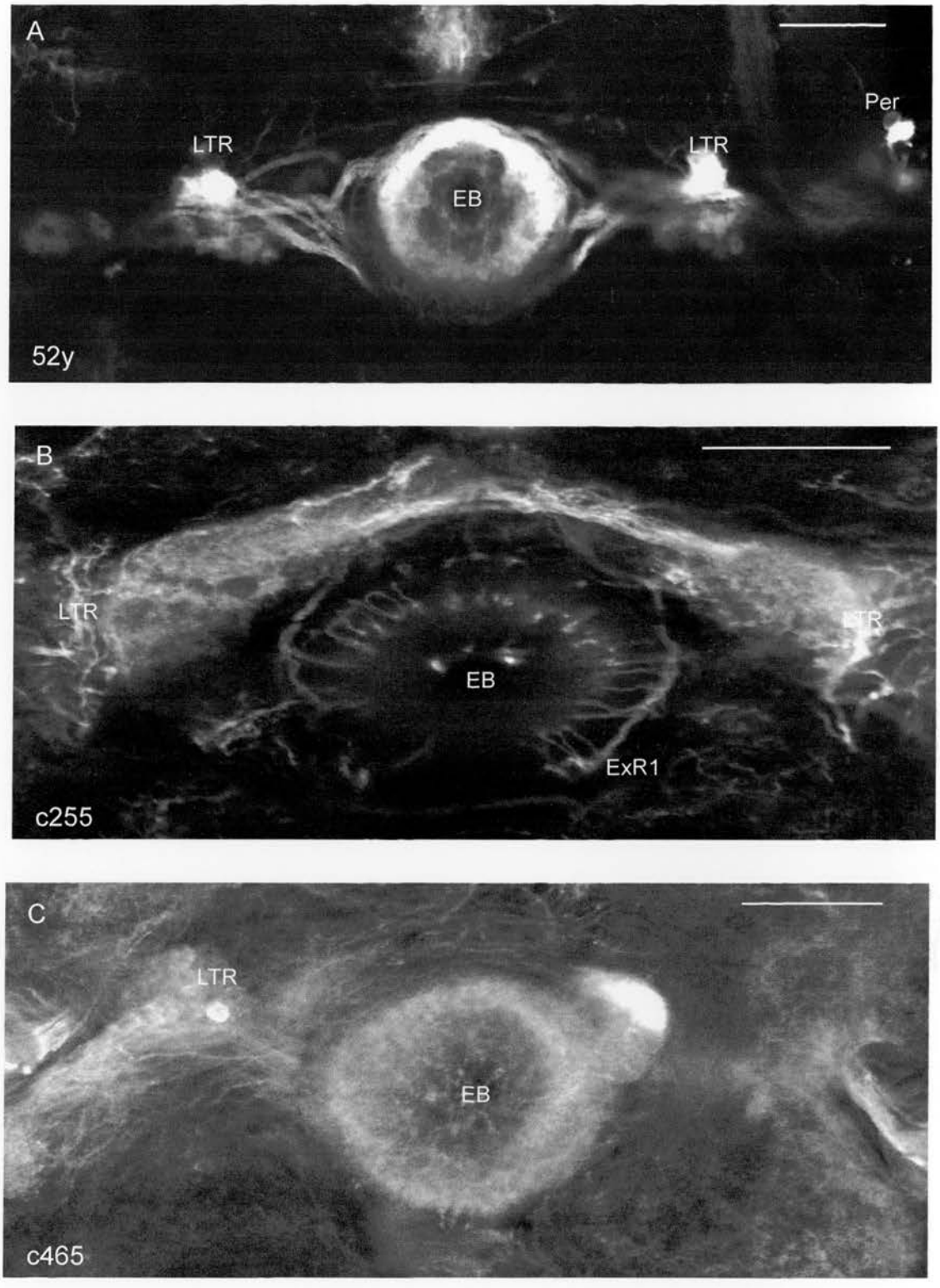

Figure 4.3: Adult EB expression patterns of enhancer trap lines used in the developmental screen visualised with an mCD8::GFP reporter line**. A**, line 52y expression in the R1-R4 neurons showing arborisations in the LTRs. **B**, line c255 expression in the ExR1 neurons(s) that can be seen branching into the EB ring. **C**, line c465 expression in the R2/R3 neurons. LTR- Lateral Triangles; Per, Perikarya. Scale bars, 25µm.

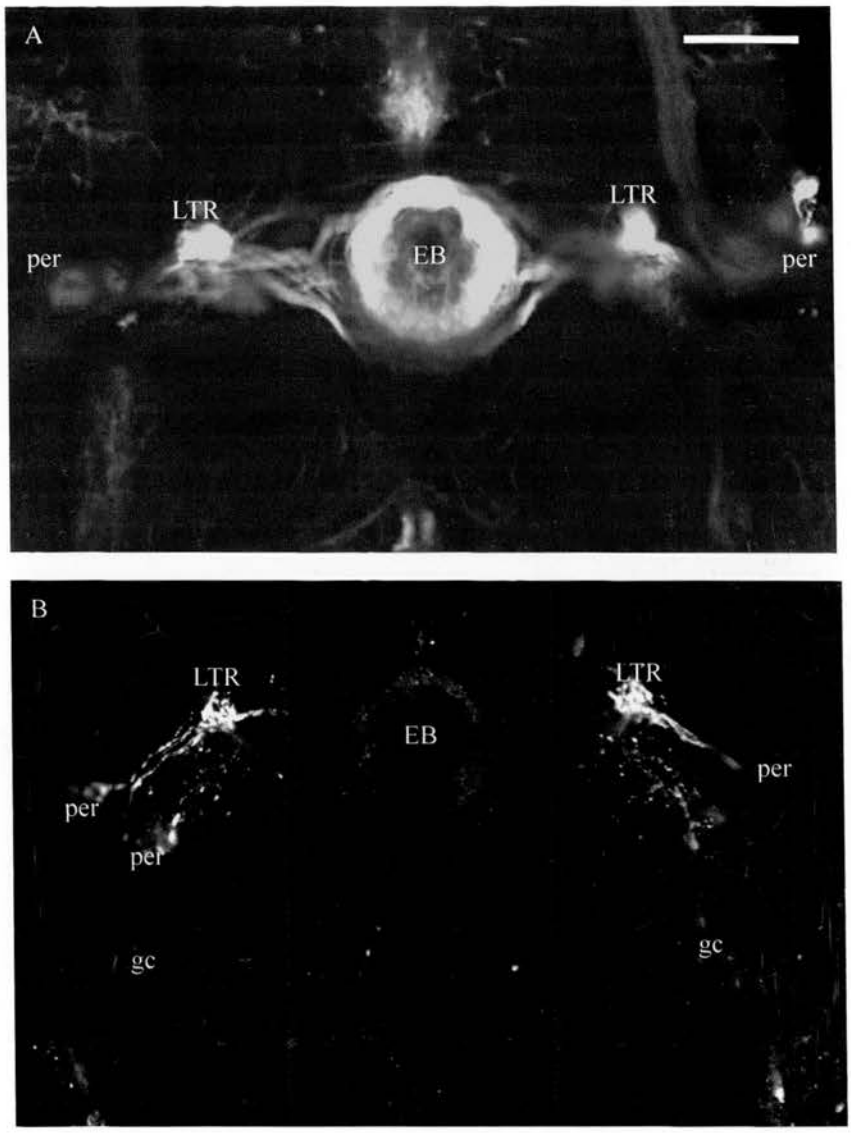

Figure 4.4: Dscam expression of P{Gal4} line 52y. A, Expression using mCD8::GFP as a marker reveals R1- R4 neurons (cell bodies not visible in this image) arborising in the LTRs and extending to form ring structures. **B,** Expression using UAS-DSCAM::GFP as a marker clearly showing cell bodies, arborisations in LTR's and connections to the gc. The ring can faintly be seen. EB; Ellipsoid body, LTR; Lateral Triangle, per; Perikarya; gc; Great Commissure. Scale bar 25μm.

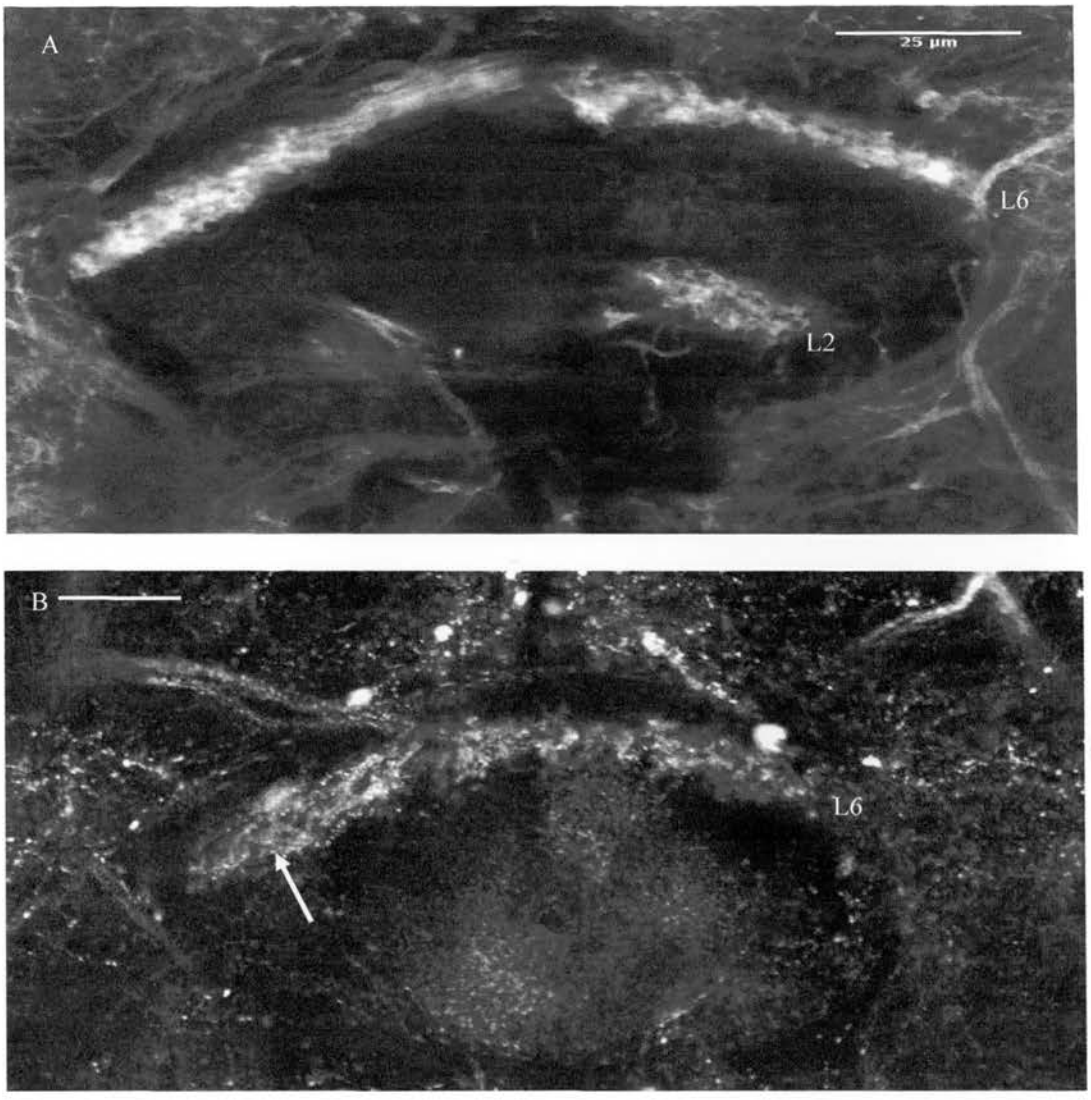

Figure 4.5: Dscam expression of P{Gal4} line 104y. A, Expression visualised with reporter line UAS-GFP::mCD8 showing arborisations from F*l* (Layer 6) and F*m* (layer 2) neurons. **B**, Expression visualised with UAS-DSCAM::GFP in the F*l* neurons in L6 (arrow) across the width of the dorsal FB. Scale bars 25µm.

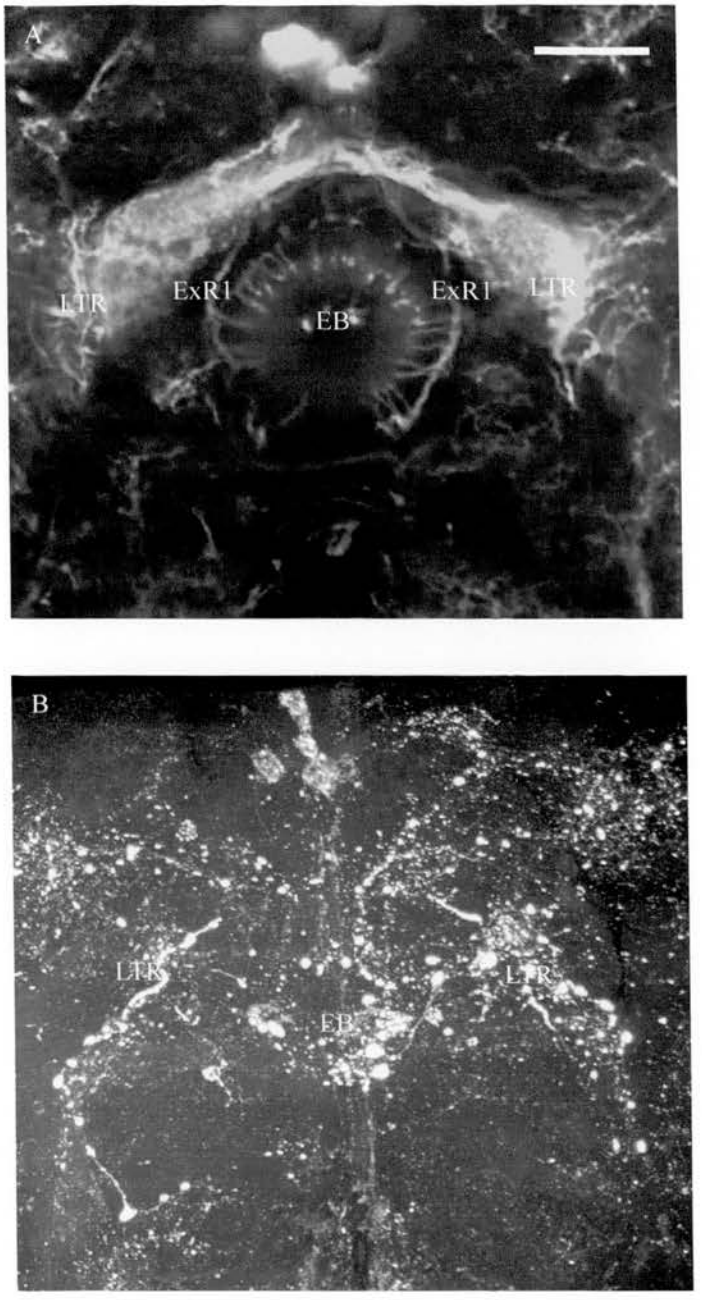

Figure 4.6: Dscam expression of enhancer trap line c255. **A**. Expression with reporter line UAS-GFP::mCD8 showing arborisation in the dorsal FB and LTR from ExR1 neurons that also has branches innervating the EB ring. **B**, Expression with reporter UAS-DSCAM::GFP appears to follow the pattern of the ExR1 neuron. LTR; Lateral Triangle, ExR1; ExR1 neurons, EB; Ellipsoid body. Scale bar 25μm.

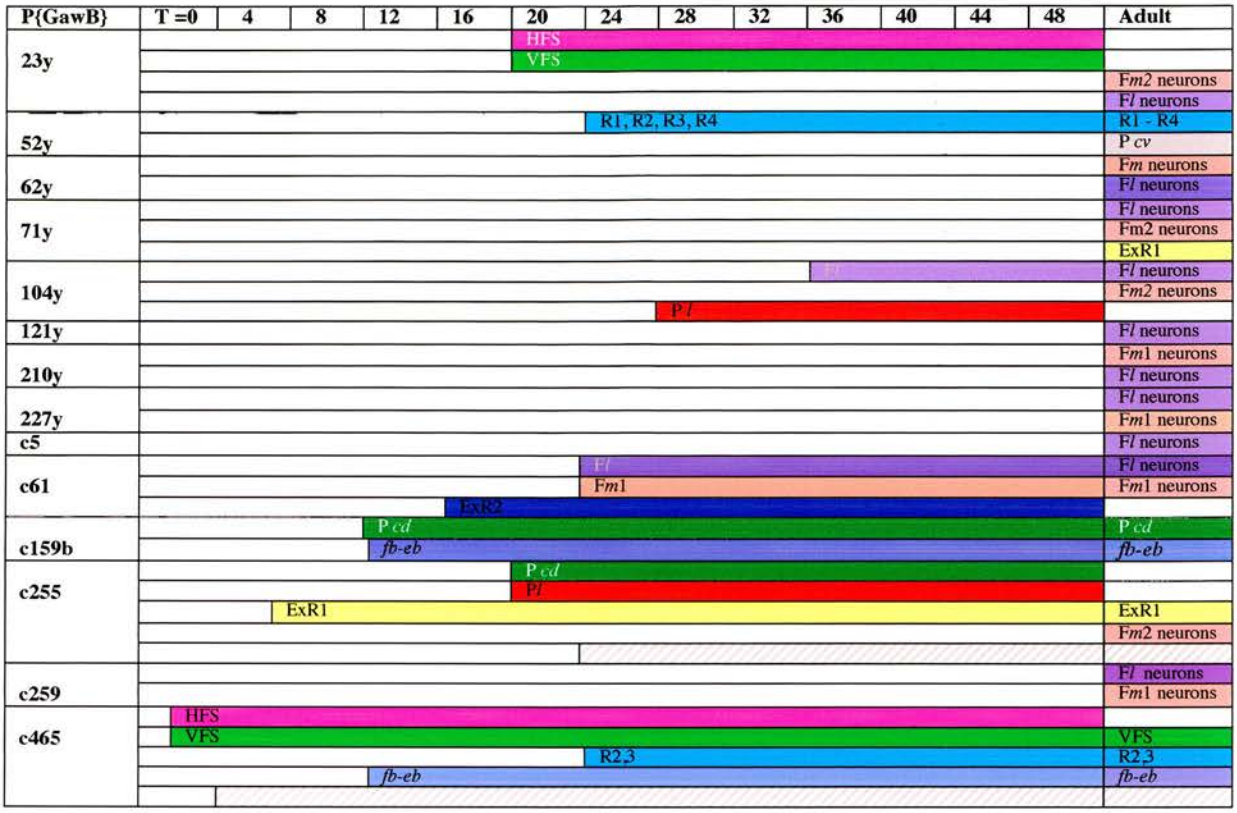

Table 4.2: Temporal expression and changes in expression pattern throughout Central Complex development. Numbers 0-48 in row 1 denote hours APF during metamorphosis. Grey type indicates faint expression in these neurons. Hatching represents a neuron type that was not possible to trace but is thought to be present (see text). Blank areas in the table represent no CC neuron expression. The rightmost column represents adult expression. F*l* , Fan shaped lateral neurons; F*m*, Fan shaped medial neurons; P *cd*, Pontine neurons crossing contralaterally in the dorsal FB; P*l*, Pontine neurons connecting layers in one segment; P *cv*, Pontine neurons crossing contralaterally in the ventral FB; R1-R4; Type A R neurons; ExR1, Type B R neurons; ExR2, Type C R neurons; ltr, Lateral triangles; HFS, Horizontal Fibre system; VFS, Vertical Fibre System. Neuron types are represented by the same colour.

4.3.1 P{Gal4} line 23y

Adult

The adult expression pattern of line 23y was restricted to the Large field F neurons that showed arborisations in FB layer two from sets of F*m2* neurons entering via the EB canal. Arborisations remained within this layer and did not extend to further layers but projected to segments in layer two only. It was not possible to detect arborisations out with the CC for these F*m* neurons. Layer six is traversed by F*l* neurons as shown in Figure 4.2(A). These first arborise lateral to the FB out with the CC. The FB is the only CC sub-structure to be innervated by these neurons.

Development

During metamorphosis expression was detected faintly at 20 APF though the pattern was different to that of the adult brain. At this early point in development no F neurons were detectable, though both of the VFS and HFS could be seen faintly. Due to the faint level and late onset of expression in the CC this line was not used further as a developmental marker.

4.3.2 P{Gal4} line 52y

Adult

Line 52y demonstrates elevated reporter expression in the adult type A R neurons of the EB [Figure 4.3(A)]. Neurons specific to the FB can also be seen with Perikarya in the dorso-posterior cortex. Axons from these neurons enter the FB laterally revealing a lattice structure projecting in a ventral direction through a segment to layer 1 [Figure 4.2(B)] where they crossed contralaterally then projected dorsally to the upper

FB layers to terminate in a different segment forming a U shape. These neurons ahave not been previously reported and therefore a new Pontine neurons subtype is proposed here. Since these neruons only innervate the FB and cross contralaterally to innervate segments in opposite hemisphere they are labelled Pontine neurons (*Pcv*). Due to the lack of developmental expression in these cells it was not possible to visualise these neurons at axonogenesis, therefore defining the precise cell number, branching and projection patterns was not possible.

The perikarya type A R neurons were detected in each hemisphere. The axons from these neurons demonstrated the same initial trajectory then arborised in the ipsilateral Lateral triangles (LTRs) before projecting to the midline where they formed their characteristic ring shape. From their positions in the EB, the R neurons could be categorised as representations of Type A. It was not possible to separate the number of neurons of each subtype. The exact number of perikarya was not observable but seemed to be much lower than the reported 100 R neurons (Renn et al.,1999). It is possible that this line represents subsets of each neuron type, and possibly further categorisation of R1-R4 neurons, though it is not possible to conclude this from this data due to staining density. This is the first time that this line has been reported for R neuron expression.

P{Gal4} driven *Dscam* expression was localised to the R neurons in the CC as shown in Figure 4.4(B). Specifically, the perikarya, axon tracts and LTRs were clearly visible though expression in the actual EB ring was barely detectable. There were also clear connections between the axons of the R neurons and the Great Commissure which lies ventro-posterior to the R neurons (see Figure 4.1). The *Dscam* expression in the Pontine neurons was faintly present as a band across the central FB.

Development

Although, there is no developmental expression in early metamorphosis, expression is faintly detectable at 24 APF in the developing type A R neurons. This

correlates with the onset of early EB development. Expression is restricted to the type A R neurons during development for this line. Expression in the Pontine neurons was only detected in the adult brain.

4.3.3 P{Gal4} line 71y

Adult

Like most lines, line 71y showed reporter expression in the F neurons in layers two and five / six of the adult FB as shown in Figure 4.2(D). F*m2* neurons could be seen entering FB through the EB canal and traversing along layer two, revealing subsequent arborisations in this layer. The F*l* neuron of the upper layers displayed arborisations in each of the segments as the axon traversed the layer. *Dscam* expression was only detected faintly in the arborisations of the upper layers (data not shown). There was also faint expression in the ExR1 neurons though precise projection patterns were difficult to visualise.

4.3.4 P{Gal4} line 104y

Adult

Adult expression in the CC was restricted to F neurons in layer six and one of the FB with this line as shown in Figure 4.2(E). In layer six the F*l* neurons showed sixteen small clumps of arborisation distributed evenly along the layer. These arborisations are restricted to this layer. F*m* neurons spanning layers two (and possibly one) show axons in the lower layer sending several branches to layer two where arborisations were detected. These F neurons are reminiscent of a type detected by Hanesch (1989). There was no expression in Small field neurons or any other cells of the Central Complex. In

terms of polarity, there was considerable expression of *Dscam* in the upper FB layers as shown in Figure 4.5(B), with faint expression in parts of the EB ring.

Development

From 28 APF P*l* neurons could faintly be detected connecting dorsal and ventral regions of the FB as reported in Hanesch et al., (1989). Expression was not strong enough to analyse these neurons properly. Expression was detected in layer six of the FB from 36 APF showing arborisations in this layer similar in position to those visualised with the Dscam reporter. This is thought to be expression in an F*l* neuron. Due to limited expression during the period of CC development this line was discontinued in the developmental screen.

4.3.5 P{Gal4} line 210y

Adult

Adult expression in the CC showed a cluster of F*m1* neurons which enter the FB through the EB canal and arborise in layer two as shown in Figure 4.2(G). Extensive arborisation was visible throughout layer two and immediately adjacent layers. In layer six there were arborisations in the upper FB layers thought to be from F*l* neurons. Visualisation of cell types with this line was difficult due to the high density of staining. No *Dscam* staining was detected.

Development

By 28 APF there was faint expression in middle layers of the FB which was likely to be the F*m* neurons but this was hardly detectable. Isolating axon tracts was

difficult with this line. Due to the lack of distinguishable developmental staining in the CC this line was excluded from any further developmental study.

4.3.6 P{Gal4} line c61

Adult

The adult expression pattern of line c61 in the Central Complex was restricted to F neurons in layers two and five (faintly) as shown in Figure 4.2(J). Staining revealed processes going through the EB canal, which were F*m1* neurons arborising in layer two. The F*l* neurons traversed layer five. Arborisations remained within this layer. No *Dscam* expression was detected.

Development

The c61 expression pattern during development was restricted to a Type C R neuron, the ExR2 neurons though the F neurons could faintly be seen [Figure 4.7]. Expression was detectable from 20 in the developing ExR2 neuron. The ExR2 neuron Perikaryon location has not been previously determined (Hanesch et al., 1989). In this study it was possible to trace the Perikaryon to the posterior-medial cortex. The ExR2 neuron has a projection pattern like that of the TL1 neurons of *Schistocerca* (Muller et al., 1997) Axons arborise in the VBO and LTR prior to innervating the EB from the lateral edge as shown in Figure 4.8. At 24 APF the EB has not fused. This neuron is represented schematically in Figure 4.9. Once the ExR2 neuron reaches the EB the axon continues contralaterally to encircle this structure. The final trajectory of the ExR2 neuron is shown in Figure 4.10 (A,B). The ExR2 neuron was not revealed in the adult brain using this enhancer trap line.

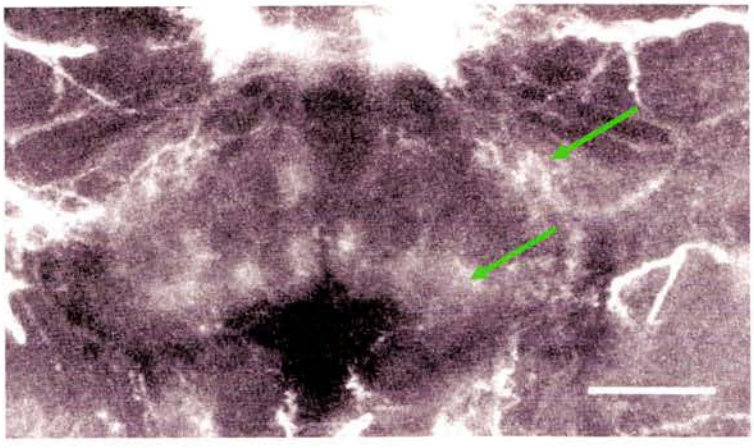

Figure 4.7: F/ neurons can be seen faintly at 24 APF in line c61. The F neurons are present in both the dorsal and ventral FB (arrows).

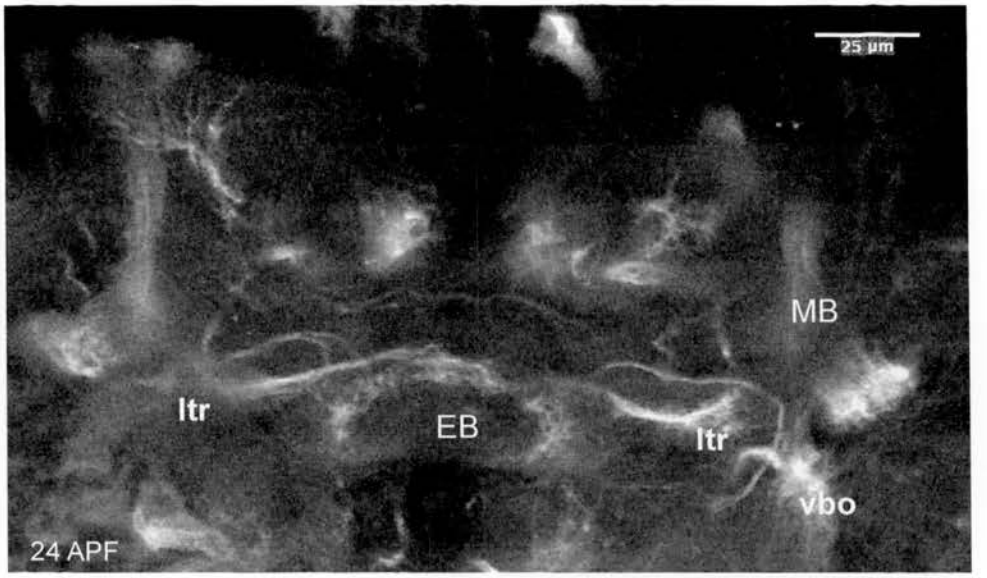

Figure 4.8: Development of the ExR2 neuron shown by enhancer trap line c61. By 24 APF the ExR2 neurons are clearly visible arborising in the posterior EB. MB, Mushroom body; EB, Ellipsoid body; ltr, Lateral triangle; vbo, Ventral body.

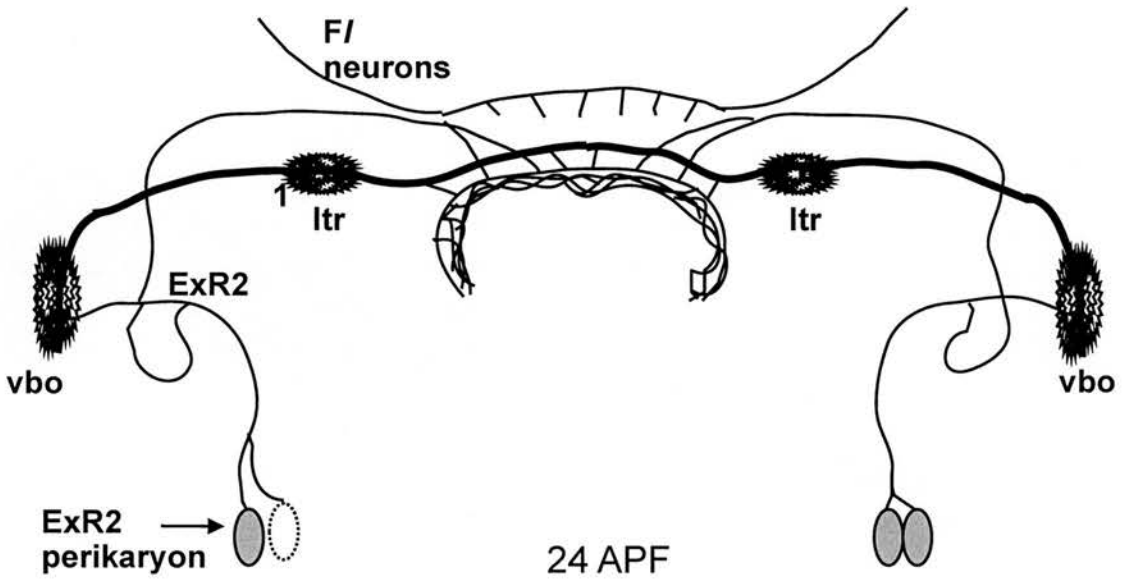

Figure 4.9: Schematic representation of c61 expression at 24 APF. By 24 APF the F/ neurons can faintly be seen in layer 4/5 of the FB where they are arborising in a regular pattern. By this stage the ExR2 neurons (1) are also clearly visible innervating the dorso posterior EB.

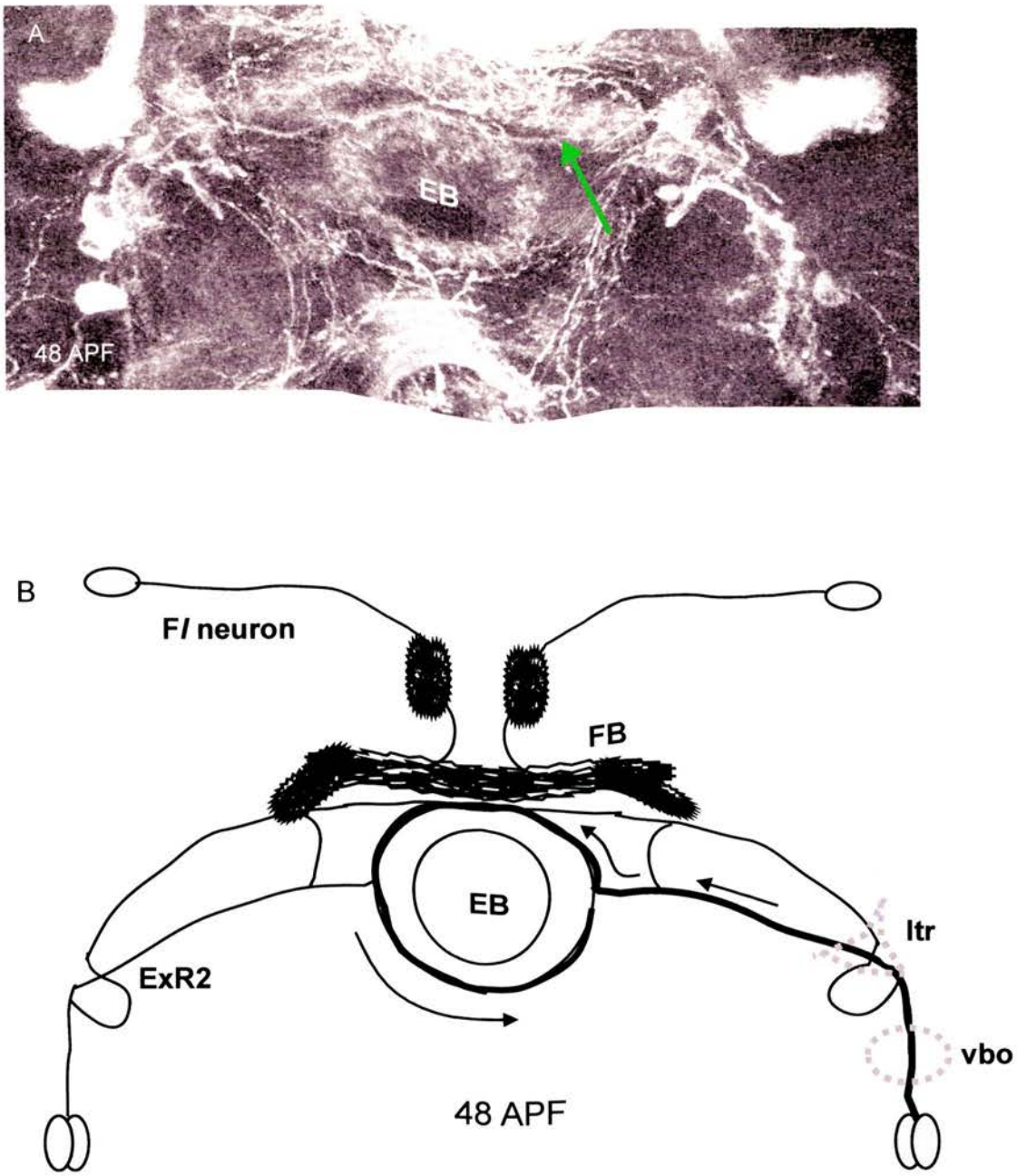

Figure 4.10: Final ExR2 projection patterns. A, The ExR2 projections encircle the EB by 48 APF. Arborisations from FI neurons can be observed in the dorsal FB (arrow). **B**, Schematic of proposed final ExR2 projections (arrows – the right hand ExR2 axons only). In this schematic the ExR2 neurons has been drawn to almost completely encircle the EB, a pattern that this data suggests, however this was deduced from a set of ExR2 neurons not a single neuron therefore may not be an exact reconstruction. FB, Fan shaped body; EB, Ellipsoid body; ltr, Lateral triangle; vbo, ventral body.

4.3.7 P{Gal4} line c159b

Adult

Adult expression of line c159b revealed Small field neurons only. Pontine neurons (P *cd*) were observed showing contralateral connections within layer five. Dense arborisation was observed in the FB as shown in Figure 4.2(K). This arborisation made visualisation of individual fibres difficult. The patterning of the Pontine neurons was determined from the developmental data (see below). In addition, expression was detected in the EB. The pattern was not reminiscent of the R neurons as no Perikarya or arborisations in regions lateral to the FB (i.e. The LTR or VBOs) was observed. Connections were observed between the FB and posterior EB. This evidence combined with the dense arborisations in the FB led to the conclusion that these were a set of the *fb-eb* neurons. No *Dscam* expression was detected.

Development

At 4 APF several Perikarya can be seen in the central brain as shown in Figure 4.11(A). By 8-12 APF clusters of neurons can be seen in the central brain targeting medially and arborising in early segments of the FB [Figure 4.11(B)]. By 16 APF the shape of the brain has altered shifting the perikarya of these neurons into a position dorsal of the FB and columnar elements have started to form as shown in Figure 4.11(B). Fibres from the P*cd* neurons can be seen crossing contralaterally from 16 APF. Figure 4.12(A) shows this pattern at 24 APF, where axons terminate in contralateral segments. This is indicated by the 'blebbed' appearance of the axon terminal. Although it is difficult to isolate precise axonal trajectories due to the condensed arrangement fibres, it is possible to trace several fibres back from their termini to segments 4 removed. This is reminiscent of the pattern of the Pontine neurons described in Hanesch et al.(1989). Innervation of two FB layers is also apparent at 24 APF [Figure 4.12(B)]. By 32 APF, six clusters of four neurons in the dorsal cortex can be counted targeting

segments B-G of the FB [Figure 4.13(A)]. Clusters of neurons innervating the lateral FB layers (A and H) can be seen latero-dorsal to the FB [Figure 4.14(B)]. From these data, it can be hypothesised that c159b shows expression in two sets of neurons (P *cd* and *fb-eb*) present as two isomorphic sets of sixteen neurons. Pairs of neurons from each set reside in one of eight dorso-posterior or latero-posterior clusters of Perikarya. This does not correlate with previously reported sets of eight Pontine neurons (Hanesch et al.,1989) however, that study did not have the advantage of visualising all neurons in an isomorphic set at once as has been shown here. Known types of Pontine neurons are represented schematically in Figure 4.15 as .

At 32 APF fibres can be seen innervating the posterior of the EB from the FB. Counting the number of these fibres was not possible due to the dense arborisations from the Pontine neurons. As mentioned above in the expression pattern of the adult brain, these neurons are likely to be the *fb-eb* neurons [Figure 4.13(B)]. Evidence supporting this can be found in the number of Perikarya and the trajectories of the axons. Axons of *fb-eb* neurons enter the FB with a trajectory like to that of the Pontine neurons (from the dorsal cortex) and have been shown to traverse both between and within segments, arborising and branching before innervating the EB (Hanesch et al., 1989). Additionally, if there are sixteen Pontine neurons (therefore two per segment) but four Perikarya observed then this suggests the presence of additional neurons. In these preparations, axon trajectories in the dorsal FB were difficult to isolate but the *fb-eb* neurons appeared to remain within the segment they originally targeted, projecting to the EB ventro-anteriorly [Figure 4.13(B)]. This, in conjunction with the observed number of Perikarya suggests that there are two *fb-eb* neurons per segment. It was not possible to discern these neurons in segments A and H. This data indicates c159b is also expressed in a set of sixteen isomorphic *fb-eb* neurons. Sets of *fb-eb* neurons have not been previously reported.

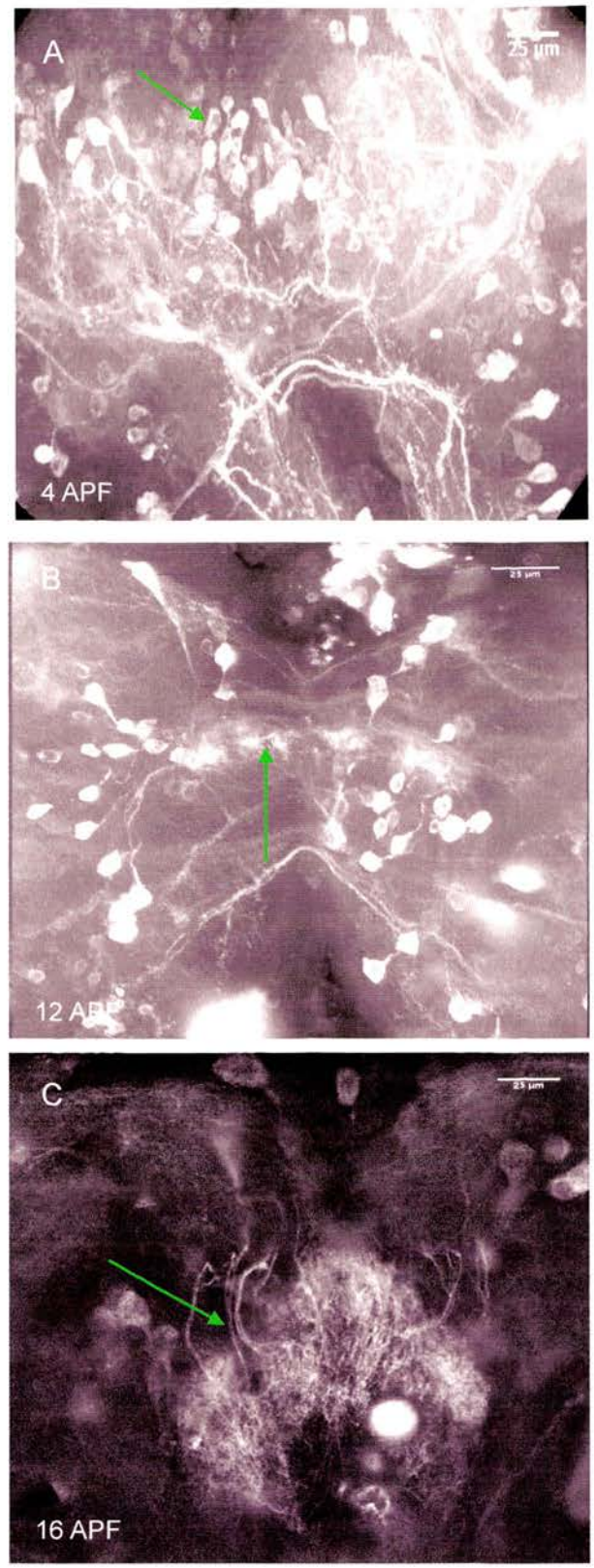

Figure 4.11:Early development of Pontine neurons visualised with ine c159b. A, At 4 APF several Perikarya can be seen in the central brain (arrow). **B**, By 12 APF Perikarya can be seen targeting segments of the early FB (arrow) from both dorso-ventral and dorso-lateral positions.. **C,** At 16 APF, clusters of four neurons (Perikarya now dorsal to FB) target individual FB segments then target contralaterally to segments in the other hemisphere. There are also connections to ventral FB layers in each segments. Scale bars 25µm.

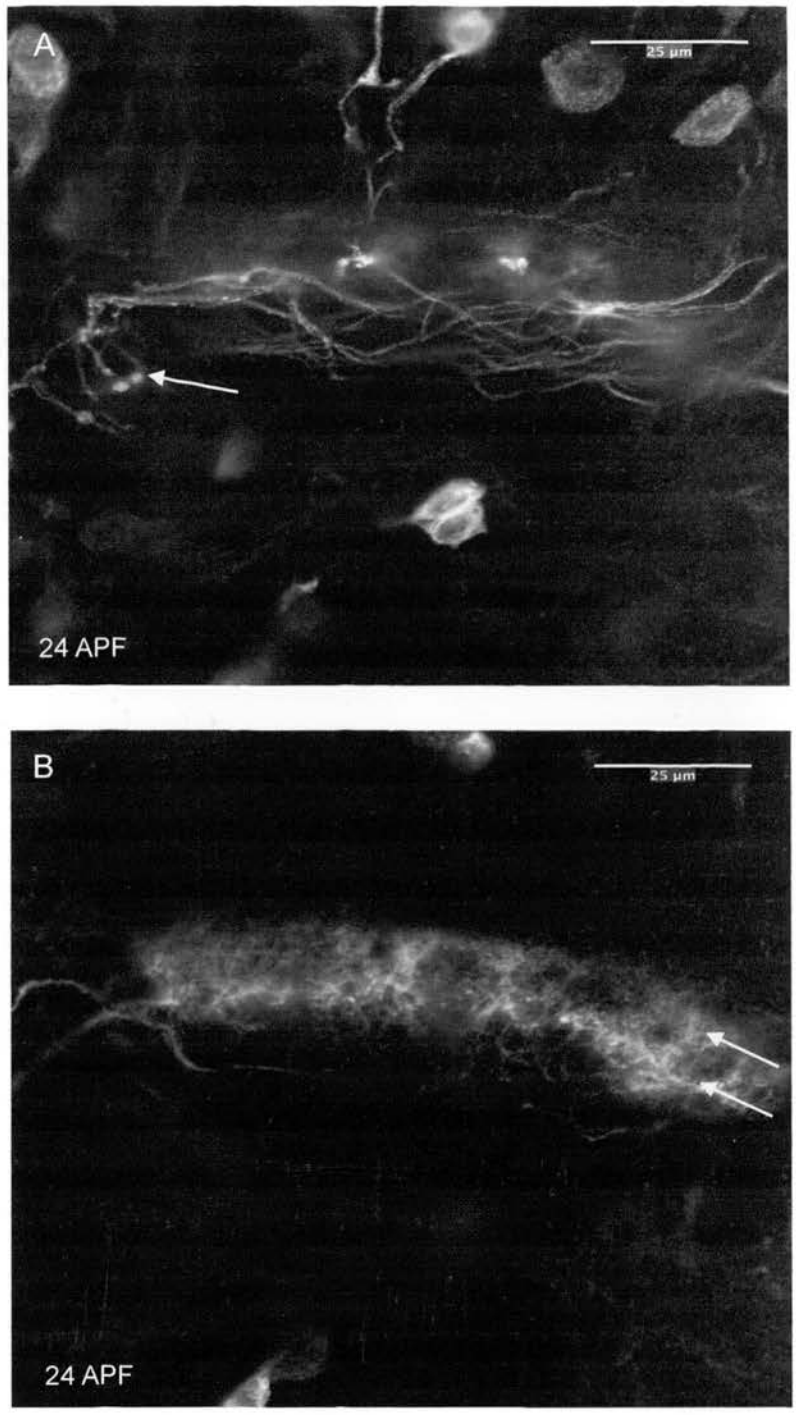

Figure 4.12: Development of Pontine neurons during mid Central Complex development as visualised with line c159b. **A**, Axons are crossing the midline and terminating with blebbed endings (arrow) in segments in the opposite hemisphere in a pattern reminiscent of the Pontine neurons. The blebs shown are from an axon that entered the FB in segment E that crossed the midline to terminate in segment A. **B**, The same timepoint as a section anterior to above showing the depth of the Pontine neurons on the antero-posterior axis (arrows) of the FB.

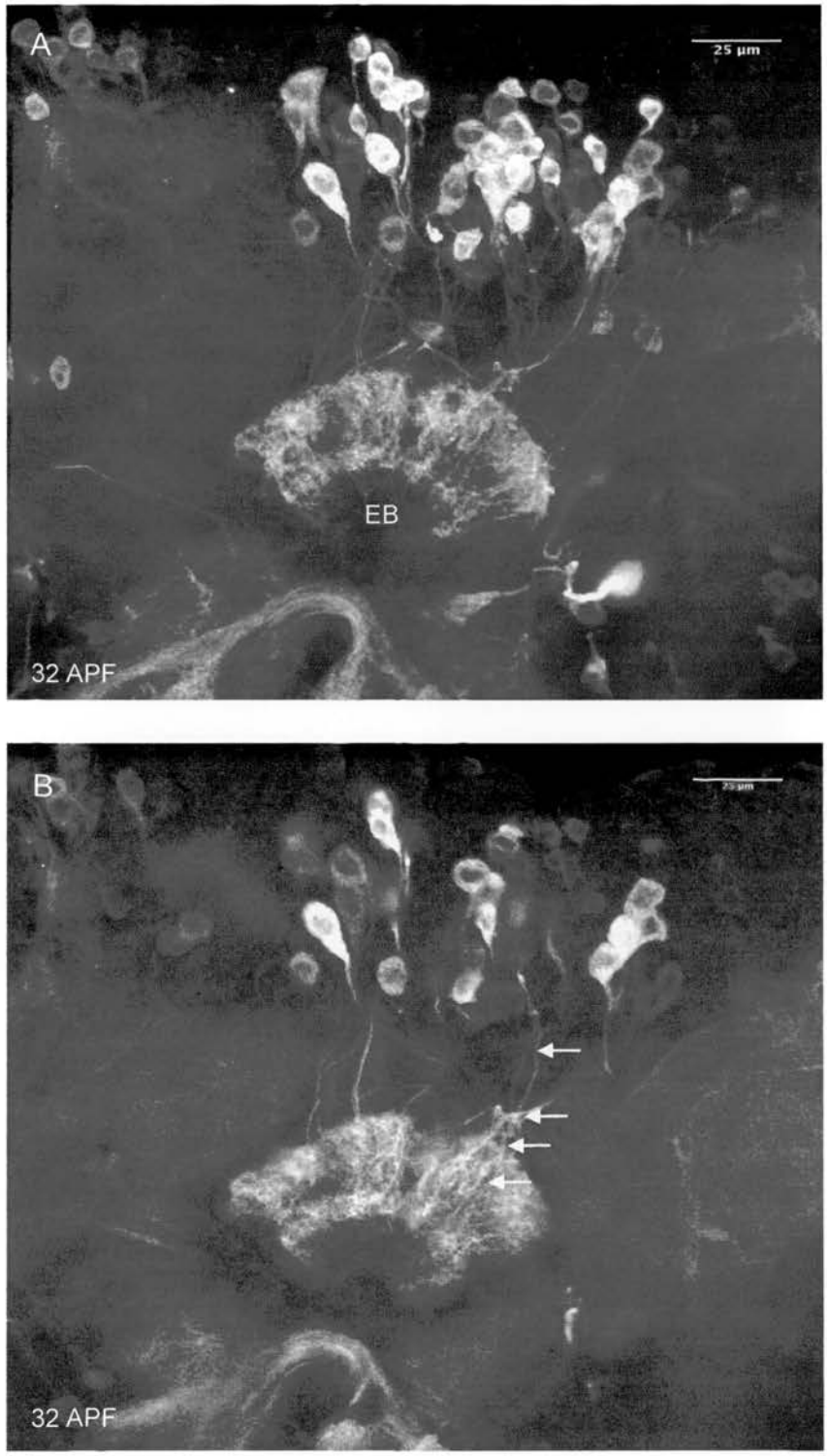

Figure 4.13: *fb-eb* neurons during mid Central Complex development as visualised with line c159b. A, Clusters of four neurons from the dorsal cortex each share trajectories to the FB. **B,** *fb-eb* trajectories from each cluster innervate a specific FB segment (only some central trajectories visible here) then continue to the EB. A columnar element extends ventro-anteriorly to the dorso-posterior EB from each segment that can be traced back to Perikarya (arrowheads). This evidence suggests these are *fb-eb* neurons in addition to Pontine neurons.

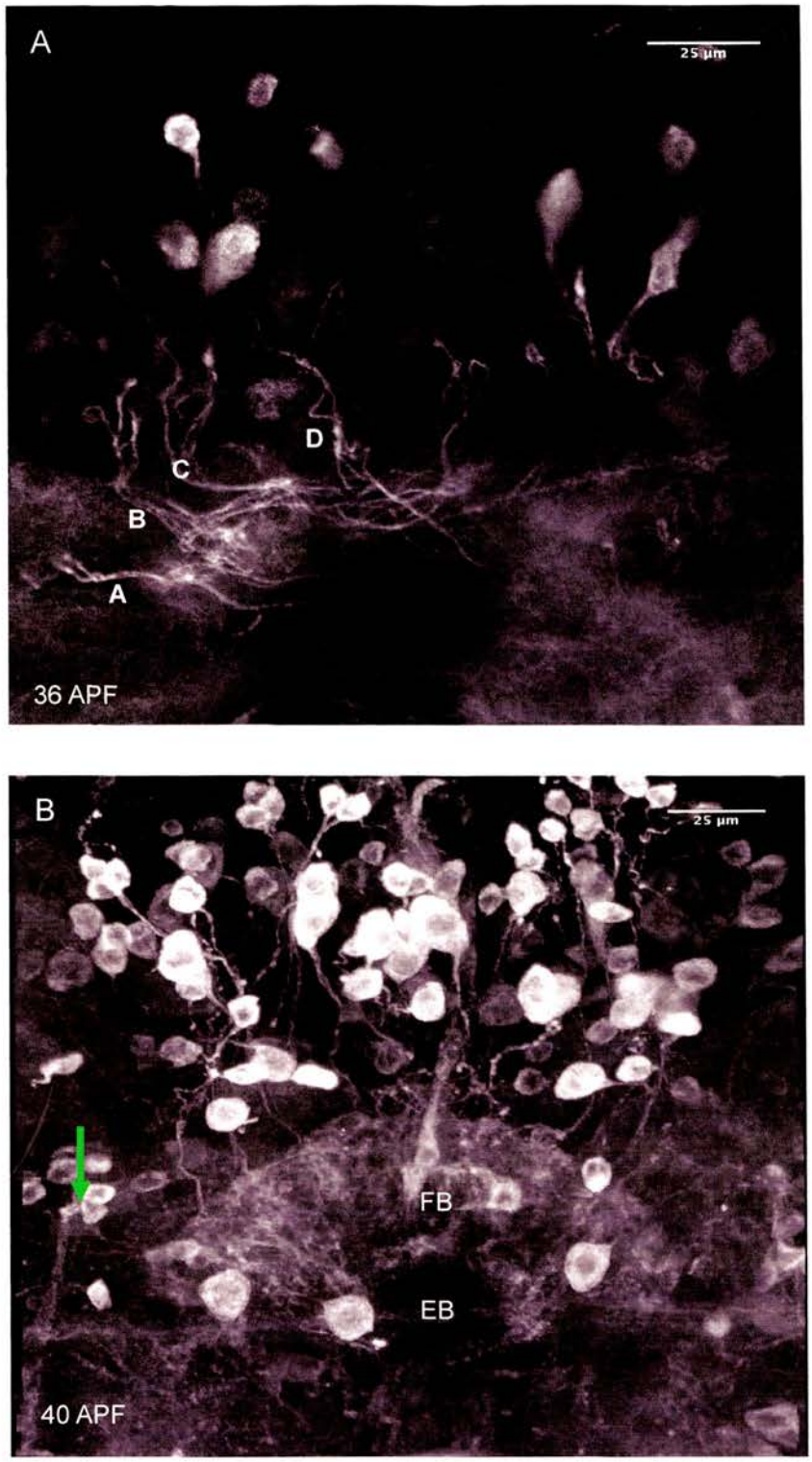

Figure 4.14: Pontine and *fb-eb* neurons during late Central Complex development as visualised with line c159b. A, Bundles of fibres innervating segements of the FB (only A-D shown) with some then crossing contralaterally. **B**, Cells innervating the FB and then the EB now revealing the EB ring. This line appears to show expression in both Pontine and *fb-eb* neurons. Clusters of these neurons lie dorsally and laterally (arrow) to the FB.

A

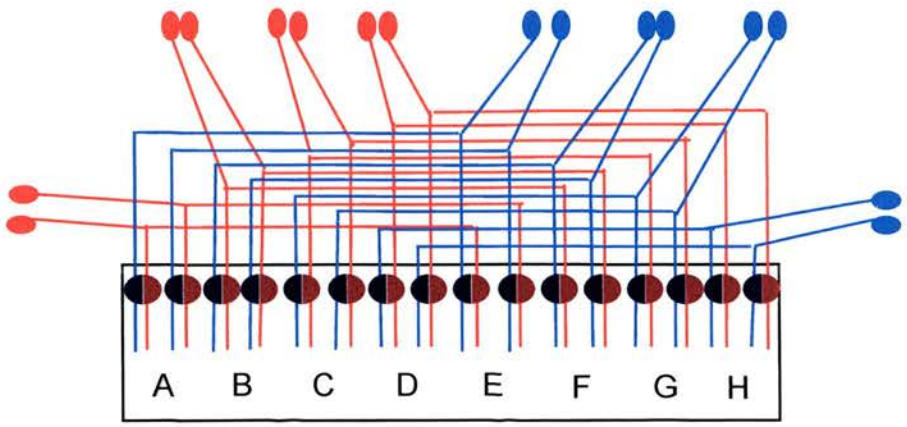

B

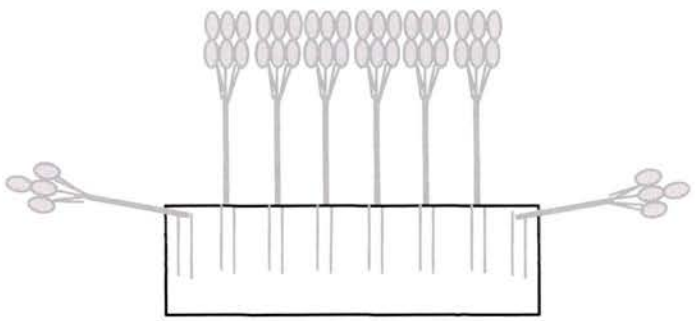

Figure 4.15: Known types of Pontine neurons also seen in this study. Numbers of neurons (16 per set) are according to the data of this thesis not previous publications. **A**, P*cd* neurons target segmentsantero- ventral to the cell cluster then turn medially to target contralateral FB segments four removed. **B**, P*l* neurons target antero-ventrally to specific segments.

4.3.8 P{Gal4} line c255

Adult

Expression was elevated in the Superior arch commissure and LTR. Two types of Large field neurons were detectable, these were F*m* neurons entering the EB canal and arborising in layer two [Figure 4.2(L)] and the type B R neuron, ExR1, that displays dense spiny arborisations in the FB, VBO and EB (Hanesch et al., 1989). Axons of ExR1 arborise in the upper FB then encircle the EB, where neurites branch off the axon at regular intervals innervating the EB in a radial pattern where they arborise [Figure 4.3(B)]. Approximately 32 (n=4) neurites (or possibly bundles of neurites) were counted innervating the EB. P{Gal4} driven *Dscam* expression was detected clearly in conjunction with the pattern of the ExR1 neuron, showing arborisations in the upper layers and LTRs [Figure 4.6(B)].

Development

During early CC development (4-16 APF) only Large field neurons, characterised by arborisations outside the CC, can be seen [Figure 4.16 (A,B) and Figure 4.17(A,B)]. By 20 APF clusters of cells in the dorsal cortex can be observed with axons projecting to the dorsal FB. By 24 APF these can clearly be seen arborising in individual FB segments as shown in Figure 4.18. Axons from clusters of 4-6 Perikarya project ventro-anteriorly to segments B-G in the dorsal FB. Perikarya of axons targeting segments A and H are located medio-posterior to the FB [Figure 4.19(A)]. Columnar projections within segments can be seen projecting to the early EB ventro-anteriorly. These morphological patterns are reminiscent of those of the Pontine neurons observed in development using enhancer trap line c159b. There seem to be two different sets of Pontine neurons with line c255, showing both columnar (P*l*) and contralateral (P *cd*) trajectories [Figure 4.19(B)] but no *fb-eb* neurons. Equally, the number of perikarya supports the theory that two sets of Pontine neurons are present. Expression is detected

in the Pontine neurons earlier in line c159b than in c255.

In addition to the Pontine neurons, line c255 also revealed a type of Large field neuron during development, the rarely observed (Hanesch et al., 1989) type A R neuron, ExR1. The ExR1 axon projects from the Pars intercerebralis (Hanesch et al.,1989). Tracing the precise projection times of this neuron was difficult due to the presence of arborisations from the Pontine and *fb-eb* neurons in the FB. It may be that the Large field neurons observed from 4-16 APF [Figure 4.16 (A,B) and Figure 4.17(A,B)] are actually the early projections of the ExR1 neurons. The positions of the Perikarya, arborisations external to the CC and projections to the FB support this suggestion. This would indicate that outgrowth of the ExR1 neuron initially occurs early during CC development (4-16 APF) then targets the EB later in CC development. The axon can be seen targeting the EB between 28-32 APF and first traverses the dorsal FB crossing contralaterally to the lateral edge of the FB before re-tracing its projection in a transverse direction across the length of the FB, through the LTR and to the VBO as shown in Figure 4.20 (A,B). The ExR1 axonal trajectory appears complete by 40 APF. The completed form is shown in Figure 4.21. This suggests that the targeting period for the ExR1 neuron may be 32-36 hours long. Axons turn antero-ventrally in the medial FB to encirlce the EB branching at regular intervals to innervate the EB as shown schematically in Figure 4.22.

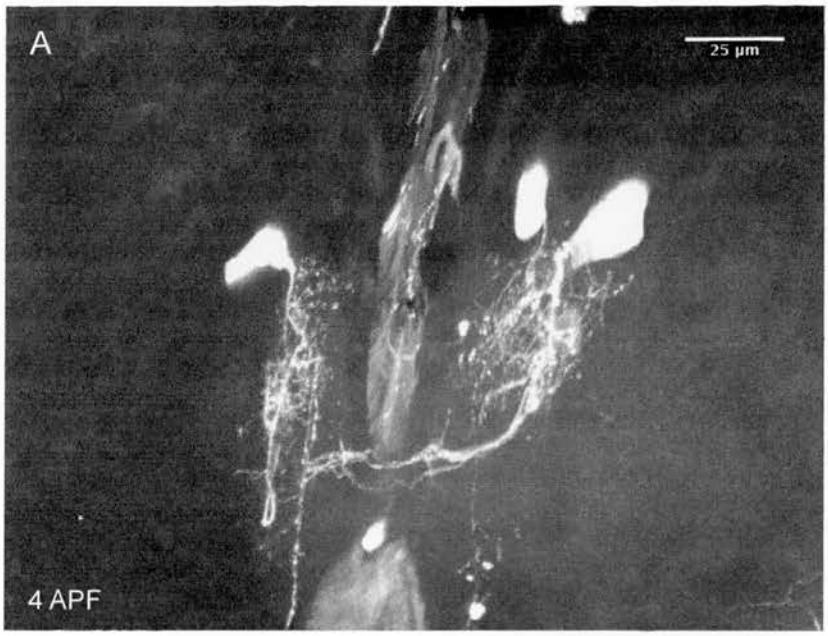

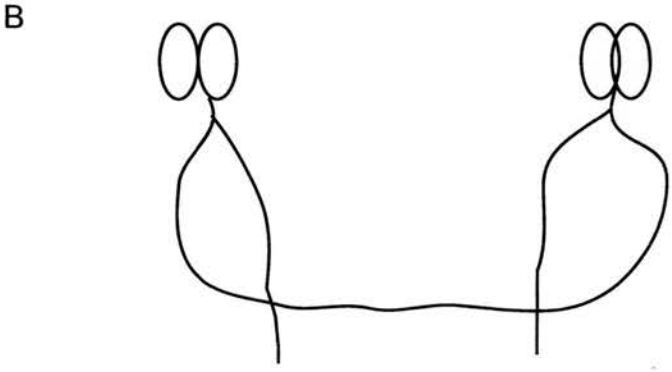

Figure 4.16: ExR1 neurons visualised with enhancer trap Line c255 at 4 APF. A. Two cells per hemisphere project ventrally, arborise then make a medial turn to traverse the midline.These may be the early projections of the ExR1 neurons. **B**, Schematic showing trajectories.

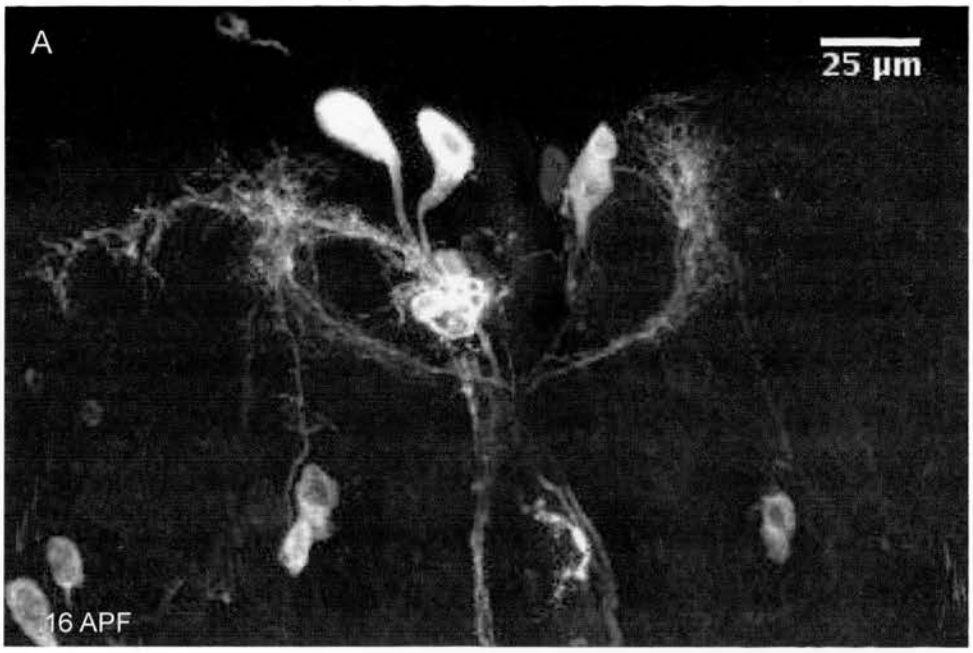

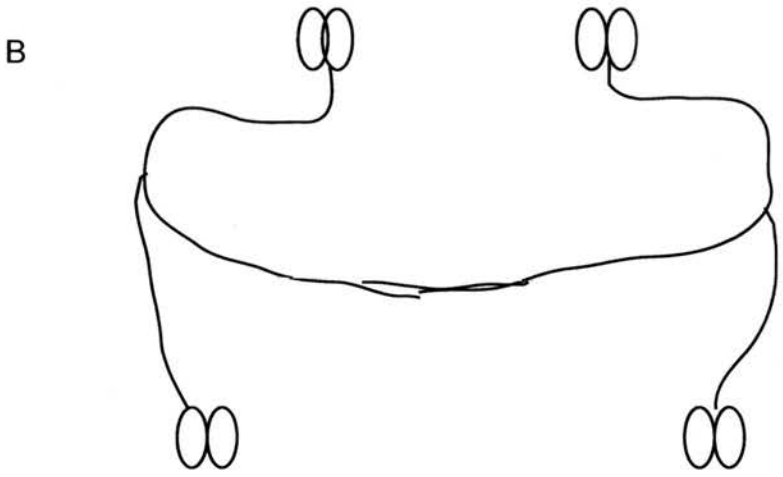

Figure 4.17: ExR1 neurons visualised with enhancer trap Line c255 at 16 APF. A, expression pattern is similar to 4 APF with additional cells ventral to the early arborisations. **B**, Schematic of projections.

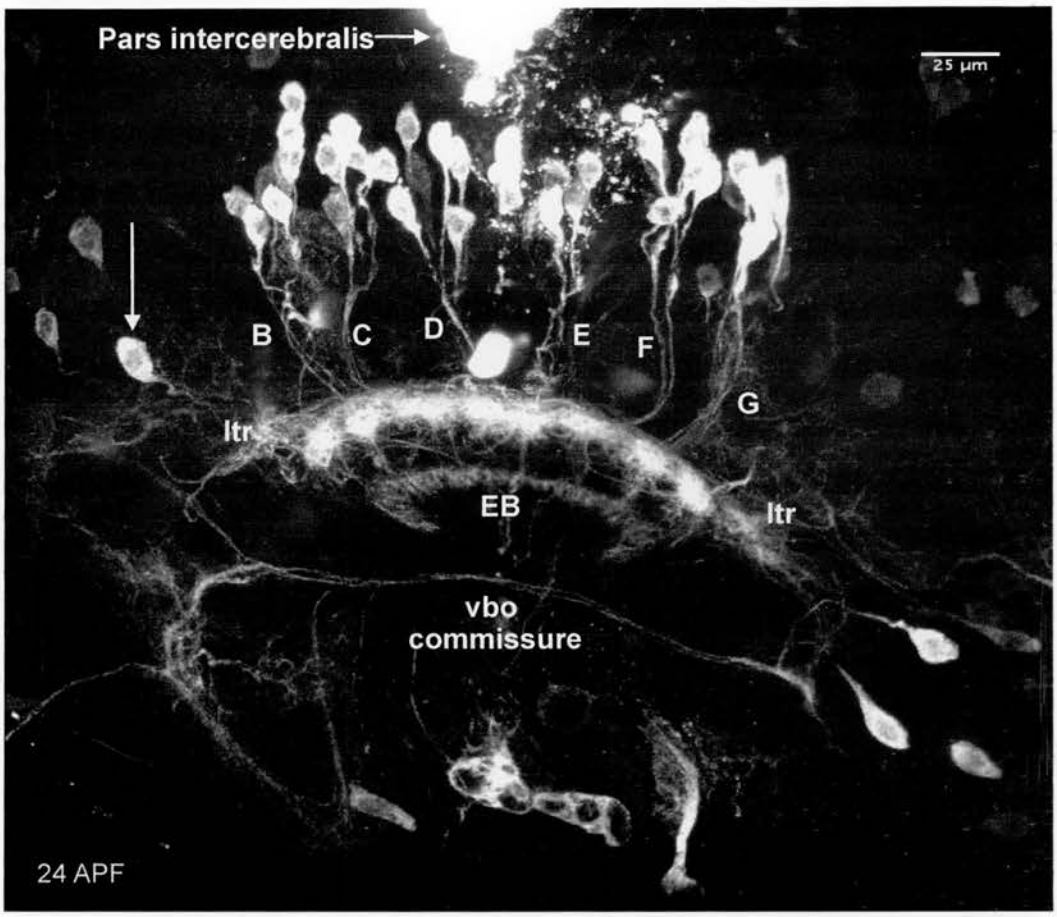

Figure 4.18 : Pontine neurons visualised with enhancer trap line c255 at 24 APF. Axons from clusters of 4-6 neurons each lie dorsal to the FB and share the same ventro-anterior trajectory targeting segments B-G of the FB. Segments A and H are not innervated by a large cluster of cells from the dorsal cortex. Neuron clusters targeting the A and H segments are not visible in this image but are shown in Figure 3.19 (A). A neuron per hemisphere can be seen innervating segment A of the FB laterally (arrow). Eight zones of arborisation are visible in the dorsal FB from the Pontine neurons due to their initial projection pattern. Columnar elements can be seen projecting anterio-ventrally from these arborisations towards the developing EB but are actually terminating posterior to the EB. The unfused EB can be seen ventral to these arborisations due to staining of the ExR1 neuron that is also marked by this line. ltr, Lateral Triangle; vbo, Ventral bodies. EB, Ellipsoid body.

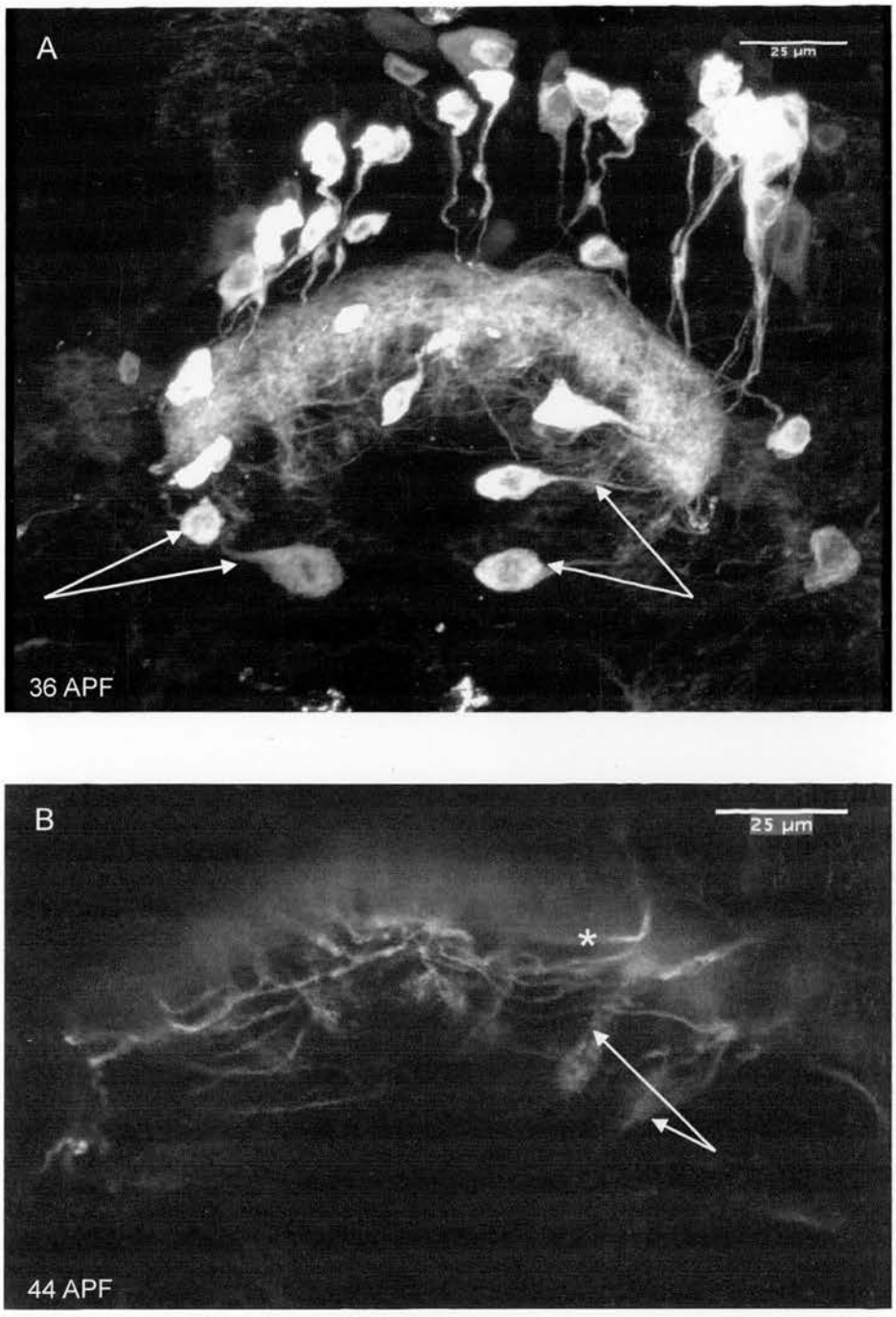

Figure 4.19: Pontine neurons visualised with enhancer trap line c255 during late Central Complex development. A. In addition to clusters of neurons targeting segments B-G from the dorsal cortex, sets of three neurons can be seen targeting the lateral segments (A and H) in this image (arrows). The ExR1 neuron is also faintly visible. **B**, Pontine neurons can clearly be seen traversing segments within the dorso-posterior FB (*asterix) and forming columnar elements (arrows) within segments.

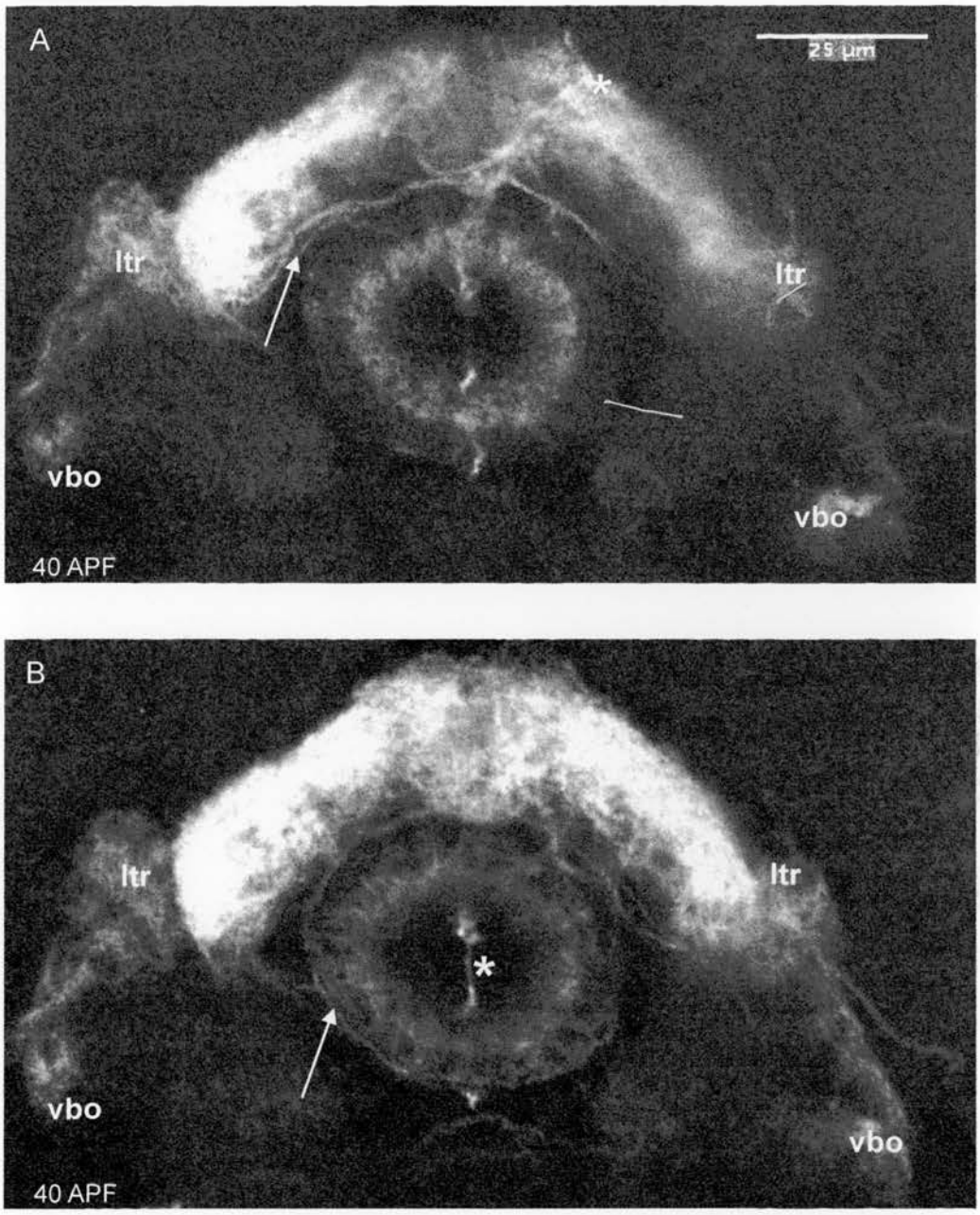

Figure 4.20: ExR1 neuron projections visualised with enhancer trap line c255. Sections from the same preparation. **A**, The ExR1 neuron can be seen crossing into the FB in a ventro-medial direction (*asterix) then traversing the dorsal FB and performing 180° turn creating a loop at the lateral edge (arrow). **B**, In this view the ExR1 neuron can be seen encirling the EB and sending processes to innervate the EB. In both images arborisations can be seen in the LTRs and VBOs. The asterisk (*) is an F*m* neuron targeting the FB through the EB canal.

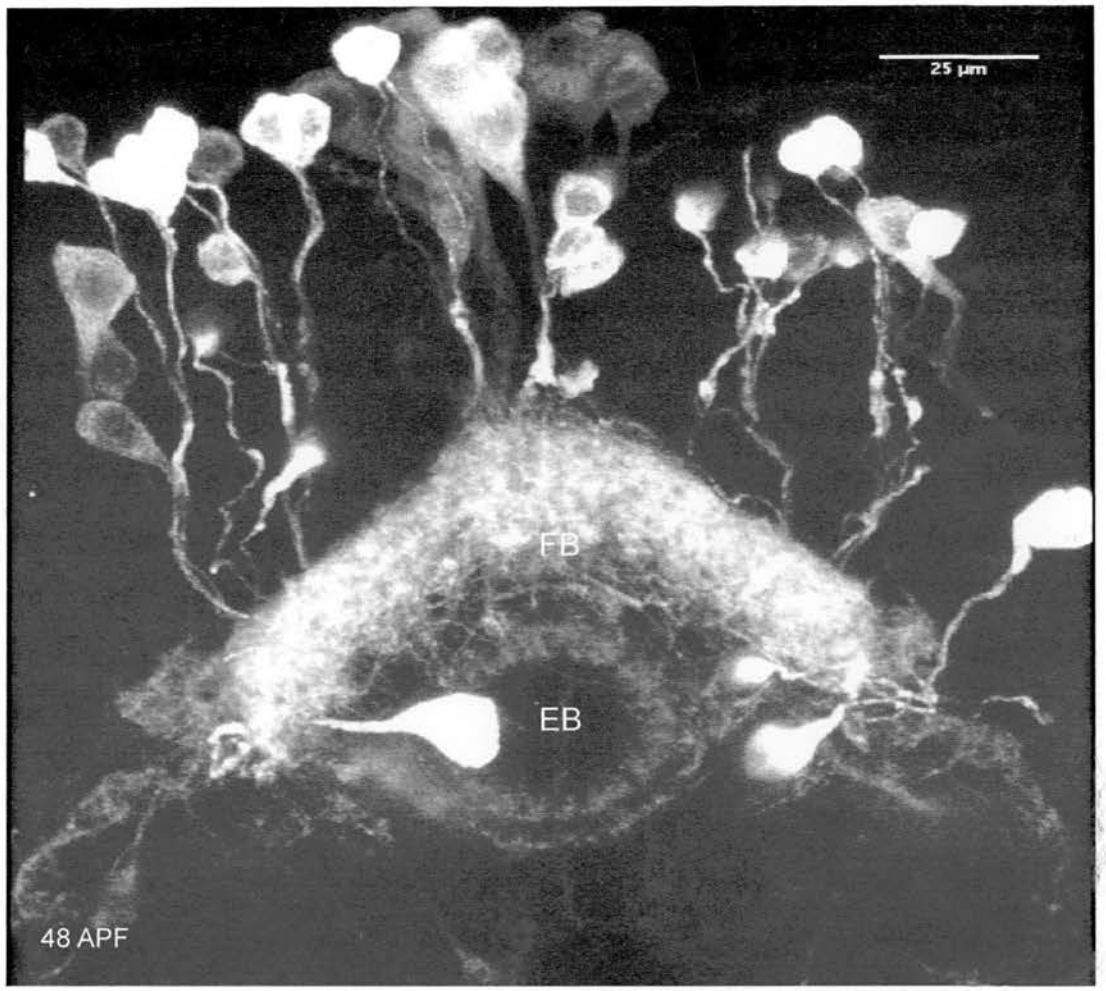

Figure 4.21: Final Pontine and ExR1 projections visualised with enhancer trap line c255. Arborisation in the Superior arch is clear from the ExR1 neurons and Pontine neurons. The EB is revealed by the ExR1 neurons.

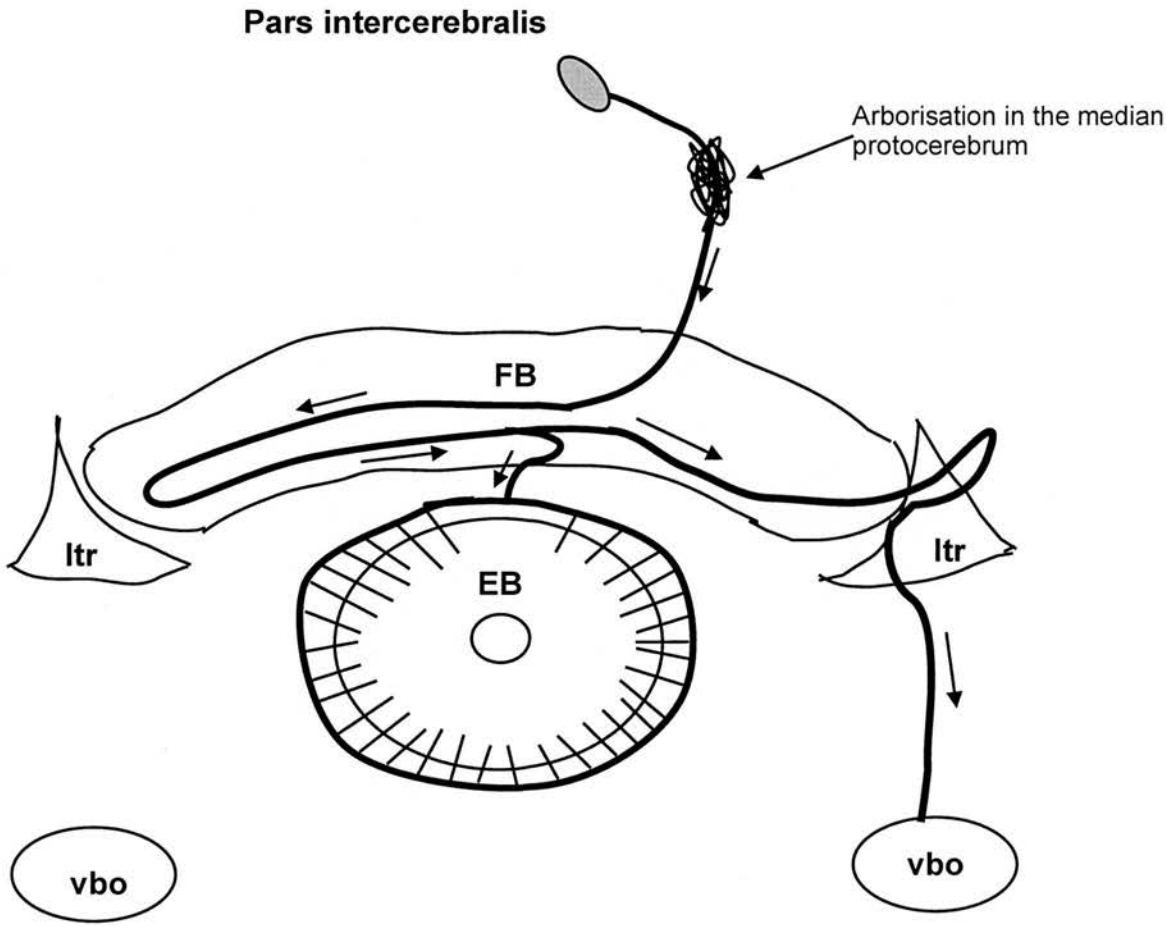

Figure 4.22: Schematic of the proposed ExR1 neuron trajectory at 48 APF. The ExR1 neuron arborises in the median protocerebrum then continues ventrally to innervate two sub-structures of the CC, the FB and the EB. The ExR1 neuron branches in the FB sending one axon to the LTR and VBO and the other to encircle the EB. 32 branches innervate the EB from the ExR1. The perikarya was not traceable though several cells in the Pars intercerebralis show reporter expression. The perikarya are known to be in this region (*Hanesch et al., 1989*). ltr, Lateral triangle; vbo, ventral bodies; FB, Fan shaped body. The ExR1 trajectory is shown by the arrows.

4.3.9 P{Gal4} line c465

Adult

Line c465 displays the most dense staining of all P{Gal4} lines used in this study. This line revealed three types of Small field neurons; the VFS, HFS and the *fb-eb* neurons. Fibres of the HFS are shown in Figure 4.2(N). These fibre systems dominate the CC revealing the PB and the NO in addition to the FB. Of the Large field neurons, c465 revealed what appeared to be the Type A R2 neurons characterised by axons growing from the EB canal outwards and arborising in the anterior EB. Another subtype of Type A neurons, the R3 neurons that are characterised by axons from the EB canal and arborisations reaching both the distal and proximal EB, as shown in Figure 4.3(C). Several additional Perikarya for cells surrounding those of the CC were visible making it difficult to discern exact cell types. It is possible that other cell types are included in this expression pattern but these were not identifiable in these preparations.

Development

The HFS is visible from 4 APF consistent with the data from α-Echinoid staining in the previous chapter. The HFS can be seen targeting the FB by 8 APF, as shown in Figure 4.23(A). Fibre bundles have reached the VBO by 16-20 APF, consistent with data from the previous chapter. In addition, c465 is expressed in the VFS also from 4 APF. It was difficult to isolate the VFS and HFS fibres, though the VFS appears to share the same temporal developmental projection characteristics as the HFS as it has also targeted the NO by 16-20 APF as shown in Figure 4.23(B). Both fibre systems can be seen at 28 APF [Figure 4.24 (A)]. At 24 APF R neurons can be seen targeting the unfused EB [Figure 4.24(B)]. At 12 APF *fb-eb* can be seen targeting the FB consistent with lines c159b. The R neurons are visible showing an unfused EB from 28 APF onwards, consistent with other lines. The R neurons and fused EB are shown at 40 APF

in Figure 4.25.

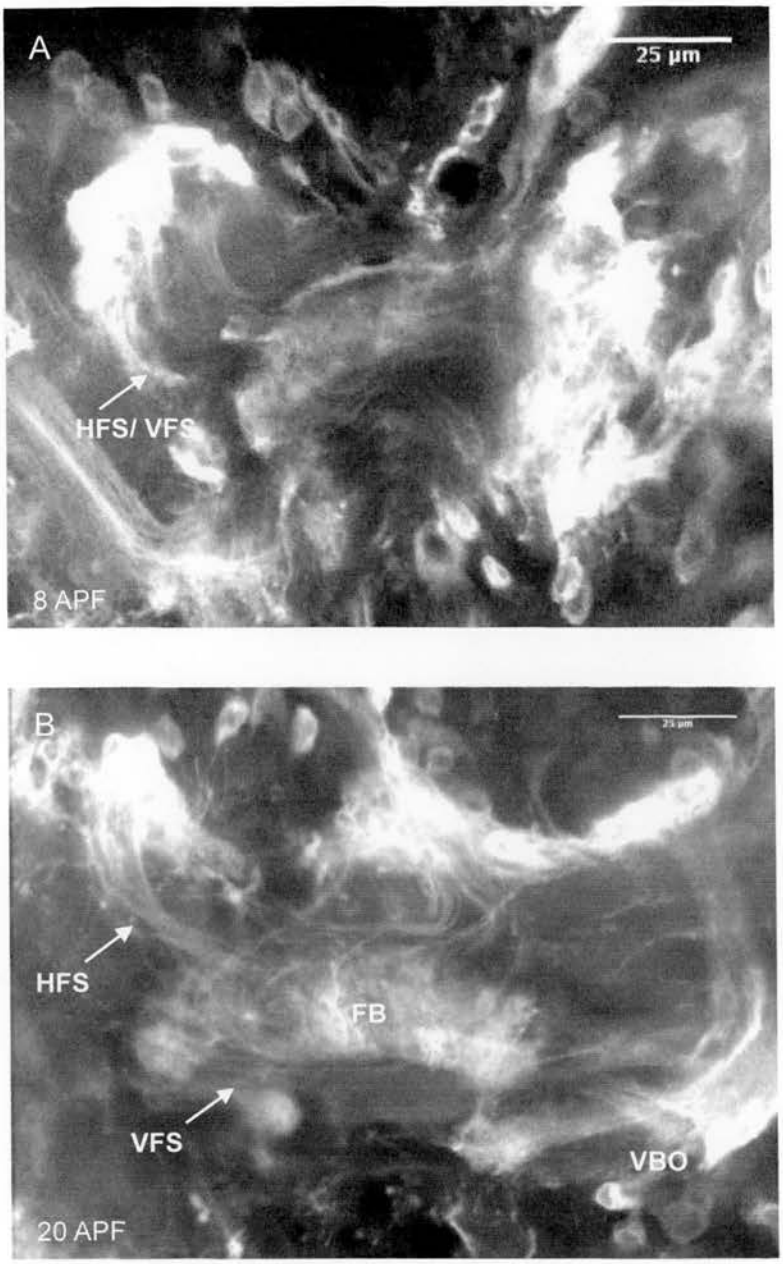

Figure 4.23: Development and projections of the HFS and VFS in early Central Complex development visualised with enhancer trap line c465. A, Perikarya and fibre of the HFS and VFS can be seen entering the FB at 8 APF (arrow). **B**, Fibres of the HFS can be seen reaching the VBO at 20 APF. Fibres that can be seen targeting the Noduli are the VFS.

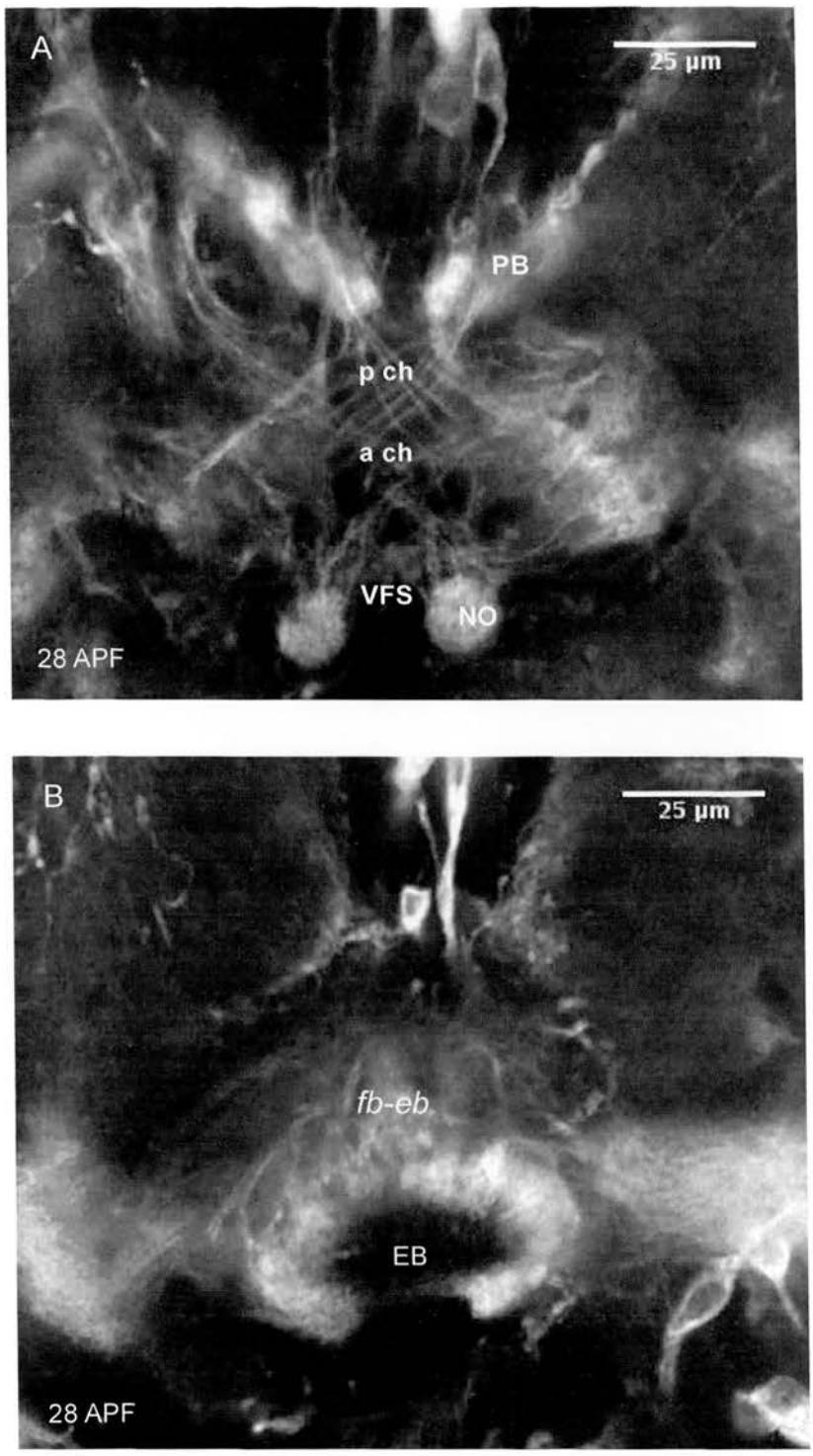

Figure 4.24: The HFS, VFS and *fb-eb* neurons during mid Central Complex development as visualised with enhancer trap line c465. A, Both the VFS and the posterior and anterior chiasma of the HFS can be seen clearly. **B**, *fb-eb* neurons can be seen targeting the unfused EB. p ch, posterior chiasma; a ch, anterior chiasma; NO, noduli.

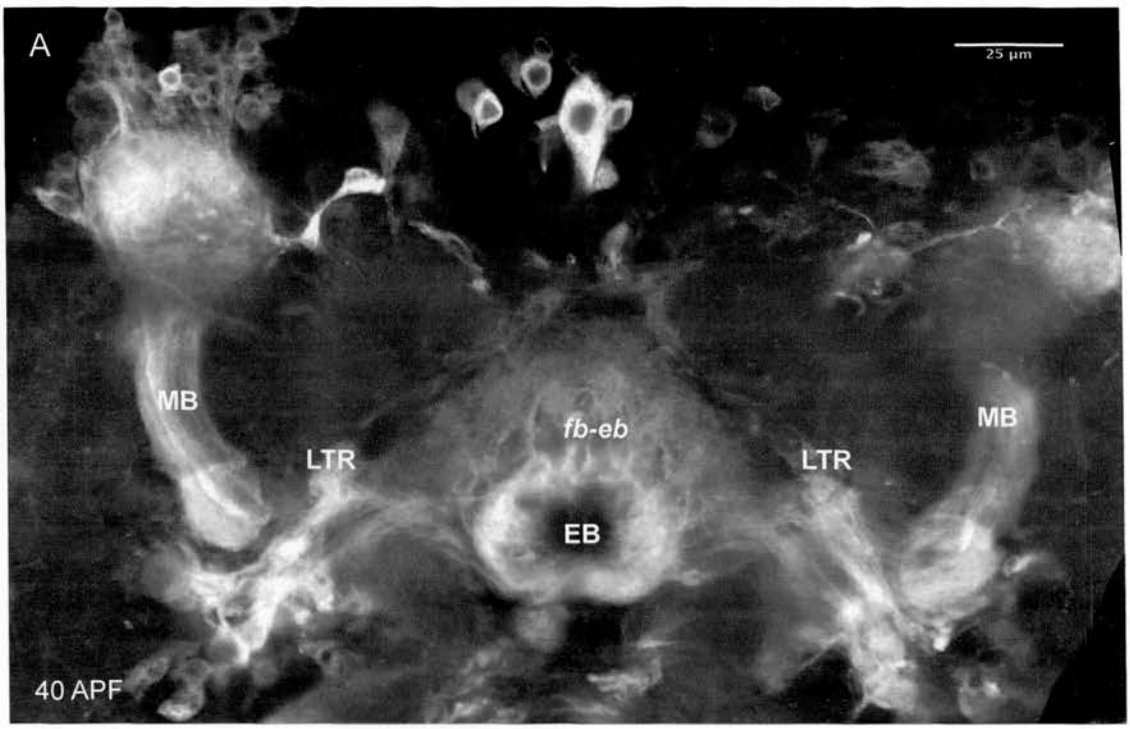

Figure 4.25 : The Type A R neurons and *fb-eb* neurons visualised during late Central Complex development by enhancer trap line c465. The R2 and R4 neurons are seen projecting to the LTRs and then the formed EB ring. The *fb-eb* neurons can also be seen targeting the dorsal EB. Neurons of the Mushroom bodies can be seen lateral to the EB ring. LTR, Lateral triangles.

4.4 Expression patterns of enhancer trap lines in the FB

In all observed specimens neurons were revealed as isomorphic sets using the enhancer trap lines. These were symmetrical and neuron numbers varied depending on the type observed. No neurons were observed individually. This allowed for a unique analysis of the adult and developing CC and revealed a large volume of new data.

4.4.1 Adult expression patterns in the whole brain

There was a high degree of overlap between expression in the FB and expression in the Optic lobes consistent with the study by Liu et al. (2006). In all cases expression in the central brain was not exclusive to the CC. In lines such as 52y and c255 the majority of expression in the central brain was restricted to the Central Complex. Conversely, lines such as c465 had a more distributed expression pattern. In six of the fourteen lines there was also expression in the Mushroom bodies though detailed patterns are not included in this study.

4.4.2 Adult expression patterns in the Central Complex

In *Drosophila*, 32 categories of small field neurons and 21 categories of large field neurons have been identified in the CC (Hanesch et al. 1989). The identified neurons mentioned in this thesis adhere to that morphological nomenclature and are presented in Tables 4.1 and 4.2. Further categorisation of the R neurons and Pontine neurons has been initiated in this study to further clarify neuron types. In some cases detecting Small field neurons was problematic due to obstruction by arborisations in the same area, therefore they may have been overlooked. All neurons observed in this study were as sets. All observed small field neurons appeared to exist as isomorphic sets of 16 (HFS, VFS, Pontine and *fb-eb*). Large field neurons varied as to the number of neurons in a set and were predominantly difficult to count due to staining density or close packing of perikarya. For sets of isomorphic neurons, lines 23y and c465 showed

expression in the HFS and VFS and subsequently were the only lines to reveal the arborisations of the PB. Three of the P{Gal4} lines revealed isomorphic sets of Pontine neurons. Lines c255 and c61 also isolated an ExR1 and ExR2 neurons respectively. These neuronal types were rarely seen in the Hanesch study (1989) and were observed here as sets of four. The majority of the enhancer trap lines showed expression in the Large field F neurons (except line c159b), some lines exclusively so. A variety of F neurons were represented, entering the FB in sets and often linking the CC with external areas by arborising in other regions of the central brain. The number and variety of F*l* neurons is unknown and it was not possible to ascertain if the same F*l* neurons were labelled when comparing patterns between enhancer trap lines.

Identifying layers of the FB has proven difficult. The layered appearance has been attributed to stratification of the Large field neurons along the transverse axis (Strausfeld 1976, Hanesch et al, 1989). On several occasions layers between these, termed 'half layers' have been detected thus it is often difficult to distinguish a particular layer (Hanesch et al., 1989). References to layers in this thesis are therefore tentative. The F neurons represented by the enhancer trap lines project tangentially to the upper (layers five & six) and lower (layers one & two) layers of the FB, with very few lines showing expression in the middle layers.

The enhancer trap lines isolated in this study were selected for their expression in the FB but the identified neurons were not exclusive to this sub-structure, as expected. Several lines also innervated the other three sub-structures. Line c465 is the only line expressed in all four sub-structures and is the only enhancer trap line marker for the PB in this study. Line 210y is the only other line that showed faint expression in the NO.

Four of the enhancer trap lines revealed dendritic patterns, visualised as a granular appearance of Dscam::GFP staining. These dendrites were mainly restricted to arborisations of Large field neurons outwith the CC or regions adjacent to the Central Complex such as the LTRs. Dscam was also detected on the Perikarya and axons of the

R neurons and revealed the formation of a zone of arborisation in the LTRs from these cells. The F*l* neurons also showed dendritic arborisations in the LTRs as well as the Superior arch and the ring of the EB. There was faint detection of Dscam in other layers of the FB from F neurons.

4.5 Timeline of development for the Central Complex

4.5.1 Large Field Neurons

The data generated from the enhancer trap study provided developmental data for 9/21 types of Large field neurons. The timeline of development is represented schematically in Figure 4.26 and in relation to enhancer trap lines in Table 4.2. Arborisations within the FB from the F*l* neurons commenced at 24 APF. The F*m* neurons were observed projecting to the FB through the early (unfused) EB canal from 28 APF using line c255 but exact projections and arborisations from these neurons were not resolvable in this study.

The characteristic ring (R) neurons of the EB were visualised with lines 52y and c465 during mid-late metamorphosis. The data showed that the EB is fully formed by 32 APF, consistent with previous observations (Renn et al., 1999). The axons of the type A R neurons are first visible arborising in the LTRs at 24 APF and are starting to adopt the characteristic ring shape by 28 APF, though the EB is still unfused at this point. Defining the exact time point of initial axon outgrowth for type A R neurons was not possible though this evidence suggests it is between 20-24 APF. Line c255 isolated an ExR1 neuron which has not been previously detected using enhancer trap studies. This neuron was first detected targeting the EB at 24 APF, consistent with the temporal differentiation of the EB. The ExR1 neuron completed projections to final EB targets by 40 APF. Tracing the axon to the Perikarya (situated near the Pars intercerebralis) was

not possible due to dense staining in the Central brain but it is thought that the axons from ExR1 neurons initially start to project as early as 4 APF.

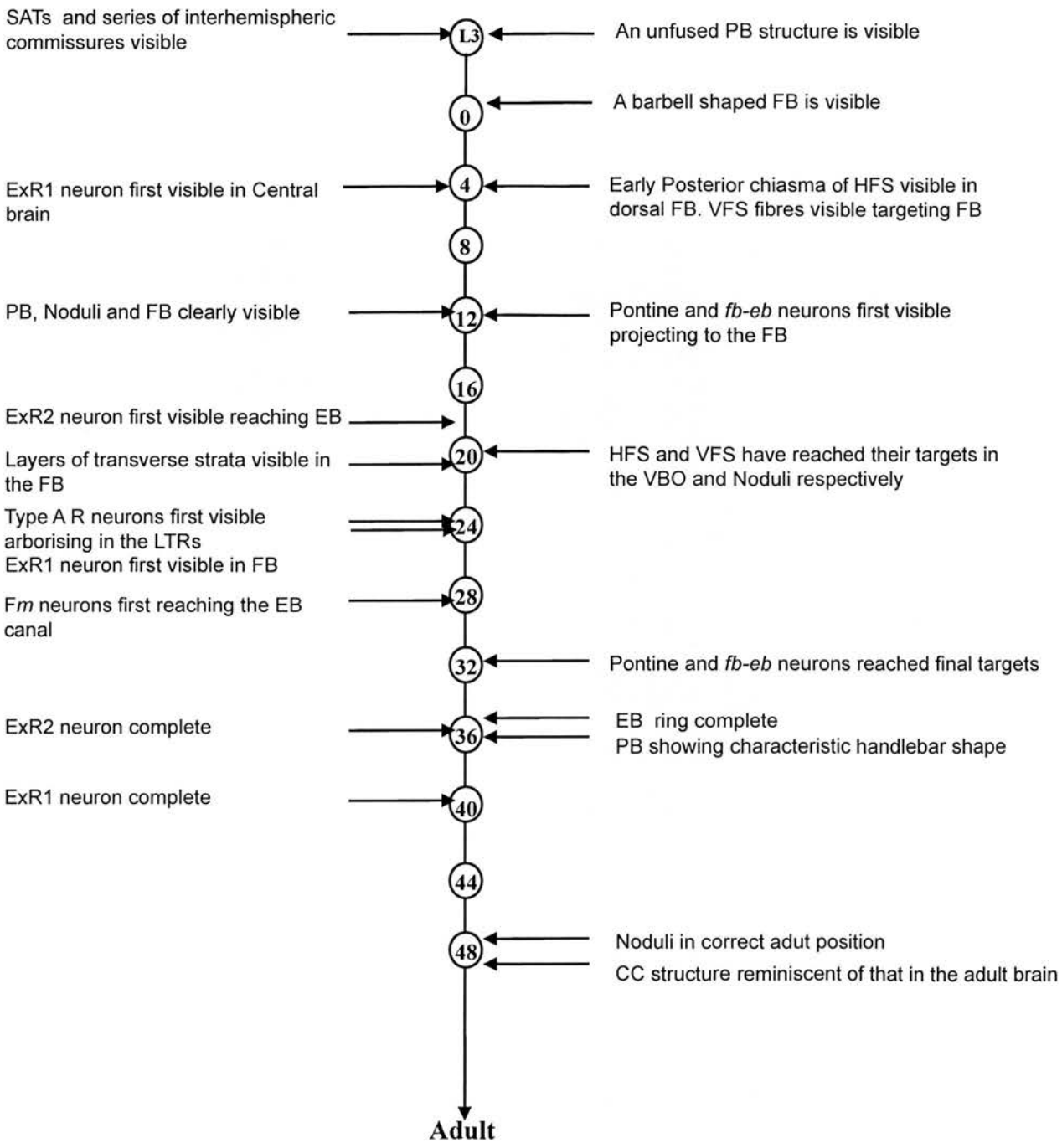

Figure 4.26: Developmental timeline of major Central Complex neurons. Numbers in the centre line refer to hours after puparium formation (APF). Large field neurons are detailed on the left and Small field neurons on the right of the line. PB, Protocerebral bridge; SATs, Secondary neuron axon tracts; FB, Fan shaped body; HFS, Horizontal Fibre System; VFS, Vertical Fibre System; LTR, Lateral Triangle; EB, Ellipsoid body.

The ExR2 neurons were observed using line c61. These neurons have not been well characterised or detected in previous studies (Hanesch et al., 1989; Renn et al., 1999). In addition the location of the ExR2 Perikaryon has not been previously reported. This study determined that the ExR2 Perikarya lie in the posterior-medial cortex. The ExR2 neurons project between 16-36 APF.

4.5.2 Small Field Neurons

The HFS can be seen at 2 APF forming the Posterior chiasma using α-Echinoid staining. This expression pattern of c465 revealed the early HFS at 4 APF using line c465 therefore confirming the previous observation. The fibres of the HFS projected to their final targets over the next sixteen hours reaching final targets in the VBO at 20 APF. Line c465 also showed expression in the VFS which had a similar timeline of development to the HFS.

The enhancer trap lines facilitated the study of the Pontine and *fb-eb* neurons which had not been revealed by the candidate genes in the previous chapter. The Pontine neurons are intrinsic to the FB and connect both segments and layers. Three lines, 52y, c159b and c255 revealed isomorphic sets of Pontine neurons. One of these isomorphic sets has previously been reported, the other two types have not been described as sets (Hanesch et al., 1989). Line 52y expression in the Pontines was restricted to the adult brain. The Perikarya of the Pontine and *fb-eb* neurons can be seen from 20 APF with line c255 but earlier (8-12 APF) for these neurons when visualised with line c159b.

4.6 Discussion

4.6.1 The Enhancer trap lines for anatomical analysis

This chapter isolated a set of enhancer trap lines expressed in the CC, determined which of these were expressed throughout CC development and utilised these lines to ascertain when certain types or populations of neurons reached their final targets. In addition to the results from the previous chapter, this data allowed a timeline of development for the CC to be generated [Figure 4.26].

The advantages of using the enhancer trap lines for an anatomical study have been demonstrated here and offer an alternative approach to classical methods of analysis such as Golgi staining. Several lines have been isolated that are expressed in specific sets of neurons allowing a detailed study of these neurons that is traceable throughout development. This has permitted visualisation of subsets of fewer cells than other techniques. Due to the reliable nature of enhancer trap technology the patterns are easily replicable allowing several specimens to be visualised at any stage. In contrast to some antibodies of the previous chapter, Perikarya, axons and dendrites are all always visible using this method and a variety of reporters allow analysis of different parts of the neuron. The expression patterns reveal a common genetic mechanism between or within morphologies which permits us to hypothesise a common functionality. This enhancer trap study also revealed certain neurons that had proved difficult to isolate with Golgi staining (Hanesch et al., 1989) or a previous enhancer trap study on the EB (Renn et al., 1999), such as the ExR1 and ExR2 neurons. In addition, novel lines were discovered that further support the Renn et al. (1999) study.

There are some limitations to the enhancer trap approach. Due to the genetic commonalities, several sets of cells were stained making visualisation of individual cell patterns problematic. Resolving precise patterns of connectivity for sets of neurons

therefore proved difficult. Conversely, the study of CC neurons with enhancer trap lines during development facillitated visualisation of some neuron types that were not in isomorphic sets (ExR1, ExR2) as arborisations external to the CC had not yet formed to obscure these tracts. An additional drawback was that enhancer trap lines may have prevented visualisation of smaller CC cell types, therefore the characterisation of some lines with wider dispersal of expression patterns may not be complete. It was not feasible that the enhancer trap lines in this collection would represent every type or subtype of known CC neuron, therefore this study is not considered comprehensive. A combination of Golgi staining, enhancer trap and antibody analysis could produce a complete analysis in future, but that was beyond the scope of this study.

Interestingly, expression patterns in the enhancer trap lines do not maintain the same cellular pattern throughout metamorphosis and into adulthood as previously reported (Ward et al., 2002). Expression often shifts to different cells (or none at all) during CC development compared to the adult pattern. Although the majority of lines used in this developmental study do maintain expression in specific cell types at least during their development, even these lines often lose/gain expression in a small number of cells as shown in Table 4.1. This may be due to the requirement of this particular transcriptional mechanism for development in certain neurons only, therefore ceases in the adult brain. It was for this reason that only lines that maintained expression in specific cell types were used for developmental analysis from the prepupal stage. Where is was possible to compare, temporal expression results in subsets were consistent with antibody staining or concurred with a previous report (Renn et al., 1999). It is likely that the enhancer trap expression patterns reveal an accurate portrayal of CC development, as in the majority of cases early axonal projections were detected. The shift in expression of enhancer trap lines provides an insight into the genetic activity of development and function, showing a genetic relationship between the two. Due to the changeable nature of P{Gal4} expression it was not considered tenable to use these lines to trace the lineage of CC neurons because single neuroblasts would be difficult to identify.

Analysis of structural development during metamorphosis facillitates the study of connectivity due to the under-developed state of neurons in the brain. Classification of cell types by enhancer trap technology can be done as subsets of cells or in some cases individual neurons. In particular, it has been possible to isolate and trace individual Large field neurons and also revealed novel sets of Pontine neurons and their targets. From the 300 original lines, 14 were isolated in this screen for FB expression. In terms of neuronal expression, all lines highlighted various Large field neurons either in the adult or at some point during CC development. This study revealed a variety of F neurons arborising in several FB layers. It was not possible to compare F neurons between lines. This genetic segregation into sets by enhancer trap lines could indicate a series of neuronal subtypes for the F*l* neurons, of which there has been no further classification to date.

The indication of a common genetic mechanism between cell morphologies isolated by the enhancer trap lines was illustrated by the identified Pontine neurons revealed by three lines (52y, c159b and c255). In c255 and c159b, clusters of neurons in the posterior cortex initially projected to one segment in the FB. From this point neurons either remained within the segment, connecting layers or projected contralaterally, joining two segments on opposing sides of the midline. The Pontine neurons visualised with line 52y were slightly different, entering at the lateral FB segments. The Pontine neurons isolated by all lines appeared as isomorphic sets of 16 neurons. A previously reported set of Pontine neurons have been described as an isomorphic set of eight neurons (Hanesch et al., 1989). This study has now identified three different sets of 16 Pontine neurons that have been named P*cv*, P*l* and P*cd* according to their trajectories. In addition, in line c159b the evidence suggests that two of the four neurons in each cluster shown by these lines are *fb-eb* neurons, targeting the FB with the same trajectory and sharing a common genetic mechanism. This suggests that the *fb-eb* neurons also exist as isomorphic sets of 16 neurons and that they have a genetic relationship with a set of Pontine neurons (P *cd* in line c159b) and the HFS and VFS (c465).

Classification of cells that comprise the CC is problematic as no study has succeeded in determining a comprehensive set of cell types. In the *Drosophila* CC over 50 cell types have been identified (Hanesch et al.,1989) though this also includes cell types outwith the CC joining satellite regions such as the VBO and LTR. The unaccounted for cell types in this study are mainly those that innervate the PB or NO, sub-structures that the enhancer trap lines were not selected for here. Subsequently, some neurons types may have been overlooked. The total number of subtypes in the classified sets of neurons is unknown, though in this study the enhancer trap lines further classified sets of Pontine neurons that had not been recorded before.

4.6.2 Development of the neurons of the Central Complex

This additional data in conjunction with the results in the previous chapter enables the generation of a timeline of development for the major neurons of the CC. This is represented schematically in Figure 4.26. Results from the previous chapter led to the conclusion that the first set of CC neurons to be identified were the isomorphic neurons of the HFS and VFS at 4 APF. New data from this chapter has revealed that Large field neurons, such as the ExR1, are also traceable at the start of metamorphosis. This is consistent with previous observations that (Wegerhoff et al.,1992) who reported that Large field neurons represent the main CC input elements of the late larva in *Tenebrio*. In this respect, *Drosophila* appears to be evolutionarily similar.

In the central brain of the 3rd instar larva, a series of interhemispheric commissures can be visualised by α-Neuroglian staining consistent with previous studies (Hanesch et al., 1989, Perenau & Hartenstein., 2006). Equally, the PB is discernable at this stage, as previously reported (Schneider et al., 1993). Using α-Echinoid staining it was possible to see one commissure in the late third instar which may be an early tract from the lateral HFS neurons. This and the early PB are the earliest recognisable evidence for the CC using the markers of this study, supporting the hypothesis that the

CC mainly differentiates during early metamorphosis. Unlike, the Mushroom bodies that are present in the late embryo and are remodelled throughout metamorphosis, no evidence was detected for neural remodelling in the CC. This is not unexpected for an imaginal structure such as the CC.

The VFS and HFS are the first neurons to project to their targets, that are reached by 16-20 APF. This supports the hypothesis that these sets of neurons act as the initial matrix framework of the CC. These are followed by the Pontine and *fb-eb* neurons and finally the R1-R4 and F neurons. Cells such as the R neurons that develop later may use the HFS or VFS as positional indicators. This data shows that CC neurons are added to the matrix incrementally.

4.6.3 Structure and information flow through the Central Complex

Enhancer trap line c255 was unique in that it revealed expression in the ExR1 neurons. The branches from this neuron to the EB have not previously been detailed. Interestingly, 32 bundles of branches were counted innervating the EB (these may also include *fb-eb* neurons). This evidence suggests the hypothesis that the EB can be divided into 16 radial segments (and 32 half segments) as in *Musca* (Strausfeld 1976). This has not previously been reported for *Drosophila*. This is further supported by the sets of 16 *fb-eb* neurons identified by line c159b. During axon outgrowth (24 APF) *fb-eb* neurons from individual FB segments were visualised projecting to the unfused EB. Although the precise projection pattern of these neurons was not determined it could be hypothesised that these neurons each innervate a segment of the EB.

The enhancer trap system reveals much about connectivity and we can use this method to drive dendrite specific reporters which provide indications of the polarity or information flow through the system. Previous studies have inferred information flow through the Central Complex from the fine structure of cells, for example 'blebbed' or

'spiny' appearances. In order to investigate this further we need to use a combination of axonal, dendritic and synaptic markers. Large field neurons are the main source of input to the CC (Strausfeld 1976; Hanesch et al., 1989; Homberg 1991, Wegerhoff & Breidbach, 1992), whereas neurons that target the VBO, such as the HFS, are thought to be the main output source (Hanesch et al., 1989). Dendritic expression, observed through the Dscam reporter in this study, was restricted to Large field neurons of the CC. This was particularly clear for the ExR1 neuron which arborised in the LTR, VBO, FB and EB and had been previously described as spiny arborisations (Hanesch et al., 1989). The spiny domains of the type A R cells were also observed using Dscam in the LTRs. This reporter appears to reveal spiny dendritic arborisations but not blebbed arborisations, suggesting it is a postsynaptic marker. This correlates with that hypothesised by Hanesch et al. (1989) that information flow to the CC is via Large field neurons with extrinsic arborisations. Dscam expression was also detected in the FB and EB suggesting postsynaptic dendrites in these regions. Dendritic arborisations of Small field neurons were not detectable with this reporter and several Large field neurons showed no arborisations when they are known to exist. It may be that blebbed terminals cannot be visualised with this specific membrane segment of Dscam as a reporter. This may have implications for functions of different Dscam isoforms that can be investigated in future. In order to analyse information flow in more detail it will be necessary to use a greater range of dendritic reporters.

5

Analysis of Central Complex structural mutants using Enhancer Trap Lines

5.1 Introduction

Central Complex structural phenotypes from three independent X-linked mutations are analysed in this chapter using the enhancer trap lines. The mutants were isolated (Heisenberg et al., 1985) have been well studied for a variety of behaviours including walking (Strauss & Heisenberg, 1990; Strauss et al., 1992; Strauss & Heisenberg, 1993) and phototaxis (Strauss & Heisenberg, 1993). Varying degrees of structural abnormalities have been reported in the CC that have not yet been characterised at the cellular level (Strauss & Heisenberg, 1993). The phenotypes observed in these mutants are not unique to the strains used here, indeed CC distortions such as these have been reported in other mutants (Bouhouche et al. 1993, Strauss & Heisenberg 1993, Ilius et al. 1994, Nicholas & Preat 2005). The gross anatomical phenotypes for these mutants have previously been described (Strauss & Heisenberg, 1993). In this study, CC lines were selected on the basis of structural abnormalities in the FB. Three of these mutants are alleles of *neuroglian* (*ceb*^{849}, *ceb*^{892} and *ibx*), two mutants are alleles of *central body defect* (*cbd* ^{KS171}, *cbd* ^{KS96}) and the final mutant is an allele of *central complex broad* (*ccb* ^{KS127}). Six of the enhancer trap lines identified in

Chapter four were used to analyse the adult Central Complex of the mutant strains at the cellular level. Lines were selected to encompass as many identified classifications of neurons as possible.

5.2 Aim

To analyse the Central Complex of structural mutants using previously isolated enhancer trap lines.

5.3 Analysis of *neuroglian* Central Complex phenotypes

neuroglian has already been implicated in CC development and there are three known alleles that demonstrate a phenotype (Strauss & Heisenberg, 1993; Carhan et al., 2005) in the CC. These have not been analysed in detail and how or when these phenotypes are initiated is unknown. This section quantifies the phenotypes of the three *neuroglian* mutants. In the CC, *neuroglian* expression in the developing and adult brain appeared to be primarily on axons, and was mainly detected on the HFS, VFS and several interhemispheric commissures (see chapter 3).

Three *neuroglian* alleles; ceb^{849} ceb^{892} and *icebox*, all displayed Central Complex phenotypes as shown in Figure 5.1. Features of these phenotypes include the failure of sub- structures to fuse across the midline and a more scattered appearance in the case of the NO. These are further described in the following section. The lack of fusion of structures across the midline is reminiscent of the phenotypes seen in Robo mutants (Nicolas & Preat, 2005). The *neuroglian* mutant phenotypes are analysed in more depth here. In all cases hemizygous males were dissected. Figure 5.2 shows quantification of these phenotypes.

In addition to *neuroglian* mutants, the brains of *echinoid* mutants were also examined for a potential CC structural phenotype. This was prompted by the expression pattern of *echinoid* in the HFS and VFS during development. Initial experiments analysed two *echinoid* mutants; a hypomorph $ed^{4.12}/ed^{4.12}$ and a null mutant $ed^{K01102}/Df(2L)ed\text{-}dp$. Staining of adult brains with both α-Fasciclin II (an adult MB and EB marker; Carhan et al., 2005) and the synaptic neuropil marker mAb nc82 (Vosshall et al., 2000) revealed no major structural abnormalities in the CC of *echinoid* mutants (data not shown). Neither of these markers stained the main fibres of the CC therefore any potential abnormalities of these neuron trajectories are unknown. Larval brains of *echinoid* mutants were also studied using α-De-cadherin as a marker for the SAT's but showed no abnormal trajectory patterns, unlike *de-cadherin* mutants (Dumstrei et al., 2003b).

5.3.1 Characterisation of *ibx* phenotype

ibx phenotypes vary in severity both between alleles and between brains of the same genotype. 80% (n= 20) of *icebox* brains display a full dorsal to ventral cleft through the middle of the FB as shown in Figure 5.1(A). The remaining 20% show only a small cleft breaking into the upper to layers of the FB. *ibx* brains also occasionally show 2-3 additional clefts laterally in the upper layers of the FB. The most striking observation of the CC however is the split EB. In *ibx* brains the EB cannot form its characteristic doughnut shape but often appears as two hemi-ellipses on either side of the midline like the ceb^{892} brain shown in Figure 5.1(B). In the some brains there are often one or two whole Ellipsoid bodies formed on either side of the midline as shown in Figure 5.1(F).

5.3.2 Characterisation of ceb^{892} phenotype

ceb^{892} shows several variations in both severity and nature of phenotype. 65% (n = 20) of brains have a full dorsal cleft through the entire FB, the remainder display small clefts in the upper 2 layers, like that of *ibx* brains. All brains analysed displayed an abnormal EB. 35% of brains showed what appeared to be a smaller FB shaped structure in the place of the EB as shown in Figure 5.1(E). 15% showed a similar phenotype to that in ibx; two fully formed EBs on either side of the midline like that shown for *ibx* brains in Figure 5.1(F). Several brains showed scattered NO not in their conventional paired form. In 35% of ceb^{892} individuals six NO can be observed, as opposed to the usual four.

5.3.3 Characterisation of ceb^{849} phenotype

ceb^{849} displays a similar phenotype to ceb^{892}. ceb^{849} has a higher incidence of fragmented NO but has fewer incidences of two fully formed EBs on either side of the midline. The mutant Fan shaped EB is also evident with this allele and occurs at a similar frequency. The midline cleft through the whole FB occurs in 50% of individuals analysed. The other 50 % show a weaker phenotype with the cleft only penetrating

between layers 6 to 4. There was no clear correlation between sub-structure phenotypes, although in cases with two EBs on either side of the midline there was commonly a cleft through the whole FB. Figure 5.2 shows a quantitative data on this phenotypic variation.

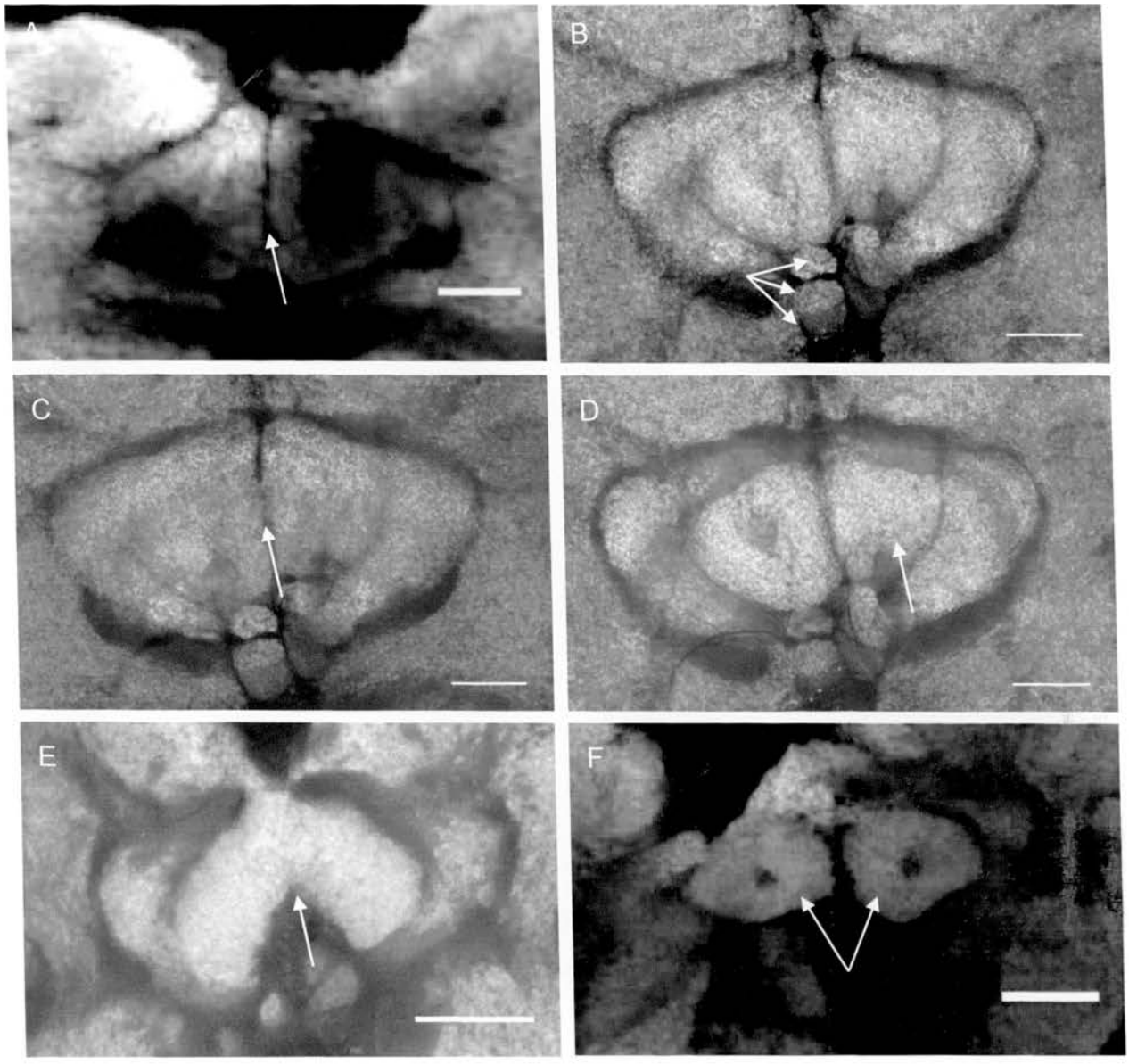

Figure 5.1: Central Complex phenotypes of alleles of neuroglian. A, cleft through the FB (arrow) in an *ibx* brain showing separation at the midline. B**,** *ceb*^{892} brain with 3 layers per NO unit (arrows). **C,D**, *ceb*^{892} brains show clefts and an unfused EB (arrows). **E**, *ceb*^{892} brain showing an abnormally shaped EB (arrow) that appears to follow the shape of the FB. **F**, Two fully formed EBs (arrows) in an *ibx* brain. Scale bars 25μm.

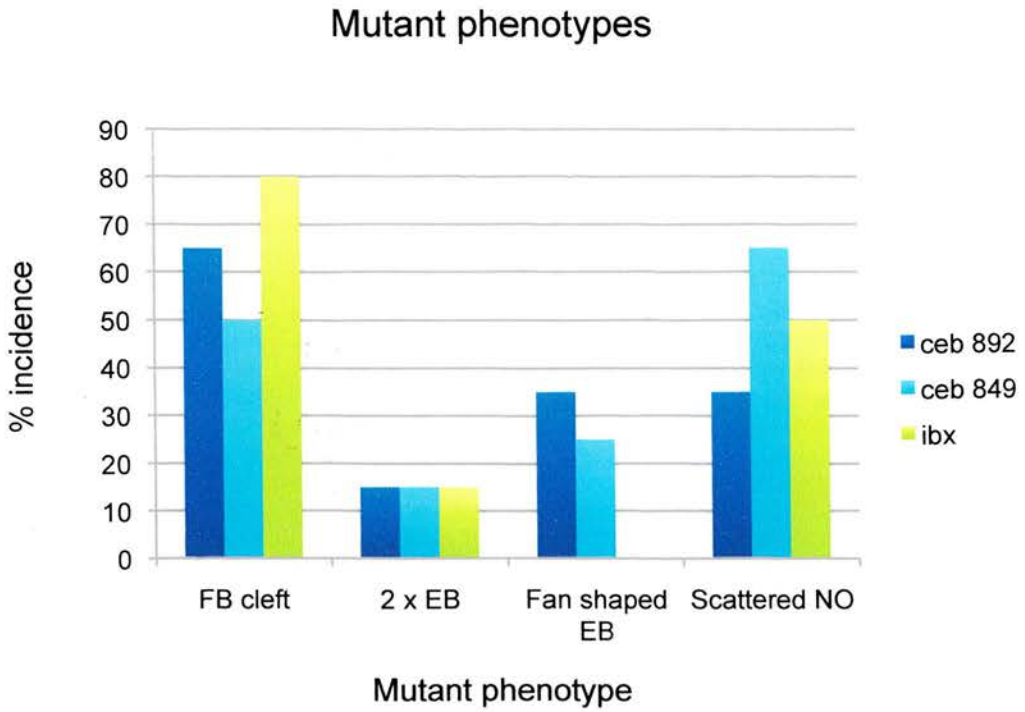

Figure 5.2: Graph showing variations in phenotypes between and within *neuroglian* strains. The strains are shown in the legend on the right of the graph.

5.4 Phenotypic characteristics of CC structural mutants observed using enhancer trap lines

In order to use the enhancer trap lines in this context it was first necessary to determine the chromosome on which each P element was located. This information is shown in Table 4.1 in the previous chapter. For further details on protocol refer to the Materials & Methods. The majority of P elements were located on chromosomes two and three. The recessively X-linked mutations of the strains used here made it too difficult to use X-linked enhancer trap lines (i.e. c61), therefore these were not included in this part of the study. The *neuroglian* strains are described together due to similarity in phenotypes between strains. Selected images are included representing each phenotype. Table 5.1 details which strains were included.

5.4.1 *neuroglian* strains (c*eb*^{849}, c*eb*^{892}, *ibx)*

Previous anatomical descriptions of *nrg* mutants in section 5.3 revealed a Central Complex phenotype that varied in severity within and between strains. The phenotype commonly displayed a split FB, disorganised NO and an unfused or additional (doubled) EB on either side of the midline. Through the use of the enhancer trap lines it has been possible to analyse this phenotype in more detail at the cellular level.

The ExR1 neuron was still clearly visible in *nrg* mutants but arborisations in the dorsal FB were profoundly reduced [Figure 5.3(C)]. Axons were still capable of crossing the midline to form the characteristic trajectory of this neuron. Axons still projected successfully to the segments of the EB despite the unfused or doubled appearance of this sub-structure [Figures 5.3 (D), 5.5(B)]. When in duplicate, each of the two EBs constituted one ExR1 cell, there was no indication of any cell fate phenotype that may cause cellular duplication resulting in two EB structures. In the majority of cases, the R neurons did not succeed in forming the characteristic circular structure of the EB

spanning the midline. The unfused EB often appeared as two hemi-ellipses (or incomplete circles) on either side of the midline and 52y expression revealed several clumps of arborisation in each of these hemi-ellipses [Figure 5.6 (B)]. This may be R neurons attempting to find their targets in segments of the EB. It was not possible to count the exact number of 'clumps' but it appeared to be between 13-18.

Line c5 revealed F*l* neurons unable to cross the midline in the dorsal FB [Figure 5.4 (B)], showing a gap in layer six between FB sections in addition to reduced arborisations. Conversely, some F neurons were still capable of making connections between layers of a distorted FB as shown by line 71y [Figure 5.4(C)]. The Pontine neurons also managed to traverse the midline in these mutants [Figure 5.3 (E)] and it was possible to see ExR1 neurons still able to connect the FB and EB despite the position of the EB [Figure 5.3 (F)]. It was not possible to count exact numbers of neurons that managed to target correctly.

There were also clear phenotypes elsewhere in the central brain. The mushroom bodies have been previously reported to develop as incomplete structures, with lobes missing in *neuroglian* mutants (Carhan et al., 2005) and this was also observed in this study. Line 52y revealed that the great commissure in mutants shows a large reduction in the number of fibres within it [Figure 5.6 (D)]. This shows that other midline spanning fibres also show defects in the mutant brains in addition to the CC.

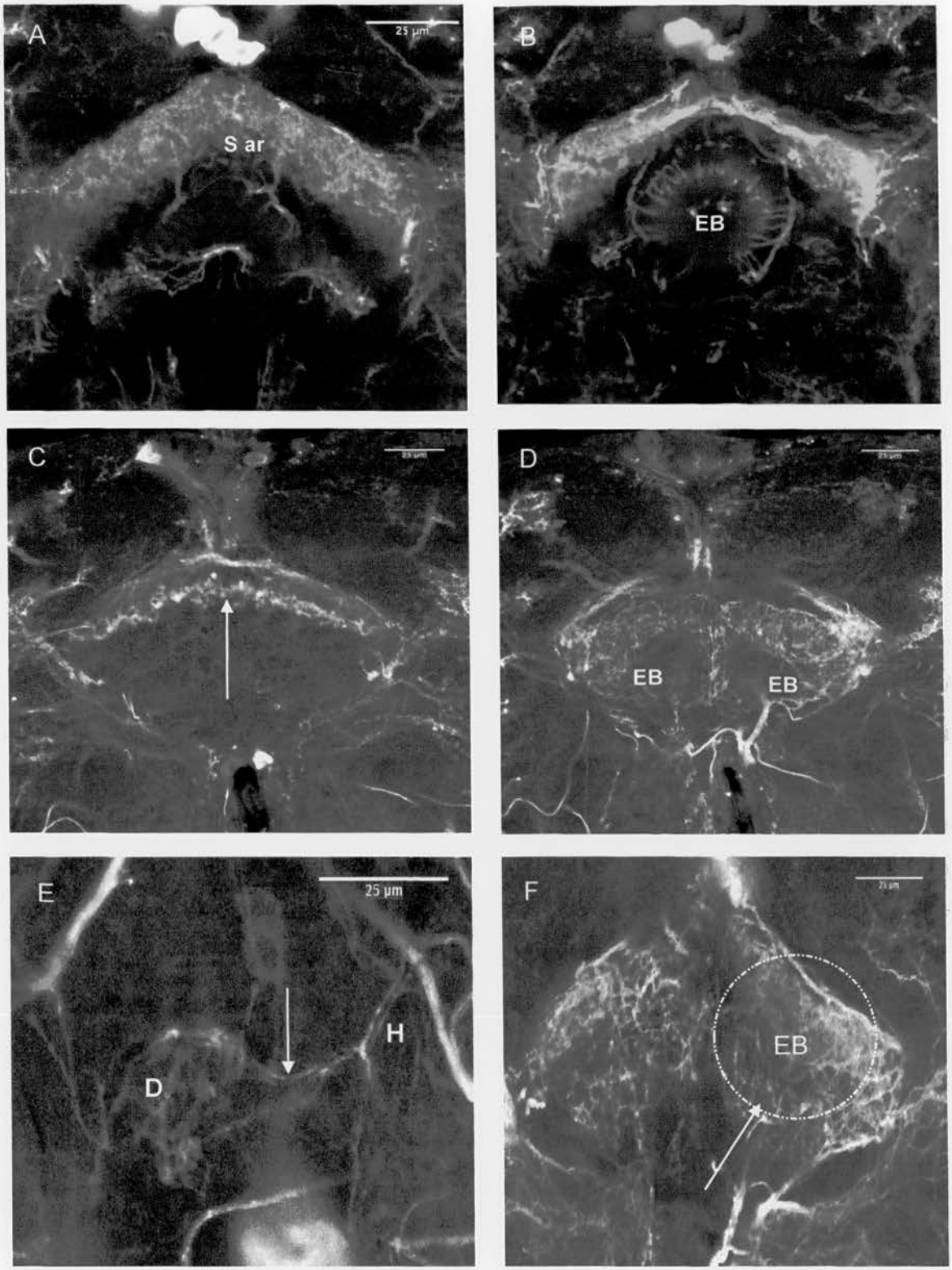

Figure 5.3: *ceb*^{849} phenotype visualised with enhancer trap line c255. A, B; c255 expression in a wildtype brain preparation. **C,** c255 expression in a *ceb*^{849} brain showing comparatively reduced arborisations (arrow) to (A) and **D**, a double EB phenotype revealed by ExR1 projections. **E**, Pontine neuron (and possible *fb-eb* neuron) projecting into segment H normally but with reduced arborisations then targeting contralateral segment D. **F**, *fb-eb* neurons (arrow) can still connect the FB and EB even with the EB out of position (shown by dotted line). Scale bars 25µm.

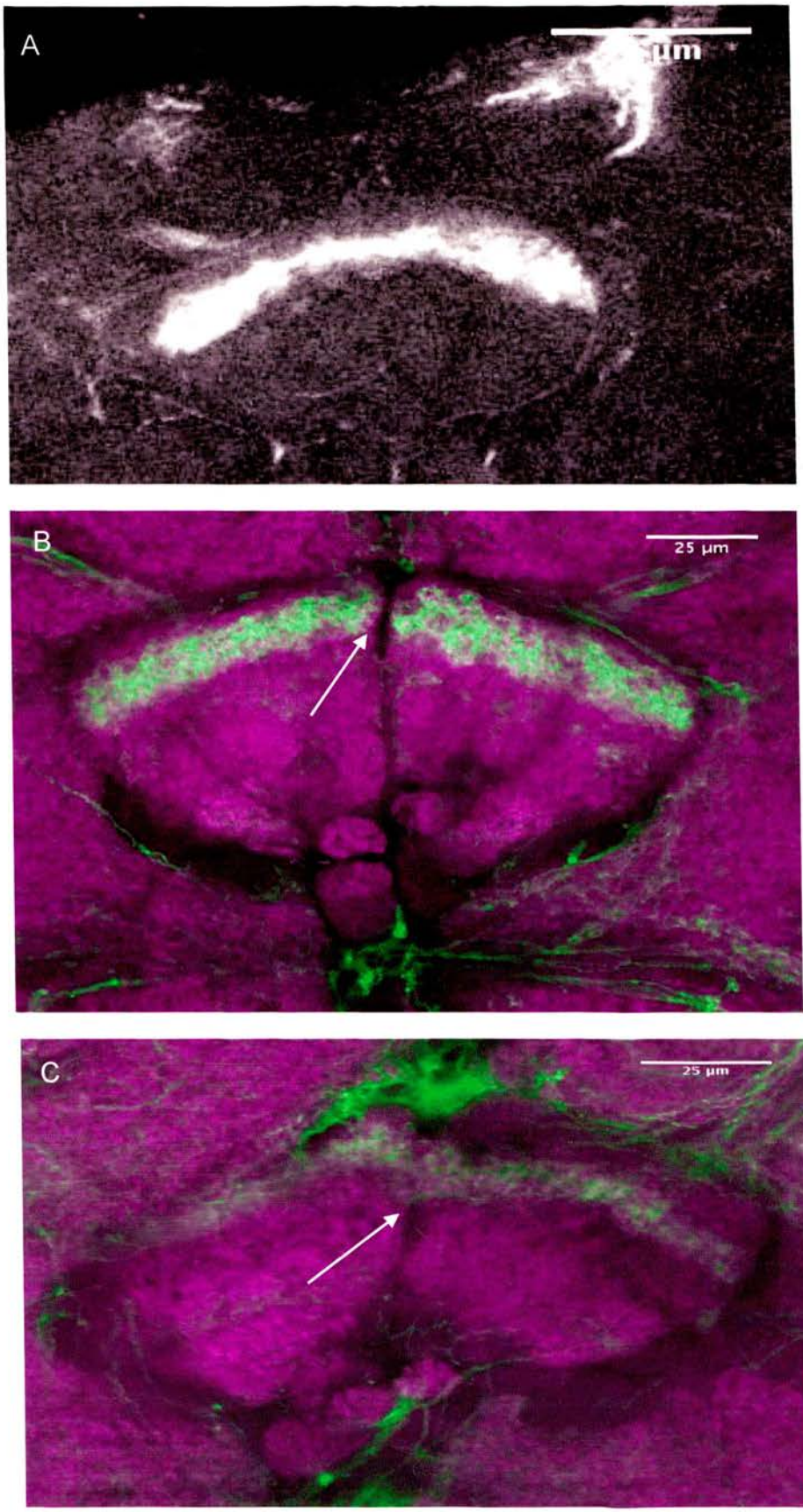

Figure 5.4: Enhancer trap line c5 expression in *ceb*^{892}. A, Expression of c5 in wildtype. **B**, expression of c5 in *ceb*^{892} showing failure of the F/ neurons to cross the midline (arrow). **C**, expression of 71y showing F neurons crossing the midline despite a distorted FB. Green – GFP, magenta – nc82. Scale bars either 50 and 25µm.

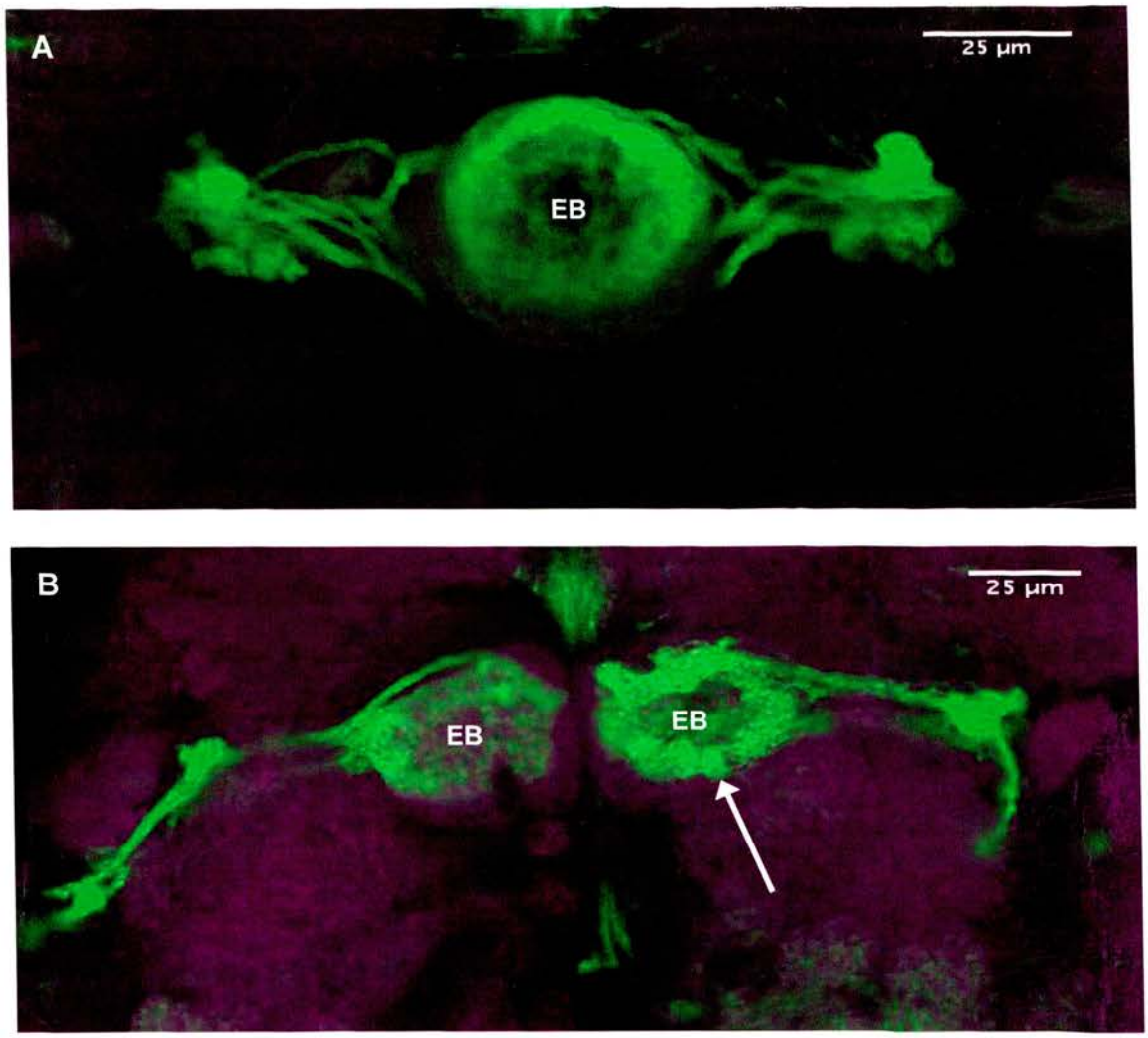

Figure 5.5: Mutant Type A R cell trajectories visualised in *ceb*^{892} brains with enhancer trap line 52y. A, 52y expression in the wildtype EB. **B**, 52y expression in *ceb*^{892} showing a double EB phenotype and clumps of arborisation within the ring (arrow). Green-GFP, magenta – nc82. Scale bars 25µm.

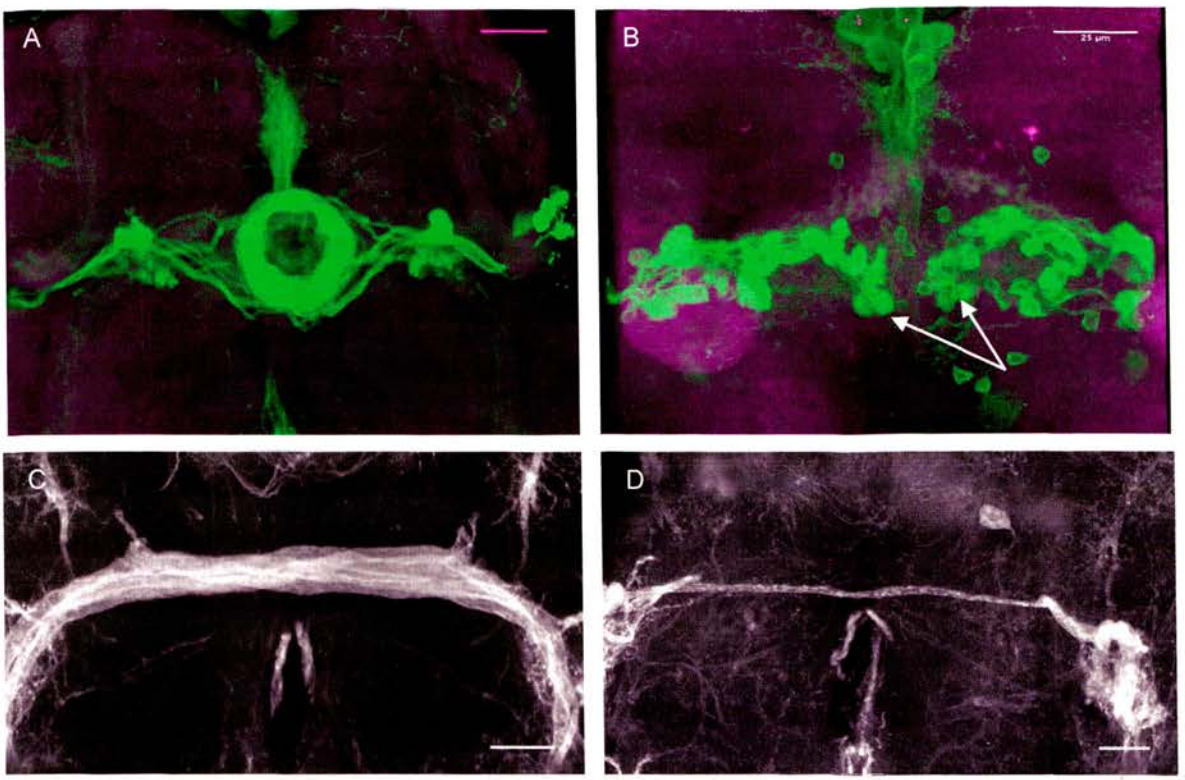

Figure 5.6: Phenotypes of the EB and the Great commissure shown by line 52y in *neuroglian* mutants. A, wildtype EB shown by 52y (*52y/UAS-mCD8::GFP*)**. B,** the EB can exist as two hemi-ellipses shown by the arrows (*ibx;;52y/UAS-mCD8::GFP*). Clumps of arborisation can be seen in each hemi-ellipse. **C**, the structure of the great commissure in a wildtype brain (*52y/UAS-mCD8::GFP)*. **D**, the great commissure in a mutant (*ceb*^{892} *;; 52y/Uas-mCD8::GFP*). Scale bars 25µm.

5.4.2 *cbd* strains (*cbd* ^{KS171}, *cbd* ^{KS96})

In addition to the *neuroglian* strains three other mutants were subjected to anatomical analysis using the selected enhancer trap lines and again the phenotypes varied in severity between individuals. In *cbd* mutants, the FB develops as distorted sections as previously reported (Strauss & Heisenberg, 1993). The EB phenotypes were like those of the other mutants was either unfused and on separate sides of the midline or fused across the midline and flattened slightly ventrally. The NO were scattered and six of these could be counted as seen in *neuroglian* mutant strains [Figure 5.1(B)]. There was often a severe Mushroom body phenotype showing aberrant trajectories (data not shown). For *cbd*^{KS171}, the FB was split into sections, which were rotated 90° laterally [Figure 5.7(A-C)]. The EB was either absent, malformed or doubled in abnormal, asymmetrical positions on both sides of the midline as shown in Figure 5.9(B).

As with other mutants, the ExR1 neuron was capable of crossing the midline in the dorsal FB and still successfully projected to the EB wherever its position. Neurites extended to meet the EB segments despite distortion of this structure. F*l* neurons were able to cross the midline and remain in the correct layer of the FB despite the abnormal split appearance of this sub-structure. This was demonstrated clearly by line c5 [Figure 5.7 (A,C)]. The distorted sections of the FB in *cbd*^{KS171} brains did not prevent the F*l* neurons from projecting to the appropriate FB layers and these neurons have still managed to achieve their normal trajectories. The neurons successfully traverse the midline and display normal branching patterns but reduced arborisations in the correct FB segments. The axons connect the distorted FB layers as a bundle (with no arborisation) traversing the space between sections in a direct trajectory. The arborisation phenotype in *cbd* strains was more severe than that of neuroglian mutants. There were no detectable arborisations in the dorsal FB from the ExR1 neuron [Figure 5.8(B)]. The axon did successfully encircle the EB branching to innervate the segments normally. There is mass disorganisation in the central brain with c255 highlighting

several unidentified fibres showing looping and abnormal trajectories [Figure 5.8 (A)]. F*m* neurons were visible attempting to enter the EB canal for arborisation in the FB but due to the were unable to do this (possibly because the EB canal was absent due to an EB phenotype) and subsequently veered off in an alternative direction.

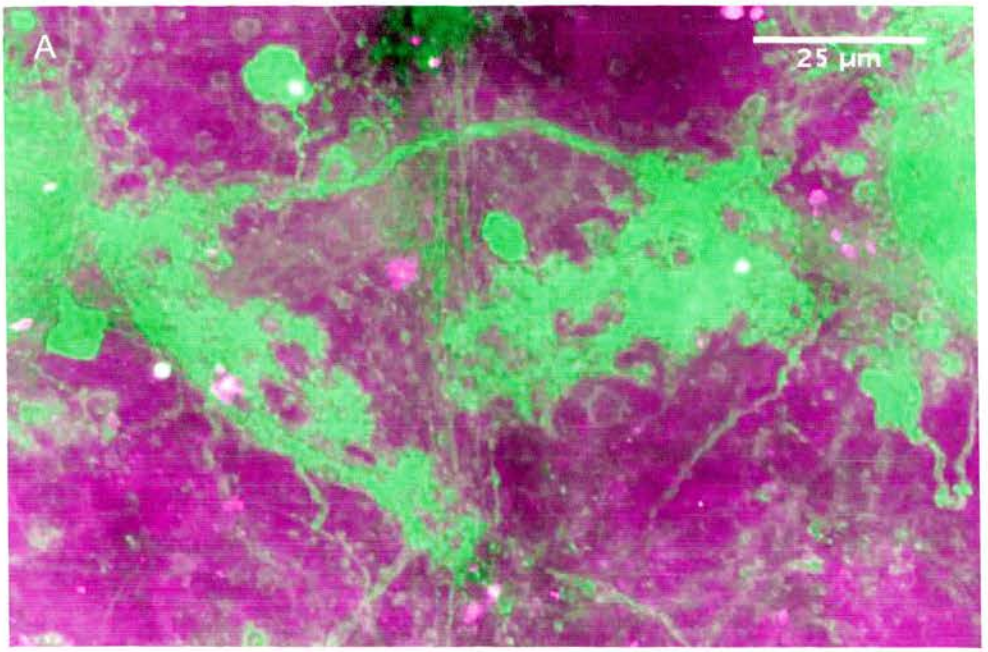

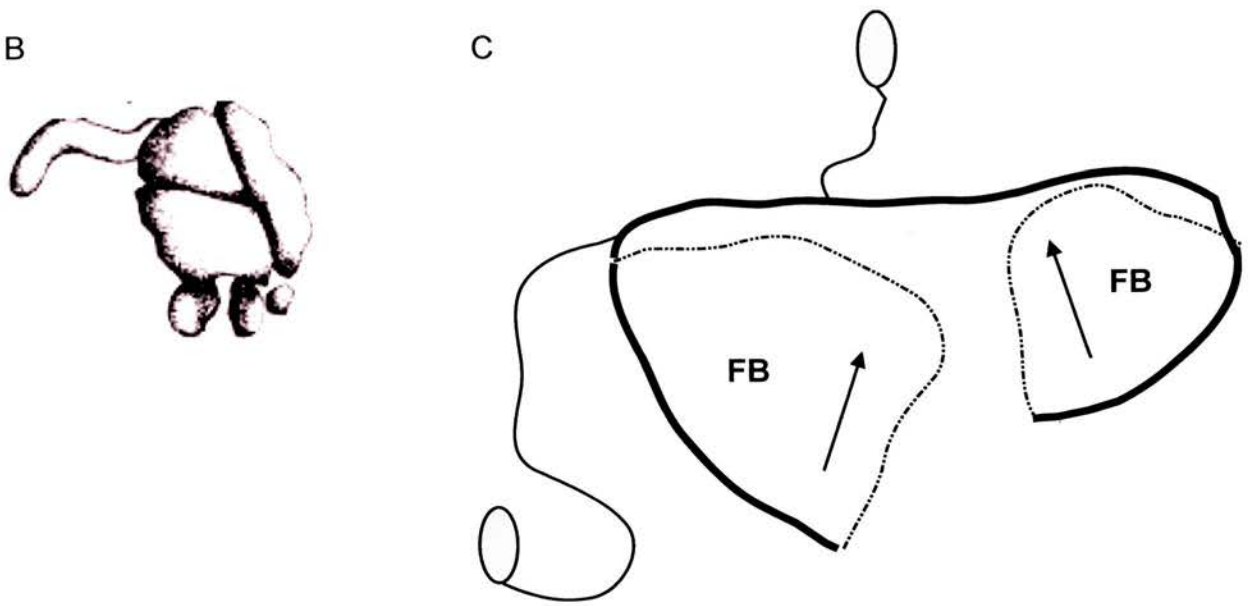

Figure 5.7: The FB of a *cbd*^{KS171} brain visualised with enhancer trap line c5. A, F*l* neurons still traverse the midline and innervate segments despite FB distortion. The use of this enhancer trap line shows the orientation of the sections FB. **B**, Schematic of previously determined *cbd*^{KS171} phenotype (Strauss & Heisenberg, 1993). **C**, Schematic of *cbd*^{KS171} phenotype using enhancer trap technology showing orientation of the distorted FB sections (arrows indicate normal dorsal to ventral orientation as observed in wildtype). Dark line is the axonal trajectories from F*l* neurons linking distorted dorsal FB sections. Scale bar 25µm.

Strain	52y	71y	210y	c5	c255
ceb ^{849}			x		x
ceb^{892}	x	x	x	x	
ibx	x	x	x	x	x
cbd^{K5171}				x	x
cbd^{KS96}			x		x
ccb^{K5127}	x	x	x	x	x

Table 5.1: Five enhancer trap lines were used to assess mutant phenotypes. Mutant strains are in column one, with enhancer trap lines denoted in row 1.

5.4.3 *ccb*^{KS127}

Line *ccb*^{KS127} showed the least severe FB phenotype of these mutants. The EB was displayed as several forms ranging from normal to a structure that has the appearance of a smaller FB as seen in the *neuroglian* alleles [Figure 5.9 (A)]. In all of these mutants the F*l* neurons and VFS/HFS projections manage to traverse the FB layers as in wildtype (data not shown). In many cases the EB appears as in wildtype brains but in a different orientation, as previously reported (Strauss & Heisenberg, 1993). The ring structure formed by the R neurons is often not affected. In the case where the EB has formed an abnormal small Fan shaped structure, the ExR1 neuron still manages to form segmental connections with the R neurons. The Fan shaped EB is due to the unfused EB R neurons that stretch across the midline creating an EB structure in line with the transverse axis of the FB. These connections are longer and form in the shape dictated by the R neurons, thus creating a smaller Fan shaped EB consisting of columnar instead of radial elements.

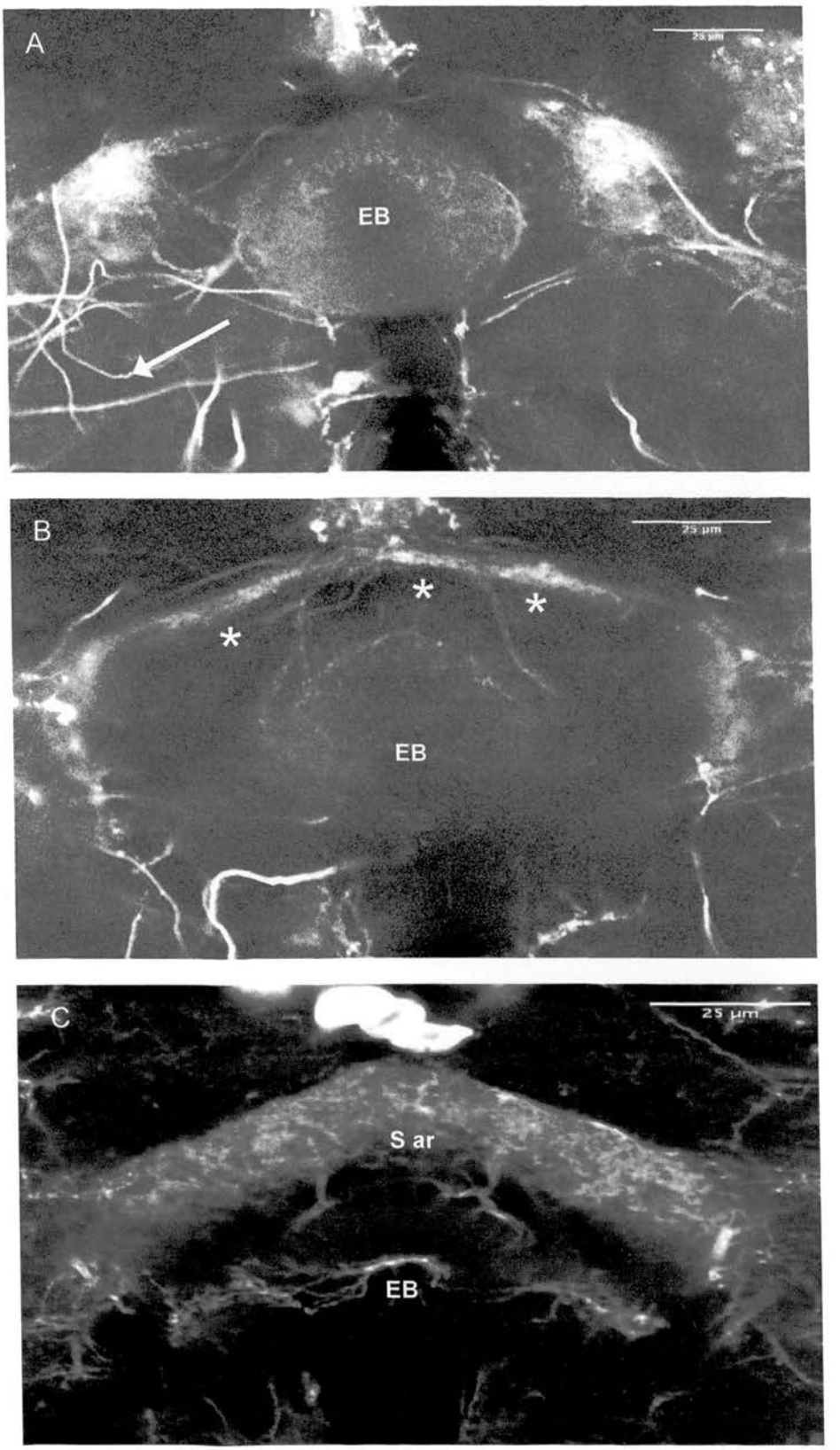

Figure 5.8: ***cbd*^{KS96} visualised with enhancer trap line c255** showing **A,** aberrant axonal trajectories outwith the CC (arrow). **B**, absent arborisations (asterix') compared to wildtype as shown by **C**, wildtype c255 expression.Scale bars 25µm.

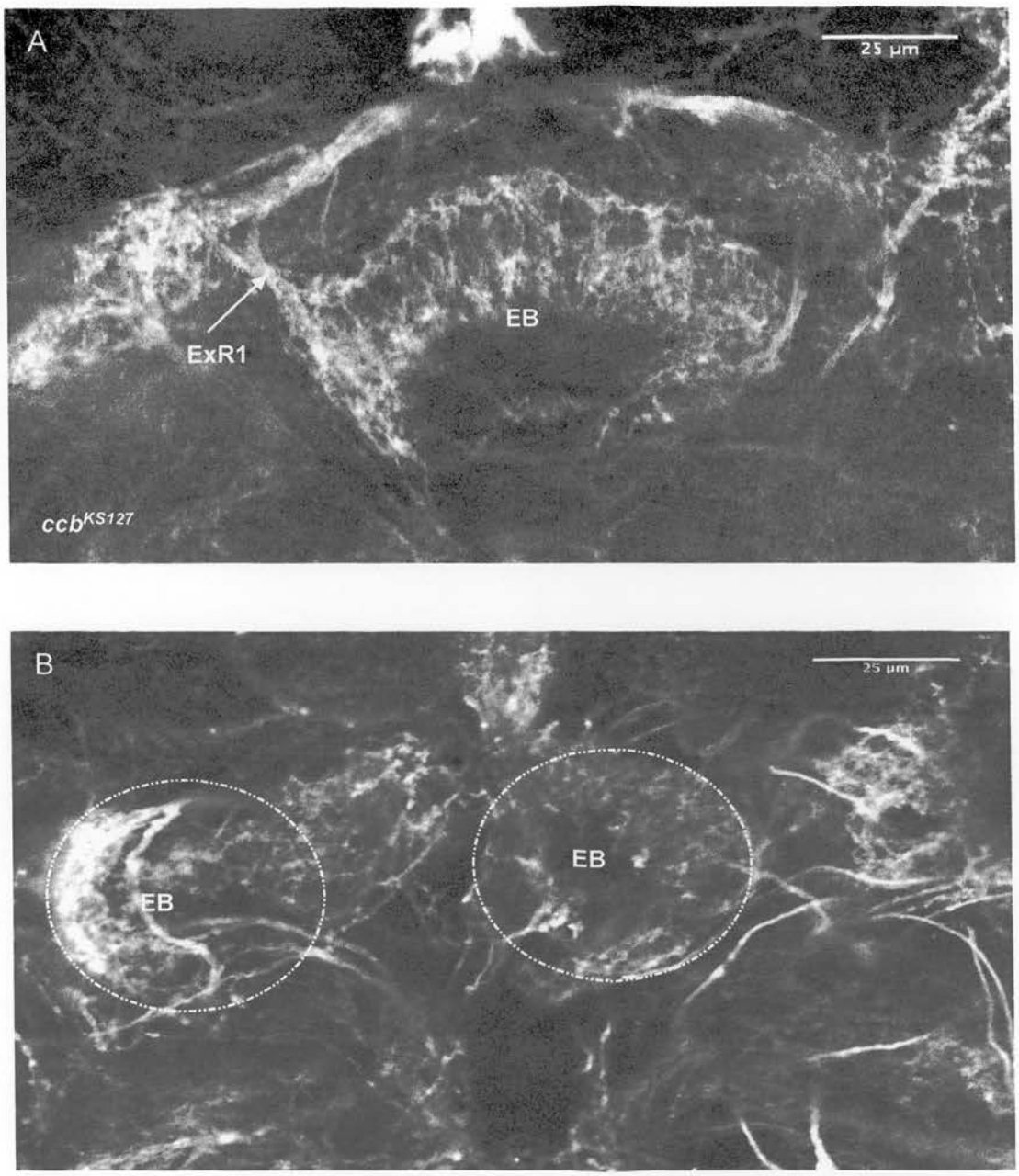

Figure 5.9: EB phenotypes for *cbd* and *ccb* strains. A, Enhancer trap line c255 revealed that the Fan shaped EB (previously observed in several mutants section 3.5) was an unfused EB. This was also observed in ccb^{KS127} flies (above). The ExR1 neurons (arrow) were unable to complete the EB ring but were still able to innervate the EB structure at regular intervals as in wildtype. **B**, cbd^{KS17} brains demonstrated displaced EB phenotypes. The dotted circles indicate malformed EB positions. Scale bars 25µm.

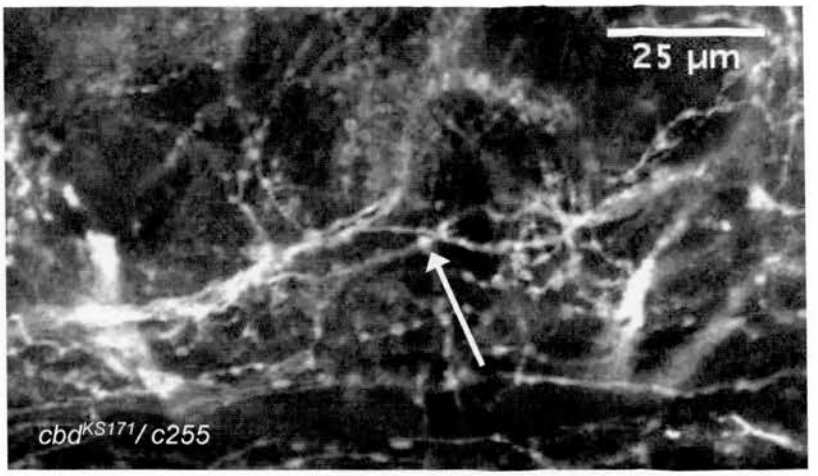

Figure 5.10: Elevated number of blebs on axons visualised with enhancer trap line c255 in *cbd*^{KS17} brains. *cbd*^{KS17} brains displayed an elevated number of blebs along axons (arrow). This phenotype was observed in all mutants. Scale bar 25µm.

5.4.4 Features in all strains

A common feature in several of the CC mutants was the high proportion of additional or aberrant synapses distributed along axons or bundles of axons in and around the CC that showed no connections to other fibres [Figure 5.10]. In addition, line c255 revealed a number of axon tracts in the Central brain that displayed aberrant trajectories, often looping back on themselves to create a disorganised set of fibres. Phenotypes such as the unfused EB or distorted FBwere often shared between all mutants.

5.5 Discussion

5.5.1 *neuroglian* mutant analysis

Interestingly, the *neuroglian* mutant phenotypes analysed here all seem to show a defect in structures at the midline. This is easily visible in the CC as it is the only major midline spanning neuropil. In all allelic variants there is a cleft (of different sizes) along the dorsal-ventral axis of the FB. Otherwise, this substructure appears normal. Likewise, the unfused EB or double EB phenotype suggests an inability for cells to cross the midline. Interestingly, *neuroglian* does not seem to be expressed in the R cells of the EB, suggesting that it may play a role in axon guidance outwith these neurons at the midline. Mutants can still often form the characteristic EB shape ipsilateral to the R cell perikarya, often resulting in two EB's but seem unable to form the sub-structure on the midline. This suggests *neuroglian* may not be required for ring formation. On the occasions when there is an EB structure that spans the midline it appears to adopt the shape of a much smaller FB with no ring formation at all. It may be that R cells adopt guidance cues intended for transverse F*l* neurons. In the case of *neuroglian* mutants, it may be that the R neurons cannot break fasciculation to form the ring structure of the EB at the midline and subsequently form a structure that mimics the F*l* neurons. Neuroglian was also expressed on several interhemispheric commissures during late larval and early metamorphosis stages. Subsequently, mutants may also have defects in these interhemispheric commissures (not visible using nc82 staining) which may contribute to the initial developing structure of the CC. These commissures could play a structural role responsible for providing a framework for the intricate CC architecture to develop at the midline. Their absence may make it difficult for structures to form properly.

The reasons for these CC mutant phenotypes are still unknown. A feature of differentiating this late in development may be that other potential defects in neurogenesis and cell fate decisions (which may explain the reduced number of fibres in the great commissure) occuring at an earlier stage may influence structural development. This is also a consideration when using these mutants for behavioural analysis. One of the most interesting features is the variation in phenotype within and between *neuroglian* strains. There does not appear to be any correlation between phenotype and specific alleles. However, there can be wide variation in severity of phenotype between

brains of one allele. As yet, this is not understood. Further analysis of *neuroglian* function in both metamorphosis and post-embryonic development is required.

Finally, central brain mutants revealed certain structural abnormalities. In the majority of *nrg* mutants, there appeared to be six NO sections as opposed to the previously reported four. This may be due to earlier developmental abnormalities (i.e. cell fate) though it is possible that analysis of these mutants has allowed visualisation of structures that are normally difficult to see or separate. This may also indicate that the NO exist with 3 dorso-ventral layers per subunit We must be careful of inferring structural information from mutants though it raises the possibility that the NO, which are characteristically difficult to visualise in wildtype brain preparations, can be further compartmentalised into 3 layers.

In addition to studying *neuroglian* mutants, several *echinoid* mutants were analysed. *echinoid* is expressed on both axons and dendrites in the CC. Like the Robo proteins (Nicolas & Preat, 2005) it is expressed in all of the CC sub-structures though faintly in the EB. Due to Echinoid's role as a Cell adhesion molecule during neurogenesis in the PNS and the strong expression pattern revealed in the CC developmental series, it was hypothesised that *echinoid* could be involved in structural development in the CC. However, analysis of both a hypomorph and a null mutant revealed no major structural abnormalities. The gross structure of the CC in *echinoid* mutants appeared normal, although this does not rule out more subtle wiring defects that may be present. Due to the lack of markers available specific to the CC it was not feasible to study this further in the adult central brain. Subsequently, third instar larvae of *echinoid* mutants were also analysed for aberrant trajectories in SAT's using α-De-cadherin (*de-cadherin* and *echinoid* are both expressed on these pioneering tracts, though *echinoid* expression is detected later than *de-cadherin*) as a marker, but trajectories also appeared normal. In order to assess a potential role for *echinoid* in neuronal development, the model of the Optic lobe was used. This study is detailed in Chapter 6.

5.5.2 Enhancer trap lines for mutant analysis of the Central Complex

Five of the isolated enhancer trap lines were used in the mutant analysis study providing novel insight into the abnormalities of the mutant Central Complex and central brain (210y did not provide useful information). The major advantage conferred by the enhancer trap lines was the ability to isolate specific neuron types in conjunction with a neuropil marker. All of the six mutant strains analysed revealed a range of anatomical CC phenotypes both within and between strains. This variation had previously been characterised for the three *neuroglian* strains in section 3.5. Due to this range of phenotypes, the results obtained using the enhancer trap lines also varied showing different characterisations for the same neuron type within a strain. The phenotypes characterised here focus only on two of the four CC sub-structures, the FB and EB. Few phenotypes were observed in the NO or PB due to the selection of mutant lines and enhancer trap reporters for the FB.

Enhancer trap analysis revealed the inability of some neuron types to traverse the midline during development. This was most clearly demonstrated by the type one R neurons, displaying a range of EB phenotypes, from unfused hemi-ellipses to the 'doubled' EB structures. The ability to form a ring, albeit from one set of R neurons remaining in one hemisphere, was seen in all strains including both alleles of *cbd,* in contrast to that reported by Renn et al. (1999) who did not observe this phenotype in *cbd* brains. Although the axons of the type A R neurons were capable of projecting towards the midline and arborising in the LTRs, in most cases they were unable to complete the EB by crossing the midline to form a ring structure with their contralateral equivalents. In some cases the R neurons did initially succeed in crossing hemispheres. Another common phenotype was the formation of a fan shaped EB spanning the midline. This was seen in conjunction with a milder FB phenotype showing no midline cleft. In this case the R neurons succeeded in forming the upper EB but failed to form the circular structure that required the axons to cross back over the midline. In contrast, analysis of

the ExR1 neurons in the mutants revealed that they successfully traversed the midline to innervate the EB whatever its position, suggesting guidance to the appropriate R neuron targets was not impaired in the mutants. This data suggests a role for the products of these genes similar to that of the Roundabout (Robo) proteins, guidance receptors that are required to traverse the midline (*Kidd et al., 1998*). Indeed, *robo* mutants show a similar Central Complex phenotype to several of the mutants used here (*Nicolas and Preat, 2005*). The Type A R neurons were often seen to terminate in ~13-18 'clumps' in the unfused EB, though the exact number could not be determined. The number of radial segments in the CC has not been reported. From this data it could be hypothesised that there are 16 segments in the EB.

The inability to cross the midline was observed less frequently for F*l* neurons and Pontine neurons than type A R neurons. F*l* neurons were still capable of reaching the appropriate FB layers, but they often stopped short at crossing hemispheres. F*l* neurons were still capable of forming connections between segments within a layer and across the midline despite profound FB spatial distortion as shown in some *cbd* brains. To explain this we can refer to the developmental characteristics obtained in earlier chapters. Several F neurons have been shown to cross contralaterally early (4 – 12 APF) in CC development. At this point the shape of the brain is still similar to that of the 3rd instar larva requiring less distance for the F neurons to travel. As the brain expands, the F neurons will expand with it but are already in position acting as the initial framework for FB formation. The subsequent distortion of the FB may occur after this point allowing the F neurons to remain but causing them to adopt an abnormal trajectory in order to continue to innervate the correct layer. This suggests that the *cbd* phenotype does not result from a problem with guidance cues. All sub-structures displayed midline defects and this may be due to an overall inability to fuse hemispheres correctly during development. The phenotype is likely to be most severe in the CC as this is the only structure that spans the midline. The Pontine neurons adopted a more disorganised appearance in the mutants but some axons could be seen crossing the midline. It was not possible to visualise all of these fibres in crossing contralaterally in the mutants,

therefore this may not always be the case. Considering the later outgrowth of Pontine neurons in CC development (12-20 APF), it may be that some axons terminate ipsilaterally.

A feature of all mutants except *ccb* was a reduced or absent arborisation phenotype in the FB as clearly demonstrated by the characterised enhancer trap expression patterns. This was most clearly observed using lines c5 and c255 which characteristically reveals arborisations in the dorsal FB in wildtype brains. These arborisations were profoundly reduced in several mutant brains. This may be due to a lack of structural cues in the deformed CC resulting in a lack of directional information for dendritic outgrowth. Alternatively, this may implicate these genes in dendritic formation. In addition, the 'clumps' observed along axon bundles observed in several mutants may be unsuccessful attempts at arborisations, that have been cropped or prevented from extending any further. Further analysis into these genes is required to ascertain these hypotheses.

These observations support the hypothesis that the various mutant phenotypes manifest during mid CC development (12-20 APF) when the brain is starting to adopt its adult formation. This is indicated by the midline effect on the late developing CC neurons such as the type A R neurons compared to the ability of some early developing F neurons to traverse the midline. Interestingly, despite the distorted FB phenotypes observed most neurons were still capable of projecting to their final intended targets.

5.5.3 Implications for *neuroglian* function

It is not possible to infer functions for the *ccb* and *cbd* genes without further information on expression but we can formulate hypotheses for *neuroglian* based on the developmental information obtained from expression patterns in Chapter Three. Neuroglian was present on several interhemispheric commissures from L3 throughout

metamorphosis. It is likely that many of these larval connections are impaired in the mutants resulting in midline defects and subsequently abnormal brain formation. In *nrg* mutants, few F*l* neurons were capable of traversing the cleft in the upper FB though they often managed to cross the midline at lower layers where there was no gap between FB segments. This suggests that the inability to cross the midline is not a cell autonomous effect but requires external cues present in the early structure of the FB. Subsequently, *neuroglian* may not be required for midline crossing, but defects that are present prior to CC formation may affect positioning of CC neurons. It is possible that the fibres of the CC use already established interhemispheric commisssures as guidance during development. If these guidance commissures are not properly formed (as shown by the great commissure phenotype) this may affect the overall development of the FB structure, including the glial sheath surrounding it.

The *neuroglian* expression pattern does not include the type A R neurons which further supports the hypothesis that *neuroglian* is not required in a cell autonomous role for midline crossing. A similar observation was formed regarding Robo protein positioning and mutant phenotypes (Nicholas & Preat, 2005). It may be that R neurons require their contralateral counterparts to form the ring structure but are prevented from reaching them by the absence of external cues in the malformed FB, itself a result of abnormally formed commissures during L3 development. This implies an indirect role for *neuroglian* in CC formation regarding the initial midline framework established in the central brain prior to CC differentiation. Further analysis of these genes is required to assess their roles in this context.

The reduced or absent arborisations on the F*l* neurons of *neuroglian* mutants supports the evidence for a dendritic branching function that has previously been reported (Yamamoto et al., 2006). Arborisations from these neurons occur during mid CC development as shown in Chapter Four, which correlates with *neuroglian* expression. Neuroglian is not detected on any dendrites in developing wildtype brains, but this data suggests that it may be involved in the initial branching from axons. It

maybe that this is also the case for *ccb* and *cbd.*

5.5.4 Whole brain abnormalities

The brains of Central Complex mutants displayed abnormal phenotypes in other areas of the brain outwith the CC. In both *neuroglian* and *central body defect* mutants there were also severe Mushroom body phenotypes. These are in the form of abnormal axon trajectories or the absence of partial or whole lobes. Several lines also revealed a number of tracts in the central brain, especially near the antennal lobes, that were not present in these locations in wildtype brains. The unusual feature of these tracts was that they did not appear to add to any determined pattern of connectivity but instead terminated what appeared to be randomly. These random trajectories suggest a potential pathfinding role for *cbd* and *neuroglian* in the central brain. Both *neuroglian* (Hall & Bieber., 1997) and its mammalian homologue L1-CAM (Kamiguchi 2003; Woolman et al., 2007) have been implicated in neuronal pathfinding and fasciculation therefore this is not surprising. Alternatively, the potential role of these molecules in structural development on the midline may affect the trajectories in mutants when the tracts cannot reach their destination, resulting in aberrant axonal pathfinding phenotypes.

6

Investigating the role of *echinoid* in axon targeting in the Optic lobe

6.1 Introduction

6.1.1 Process of Photoreceptor development

The *Drosophila* compound eye consists of approximately 800 Ommatidia organised in a regular topographic array. Each Ommatidium contains eight photoreceptors (R1-R8 cells). The establishment of each of the R cells occurs as the morphogenetic furrow travels across the eye disc during the late 3rd instar, a process that includes the proneural genes and EGFR signalling. The R1-R6 cells fasciculate and project from the retina via the optic stalk to terminate in the Lamina. The R7-R8 cells also fasciculate and project with the other R cells but continue past the optic chiasm to terminate in the Medulla in two separate layers (layers M3 and M6 respectively) as shown in Figure 6.1 (A,B). R cell outgrowth commences in the 3rd instar larva, with R8 axons extending first followed by R1-R6 cells. After a lag, the R7 cells project through the lamina into the developing medulla neuropil during early metamorphosis. In the first targeting phase, both the R7 and R8 cells stop at a temporary layer (between L3-15 APF) in the medulla. Projection to their final termination points in the second targeting phase commences at 48 APF and is complete by 70 APF (Meinertzhagen & Hanson,

1991). This is represented schematically in Figure 6.1(C).

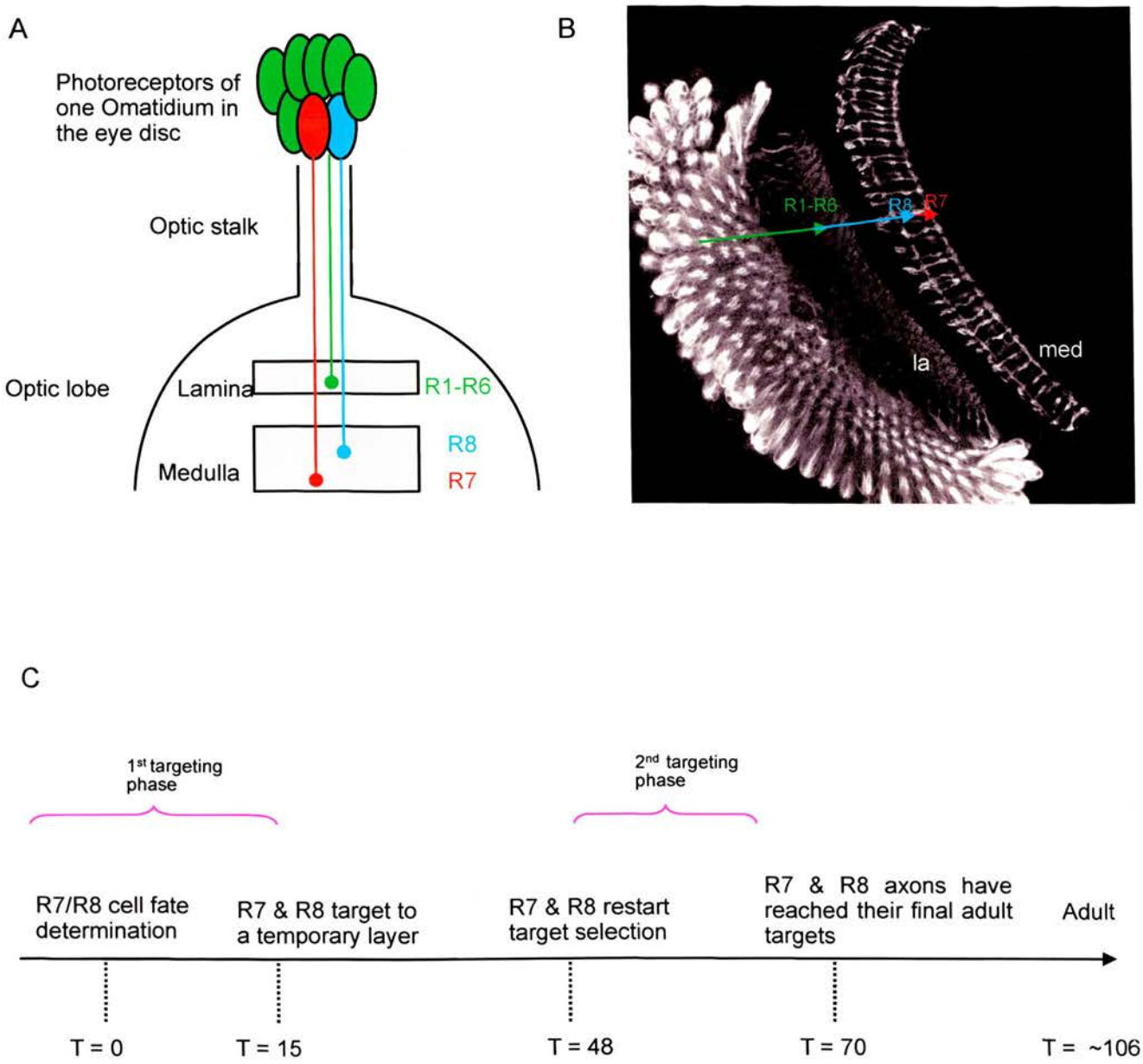

Figure 6.1: R cell targeting in the Optic lobes. A, Schematic representation of R cell targeting layers in the Lamina and Medulla in the adult. (green -R1-R6, blue-R8, red-R8). **B**, R cells stained with mAb 24B10 revealing individual R cell targets in the adult. **C**, Developmental R cell targeting timeline. The targeting phases refer to the two periods of R cell axonogenesis.'T' denotes the number of hours after puparium formation, therefore T=0 is the white prepupa. la-Lamina, med-Medulla.

6.1.2 The genetics of visual system assembly

The mechanism by which neuronal connections are created and how axons find the correct targets is still not fully understood. What is known is that cell adhesion molecules play a role in fasciculation and pathfinding often due to their homophillic binding capabilities (Kristiansen et al., 2005; Godenschwege et al., 2006). Several CAMs are known to be involved in pathfinding and synapse formation in the visual system (N-cadherin: Lee et al, 2001; Iwai et al., 2002; Prakash et al., 2005; Ting et al., 2005; Flamingo; Senti et al., 2003; Lee et al., 2003; LAR; Clandinin et al., 2001; Maurel-Zaffran et al., 2001; Capricious: Shinza-Kameda et al., 2006. Reviewed in Clandinin & Zipursky, 2002; Ting & Lee, 2007). Axonogenesis can be thought of as three steps; Firstly, guidance to the target field, secondly, choice of the correct target in this field and thirdly, assembly of a functional synapse (Clandinin & Zipursky, 2002). Accurate execution of these steps is likely to require a genetically hardwired system involving a series of molecular interactions and several cell surface recognition molecules.

6.1.3 *echinoid*

The *Drosophila* Cell adhesion molecule (CAM) Echinoid has been characterised in peripheral nervous system development and has been implicated in neurogenesis through two major pathways (Bai et al., 2001; Rawlins et al., 2003a; Spencer and Cagan., 2003). Echinoid is a member of the IgG superfamily and is similar to L1-type molecules (such as Neuroglian) which are strongly associated with neurite extension and axon pathfinding (Hortsch, 2003) and more recently synaptic function (Godenschwegge et al., 2006). The role of Echinoid in the developing CNS is not known and has not been studied to date. This project has found extensive *echinoid* expression at various points during CNS development, specifically between the late 3rd instar and early adult stages in the brain.

Echinoid demonstrates both homophilic and heterophilic (with Neuroglian; Islam et al., 2003) interactions. Functions of Echinoid include; facilitating Notch signalling (Escudero et al., 2003; Rawlins et al., 2003a), negatively regulating EGFR signalling (Bai et al., 2001; Rawlins et al., 2003b; Spencer and Cagan., 2003), cooperating with De-cadherin at Adherens junctions (Wei et al., 2005) and cell signalling during muscle morphogenesis (Swan et al., 2006). The pleiotropic nature of Echinoid indicates it may be involved in several pathways. The Echinoid protein contains seven immunoglobulin domains and two fibronectin type III-protein domains. This is similar to L1-type proteins with six immunoglobulin domains and five FNIII-protein domains. L1 type proteins have been shown to be involved in pathfinding and synapse formation (Burden-Gulley et al., 1997; Godenschwege et al., 2006). IgSF CAMs play major roles in nervous system development and many have been studied in detail, e.g. Robo (Dickson & Gilestro, 2006), Fas II (Baines et al., 2002) and DSCAM (Rougon & Hober, 2003). These molecules are found in a variety of cell types and appear to be pleiotropic in character.

A complete study is yet to be carried out on the role of the IgSFs in the CNS. They are one of the major groups of CAMs required for CNS development and function, along with Netrins and Semaphorins. Their actions are vital to the functioning of the nervous system. Mutations of several IgSFs show gross defects and have been linked to a variety of nervous system diseases. Determining their functions, signalling properties and network connections is pivotal in our understanding of the nervous system from flies to humans.

echinoid expression analysis in section 3.3 revealed extensive *ed* expression on axons throughout the brain including those in the Optic lobe. This was the first time *echinoid* expression had been recorded in the *Drosophila* CNS. In order to assess the role of *echinoid* in pathfinding it was decided to utilise the well characterised topographic system of the Optic lobe photoreceptors due to the range of genetic tools available.

6.2 Aim

To investigate the potential role of *echinoid* in pathfinding and target selection in the visual system.

6.3 *echinoid* is expressed on the developing photoreceptors

In section 3.3, *echinoid* expression was faintly detected in the optic lobe of the early adult brain. The subsequent expression analysis revealed *echinoid* expression in the developing brain, particularly the Central Complex and the Optic lobes. In order to ascertain the developmental profile for *ed* in the optic lobes, brains were dissected at a series of stages; the white prepupal stage, 12, 20, 48 and 72 APF. Brains were double labelled with α-Echinoid and mAb 24B10 (α-Chaoptin), a photoreceptor marker. Echinoid was detected at the growth cones of the developing R7 and R8 photoreceptors and faintly on the axons in the medulla and optic stalk. At the prepupal stage Echinoid was detected faintly in the projecting R8 cells (data not shown). By 12 APF (near the end of the first targeting phase) *echinoid* expression was detected faintly in growth cones of R7 and R8 cells and more strongly on R1-R6 growth cones [Figure 6.2 (A,B)]. Expression continued through to 48 APF at the initiation of the second targeting phase, where expression at the growth cones of the R7 cells was particularly strong [Figure 6.2(C,D)]. *echinoid* was expressed in the M3 and M6 medulla layers (and layers 7, 8 and 10) at 48 APF. Expression was also detected faintly on R cell axons. Echinoid immunoreactivity was detected at the R1-R6 cell growth cones in the Lamina at 20 APF but not after this point. There was very faint Echinoid detection in the photoreceptors at 72 APF but there was immunoreactivity in the M1 and M2 (medulla) layers at this stage [Figure 6.2 (E,F)]. The M2 layer is the target of L2 (Laminar) neurons.

At 48 APF there was also detection in several of the deeper (more medial) medulla layers, indicating Echinoid was also present on growth cones of the laminar neurons, although this was not investigated any further in this study [see Figure 6.2(E)]. Restriction of expression to certain layers was apparent by this timepoint. The layers between the temporary R7 and R8 neurons were either faint or negative for *echinoid* expression. These data, in conjunction with temporal expression data mentioned above, permits the hypothesis that *echinoid* expression is correlated with R cell targeting. The detection of *echinoid* expression at the R cell growth cones during the two targeting

phases suggested a potential role in axon guidance and choice of the appropriate R cell target. Considering these developmental expression results and the ease of identification of the R7 and R8 cell layers, further analysis was restricted to these cell types. Analysis of growth cones of the R1-R6 cells that terminate in the Lamina was not feasible in this study due to the densely packed arrangement of cells.

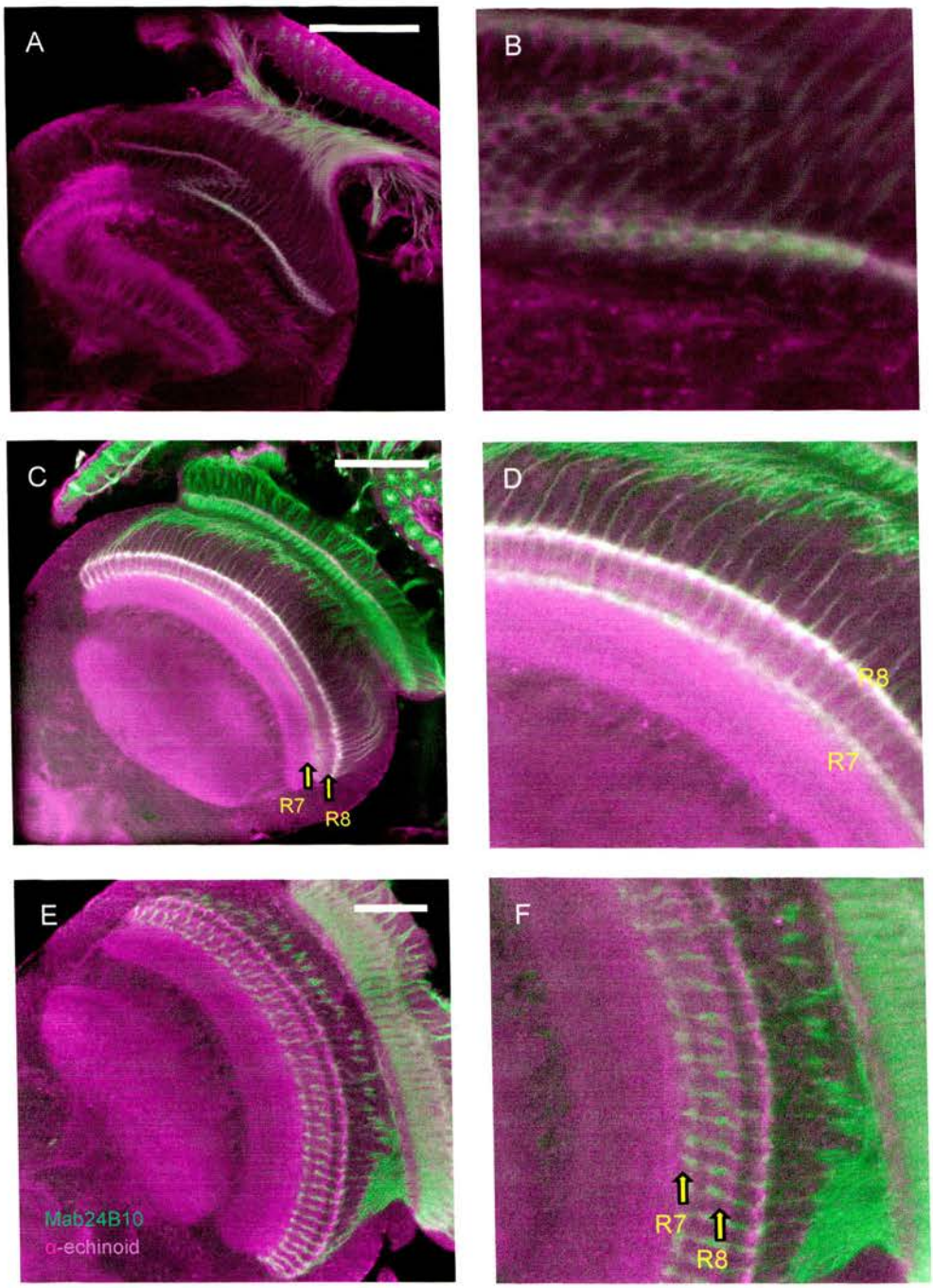

Figure 6.2: *echinoid* expression in wildtype brains. A,C,E; whole lobe. B, D,F; higher magnification of A, C, E. **A,B**; 12 APF shows expression in the R1-R6 cells targeting the lamina. **C,D;** 48 APF shows *echinoid* expression in the temporary R7 and R8 layers. **E,F**; 72 APF shows reduced *echinoid* expression in the target regions. Green – mAb 24B10, magenta – α-Echinoid. Scale bars 50μm.

6.4 *echinoid* mutants display aberrant trajectories to the medulla

To assess the potential role for *echinoid* in axon targeting it was first necessary to analyse *echinoid* mutants. Three alleles of *echinoid* were assessed; a viable hypomorph $ed^{4.12}$, a null allele ed^{K01102} (Rawlins et al., 2003a) which when crossed over a deficiency produced escapers (delayed hatching) and $ed^{6.1}$ (null). Photoreceptor trajectories were assessed using mAb24B10. Mutants were analysed at three developmental stages; 24, 48 and 72 APF in order to analyse phenotypes at different stages of targeting.

6.4.1 $ed^{4.12}$

In wildtype control experiments R7 and R8 cells projected to the medulla terminating in an even topographic array [Figure 6.3 (C)]. In contrast, $ed^{4.12}$ homozygotes displayed a more disorganised projection pattern. Observations of mutants at all stages showed several R cell fascicles overshooting their usual point of termination. In several cases these axons overshot their target layer and then looped back again as if correcting themselves [Figure 6.3(A)]. The looping phenotype was observed in adults (n = 4/6), at 72 APF (n=7/10 and in brains at 48 APF (n=3/6). This form of phenotype has not been reported in the *Drosophila* nervous system before, though a looping phenotype similar to this has been reported *neurolin* mutants in retinal axon guidance in Goldfish (Ott et al., 1998).

In wildtype brains at 48 APF, R7 and R8 axons projected directly to the medulla where they stopped displaying two distinct temporary layers. In contrast, at 48 APF $ed^{4.12}$ brains showed three targeting phenotypes. Firstly, several axons stopped beyond the R7 and R8 layers, in other medulla layers. Secondly, axons often crossed trajectories between the two termination layers instead of continuing in a direct line. This is shown in Figure 6.3(B) Thirdly, the looping phenotype was observed [Figure 6.3(A)]. This is shown in Figure 6.3(B). A similar phenotype was observed in brains at 72 APF and in adults.

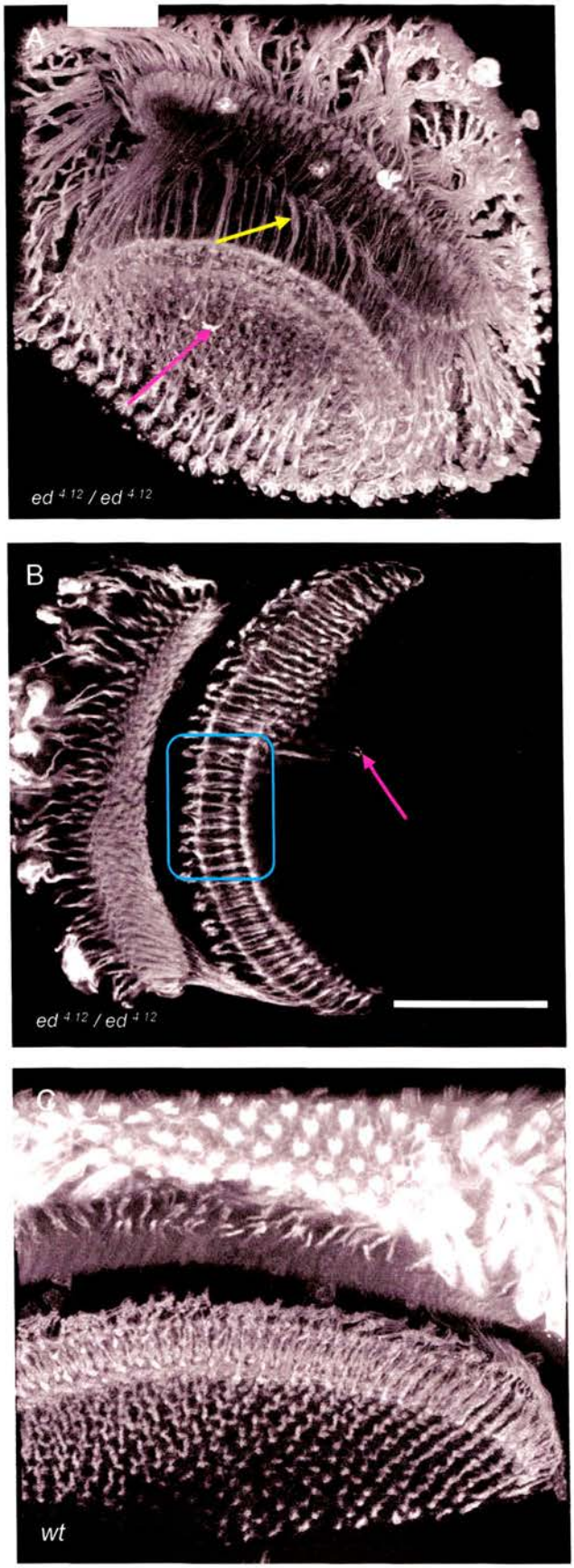

Figure 6.3: *ed*$^{4.12}$/ *ed*$^{4.12}$ mutant phenotypes. A,B; *ed*$^{4.12}$ /*ed*$^{4.12}$ at 48APF, magenta arrow points to R cell axons looping. Yellow arrow points to increased fasciculation between axons. Blue box shows region where fibres seem to be terminating in incorrect positions. **C**, Wildtype showing normal R cell trajectories to medulla.. All brains stained with mAb 24B10 at 48 APF. Scale bar 50µm.

6.4.2 $ed^{K01102}/ ed^{6.1}$

In order to assess this phenotype in a more severe mutant, a null allele of *echinoid* was subjected to the same evaluation as the hypomorph. ed^{K01102}, a larval lethal recessive allele (Spencer and Cagan., 2003) allows escapers when crossed to $ed^{6.1}$(Rawlins et al., 2003b). The escapers were rare (n=1/68 adults) and had several additional nervous system phenotypes. Obtaining individual brains at the required developmental stages proved problematic due to the limited number of individuals with the desired genotype. Optic lobes from $ed^{K01102}/ ed^{6.1}$ individuals showed a disorganised topography [Figure 6.4 (B)] with R7 and R8 cells often terminating too close together [Figure 6.4 (B')] (n = 3). Projections were capable of initial straight trajectories but showed aberrant termination patterns in the medulla.

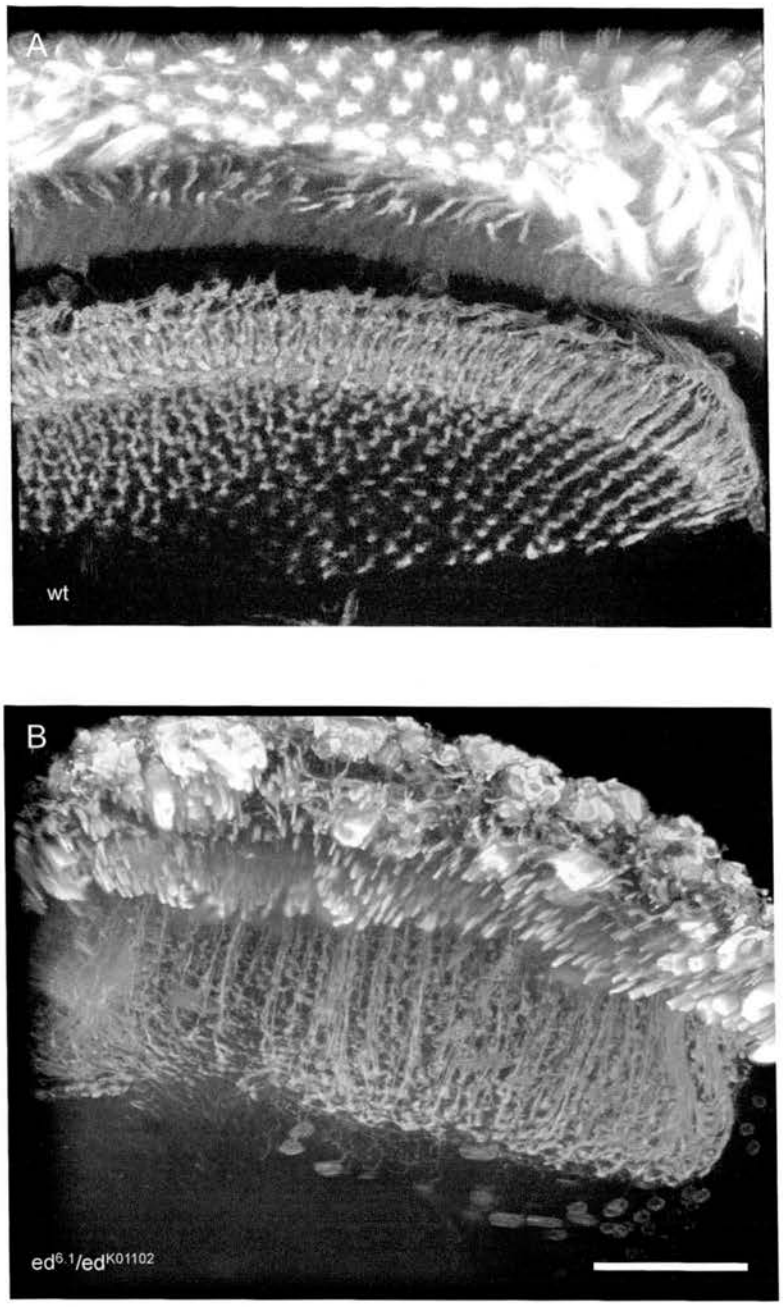

Figure 6.4: *ed*$^{6.1}$ / *ed*^{K01102} mutant phenotypes. A, Adult wildtype. **B**, *ed*$^{6.1}$ / *ed*^{K01102} (mid pupal development) displaying disorganised topography . **B'**, Aberrant topography with R cell termini often located very close together as shown by the magenta arrow (n=3). All brains stained with mAb 24B10. Scale bar 50 µm.

6.5 Analysis of R cell afferents

The results from the mutants suggested an R cell targeting function for *echinoid*, though the data obtained was not sufficient to confirm this hypothesis. There are limitations when using the mutants for this type of study. The low survival rate of null mutants reduces numbers for analysis. Also, both R cell afferents and their medulla target cells are mutant, preventing autonomous analysis of one cell type. In order to examine if the phenotypes observed were due to an autonomous effect within the R cells it was necessary to perform experiments in which the R cell afferents, but not the targets, were deficient for *echinoid*. In addition, mAb 24B10 does not allow visualisation of separate R cell types, therefore it is not possible to visualise individual R cells or single types of R cells.

An alternative hypothesis for the observed *echinoid* mutant phenotypes can be formed from previous studies on signalling pathways. *echinoid* has been shown to be required to moderate Egfr signalling during R8 photoreceptor selection by the proneural gene *atonal* during eye development (Rawlins et al., 2003b, Spencer and Cagan., 2003). Subsequently, *echinoid* mutants display 'twinned' R7 and R8 cells in several ommatidia. As a result the targeting phenotype observed in *echinoid* mutants may be due to the surplus of axons competing for the same target, a secondary defect of cell fate specification indicating the pleiotropy of *echinoid*.

Common methods of choice by which to assess the development of individual groups of cells in this context is through the FLP/FRT (Newsome et al., 2000; Lee et al., 2001; Lee et al., 2003), MARCM (Lee et al., 2001, Senti et al., 2003) or EGUF/Hid (Shinza-Kameda et al., 2006) systems. These techniques induce homozygous mutations in individual cells or small subsets of cells deriving from a single progenitor, resulting in all cells derived form this progenitor being homozygous mutant. For experiments assessing *echinoid* however, these methods are not feasible. The pleiotropic effects of Echinoid determine multiple phenotypes as displayed by the mutants. These are likely to

still be displayed by the clones, subsequently affecting the R cells before axonogenesis.

The extensive study of the *echinoid* gene has provided several alternative tools that can be utilised to compensate for the lack of a clonal analysis. Therefore the role of *echinoid* in R cell targeting was tested using a range of genetic tools including photoreceptor specific P{Gal4} lines, temperature sensitive strains and dominant negative (Rawlins et al., 2003a) strains.

Initial experiments utilised an ed^{ts} strain (gift from H.Vaessin). The aim of using the temperature sensitive strain in this study was to knock down *echinoid* during specific developmental timepoints by moving pupae to the restrictive temperature. There are two main targeting phases during photoreceptor development as shown in Figure 6.1 (C). Sets of ed^{ts} pupae could be aged and moved to the restrictive temperature during either the first or second targeting phase and then removed and placed at 18°C until eclosion. Adult flies would be dissected and analysed for R cell targeting phenotypes. This particular ed^{ts} strain was maintained over CyO, though ed^{ts}/ed^{ts} flies are homozygous viable at temperatures below 25°C (Ahmed et al., 2003). Flies were raised at either 18°C or 21°C however no ed^{ts}/ ed^{ts} individuals eclosed.

To test if the ed^{ts} allele was present, a complementation test was performed. The ed^{ts} /CyO flies were crossed to a deficiency (Df(2L)ed-dp/CyO) and crosses were placed at both 18°C and 30°C after one day. In theory, the ed^{ts} /Df(2L)ed-dp should survive at 18°C and die at 30°C. In the resulting F1 progeny from both temperatures both Curly and straight winged flies were observed meaning ed^{ts} /Df(2L)ed-dp flies had survived being raised at 30°C. These results suggested that no ed^{ts} allele was present. Subsequently, it was not possible to use this strain in further experiments.

6.5.1 R cell afferents do not show an abnormal targeting phenotype

To assess the targeting of *echinoid* mutant R cells a form of Echinoid protein lacking the extracellular domain (UAS-ed^{ICD}-HA) was expressed in the R cells driven by a set of three different Gal4 drivers; GMR-Gal4, PANR7-Gal4 and PM181-Gal4. There is evidence to suggest that this form of Echinoid protein acts as a dominant negative. Over-expression of a truncated Echinoid protein late in proneural clusters, the eye disc and the dorsal compartment of the wing discs has been shown to result in phenotypes similar to those of loss of function *ed* mutations (Ahmed et al., 2003; Escudero et al., 2003; A.Jarman, personal communication). The mechanism by which this dominant negative form of Echinoid acts is unknown but evidence from the latter studies suggests that it can be used to interfere with Echinoid function in several cell types. Therefore in this study, the dominant negative form of Echinoid can be expressed using a variety of driver lines to interfere with Echinoid function in R cells. This makes it possible to alter Echinoid function in the afferent (R cells) but not the target cells in the Medulla.

Three P{Gal4} lines were selected to drive expression of the dominant negative Echinoid protein. GMR (Glass multimer receptor) is expressed in the eye imaginal discs in cells posterior to the morphogenetic furrow. Flies homozygous for GMR-Gal4 have been shown to have effects on eye development (Kramer & Staveley, 2003) therefore heterozygotes were used. In addition GMR-Gal4 driven dominant negative Echinoid has been shown to result in flies with a rough eye phenotype (Escudero et al.,2003). In order to avoid effects of the dominant negative *echinoid* on cell fate determination in the 3rd instar larva, the Gal80^{ts} repressor of Gal4 was used. Flies were moved to the restrictive temperature at either 0-10 APF or 45-55 APF to allow Gal4 expression during the two R cell targeting phases. Results showed no abnormal targeting (data not shown).

echinoid expression was strongest on the R7 afferents (see section 6.3) therefore R7 driver lines were used to express the dominant negative *echinoid.* Initial experiments were performed using PANR7-Gal4 (Lee et al., 2001) and PM181-Gal4 (Clandinin et

al., 2001) drivers, that both drive expression in R7 cells, to drive dominant negative UAS-ed^{ICD}-HA. *PANR7-Gal4/ UAS-ed^{ICD}-HA* adults did not display an abnormal R cell targeting phenotype (data not shown). It was thought that this may be due to temporal expression of this driver line. To test the expression timeline for PANR7-Gal4, this line was crossed to UAS-mcd8::GFP and dissected at 12 and 48 APF. Results showed that this line was not expressed during the two main R7 photoreceptor targeting phases, thereby accounting for a lack of phenotype. This driver was therefore discontinued. Instead, an alternative driver, PM181-Gal4 (Gift from L.Zipursky) that is expressed in the late larval stage (Lee et al., 2001) was used. The expression of the PM181-Gal4 driver overlapped with the early part of the first R cell targeting phase.

Staining with mAb 24B10 revealed that *PM181-Gal4/ UAS-ed^{ICD}-HA* adults showed a looping phenotype in 5/24 individuals. However, this was not like that of the previously observed mutant phenotypes (data not shown). Often only individual axons were seen overshooting, a phenotype also detected occasionally in Oregon R adult flies (n = 3/10). In all brains the topographic array in the medulla was normal, unlike that of *ed ^{K01102}/ ed$^{6.1}$* individuals. To ensure the dominant negative construct was being expressed in the correct cells an α-HA antibody was used to detect the HA tag in the late 3rd instar eye disc. It tested positive. This confirmed the presence of the dominant negative form of Echinoid in the R7 cells during the early part of the first targeting phase.

The PM181-Gal4 driver in this instance was used to assess the role of *echinoid* in the first targeting phase and results indicated that loss of Echinoid function in the R7 cells at this time did not affect targeting. A previous study reported that *PM181-Gal4 UAS-mCD8::GFP* expression was still detectable at 15 APF (Lee et al., 2001) but in this study no *PM181-Gal4* expression was detected at this timepoint or even earlier, at 5 APF. Therefore the reason for the lack of targeting phenotype in *PM181-Gal4/ UAS-ed^{ICD}-HA* individuals may be due to *PM181-Gal4* expression ceasing too early to have an effect on R7 axonogenesis (which commences near the onset of metamorphosis). In

order to assess if this was the case throughout both of the R cell targeting phases it was necessary to express the dominant negative form of Echinoid for a longer period of time. The total expression time for the *PM181-Gal4* driver was unknown.

To determine if the *PM181-Gal4* driver was expressed during the second targeting phase, *PM181-Gal4; Uas-mCD8::GFP* pupae were dissected at 48 APF and assessed for GFP expression in R7 cells. No GFP expression was detected at this timepoint. In order to allow constitutive expression of Pm181-Gal4 through to the second targeting phase at 48 APF a strain containing *Pm181-UAS-mCD8::GFP/ UAS-Gal4 ; UAS- ed^{ICD}-HA/ UAS-Gal4* was generated. The *UAS-Gal4* construct allows continual expression of all UAS constructs, thereby maintaining expression of *PM181-UAS-mCD8::GFP* and *UAS- ed^{ICD}-HA* throughout the second targeting phase. This also allows visualisation of the R7 cells alone in the adult with GFP in addition to visualisation of all the photoreceptors with mAb 24B10. Results (n=7) showed no abnormal R7 cell targeting phenotype (data not shown). This suggests that Echinoid function is not required cell autonomously in R cell afferents during axonogenesis.

6.6 Discussion

6.6.1 A role for *echinoid* in pathfinding and target selection?

echinoid is expressed on R cell axons and growth cones in the first targeting phase and in the M3 and M6 medulla layers (and layers 7, 8 and 10) in the second targeting phase. Expression was not detected in other medulla layers including those separating the R7 and R8 layers. Expression had ceased by 72 APF when R cells had projected to their final adult targets. These expression patterns indicated a developmental targeting function for *echinoid* that was further supported by abnormal targeting phenotypes in two strains of *echinoid* mutants during metamorphosis and in adults. Cell adhesion molecules that have been shown to co-operate or interact with Echinoid (De-cadherin; Wei et al 2005, Neuroglian; Islam et al 2003), are known to be involved in pathfinding and targeting (De-cadherin; Dumstrei et al. 2003, Dn-cadherin; Lee et al. 2001, Neuroglian; Hall & Bieber 1997) in the *Drosophila* nervous system therefore this function was investigated for *echinoid*. This is the first study of the role of *echinoid* in neuronal pathfinding and target selection.

Subsequent loss of function experiments that generated mutant R cell afferents in an otherwise wildtype brain did not support this hypothesis. These results indicate that *echinoid* is not required for targeting in the R cell afferents of the optic lobes. This does not rule out a role for *echinoid* in target selection in the medulla as it was detected in the target region. Therefore Echinoid may mediate an interaction between medulla layers and R cells. The results further imply that *echinoid* is not required for axon-axon fasciculation as R cells targeted normally. Alternatively, it could be hypothesised that *echinoid* has an indirect function in pathfinding that is compensated for in its absence. This study investigated the role of *echinoid* in targeting of R cell afferents. Due to time constraints, further experiments to determine the potential role of *echinoid* in the target region were not possible. It is feasible that the phenotypes seen in the *echinoid* mutants may be due to the higher number of R7 and R8 cells competing for targets in the same

location resulting in aberrant targeting.

6.6.2 Limitations to studying *echinoid* for pathfinding and targeting

Extensive expression of *echinoid* in the brain suggests it may be a pleiotropic molecule. Cell adhesion molecules do not only have a role in adhesion but also in cell-cell communication and signaling (Islam et al. 2003). They also play important roles in promoting and directing neurite outgrowth (Hall & Bieber, 1997). The presence of the Echinoid cell adhesion molecule on axons (i.e. Photoreceptors, VFS, HFS) and in regions of synaptic formation (medulla layers) may indicate roles in fasciculation or synapse formation, though this will require further analysis.

A limitation to studying *echinoid* in the photoreceptors was the cell specification phenotype that manifests in these cells in mutants prior to axonogenesis. This requirement for Echinoid during R8 and R7 specification (R8; Rawlins et al., 2003b, R7; Bai et al., 2001) prevented the used of clonal analysis in this investigation as mutant clones would have affected equivalence group signalling. A combination of R cell specific Gal4 drivers active after cell specification and a dominant negative *echinoid* construct were employed that also avoided the cell specification phenotype. The observations made from these methods disproved the hypothesis.

How the dominant negative version of the protein works is not completely understood therefore this is not perhaps an ideal substitute for a clonal analysis. However this was the best method available when considering the cell signalling phenotype and in the absence of a viable ed^{ts} strain. To further analyse *echinoid's* role in R cell targeting it would be necessary to assess the role of an *echinoid* mutant target with wild type afferents. To do this, the GMR-Gal4 could be used to drive UAS-ed in $ed^{4.12}/ed^{4.12}$ mutants thus rescuing both the R cell signalling and potential axonogenesis

phenotype. To perform rescue experiments specific R cell drivers (i.e. PM181-Gal4) could not be used as this would still result in signalling phenotypes in other R cells. Equally, using RNAi technology would be a suitable alternative to a dominant negative construct. Had the temperature sensitive allele of *echinoid* been usable it would have made testing the hypothesis more straightforward. It was possible to test for a targeting phenotype while avoiding the cell fate phenotype induced by the absence of *echinoid,* but it is a challenging problem that requires further extensive study.

7

Discussion

7.1 A combined marker approach for neuroanatomical study

This study of the developing neuroarchitecture of the CC was conducted using both immunohistochemical markers and enhancer trap lines. In section 3.3.3 expression patterns for three markers were determined that could be used to trace CC development through metamorphosis. This is the first study to examine these expression patterns in the developing Central Complex, thereby revealing novel markers (in addition to isolating potential molecules for functional investigation) for CC neuron development. In particular, Echinoid proved to be a reliable marker with which to trace the development of the HFS as well as to track the differentiation of the whole CC structure. This proved to be beneficial when the enhancer trap lines did not yield a line allowing clear visualisation of this fibre system. The results from these markers successfully provided a developmental timeline for the whole CC structure and the HFS. However, it is also important to note the drawbacks of the immunohistochemistry technique in this study. In addition to the three selection criteria for effective markers initially outlined in section 1.4, it is now possible to add further points that should be considered when using

immunohistochemical analysis for developmental studies. Firstly, the markers used did not reveal any Perikarya therefore isolating the number of cells sending axons into certain fibre bundles was not possible. This would have been particularly useful for the investigation of the neurons of the HFS. Secondly, isolating fibre bundles often proved difficult due to extensive staining in nearby regions.

In order to assess these issues the developmental study was repeated using enhancer trap lines. This yielded a large volume of data for both adult and developmental structural analysis as detailed in Section 4.3. The enhancer trap lines and the two different reporters revealed neuronal Perikarya, projection patterns, sets of morphologically related neurons and polarity data. In several cases novel morphological relationships between neurons were identified. The reproducibility of this technique makes it ideal for developmental studies. Although temporal and spatial changes in Gal4 expression occurred between CC development and adult expression (e.g. line 23y, see Table 4.2), expression patterns often appeared to be consistent with axon outgrowth and circuit establishment, meaning neurons could be easily traced as they projected. This was demonstrated clearly by lines c255, c61 and c159b (section 4.3, Table 4.2). These patterns were often absent or reduced in these neurons in adult brains showing expression in different neurons, suggesting a common transcriptional mechanism for separate processes of axon outgrowth and adult function. This inference of function is a further advantage of using the enhancer trap lines for developmental analysis. From this study it can be concluded that the two techniques complimented each very successfully. Both yielded a large volume of novel data on the differentiating CC.

It is important to note that this is not a comprehensive analysis as not all CC neuron types were accounted for in this study. This is a consideration regardless of the technique employed as no one method reliably labels every neuron of interest. By building on the present study through the use of novel enhancer trap lines and immunohistochemical markers in addition to other techniques (see Future work, below) we can aim to build an atlas of CC development that can be subdivided by a series of

reliable markers.

7.2 Central Complex development

7.2.1 Comparison of Central Complex development across the Insects

The adult structure of the Central Complex is highly conserved throughout the arthropods (Loesel et al., 2002, Williams et al., 2005) even though members of this phyla display a wide variety of behaviours that varies in complexity. This is in contrast to the Mushroom bodies where structural differences have been demonstrated (Strausfeld et al., 1998). This suggests come commonality in adult CC function across the insects. Suggested functions of the CC include that it is a common control centre for locomotion (Loesel et al., 2002; Strauss, 2002) or is involved in visual processing (Liu et al., 2006). Despite the fundamental importance of the Central Complex demonstrated by behavioural analyses (Strauss et al., 1992; Bonhouche et al., 1993; Strauss & Heisenberg, 1993; Liu et al., 2006) our knowledge of the ontogeny of this structure previous to this study was limited. This study of the developing CC has established the intricate temporal projection pattern for the major neurons that comprise this neuropil as shown in Figure 4.26. Unlike the CC of the holometabolous beetle *Tenebrio molitor* (Wegerhoff & Breidbach., 1992) and the hemimetabolous grasshopper *Schistocerca* (Boyan & Williams., 1997), the CC of the holometabolous *Drosophila* is an imaginal structure like that of *Musca domestica* (Strausfeld, 1976).

7.2.2 Central Complex development in *Drosophila*

Initial analysis of metamorphosis of the brain revealed temporal development of the four CC neuropil occurs in the first 48-52 hours APF (section 3.4), confirming reports that the CC appears in the early part of metamorphosis (Hanesch et al., 1989;

Renn et al., 1999). The first identifiable whole sub-structure was the PB (L3) followed by the FB and NO. This correlates with that of *Tenebrio*, with the FB and PB being the first discernible CC sub-structures. *Drosophila* differ in that NO are also present at this early stage. Like that of *Tenebrio* however, the EB differentiates later in development. As to why *Tenebrio* develops a CC at this earlier stage is not clear, although in the case of *Schistocerca* this earlier requirement for a CC may be a feature of hemimetabolous life.

The early appearance of the PB, FB and NO is likely to be due to the early developing fibre systems (HFS and VFS) that innervate these sub-structures but not the EB, that is mainly formed by the Large field R neurons. Compartmentalisation of the FB is apparent at 8 APF as demonstrated by the developing HFS (section 3.4). This was further exemplified by the enhancer trap lines that revealed a potential initial structural framework is established in the first 12 hours of metamorphosis (section 4.5). This consists of the two major fibre systems, the VFS and the HFS and an unknown number of F neurons. Establishing the precise number of F neurons involved at this stage was not possible in this study as we were limited by the expression characteristics of the enhancer trap lines and immunohistochemical markers. This framework may provide an initial structural lattice for projections from the later developing CC neurons to use as spatial guidance cues. The two fibre systems innervate the eight segments of the FB before targeting neuropil external to the CC. The F neurons may perform a similar function by innervating the transverse FB layers.

From these data (sections 3.4 and 4.5) it can be concluded that CC neuron outgrowth occurs incrementally, with successive neuron types being added to the CC framework at defined intervals. Firstly, the F*l* neurons shown by line c61, the HFS and VFS (α-Echinoid staining and enhancer trap line c465), secondly the *fb-eb* neurons and Pontine neurons (c159b and c255) and finally the R neurons (52y, c61, c255) and F*m* neurons (c255). This observation of temporal augmentation of cell types to the CC has also been observed in *Tenebrio*, where projections from certain cell types innervate the

CC additively over consecutive larval instars (Wegerhoff & Breidbach, 1992), and in *Schistocerca*, where w, x, y and z tracts pioneer successively during mid-embryogenesis (Williams et al., 2005).

Analysis of staining patterns from *echinoid* and *shotgun* expression yielded preliminary information on lineage for the HFS (section 3.4.1). Both the *z* and *y* fibres were each traced to separate clusters of neuroblasts and secondary neurons suggesting the each of the four fibre bundles originated from one of four protocerebral neuroblasts per hemisphere as seen in *Schistocerca*. Positions and trajectories of the clusters of Perikarya for the later developing *fb-eb* and Pontine neurons were reminiscent of the pattern of the HFS, suggesting that each of the eight clusters have separate origins, but equally that pairs of *fb-eb* and Pontine neurons share a common lineage. This type of clonal segregation can be seen in the Kenyon cells of the Mushroom bodies that differentiate from four neuroblasts to form a four unit structure (Armstrong et al., 1998). The enhancer trap lines reveal this potential shared lineage between *fb-eb* and Pontine neurons and indicate that cell type specification occurs as a further differentiation. This hypothesis is consistent with that suggested for the type A R neurons of the EB (Renn et al., 1999).

7.3 Insights into Central Complex structure

7.3.1 Genetic relationships between neurons

This is the first study to isolate the perikaryon of the ExR2 neuron and trace the complete projection pattern of this neuron (line c61, section 4.3.6). Indeed, this study has isolated enhancer trap lines that allow visualisation of the projection patterns of both the ExR2 and ExR1 (c255, section 4.3.8) neurons. These were not fully represented using Golgi staining in previous studies (Hanesch et al.,1989). Early in development,

sets of F*l* neurons were observed in two pairs suggesting a common morphology (c61, section 4.3.6). The F*l* neurons have not been further categorised in previous studies though many different subtypes have been observed (Hanesch et al., 1989). F neuron branching patterns can be most accurately analysed using Golgi staining, as this allows analysis at single cell resolution. In this study the enhancer trap lines revealed potential relationships between two pairs of F*l* neurons which may indicate further categorisation and a possible shared lineage. Several enhancer trap lines showed expression in F neurons but these were not always observed during development. Tracing and identifying the F neurons in the adult brain was problematic due to the high density of arborisations from these cells. Therefore it was not possible to resolve neuronal relationships for all of these cells.

7.3.2 Connections to other regions of the Nervous System

Echinoid staining revealed that fibre bundles of the HFS project ventrally past the VBOs (section 3.4.1.1). The final targets of these neurons were not resolvable in this study. It may be that these fibres target to the Ventral nerve cord (VNC) and connect to a motor circuit. Indeed, in *Schistocerca*, connections to the EB from the VNC via structures homologous to the VBO have been reported (Homberg, 1994). In *Drosophila* it may be that information is relayed from the HFS via the VBO to the VNC. Further study and a specific HFS marker is required to investigate this fully. The major fibre systems (HFS and VFS) have been well characterised in adult diptera (Power 1943, Williams 1975, Strausfeld 1976, Hanesch et al.1989) but the intrinsic Pontine neurons have remained more elusive (Hanesch et al., 1989). These data suggest that isomorphic sets of both Pontine and *fb-eb* neurons exist in the CC, shown by the expression patterns of enhancer trap lines c159b and c255 (sections 4.3.7 and 4.3.8). These enhancer trap lines have revealed that these neurons share a common morphology and this has allowed inference of cellular patterns. The Pontine neurons display a range of morphologies all

of which are intrinsic to the FB. These neurons, like the HFS and VFS, exist as isomorphic sets. One type of Pontine neurons, the *Pcd* neurons, appear to relay information between hemispheres within the FB. Future studies focusing on the functions of the FB could start with an investigation of these neurons.

7.3.3 Compartmentalisation and information flow in the Central Complex

The expression patterns revealed in this study allow us to further clarify the compartmentalisation of the CC. Projection patterns of the HFS, VFS, Pontine and *fb-eb* neurons define the columnar matrix elements with the F neurons forming the transverse strata. Projections of all the columnar elements target the 8 segments of the FB, with the VFS and HFS arborising in the 16 glomeruli of the PB. In addition to this projection patterns of the ExR1 neurons revealed 32 radial branches innervating the EB ring [Figure 4.3(B)]. The mutant data was also informative in this respect, revealing ~16 areas of arborisation from Type A R neurons in the unfused EB sections adjacent to the midline (Figure 5.4). These data suggest the hypothesis that the *Drosophila* EB is divided into 16 radial segments (that can be further subdivided into 32 half segments). It may be that the *fb-eb* neurons each innervate a segment displaying homolateral connections between the FB and the EB, as seen in *Musca domestica* (Strausfeld, 1976), although this was not resolvable in this study. The projection patterns from the *fb-eb* and Pontine neurons also suggest that the FB segments can be further subdivided into half segments, revealing 16 segments/glomeruli for each of the PB, FB and EB thereby forming a one dimensional array of columnar elements as hypothesised by Hanesch et al. (1989).

From this study we can also tentatively infer more about the information flow through the CC. It has been previously reported that the main input to the CC is through the Large field F and R neurons that first arborise in regions such as the VBO and LTR,

and the chief output neurons are the small field HFS neurons (Hanesch et al., 1989; Strauss, 2002). Data from the Dscam marker used in this study only revealed spiny dendrites of some Large field neurons, but this does suggest that the previously reported hypothesis may be correct. These data also reveal that Large field neurons (i.e. ExR1) are not exclusive to one sub-structure (Hanesch et al.,1989), as the ExR1 neuron innervates both the FB and the EB with spiny terminals, suggesting data flow from outwith and within the CC by Large field neurons. The Pontine neurons were previously shown to have both blebbed and spiny endings (Hanesch et al., 1989) and this was also seen in this study. These neurons are intrinsic to the FB and do not arborise until they reach the FB segments. *Pc d* neurons innervate one segment then terminate contralaterally prompting the hypothesis that their function is to allow data flow between hemispheres albeit in one sub-structure. Further studies are required to determine the CC polarity.

7.4 Significance of research

This study presents the first detailed analysis of the differentiating Central Complex and has provided novel insight into the structural, genetic and lineage components of this neuropil. In addition, a set of enhancer trap lines have been isolated and characterised for both the developing and adult Central Complex. The combined approach of antibodies and enhancer trap lines proved to be an effective method for structural and developmental analysis. Using these methods this study successfully built on the previous structural analyses of the insect CC (*Drosophila*; Power 1943; Hanesch et al., 1989; Renn et al., 1999: *Musca*; Strausfeld 1976*; Tenebrio molitor;* Wegerhoff & Breidbach, 1992*; Schistocerca gregaria;* Boyan & Williams, 1997; Williams et al., 2004: *Arthropods*; Loesel et al., 2002). In addition, novel markers for neurons of the CC were identified. Echinoid proved to be an effective structural marker, although the exact function of this Cell adhesion molecule could not be confirmed. This work also provided

an insight into the function of *neuroglian*. Analysis of CC mutants with the enhancer trap lines yielded further data on the structure of the CC and provided an indication of the functions of the genes that had been mutated.

7.5 Future work

7.5.1 Lineage Analysis

This thesis did not set out to identify the lineage of the CC but it has been possible to infer lineage from the data. Early results from section 3.6.1 permitted the inference of lineage for the HFS but this was not investigated further. These results were interpreted after consulting two studies that were published after the work for this section had been completed (Pereanu & Hartenstein, 2006; Younoussi-Hartenstein et al., 2006). Lineage tracing has been performed for the MBs (Ito & Hotta, 1992) and this information has been utilised successfully to ablate these structures in more recent studies (Armstrong et al., 1998). Performing a lineage analysis of the CC would not only provide valuable information on the origins of the intricate framework of this structure but would be useful for further structural and functional studies.

To conduct further investigation of both the lineage and structural elements of the CC, it would now be beneficial to perform a clonal analysis. The MARCM technique (Lee & Luo, 1999; Lee & Luo, 2001) is ideal for visualising small populations of neurons (like the enhancer trap system) and for tracing lineage as previously reported for the MBs (Lee et al., 1999). The data presented in this thesis has provided valuable information on P{Gal4} drivers that can be used for such an analysis in the CC. Prior to this, performing a MARCM analysis would have been considerably more challenging. In addition, investigation of the connections that the CC has to other regions of the CNS

would provide an insight into function of this neuropil.

Isolation of novel enhancer trap lines and cellular markers in addition to modern techniques mentioned above will allow us to build on the developmental CC data presented in this thesis. Several such collections of enhancer trap lines exist to screen for CC expression (including the laboratories of Kei Ito, Julie Simpson and Volker Hartenstein). In addition to this analysis, further structural and functional analyses are required of the larval counterpart(s) or primordium of the CC. This is referred to either a series of interhemispheric commissures (Hanesch et al., 1989; Strauss, 2002), a set of different fibre systems (Pereanu & Hartenstein, 2006) or an early sub-structure (Schneider et al., 1993). A common nomenclature system for the CC at both ends of development is required to study this. Indeed, the issue of a common nomenclature can be extended to encompass the structural descriptions of the CC in all insects. In order to effectively compare CC data between species a single nomenclature system would facilitate exchange of ideas.

7.5.2 Computational tools for structural analysis of the Fly brain

There is an ongoing need to provide a common source of structural information on the *Drosophila* brain. In addition to this, it is necessary to have a consistent neuronal nomenclature system on the insect brain. The computational power and tools available to us can facilitate the analysis and presentation of this structural data that were not available previously. Programs such as Amira allow construction of schematics representative of brain structures and neuronal systems that can be subsequently visualised in 3D (Rein et al., 2002). These programs are hugely valuable for converting raw images into comprehensible schematics. The use of computational tools is also practical when dealing with large volumes of data. Learning algorithms can be applied to trace neurons directly from images, thereby facilitating the process of manual marking

of Z stacks. By using a combination of advanced imaging techniques and computational tools it should be possible to build a map of known connectivity in the Fly brain. This, in combination with raw image data, could then be incorporated into an online archive to facilitate future developmental, structural and behavioural studies.

7.5.3 Behavioural and Genetic Analyis

These data can also be utilised in studies investigating the opposite point of development; behavioural analysis. This study has isolated enhancer trap lines for certain populations of neurons. Lines could be used to drive toxins (i.e. CntE; Liu et al., 2006), *shibere*^{ts} (Kitamoto, 2002) or specific RNAi constructs (Dietzl et al., 2007) in these neurons to assess their functional role, building on previous behavioural studies for the *Drosophila* CC (Strauss & Heisenberg, 1992; Strauss & Heisenberg, 1993; Bouhouche et al.,1993; Strauss 2002; Liu et al., 2006). In addition, functions of specific genes in these cells can be investigated. These lines can be used to assess genetic components involved in axons crossing the midline, indeed the neurons of the CC are an ideal model for this type of study. These studies will hopefully reveal more about the functions of the CC as a whole.

Renewed interest in the CC is rapidly rising in the research community. Several groups focusing on behavioural studies including learning and memory, locomotion and aggression behaviour have expressed an interest in the functions of the CC (Waddell S; Simpson J; Strauss, R; Rene-martin J; Penn J. Personal communications.). Recent behavioural experiments on Learning and memory have focused on the Mushroom bodies, this is partially due to the well known memory circuit link to the antennal lobes (de Belle & Heisenberg, 1994). It would be interesting to study the CC in relation to learning and memory and to test for potential shared functionality with the Mushroom bodies.

Understanding the genetic components involved in brain development is critical to the study of the brain. Further study of genes such as *cbd*, *ccb*, *neuroglian*, *echinoid* and the Cadherins is required to determine their neuronal functions and potential interactions. This may eventually allow us to infer functional pathways. This knowledge will not only be of interest to the *Drosophila* community, but due to a high degree of shared molecular mechanisms between invertebrates and vertebrates will also be valuable in medical research.

7

Discussion

7.1 A combined marker approach for neuroanatomical study

This study of the developing neuroarchitecture of the CC was conducted using both immunohistochemical markers and enhancer trap lines. In section 3.3.3 expression patterns for three markers were determined that could be used to trace CC development through metamorphosis. This is the first study to examine these expression patterns in the developing Central Complex, thereby revealing novel markers (in addition to isolating potential molecules for functional investigation) for CC neuron development. In particular, Echinoid proved to be a reliable marker with which to trace the development of the HFS as well as to track the differentiation of the whole CC structure. This proved to be beneficial when the enhancer trap lines did not yield a line allowing clear visualisation of this fibre system. The results from these markers successfully provided a developmental timeline for the whole CC structure and the HFS. However, it is also important to note the drawbacks of the immunohistochemistry technique in this study. In addition to the three selection criteria for effective markers initially outlined in section 1.4, it is now possible to add further points that should be considered when using

immunohistochemical analysis for developmental studies. Firstly, the markers used did not reveal any Perikarya therefore isolating the number of cells sending axons into certain fibre bundles was not possible. This would have been particularly useful for the investigation of the neurons of the HFS. Secondly, isolating fibre bundles often proved difficult due to extensive staining in nearby regions.

In order to assess these issues the developmental study was repeated using enhancer trap lines. This yielded a large volume of data for both adult and developmental structural analysis as detailed in Section 4.3. The enhancer trap lines and the two different reporters revealed neuronal Perikarya, projection patterns, sets of morphologically related neurons and polarity data. In several cases novel morphological relationships between neurons were identified. The reproducibility of this technique makes it ideal for developmental studies. Although temporal and spatial changes in Gal4 expression occurred between CC development and adult expression (e.g. line 23y, see Table 4.2), expression patterns often appeared to be consistent with axon outgrowth and circuit establishment, meaning neurons could be easily traced as they projected. This was demonstrated clearly by lines c255, c61 and c159b (section 4.3, Table 4.2). These patterns were often absent or reduced in these neurons in adult brains showing expression in different neurons, suggesting a common transcriptional mechanism for separate processes of axon outgrowth and adult function. This inference of function is a further advantage of using the enhancer trap lines for developmental analysis. From this study it can be concluded that the two techniques complimented each very successfully. Both yielded a large volume of novel data on the differentiating CC.

It is important to note that this is not a comprehensive analysis as not all CC neuron types were accounted for in this study. This is a consideration regardless of the technique employed as no one method reliably labels every neuron of interest. By building on the present study through the use of novel enhancer trap lines and immunohistochemical markers in addition to other techniques (see Future work, below) we can aim to build an atlas of CC development that can be subdivided by a series of

reliable markers.

7.2 Central Complex development

7.2.1 Comparison of Central Complex development across the Insects

The adult structure of the Central Complex is highly conserved throughout the arthropods (Loesel et al., 2002, Williams et al., 2005) even though members of this phyla display a wide variety of behaviours that varies in complexity. This is in contrast to the Mushroom bodies where structural differences have been demonstrated (Strausfeld et al., 1998). This suggests come commonality in adult CC function across the insects. Suggested functions of the CC include that it is a common control centre for locomotion (Loesel et al., 2002; Strauss, 2002) or is involved in visual processing (Liu et al., 2006). Despite the fundamental importance of the Central Complex demonstrated by behavioural analyses (Strauss et al., 1992; Bonhouche et al., 1993; Strauss & Heisenberg, 1993; Liu et al., 2006) our knowledge of the ontogeny of this structure previous to this study was limited. This study of the developing CC has established the intricate temporal projection pattern for the major neurons that comprise this neuropil as shown in Figure 4.26. Unlike the CC of the holometabolous beetle *Tenebrio molitor* (Wegerhoff & Breidbach., 1992) and the hemimetabolous grasshopper *Schistocerca* (Boyan & Williams., 1997), the CC of the holometabolous *Drosophila* is an imaginal structure like that of *Musca domestica* (Strausfeld, 1976).

7.2.2 Central Complex development in *Drosophila*

Initial analysis of metamorphosis of the brain revealed temporal development of the four CC neuropil occurs in the first 48-52 hours APF (section 3.4), confirming reports that the CC appears in the early part of metamorphosis (Hanesch et al., 1989;

Renn et al., 1999). The first identifiable whole sub-structure was the PB (L3) followed by the FB and NO. This correlates with that of *Tenebrio*, with the FB and PB being the first discernible CC sub-structures. *Drosophila* differ in that NO are also present at this early stage. Like that of *Tenebrio* however, the EB differentiates later in development. As to why *Tenebrio* develops a CC at this earlier stage is not clear, although in the case of *Schistocerca* this earlier requirement for a CC may be a feature of hemimetabolous life.

The early appearance of the PB, FB and NO is likely to be due to the early developing fibre systems (HFS and VFS) that innervate these sub-structures but not the EB, that is mainly formed by the Large field R neurons. Compartmentalisation of the FB is apparent at 8 APF as demonstrated by the developing HFS (section 3.4). This was further exemplified by the enhancer trap lines that revealed a potential initial structural framework is established in the first 12 hours of metamorphosis (section 4.5). This consists of the two major fibre systems, the VFS and the HFS and an unknown number of F neurons. Establishing the precise number of F neurons involved at this stage was not possible in this study as we were limited by the expression characteristics of the enhancer trap lines and immunohistochemical markers. This framework may provide an initial structural lattice for projections from the later developing CC neurons to use as spatial guidance cues. The two fibre systems innervate the eight segments of the FB before targeting neuropil external to the CC. The F neurons may perform a similar function by innervating the transverse FB layers.

From these data (sections 3.4 and 4.5) it can be concluded that CC neuron outgrowth occurs incrementally, with successive neuron types being added to the CC framework at defined intervals. Firstly, the F*l* neurons shown by line c61, the HFS and VFS (α-Echinoid staining and enhancer trap line c465), secondly the *fb-eb* neurons and Pontine neurons (c159b and c255) and finally the R neurons (52y, c61, c255) and F*m* neurons (c255). This observation of temporal augmentation of cell types to the CC has also been observed in *Tenebrio*, where projections from certain cell types innervate the

CC additively over consecutive larval instars (Wegerhoff & Breidbach, 1992), and in *Schistocerca*, where w, x, y and z tracts pioneer successively during mid-embryogenesis (Williams et al., 2005).

Analysis of staining patterns from *echinoid* and *shotgun* expression yielded preliminary information on lineage for the HFS (section 3.4.1). Both the *z* and *y* fibres were each traced to separate clusters of neuroblasts and secondary neurons suggesting the each of the four fibre bundles originated from one of four protocerebral neuroblasts per hemisphere as seen in *Schistocerca*. Positions and trajectories of the clusters of Perikarya for the later developing *fb-eb* and Pontine neurons were reminiscent of the pattern of the HFS, suggesting that each of the eight clusters have separate origins, but equally that pairs of *fb-eb* and Pontine neurons share a common lineage. This type of clonal segregation can be seen in the Kenyon cells of the Mushroom bodies that differentiate from four neuroblasts to form a four unit structure (Armstrong et al., 1998). The enhancer trap lines reveal this potential shared lineage between *fb-eb* and Pontine neurons and indicate that cell type specification occurs as a further differentiation. This hypothesis is consistent with that suggested for the type A R neurons of the EB (Renn et al., 1999).

7.3 Insights into Central Complex structure

7.3.1 Genetic relationships between neurons

This is the first study to isolate the perikaryon of the ExR2 neuron and trace the complete projection pattern of this neuron (line c61, section 4.3.6). Indeed, this study has isolated enhancer trap lines that allow visualisation of the projection patterns of both the ExR2 and ExR1 (c255, section 4.3.8) neurons. These were not fully represented using Golgi staining in previous studies (Hanesch et al.,1989). Early in development,

sets of F*l* neurons were observed in two pairs suggesting a common morphology (c61, section 4.3.6). The F*l* neurons have not been further categorised in previous studies though many different subtypes have been observed (Hanesch et al., 1989). F neuron branching patterns can be most accurately analysed using Golgi staining, as this allows analysis at single cell resolution. In this study the enhancer trap lines revealed potential relationships between two pairs of F*l* neurons which may indicate further categorisation and a possible shared lineage. Several enhancer trap lines showed expression in F neurons but these were not always observed during development. Tracing and identifying the F neurons in the adult brain was problematic due to the high density of arborisations from these cells. Therefore it was not possible to resolve neuronal relationships for all of these cells.

7.3.2 Connections to other regions of the Nervous System

Echinoid staining revealed that fibre bundles of the HFS project ventrally past the VBOs (section 3.4.1.1). The final targets of these neurons were not resolvable in this study. It may be that these fibres target to the Ventral nerve cord (VNC) and connect to a motor circuit. Indeed, in *Schistocerca*, connections to the EB from the VNC via structures homologous to the VBO have been reported (Homberg, 1994). In *Drosophila* it may be that information is relayed from the HFS via the VBO to the VNC. Further study and a specific HFS marker is required to investigate this fully. The major fibre systems (HFS and VFS) have been well characterised in adult diptera (Power 1943, Williams 1975, Strausfeld 1976, Hanesch et al.1989) but the intrinsic Pontine neurons have remained more elusive (Hanesch et al., 1989). These data suggest that isomorphic sets of both Pontine and *fb-eb* neurons exist in the CC, shown by the expression patterns of enhancer trap lines c159b and c255 (sections 4.3.7 and 4.3.8). These enhancer trap lines have revealed that these neurons share a common morphology and this has allowed inference of cellular patterns. The Pontine neurons display a range of morphologies all

of which are intrinsic to the FB. These neurons, like the HFS and VFS, exist as isomorphic sets. One type of Pontine neurons, the *Pcd* neurons, appear to relay information between hemispheres within the FB. Future studies focusing on the functions of the FB could start with an investigation of these neurons.

7.3.3 Compartmentalisation and information flow in the Central Complex

The expression patterns revealed in this study allow us to further clarify the compartmentalisation of the CC. Projection patterns of the HFS, VFS, Pontine and *fb-eb* neurons define the columnar matrix elements with the F neurons forming the transverse strata. Projections of all the columnar elements target the 8 segments of the FB, with the VFS and HFS arborising in the 16 glomeruli of the PB. In addition to this projection patterns of the ExR1 neurons revealed 32 radial branches innervating the EB ring [Figure 4.3(B)]. The mutant data was also informative in this respect, revealing ~16 areas of arborisation from Type A R neurons in the unfused EB sections adjacent to the midline (Figure 5.4). These data suggest the hypothesis that the *Drosophila* EB is divided into 16 radial segments (that can be further subdivided into 32 half segments). It may be that the *fb-eb* neurons each innervate a segment displaying homolateral connections between the FB and the EB, as seen in *Musca domestica* (Strausfeld, 1976), although this was not resolvable in this study. The projection patterns from the *fb-eb* and Pontine neurons also suggest that the FB segments can be further subdivided into half segments, revealing 16 segments/glomeruli for each of the PB, FB and EB thereby forming a one dimensional array of columnar elements as hypothesised by Hanesch et al. (1989).

From this study we can also tentatively infer more about the information flow through the CC. It has been previously reported that the main input to the CC is through the Large field F and R neurons that first arborise in regions such as the VBO and LTR,

and the chief output neurons are the small field HFS neurons (Hanesch et al., 1989; Strauss, 2002). Data from the Dscam marker used in this study only revealed spiny dendrites of some Large field neurons, but this does suggest that the previously reported hypothesis may be correct. These data also reveal that Large field neurons (i.e. ExR1) are not exclusive to one sub-structure (Hanesch et al.,1989), as the ExR1 neuron innervates both the FB and the EB with spiny terminals, suggesting data flow from outwith and within the CC by Large field neurons. The Pontine neurons were previously shown to have both blebbed and spiny endings (Hanesch et al., 1989) and this was also seen in this study. These neurons are intrinsic to the FB and do not arborise until they reach the FB segments. *Pc d* neurons innervate one segment then terminate contralaterally prompting the hypothesis that their function is to allow data flow between hemispheres albeit in one sub-structure. Further studies are required to determine the CC polarity.

7.4 Significance of research

This study presents the first detailed analysis of the differentiating Central Complex and has provided novel insight into the structural, genetic and lineage components of this neuropil. In addition, a set of enhancer trap lines have been isolated and characterised for both the developing and adult Central Complex. The combined approach of antibodies and enhancer trap lines proved to be an effective method for structural and developmental analysis. Using these methods this study successfully built on the previous structural analyses of the insect CC (*Drosophila*; Power 1943; Hanesch et al., 1989; Renn et al., 1999: *Musca*; Strausfeld 1976*; Tenebrio molitor;* Wegerhoff & Breidbach, 1992*; Schistocerca gregaria;* Boyan & Williams, 1997; Williams et al., 2004: *Arthropods*; Loesel et al., 2002). In addition, novel markers for neurons of the CC were identified. Echinoid proved to be an effective structural marker, although the exact function of this Cell adhesion molecule could not be confirmed. This work also provided

an insight into the function of *neuroglian*. Analysis of CC mutants with the enhancer trap lines yielded further data on the structure of the CC and provided an indication of the functions of the genes that had been mutated.

7.5 Future work

7.5.1 Lineage Analysis

This thesis did not set out to identify the lineage of the CC but it has been possible to infer lineage from the data. Early results from section 3.6.1 permitted the inference of lineage for the HFS but this was not investigated further. These results were interpreted after consulting two studies that were published after the work for this section had been completed (Pereanu & Hartenstein, 2006; Younoussi-Hartenstein et al., 2006). Lineage tracing has been performed for the MBs (Ito & Hotta, 1992) and this information has been utilised successfully to ablate these structures in more recent studies (Armstrong et al., 1998). Performing a lineage analysis of the CC would not only provide valuable information on the origins of the intricate framework of this structure but would be useful for further structural and functional studies.

To conduct further investigation of both the lineage and structural elements of the CC, it would now be beneficial to perform a clonal analysis. The MARCM technique (Lee & Luo, 1999; Lee & Luo, 2001) is ideal for visualising small populations of neurons (like the enhancer trap system) and for tracing lineage as previously reported for the MBs (Lee et al., 1999). The data presented in this thesis has provided valuable information on P{Gal4} drivers that can be used for such an analysis in the CC. Prior to this, performing a MARCM analysis would have been considerably more challenging. In addition, investigation of the connections that the CC has to other regions of the CNS

would provide an insight into function of this neuropil.

Isolation of novel enhancer trap lines and cellular markers in addition to modern techniques mentioned above will allow us to build on the developmental CC data presented in this thesis. Several such collections of enhancer trap lines exist to screen for CC expression (including the laboratories of Kei Ito, Julie Simpson and Volker Hartenstein). In addition to this analysis, further structural and functional analyses are required of the larval counterpart(s) or primordium of the CC. This is referred to either a series of interhemispheric commissures (Hanesch et al., 1989; Strauss, 2002), a set of different fibre systems (Pereanu & Hartenstein, 2006) or an early sub-structure (Schneider et al., 1993). A common nomenclature system for the CC at both ends of development is required to study this. Indeed, the issue of a common nomenclature can be extended to encompass the structural descriptions of the CC in all insects. In order to effectively compare CC data between species a single nomenclature system would facilitate exchange of ideas.

7.5.2 Computational tools for structural analysis of the Fly brain

There is an ongoing need to provide a common source of structural information on the *Drosophila* brain. In addition to this, it is necessary to have a consistent neuronal nomenclature system on the insect brain. The computational power and tools available to us can facilitate the analysis and presentation of this structural data that were not available previously. Programs such as Amira allow construction of schematics representative of brain structures and neuronal systems that can be subsequently visualised in 3D (Rein et al., 2002). These programs are hugely valuable for converting raw images into comprehensible schematics. The use of computational tools is also practical when dealing with large volumes of data. Learning algorithms can be applied to trace neurons directly from images, thereby facilitating the process of manual marking

of Z stacks. By using a combination of advanced imaging techniques and computational tools it should be possible to build a map of known connectivity in the Fly brain. This, in combination with raw image data, could then be incorporated into an online archive to facilitate future developmental, structural and behavioural studies.

7.5.3 Behavioural and Genetic Analyis

These data can also be utilised in studies investigating the opposite point of development; behavioural analysis. This study has isolated enhancer trap lines for certain populations of neurons. Lines could be used to drive toxins (i.e. CntE; Liu et al., 2006), *shibere*^{ts} (Kitamoto, 2002) or specific RNAi constructs (Dietzl et al., 2007) in these neurons to assess their functional role, building on previous behavioural studies for the *Drosophila* CC (Strauss & Heisenberg, 1992; Strauss & Heisenberg, 1993; Bouhouche et al.,1993; Strauss 2002; Liu et al., 2006). In addition, functions of specific genes in these cells can be investigated. These lines can be used to assess genetic components involved in axons crossing the midline, indeed the neurons of the CC are an ideal model for this type of study. These studies will hopefully reveal more about the functions of the CC as a whole.

Renewed interest in the CC is rapidly rising in the research community. Several groups focusing on behavioural studies including learning and memory, locomotion and aggression behaviour have expressed an interest in the functions of the CC (Waddell S; Simpson J; Strauss, R; Rene-martin J; Penn J. Personal communications.). Recent behavioural experiments on Learning and memory have focused on the Mushroom bodies, this is partially due to the well known memory circuit link to the antennal lobes (de Belle & Heisenberg, 1994). It would be interesting to study the CC in relation to learning and memory and to test for potential shared functionality with the Mushroom bodies.

Understanding the genetic components involved in brain development is critical to the study of the brain. Further study of genes such as *cbd*, *ccb*, *neuroglian*, *echinoid* and the Cadherins is required to determine their neuronal functions and potential interactions. This may eventually allow us to infer functional pathways. This knowledge will not only be of interest to the *Drosophila* community, but due to a high degree of shared molecular mechanisms between invertebrates and vertebrates will also be valuable in medical research.

Bibliography

Ahmed A, Chandra S, Magarinos M, Vaessin H. (2003) *echinoid* mutants exhibit neurogenic phenotypes and show synergistic interactions with the Notch signaling pathway. Development 130, 6295-6304.

Appel F, Holm J, Conscience JF, Schachner M. (1993). Several extracellular domains of the neural cell adhesion molecule L1 are involved in neurite outgrowth and cell body adhesion. *J. Neurosci.* **13**: 4763-4775.

Armstrong JD. (1995) Structural characterisation of the *Drosophila* Mushroom bodies. Ph.D Thesis. University of Glasgow.

Armstrong JD, de Belle S, Wang Z, Kaiser K. (1998) Metamorphosis of the Mushroom Bodies; Large scale rearrangements of the Neural Substrates for Associative Learning and Memory in *Drosophila*. Learning and Memory 5: 102-114.

Armstrong JD, Texada MJ, Munjaal R, Baker DA, Beckingham KM. (2006) Gravitaxis in *Drosophila melanogaster*: a forward genetic screen. Genes, Brain & Behavior, Volume 5,Number 3 , pp. 222-239(18)

Ashburner M, Golic K, Hawley R. (2005) *Drosophila*: a laboratory handbook. 2nd edition.

Bai JM, Chiu WH, Wang JC, Tzeng TH, Perrimon N, Hsu JC. (2001) The cell adhesion molecule Echinoid defines a new pathway that antagonizes the *Drosophila* EGF receptor signaling pathway. Development 128, 591-601.

Baines RA, Seugnet L, Thompson A, Salvaterra PM, Bate M. (2002) Regulation of synaptic connectivity: levels of Fasciclin II influence synaptic growth in the Drosophila CNS. J Neurosci. 2002 Aug 1;22(15):6587-95.

Baker DA, Beckingham KM, Armstrong JD. (2007) Functional dissection of the neural substrates for gravitaxic maze behavior in *Drosophila melanogaster.* Journal Comp Neurology, Volume 501, Issue 5 , Pages 756 – 764

Baker NE. (2000) Notch signaling in the nervous system. Pieces still missing from the puzzle. Bioessays. 2000 Mar;22(3):264-73.

Bieber AJ, Snow PM, Hortsch M, Patel NH, Jacobs JR, Traquina ZR, Schilling J, Goodman CS. (1989) *Drosophila* Neuroglian: A member of the immunoglobulin superfamily with extensive homology to the vertebrate neural adhesion molecule L1. Cell, Vol 59, 447-460, 3 November.

de Belle S. (1995) *Drosophila* Mushroom Body subdomains: Innate or learned representations of odor preference and sexual orientation? Neuron, Vol. 15, 245-247.

Benson DL, Schnapp LM, Shapiro L, Huntley GW. (2000) Making memories stick: cell adhesion molecules in synaptic plasticity. Trends in Cell biology. 10. November.

Boquet I, Hitier R, Dumas M, Chaminade M, Preat T. (2000) Central brain postembryonic development in *Drosophila*: Implication of genes expressed at the interhemispheric junction. Journal of Neurobiology. Jan;42(1):33-48.

Bouhouche A, Vaysse G, Corbiere M. (1993) Immunocytochemical and learning studies of a *Drosophila melanogaster* neurological mutant, NO-BRIDGE^{KS49}, as an approach to the possible role of the Central Complex. J. Neurogenetics, Vol.9, pp.105-121.

Boyan GS, Williams JLD. (1997) Embryonic development of the pars intercerebralis/ central complex of the Grasshopper. Dev Genes Evol 207: 317-329.

Brand AH, Perrimon N. (1993) Targeted gene expression as a means of altering cell fates and generating dominant phenotypes. Development, Vol 118, Issue 2 401-415.

Brand AH. (1995) GFP in *Drosophila*. Trends Genetics 11: 324-325.

Buchner E, Buchner S, Crawford G, Mason WT, Salvaterra PM, Sattelle DB. (1986) Choline acetyltransferase-like immunoreactivity in the brain of *Drosophila melanogaster*. Cell tissue res 246: 57-62.

Burden-Gulley SM, Pendergast M, Lemmon V. (1997) The role of cell adhesion molecule L1 in axonal extension, growth cone motility, and signal transduction. Cell Tissue Res. 1997 Nov;290(2):415-22.

Callaerts P, Leng S, Clements J, Benassayag C, Cribbs D, Kang YY, Walldorf U, Fischback KF, Strauss R. (2000) *Drosophila* Pax-6/eyeless is Essential for Normal Adult Brain Structure and Function. . J. Neurobiology. Feb 5;46(2):73-88.

Carhan A, Allen F, Armstrong JD, Hortsch M, Goodwin SF, O'Dell KM. (2005) Female receptivity phenotype of *icebox* mutants caused by a mutation in the L1-type cell adhesion molecule neuroglian. Genes Brain Behav.4(8):449-65

Clandinin TR, Lee CH, Harman T, Lee RC, Yang AY, Ovasapyan S, Zipursky SL. (2001) *Drosophila* LAR regulates R1-R6 and R7 target specificity in the visual system. Neuron Vol. 32, 237-248, Oct 25.

Clandinin TR, Zipursky L. (2002) Making connections in the fly visual system. Neuron Vol. 35, 827-841, Aug 29. Review.

Connelly JB, Tully T. (1998) Integrins: a role for adhesion molecules in olfactory memory. Curr Biol. 1998 May 21;8(11):R386-9.

Cowan WM. (1998) The emergence of modern neuroanatomy and developmental neurobiology. Neuron Vol 20: 413-426.

de Belle JS, Heisenberg M. (1994) Associative odor learning in *Drosophila* abolished by chemical ablation of mushroom bodies. Science. Feb 4;263(5147):692-5.

Dickson BJ, Gilestro GF. (2006) Regulation of commissural axon pathfinding by slit and its Robo receptors. Annu Rev Cell Dev Biol. 2006;22:651-75.

Dietzl G, Chen D, Schnorrer F, Su KC, Barinova Y, Fellner M, Gasser B, Kinsey K, Oppel S, Scheiblauer S, Couto A, Marra V, Keleman K, Dickson BJ. (2007) A genome-wide transgenic RNAi library for conditional gene inactivation in *Drosophila*. Nature. Jul 12;448(7150):151-6.

Dubreuil RR, MacVicar G, Dissanayake S, Liu C, Homer D, Hortsch M. (1996) Neuroglian-mediated cell adhesion induces assembly of the membrane skeleton at cell contact sites. J Cell Biol. 1996 May;133(3):647-55.

Dubreuil RR, Grushko T. (1999) Neuroglian and DE-cadherin activate independent cytoskeleton assembly pathways in *Drosophila* S2 cells. Biochem Biophys Res Commun. Nov 19;265(2):372-5.

Dumstrei K, Wang F, Nassif C, Hartenstein V. (2003a) Early development of the Drosophila brain: V. Pattern of postembryonic neuronal lineages expressing DE-cadherin. Jour. Comp. Neurology. Jan 20;455(4):451-62.

Dumstrei K, Wang F, Hartenstein V. (2003b) Role of DE-cadherin in neuroblast proliferation, neural morphogenesis, and axon tract formation in *Drosophila* larval brain development.J. Neurosci. Apr 15;23(8):3325-35.

Dumstrei K, Wang F, Haag T, Hartenstein V. (2004) The role of DE-cadherin during cellularization, germ layer formation and early neurogenesis in the *Drosophila* embryo. Dev Biol. 2004 Jun 15;270(2):350-63.

Escudero LM, Wei SY, Chiu WH, Modolell J, Hsu JC. (2003) Echinoid synergizes with the Notch signaling pathway in *Drosophila* mesothorax bristle patterning. Development. 2003 Dec;130(25):6305-16.

Finnigan DJ. (1992) Transposable elements. Current Opinion in Genetics and Development, 2, pp 861-867.

Ge X, Hannan F, Xie Z, Feng C, Tully T, Zhou H, Xie Z, Zhong Y. (2004) Notch signaling in *Drosophila* long-term memory formation. Proc. Natl. Acad. Sci. USA. 2004 Jul 6;101(27):10172-6.

Ghysen A. (2003) The origin and evolution of the nervous system. Int. J Dev Biol. 47(7-8):555-62.

Godenschwege TA, Kristiansen LV, Uthaman SB, Hortsch M, Murphey RK. (2006) A conserved role for *Drosophila* Neuroglian and human L1-CAM in central-synapse formation. Curr. biol. Jan 10;16(1):12-23

Greenspan R. (2004) Fly Pushing: The Theory and Practice of *Drosophila* Genetics. 2nd Edition. Cold Spring Harbor Laboratory Press. New York.

Hall SG, Bieber AJ. (1997) Mutations in the *Drosophila* Neuroglian Cell Adhesion

Molecule Affect Motor Neuron Pathfinding and PeripheralNervous System patterning. J.Neurobiology. Mar ; 32(3):325-40.

Hanesch U, Fischbach KF, Heisenberg M. (1989) Neuronal architecture of the Central Complex in *Drosophila melanogaster*. Cell Tissue Res 257: 343-366.

Heinze S, Homberg U (2007) Maplike representation of celestial E-vector orientations in the brain of an insect. Science 16;315(5814):995-7.

Heisenberg M, Bohl K. (1979) Isolation of anatomical brain mutants of *Drosophila* by histological means. Z Naturforsch 34c: l43-147.

Heisenberg M, Borst A, Wagner S, Byers D. (1985) *Drosophila* mushroom body mutants are deficient in olfactory learning. *J.Neurogenet* 2:1-30.

Heisenberg M. (2003) Mushroom body memoir: From maps to models. Nature Reviews Neuroscience Nat Rev Neurosci. Apr;4(4):266-75.

Hirsch J & Ksander G. (1969) Studies in experimental behavior genetics. V. Negative geotaxis and further chromosome analyses in *Drosophila melanogaster*. J Comp Physiol Psychol 67,118–122.

Homberg U. (1991) Neuroarchitecture of the Central Complex in the brain of the locust *Schistocerca gregaria* and *S.americana* as revealed by serotonin immunocytochemistry. J Comp. Neurology 303: 245-254.

Homberg U. (1994) Flight-correlated activity changes in neurons of the lateral accessory lobes in the brain of the locust *Schistocerca gregaria* J. Comp. Physiol 175. p597 - 610.

Homberg U. (2004) In the search of the sky compass in the insect brain Naturwissenschaften 91 199–208.

Hortsch M. (2000). Structural and functional evolution of the L1-family: are four adhesion molecules better than one? *Mol. Cell. Neurosci.* 15,1 -10.

Hortsch M, Wang YME, Marikar Y, Bieber AJ. (1995). The cytoplasmic domain of the Drosophila cell adhesion molecule neuroglian is not essential for its homophilic adhesive properties in S2 cells. *J. Biol. Chem.* **270**: 18809-18817.

Hortsch M. (2003) Drosophila Echinoid is an antagonist of Egfr signalling, but is not a member of the L1-type family of cell adhesion molecules. Development. Nov;130(22):5295.

Hortsch M. (2003) Neural cell adhesion molecules - brain glue and much more!
Jan 1;8:d357-9. Review.

Hotta Y & Benzer S. (1972) Mapping of behaviour in *Drosophila* mosaics. Nature. Dec 29;240(5383):527-35.

Ilius M, Wolf R, Heisenberg M. (1994) The Central Complex of *Drosophila melanogaster* is involved in flight control: studies on mutants and mosaics of the gene *ellipsoid body open*. J Neurogenet 9: 189-206.

Islam R, Wei SY, Chiu WH, Hortsch M, Hsu JC. (2003) Neuroglian activates Echinoid to antagonize the *Drosophila* EGF receptor signaling pathway. Development. 2003 May;130(10):2051-9.

Ito K, Hotta Y. (1992) Proliferation pattern of postembryonic neuroblasts in the brain of

Drosophila melanogaster. Developmental biology 149, 134-148.

Ito K, Suzuki K, Estes P, Ramaswami M, Yamamoto D, Strausfeld NJ. (1998) The organization of extrinsic neurons and their implications in the functional roles of the mushroom bodies in *Drosophila melanogaster* Meigen. Learn Mem. May-Jun;5(1-2):52-77.

Iwai Y, Hirota Y, Ozaki K, Okano H, Takeichi M, Uemura T. (2002) DN-Cadherin is required for spatial arrangement of nerve terminals and ultrastructural organization of synapses. Mol & Cell Neuro. Volume 19,Number 3, March, pp. 375-388(14)

Jarman A. (2002) Studies of mechanosensation using the fly. Human Molecular Genetics. Vol 11, No.10. 1215-1218

Kamiguchi H. (2003) The mechanism of axon growth: what we have learned from the cell adhesion molecule L1. Mol Neurobiol. Dec;28(3):219-28.

Kamiguchi H, Hlavin ML, Yamasaki M, Lemmon V. (1998). Adhesion molecules and inherited diseases of the human nervous system. *Annu. Rev. Neurosci.* **21**, 97-125.

Keene A, Waddell S. (2007) *Drosophila* olfactory memory: single genes to complex neural circuits. Nature Reviews Neuroscience 8, 341-354

Kenyon FC. (1896) The brain of the bee: A preliminary contribution to the morphology of the nervous system of the arthropoda. J. Comp Neurology 6, 133-210.

Kidd T, Russell C, Goodman CS, Tear G. (1998) Dosage-sensitive and complementary functions of roundabout and commissureless control axon crossing of the CNS midline. Neuron. 1998 Jan;20(1):25-33.

Kitamoto, T. (2002) Conditional disruption of synaptic transmission induces male-male courtship behavior in *Drosophila*. Proc. National. Acad. Sci. Oct 1;99(20):13232-7.

Kramer J & Staveley B. (2003) GAL4 causes developmental defects and apoptosis when expressed in the developing eye of *Drosophila melanogaster*. Genet. Mol. Res. 2 (1): 43-47 (2003)

Kristiansen LV, Velasquez E, Romani S, Baars S, Berezin V, Bock E, Hortsch M, Garcia-Alonso L. (2005) Genetic analysis of an overlapping functional requirement for L1- and NCAM-type proteins during sensory axon guidance in *Drosophila*. . Mol cell Neurosci. Jan;28(1):141-52.

Landgraf M, Sanchez-Soriano N, Technau GM, Urban J, Prokop A. (2003) Charting the *Drosophila* neuropile: a strategy for the standardised characterisation of genetically amenable neurites. Developmental Biology, Volume 260, Issue 1, 1 August 2003, Pages 207-225

Lee T, Luo L. (1999) Mosaic Analysis with a Repressible Cell Marker for studies of Gene Function in Neuronal Morphogenesis. Neuron, Vol.22, 451-61, March.

Lee T, Lee A, Luo L. (1999) Development of the *Drosophila* Mushroom bodies: sequential generation of three distinct types of neurons from a neuroblast. Development 126, 4065-4076.

Lee T, Luo L. (2001) Mosaic analysis with a repressible cell marker (MARCM) for *Drosophila* neural development. Trends in Neurosciences. Vol 24, No.5 May.

Lee CH, Herman T, Clandinin TR, Lee R, Zipursky SL. (2001) N-cadherin regulates target specificity in the *Drosophila* visual system. Neuron 30, 437-450.

Lee RC, Clandinin TR, Lee CH, Chen PL, Meinertzhagen IA, Zipursky SL. (2003) The Protocadherin Flamingo is required for axon target selection in the *Drosophila* visual system. Nature Neuroscience 6, p.557-564. June.

Liu G, Seiler H, Wen A, Zars T, Ito K, Wolf R, Heisenberg M, Liu L. (2006) Distinct memory traces for two visual features in the *Drosophila* brain. Nature. Feb 2;439 (7076):551-6.

Loesel R, Nassel DR, Strausfeld NJ. (2002) Common design in a unique midline neuropil in the brains of arthropods. Arthropod Structure & Development 31: 77-91.

Marguiles C, Tully T, Dubnau J. (2005) Deconstructing Memory in *Drosophila.* Current Biology, Vol.15, R700-R713, September 6.

Martin JR, Raabe T, Heisenberg M. (1999) Central Complex substructures are required for the maintenance of locomotor activity in *Drosophila melanogaster*. J Comp Physiol [A]. 1999 Sep;185(3):277-88.

Martinek S, Gaul U. (1997) Neural development: how cadherins zipper up neural circuits Current Biology. Nov 1;7(11):R712-5.

Maurel-Zaffran C, Suzuki T, Gahmon G, Treisman JE, Dickson BJ. (2001) Cell-autonomous and -nonautonomous functions of LAR in R7 photoreceptor axon targeting. Neuron. 2001 Oct 25;32(2):225-35.

Meinertzhagen IA & Hanson TE. (1993) The development of the Optic lobe. In 'The development of *Drosophila melanogaster*', M Bate & AM Arias eds. (New York: Cold Spring Harbor University press). PP. 1363-1492.

Meinertzhagen IA, Emsley JG, Sun XJ. (1998) Developmental anatomy of the

Drosophila brain: Neuroanatomy is gene expression. Journal of Comparative Neurology. 402:1-9.

Muller M, Homberg U, Kuhn A. (1997) Neuroarchitecture of the lower division of the central body in the brain of the locust (*Schistocerca gregaria*). Cell Tissue Res 288: 159-176.

Nassif C, Noveen A, Hartenstein V. (1998) Embryonic development of the *Drosophila* brain. I. Pattern of pioneer tracts. Journal Comp. Neurology. Dec 7;402(1):10-31. Dec 7;402(1):10-31.

Nassif C, Noveen A, Hartenstein V. (2003) Early development of the *Drosophila* brain: III. The pattern of neuropile founder tracts during the larval period. Jour. Comp. Neurology. Jan 20;455(4):417-34.

Newsome TP, Asling B, Dickson BJ. (2000) Analysis of *Drosophila* photoreceptor axon guidance in eye-specific mosaics. Development. Feb;127(4):851-60.

Nicolas E & Preat, T (2005) *Drosophila* central brain formation requires Robo proteins. Development Genes and Evolution Volume 215, Number 10. October, 2005.

Noveen A, Daniel A, Hartenstein V. (2000) Early development of the *Drosophila* mushroom body: the roles of eyeless and dachshund. Development. Aug;127(16):3475-88.

Ott H, Bastmeyer M, Stuermer CA. (1998) Neurolin, the goldfish homolog of DM-GRASP, is involved in retinal axon pathfinding to the optic disk. . Journal neurosci. May 1;18(9):3363-72.

Pereanu W, Hartenstein V. (2006) Neural lineages of the *Drosophila* brain: A three-

dimensional digital atlas of the pattern of lineage location and projection at the late larval stage. Journal of Neuroscience, May 17, 26(20):5534-5553.

Popov AV, Peresleni AI, Ozerskii PV, Shchekanov EE, Savvateeva-Popova EV. (2003) On the Role of the Protocerebral Bridge in the Central Complex of *Drosophila melanogaster* Brain in Control of Courtship Behavior and Sound Production. J Evolutionary Biochemistry & Physiology, Vol 39(6): 530-9.

Popov AV, Peresleni AI, Savvateeva-Popova EV, Wolf R, Heisenberg M. (2004) The role of the mushroom bodies and of the central complex of *Drosophila melanogaster* brain in the organization of courtship behavior and communicative sound production. J Evolutionary Biochemistry & Physiology, Vol 40 (6): 641-52.

Power M. (1943) The brain of *Drosophila Melanogaster*. Journal of Morphology, Volume 72, Issue 3 , Pages 517 - 559.

Prakash S, Caldwell JC, Eberl DF, Clandinin TR. (2005) *Drosophila* N-cadherin mediates an attractive interaction between photoreceptor axons and their targets, *Nat Neurosci* 8, pp. 443–450

Presente A, Boyles RS, Serway CN, de Belle JS, Andres AJ. (2003) *notch* is required to long term memory in *Drosophila*. PNAS, Vol.101, no.6, 1764-1768.

Quinn WG. (2006) Memories of a Fruitfly. Nature, Vol 439. pp.546-548.

Rawlins EL. (2001) The characterisation of dominant second site modifiers of an activated *atonal* phenotype in *Drosophila melanogaster*. Ph.D Thesis. University of Edinburgh.

Rawlins EL, Lovegrove B, Jarman AP. (2003a) Echinoid facilitates Notch pathway

signalling during *Drosophila* neurogenesis through functional interaction with Delta. Development. Dec;130(26):6475-84.

Rawlins EL, White NM, Jarman AP. (2003b) Echinoid limits R8 photoreceptor specification by inhibiting inappropriate EGF receptor signalling within R8 equivalence groups. Aug;130(16):3715-24.

Rein K, Zockler M, Mader M, Grubel C, Heisenberg M. (2002) The *Drosophila* standard brain. Current biology 12: 227-231.

Renn SCP, Armstrong JD, Yang M, Wang Z, An X, Kaiser K, Taghert PH. (1999) Genetic analysis of the *Drosophila* ellipsoid body neuropil: Organisation and development of the Central Complex. J. Neurobiology Nov 5;41(2):189-207,

Riddiford LM, Hiruma K, Zhou X, Nelson CA. (2003) Insights into the molecular basis of the hormonal control of molting and metamorphosis from *Manduca sexta* and *Drosophila melanogaster*. Insect Biochem Mol Biol. 2003 Dec;33(12):1327-38

Rohrbough J, O'Dowd DK, Baines R, Broadie K. (2003) Cellular bases of behavioural plasticity : Establishing and modifying synaptic circuits in the *Drosophila* genetic system. J Neurobiol. Jan;54(1):254-71.

Rougon G, Hober O. (2003) New insights into the diversity and function of the neuronal immunoglobulin superfamily molecules. Annual Review of Neuroscience Vol. 26: 207-238.

Rosay P, Armstrong JD, Wang Z, Kaiser K. (2001) Synchronized neural activity in the *Drosophila* memory centers and its modulation by *amnesiac*. Neuron, Vol. 30, 759-770, June 2001.

Sanchez-Soriano N, Bottenberg W, Fiala A, Haessler U, Kerassoviti A, Knust E, Lohr R, Prokop A. (2005) Are dendrites in *Drosophila* homologous to vertebrate dendrites? Developmental Biology, 288: 126-138.

Schneider L, Sun ET, Garland DJ, Taghert PH. (1993). An immunocytochemical study of the FMRFamide neuropeptide gene products in *Drosophila*. Journal of Comparative Neurology 337:446 - 460.

Senti KA, Usui T, Boucke K, Greger U, Uemure T, Dickson BJ. (2003) Flamingo regulates R8 axon-axon and axon-target interactions in the *Drosophila* visual system. Current Biology, Vol 13, 828- 832, May 13.

Shinza-Kameda M, Takasu E, Sakurai K, Hayashi S, Nose A. (2006) Regulation of layer-specific targeting by reciprocal expression of a cell adhesion molecule, Capricious, Neuron 49, pp. 205–213.

Spencer SA, Cagan RL. (2003) Echinoid is essential for regulation of Egfr signaling and R8 formation during *Drosophila* eye development. Development. 2003 Aug;130(16):3725-33.

Strausfeld NJ. (1976) Atlas of an insect brain. Berlin ; New York: Springer-Verlag.

Strausfeld NJ, Miller TA. (1980) Neuroanatomical techniques. Springer-Verlag.

Strausfeld NJ, Hansen L, Li Y, Gomez RS, Ito K. (1998) Evolution, discovery and interpretations of Arthropod Mushroom Bodies. Learning and Memory, 5:11-37.

Strauss R, Hanesch U, Kinkelin M, Wolf R, Heisenberg M. (1992) No-bridge of *Drosophila melanogaster*: portrait of a structural brain mutant of the central complex. J

Neurogenet. Sep;8(3):125-55.

Strauss R & Heisenberg M. (1993) A higher center of locomotor behaviour in the *Drosophila* brain. Journal of Neuroscience 13(5): 1852-1861.

Strauss R. (2002) The Central Complex and the genetic dissection of locomotor behaviour. Curr. Op. Neurobiology. 12: 633-638.

Sullivan W, Ashburner M, Scott Hawley R. (2000) *Drosophila* Protocols. Cold Spring harbor Laboratory press.

Swan LE, Schmidt M, Schwarz T, Ponimaskin E, Prange U, Boeckers T, Thomas U, Sigrist SJ. (2006) Complex interaction of *Drosophila* GRIP PDZ domains and Echinoid during muscle morphogenesis. EMBO J. 2006 Aug 9;25(15):3640-51

Tettamanti M, Armstrong JD, Endo K, Yang MY, Furukubo-Tokunaga K, Kaiser k, Reichert H. (1997) Early development of the *Drosophila* mushroom bodies, brain centers for associative learning and memory. Dev Genes Evol 207: 242-252.

Ting CY, Yonekura S, Chung P, Hsu SN, Robertson HM, Chiba A, Lee CH. (2005) *Drosophila* N-cadherin functions in the first stage of the two-stage layer-selection process of R7 photoreceptor afferents, *Development* **132**, pp. 953–963.

Ting CY, Lee CH. (2007) Visual circuit development in *Drosophila*. Curr. Opin. Neur. Biology. Feb;17(1):65-72. Epub 2007 Jan 3. Review.

Truman JW. (1990) Metamorphosis of the central nervous system of *Drosophila*. Journal of Neurobiology, Vol.21 No.7, pp.1072-1084.

Truman, JW, Taylor, BJ, Award, TA. (1993) Formation of the adult nervous system. The Development of *Drosophila melanogaster*. II, M. Bate and A.M. Arias, Cold Spring

Harbor Laboratory Press, Cold Spring Harbor, NY pp. 1245–1275. .

Truman JW, Schuppe H, Shepherd D, Williams DW. (2004) Developmental architecture of adult-specific lineages in the ventral CNS of *Drosophila*. J Neurobiol. Oct;131(20):5167-84.

Uchida N, Honjo Y, Johnson KR, Wheelock MJ, Takeichi M. (1996) The catenin/ cadherin adhesion system is localized in synaptic junctions bordering transmitter release zones. J Cell Biol. 1996 Nov;135(3):767-79.

Uemura K, Kuzuya A, Shimohama S. (2004) Protein trafficking and Alzheimer's disease. Curr Alzheimer Res. 2004 Feb;1(1):1-10.

Varnam CJ, Strauss R, de Belle JS & Sokolowski MB. (1996) Larval behavior of Drosophila central complex mutants: Interactions between no bridge, foraging, and chaser. Journal of Neurogenetics 11, 99-115.

Vosshall LB, Wong AM, Axel R. (2000) An olfactory sensory map in the fly brain. Cell 102:147.

Wang J, Ma X, Yang J, Zheng X, Zugates C, Lee CH, Lee T. (2004) Transmembrane/ juxtamembrane domain-dependent Dscam distribution and function during Mushroom Body neuronal morphogenesis. Volume 43, Issue 5, 2 September, P. 663-672.

Ward EJ, Thaipisuttikul I, Terayama M, French RL, Jackson SM, Cosand KA, Tobler KJ, Dorman JB, Berg CA. (2002) GAL4 enhancer trap patterns during *Drosophila* development. Genesis 34: 46-50.

Wegerhoff R, Breidbach O. (1992) Structure and development of the larval central complex in a holometabolous insect, the beetle *Tenebrio molitor*. Cell Tissue Res. 268:

341-358.

Wei SY, Escudero LM, Yu F, Chang LH, Chen LY, Ho YH, Lin CM, Chou CS, Chia W, Modolell J, Hsu JC. (2005) Echinoid is a component of adherens junctions that cooperates with DE-Cadherin to mediate cell adhesion. Dev Cell. 2005 Apr;8(4):493-504.

Wessnitzer J, Webb B. (2006) Multimodal sensory integration in insects – towards insect brain control architectures. Bioinsp. Biomim. 1 (2006) 63–75.

Williams JLD. (1975) Anatomical studies of the insect central nervous system: a ground plan of the midbrain and an introduction to the central complex in the locust, *Schistocerca gregaria* (Orthoptera). J Zool Lond 176:67-86.

Williams DW, Truman JW. (2004) Mechanisms of dendritic elaboration of sensory neurons in *Drosophila*: Insights from *in vivo* time lapse. Journal of Neuroscience, February 18, 2004, 24(7):1541-1550.

Williams DW, Truman JW. (2005) Remodeling dendrites during insect metamorphosis. J. Neurobiology. 2005 Jul;64(1):24-33.

Williams JLD, Guntner, Boyan GS. (2005) Building the Central Complex of the grasshopper *Schistocerca gregaria*: temporal topology organises the neuroarchitecture of the w, x, y, z tracts. Arthropod Structure & Development. 34:97-110.

Wolman MA, Regnery AM, Becker T, Becker CG, Halloran MC. (2007) Semaphorin3D regulates axon axon interactions by modulating levels of L1 cell adhesion molecule. J Neurosci. 2007 Sep 5;27(36):9653-63.

Yamamoto M, Ueda R, Takahashi K, Saigo K, Uemura T. (2006) Control of axonal sprouting and dendrite branching by the Nrg-Ank complex at the neuron-glia interface.

Curr Biol. 2006 Aug 22;16(16):1678-83.

Yang MY, Armstrong JD, Vilinsky I, Strausfeld NJ, Kaiser K. (1995) Subdivision of the *Drosophila* Mushroom bodies by enhancer trap expression patterns. Neuron Vol 15, 45-54 July.

Younossi-Hartenstein A, Nassif C, Green P, Hartenstein V. (1996) Early neurogenesis of the *Drosophila* brain. Jour. Comp. Neurology. Jul 1;370(3):313-29.

Younoussi-Hartenstein A, Nguyen B, Shy D, Hartenstein V. (2006) Embryonic origin of the *Drosophila* brain neuropile. Jour. Comp Neurology. Aug 20;497(6):981-98.

Zhu H, Luo L. (2004) Diverse functions of N-cadherin in dendritic and axonal terminal arborization of olfactory projection neurons. Neuron. 2004 Apr 8;42(1):63-75.

Zhu H, Hummel T, Clemens JC, Berdnik D, Zipursky SL, Luo L. (2006) Dendritic patterning by Dscam and synaptic partner matching in the *Drosophila* antennal lobe. Nat Neuroscience Mar;9(3):349-55.